Attis Media

Interplay between host and pathogen

Kim Stol

OTMS MEDIA

Interplay between host and pathogen

Kim Stol

ISBN 978-90-9027766-0

Printed by
Off Page, Amsterdam

Published by
K. Stol

Cover design
Anna Hoving
www.ANNAontwerp.nl

Layout
Arthur Klijn

OTITIS MEDIA

Interplay between host and pathogen

MIDDENOORONTSTEKING

samenspel tussen gastheer en pathogeen

Proefschrift

ter verkrijging van de graad van doctor aan de Radboud Universiteit Nijmegen op gezag van de rector magnificus prof. mr. S.C.J.J. Kortmann,
volgens besluit van het college van decanen in het openbaar te verdedigen op
vrijdag 18 oktober 2013 om 10.30 uur precies

door
Kim Stol
geboren op 18 januari 1980 te IJsselstein

Promotiecommissie

Promotoren
Prof. dr. P.W.M. Hermans
Prof. dr. R. de Groot

Co-promotor
Dr. A. Warris

Overige leden
Prof. dr. M.M. Rovers
Prof. dr. E.A.M. Sanders
Prof. dr. K. Graamans

Financial support
Research: Financial support was obtained from the European Union Sixth Framework Program (Project Title: OMVac. Project No. 037653).

voor Arthur

Contents

General introduction

Introduction

Epidemiology and background

Otitis media (OM), or middle ear infection, is one of the most frequent diseases during childhood and the most common motive for young children to visit a physician. In many countries, OM is the most common reason for children to receive antibiotics or to undergo surgery (1-4). Although severe complications such as mastoiditis and meningitis are rare, their morbidity is high (5). Costs for general healthcare, in which OM plays a very significant role, are estimated to be around 5 billion dollars in the US annually (1,4,6,7).

OM is a common denominator for a variety of middle ear diseases that can be divided into different categories. These include acute otitis media (AOM) and otitis media with effusion (OME) (8,9). AOM is defined as the presence of middle ear effusion accompanied by signs of acute inflammation of the middle ear, such as otalgia, otorrhea, fever, and malaise or irritability of the child (4). OME on the other hand can either develop as a sequel of AOM or develop *de novo*, the primary symptom being hearing loss due to the presence of middle ear fluid in the middle ear cavity but in the absence of signs of acute inflammation (10).

Seventy-five percent of all individuals are confronted with at least one episode of AOM in a life-time, with a peak during the first 6-18 months of life (7,11). In 10-20% of all children up to one year old, recurrence of at least three AOM episodes will occur. Recurrent AOM is defined as 3 or more episodes within 6 months time, or 4 or more episodes in a period of 12 months. In 50%, middle ear effusions are present 4-6 weeks after the acute onset, which diminish by half after 3 months. In case the effusion persists for more than 3 months, the disease is defined as chronic OME (COME) (12).

A number of factors are associated with an increased risk to develop OM. Although family predisposition is not well understood (11), it is generally assumed that there is a genetic basis. For example, Emonts et al. have demonstrated an association between the PAI 1 4G/4G genotype and recurrent AOM in children under the age of 4 (13). In another study, they observed that polymorphisms in the inflammatory response genes of TNF-α, IL-6 and IL-10 contributed to increased susceptibility to AOM in otitis-prone children (14). There is also an increased prevalence among Native Americans, Aboriginals and Inuit, suggesting genetic predisposition for OM (15).

Related to the home environment, the presence of older siblings increases the exposure to potential middle ear pathogens and respiratory viruses, and consequently, the risk

to develop OM. In addition, lack of breast-feeding, pacifier use, low socioeconomic status and exposure to tobacco smoke also contribute to the risk of developing otitis media. Furthermore, daycare center attendance is another environmental factor which increases the risk for OM as a result of increased exposure to respiratory viruses and middle ear pathogens (4,11,16). Finally, children younger than 6 months of age, with craniofacial abnormalities, immune deficiencies, or a history of recent ear surgery are at risk to develop OM (17).

Diagnosis, complications and sequelae

Initial OM diagnosis is based on signs, symptoms and otoscopic findings with physical examination. In case of complicated, recurrent or persistent OM episodes, referral to an otolaryngologist or pediatrician (in particular when immune deficiencies are suspected) is warranted. To confirm OM diagnosis, otoscopy needs to be supported by audiometry and tympanometry (18). Sequelae of OM manifested in the tympanic membrane include atrophy, myringosclerosis, retraction, adhesion and perforation (19). Complications of OM, for example mastoiditis, meningitis, petrositis, labyrintitis and cerebral venous thrombosis, appear in approximately 0.5% of the OM cases (20).

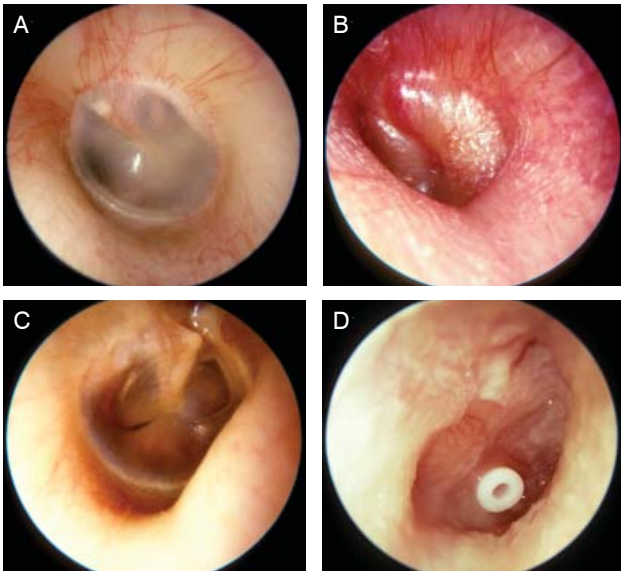

Figure 1. Typical otoscopic findings of the tympanic membrane in the unaffected middle ear and during OM: (A), healthy tympanic membrane; (B), tympanic membrane during AOM; (C), tympanic membrane during COME; (D) tympanic membrane after insertion of a ventilation tube (adapted from http://me.hawkelibrary.com).

Treatment

Although OM management has no universal standard yet, it may imply watchful waiting, antibiotic treatment, adenoidectomy, insertion of ventilation tubes or vaccination (Figure 2). Accurate diagnosis is often difficult, because signs and symptoms might overlap with symptoms of other respiratory infections (21). In addition, diagnosis relies on otoscopy (inspection of the tympanic membrane) and tympanometry (functional testing of the tympanic membrane), which is done inconsistently. Hence, AOM diagnosis is estimated to be incorrect in 30% of the cases (Figure 2).

The Wait and See Approach is a primary care strategy designed in The Netherlands, in which children suffering from AOM do not receive antibiotic treatment in the first 48-72 hours, but do receive adequate analgesics (4,22). This strategy, at present implemented in most international guidelines, is preferred in uncomplicated AOM for selected children based upon diagnostic certainty, age, illness severity, and assurance of follow-up (22). Although guidelines among countries are fairly similar, adherence of physicians to these guidelines is poor (23,24)(Figure 2). Importantly, untreated AOM has a high rate of spontaneous resolution, and a plausible viral origin is often neglected. Nevertheless antibiotic prescription rates to treat OM remain high, varying from 31% in the Netherlands to 98% in Australia and the United States (1). Consequently, if antibiotics are used in diseases which are mostly self-limiting, development of antimicrobial resistance will be enhanced (7) (Figure 2).

Whether antibiotic treatment contributes to the cure of rAOM or COME is still a matter of debate (25-27). Tympanostomy tube insertion and adenoidectomy are two surgical interventions for children suffering from rAOM or COME, primarily to establish (transient) improvement of hearing levels (8,28,29). Nevertheless, optimal treatment with regard to these children remains highly controversial (Figure 2). For example, Schilder et al. demonstrated a wide discrepancy in ventilation tube insertion among countries for the treatment of COME in children aged 0-14 years (29), and a similar phenomenon holds true for adenoidectomy: annual adenoidectomy rates differ significantly between countries (30). For adenoidectomy there is a significant benefit regarding the resolution of middle ear fluid, the benefits to hearing are small. The benefits of ventilation tubes to hearing improvement diminishes during the first year. Thus far, the effect of ventilation tube insertion on speech and language development has not been demonstrated (29).

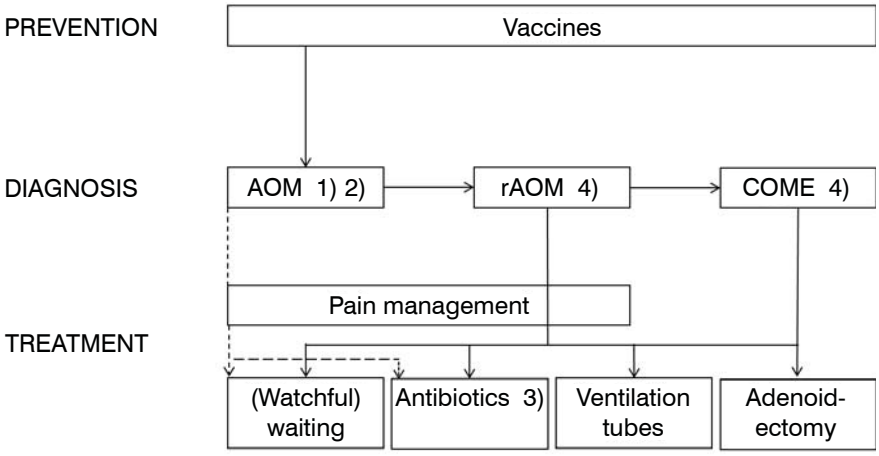

Figure 2. OM diagnosis, treatment and obstacles to overcome. 1) AOM diagnosis estimated to be wrong in 30% of the cases; 2) International consensus on AOM guidelines, however, interpretation of the guideline remains difficult; 3) Empirical prescription of antibiotics, and consequently increasing antibiotic resistance; 4) No international consensus in rAOM and COME treatment.

Vaccines and vaccine development

Vaccines are a relatively new treatment strategy to combat OM. Vaccination efficacy against OM diseases is currently limited, and directed against very few bacterial OM pathogens, and even fewer viral OM pathogens. The pneumococcal conjugate vaccine (PCV7), implemented in the Dutch National Immunization Program in 2006, is primarily designed to target pneumococcal invasive disease, and the introduction of this vaccine reduced the overall OM incidence by 6-9% (31-34). Moreover, PCV7 and the recently launched PCV10 and PCV13 vaccines are thought (i) to delay the first pneumococcal AOM episode in children, (ii) to reduce emergency room visits, (iii) to reduce antibiotic resistance, and (iv) to reduce the need for ventilation tube insertion (35). However, once recurrent acute otitis media has been established, no reduction in otitis media episodes occurs after vaccination, not even reduction of OM caused by the serotypes included in the conjugate vaccine (36).

In the Netherlands, PCV7 has recently been replaced by PCV10 (PHiD-CV, Synflorix) (37,38). PCV13 (13-valent, Prevenar) has replaced PCV7 in the childhood immunization schedules of the USA and UK in 2010 (39). Since the current conjugate vaccines are only directed against a limited number of pneumococcal serotypes, serotype replacement and pathogen replacement can occur, with a reduced overall vaccine effect as a consequence. PCV10 is the first vaccine in which components of multiple OM pathogens are combined:

the *Haemophilus influenzae* protein D is combined with 10 distinct pneumococcal polysaccharides in a conjugate formulation in order to reduce OM induced by *Streptococccus pneumoniae* and *H. influenzae* (40). Future vaccines that are protective against all *S. pneumoniae* serotypes and that contain bacterial components that elicit protection against all three major bacterial OM pathogens (*S. pneumoniae*, *H. influenzae* and *Moraxella catarrhalis*), are considered to have a very significant potential to reduce the burden of OM disease (2,7,41,42). Viral relevance in OM should not be underestimated, however, due to the manufacturing complexity it is unlikely to produce a combined multiple bacterial-viral vaccine in the near future (16).

Clinical microbiology

OM episodes are usually preceded by asymptomatic nasopharyngeal colonization with one or more of the major OM pathogens, i.e. *S. pneumoniae*, *H. influenzae* and/or *M. catarrhalis* (Figure 3) (9). The rate of colonization is age-dependent, increases from infancy to early childhood and remains high in adulthood (43). A population-based prospective cohort study in the Netherlands enrolled 1079 children and determined the carriage rate of the aforementioned pathogens: *S. pneumoniae* (8.3%, 31.3% and 44.5%, measured at 1.5 months, 6 months and 14 months, respectively), *H. influenzae* (7.2%, 23.8% and 31.7%, respectively) and *M. catarrhalis* (11.8%, 29.9% and 29.7% respectively) (44). The prevalence of nasopharyngeal carriage is increased in those coming in close inter-individual contact, for example when attending day-care or when having older siblings (45). Some studies conclude that colonization of the nasopharynx at an early stage, predisposes children for development of rAOM (46), whereas others cannot confirm this association (47). In addition, OM-prone children display increased carriage rates of these bacterial pathogens compared to healthy controls (31,48,49). Furthermore, the density of colonization appears to be important in determining the likelyhood of progression to OM (50).

As determined by clinical studies performed in the US and Europe *S. pneumoniae* and *H. influenzae* are responsible for 80% of all AOM episodes, and *M. catarrhalis* in 3 to 20% (11,51). Since OME can develop as a sequel of AOM, these pathogens are often found in middle ear effusions from children with OME. Whether these bacteria are also important in the development of *de novo* OME, is not yet clear (11,52).

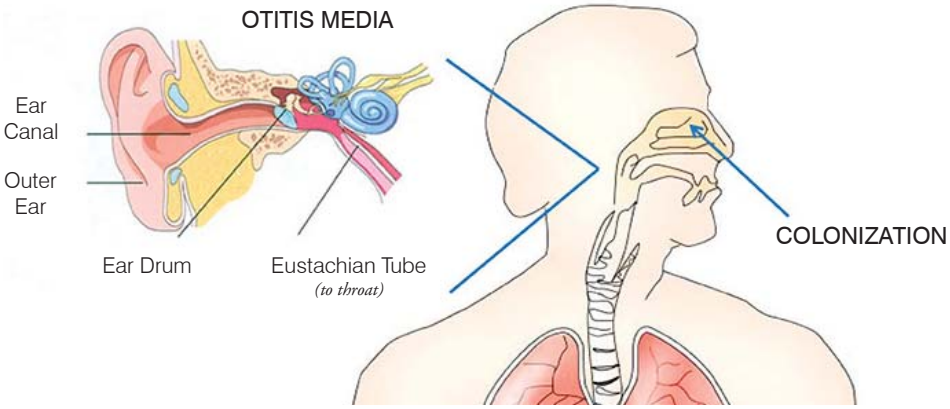

Figure 3. Schematic representation of nasopharyngeal colonization and OM (adapted from K.M. Mason, http://masonlab.nchresearch.org/).

Microbial pathogenesis

S. pneumoniae is an encapsulated, Gram-positive diplococcus, whereas *H. influenzae* is a Gram-negative rod-shaped bacterium that can be either capsulated (typeable) or unencapsulated (non-typeable). *M. catarrhalis* is an unencapsulated, Gram-negative diplococcus.

Since the introduction of the heptavalent conjugate vaccine, a significant reduction in otitis media due to *S. pneumoniae* strains and an increase in otitis media due to non-typeable *H. influenzae* have been reported (32). Non-typeable *H. influenzae* is a significant cause of OM in children, but is also known to exacerbate COPD or persist chronically in adults with COPD (53). *M. catarrhalis,* although previously thought to be primarily a commensal, is currently considered to be a true pathogen of the upper and lower respiratory tract.

S. pneumoniae

Adhesion. In order to reside in the middle ear cavity, *S. pneumoniae* needs to adhere to the epithelium. Various factors e.g. Ami/AliAB, IgA1 protease, PavA, NanA, PsaA, PspA, PspC, and pneumolysin have shown their significant contribution to nasopharyngeal colonization (54-59). Thus far, research investigating the contribution of the specific virulence factors in OM has been scarce. Type four pili (TFP), adhesins which are believed to also mediate colonization of the nasopharynx and OM, have been investigated extensively over the last years and have shown to be present in pathogen *S. pneumoniae*, albeit not invariably present in all strains (60,61).

Invasion. The proportion of internalized pneumococci in resting pulmonary cells is only 0.1% of the adherent bacteria (62).

Toxicity. Another important molecule that is associated with pneumococcal virulence is pneumolysin. This hemolysin is intracellularly produced by *S. pneumoniae* and released by the action of cell-bound autolysin. The multiple biological activities of pneumolysin, such as inhibition of ciliar function on epithelial and endothelial cells and masking of hydrogen peroxide release have been shown to interfere with eukaryotic host-cell function and the immune system (63).

Immune evasion. The capsular polysaccharide of *S. pneumoniae* is considered to be the major virulence factor (64). The role of the capsule is mainly of protective nature, as it allows pneumococci to evade phagocytosis by immune cells by inhibiting complement deposition and activation at the bacterial surface. The pneumococcus can regulate the thickness of its capsule during colonization, allowing the bacterium to expose surface molecules that facilitate adherence to the epithelium (64,65). At present, over 90 pneumococcal capsular polysaccharide types are recognized. The distinct capsular structures are used to serologically discriminate *S. pneumoniae* strains. *S. pneumoniae* has developed several mechanisms to resist the effects of complement in innate immunity (66). The pneumococcal capsule is a key factor in this resistance, acting not only to limit access to cell bound complement, but also reducing the amount of complement deposited. In addition, the toxin pneumolysin and the pneumococcal surface proteins PhtB, PspA and PspC contribute to serum resistance (63).

H. influenzae

Adhesion. Hap adhesin, HMW1/2 and Hia are all virulence factors involved in *H. influenzae* adhesion (for review, see (67)). Type four pili have also been found to be expressed by *H. influenzae*. Fifteen percent of *H. influenzae* strains, both typeable and non-typeable, is able to express these pili (67). Phosphorcholine (ChoP), a phase variable LOS-component, has been shown to contribute to the LOS-dependent adherence of NTHi to epithelial cells (67).

Invasion. ChoP may influence invasion via interaction with the platelet activating factor (PAF) receptor on the host cell surface (67). Tong et al. demonstrated a critical role for ChoP in a chinchilla model of infection: *H. influenzae* infection with the ChoP positive phenotype promoted enhanced nasopharyngeal colonization and development of OM.

H. influenzae, like *M. catarrhalis*, is found in reticular crypt epithelial cells of adenoids removed from children with chronic OM or adenoidal hypertrophy (68,69). Experiments with human bronchial epithelial cells revealed that *H. influenzae* invasion begins with extension of host cell microvilli and the formation of lamellipodia (70).

Immune evasion. Some of the *H. influenzae* isolates are covered with an immune evasive polysaccharide capsule, with six antigenic serotypes, designated a to f, being identified (43). In contrast to *S. pneumoniae*, most *H. influenzae* pathogens cultured from the upper respiratory tract are unencapsulated (64,71).

Non-typeable *H. influenzae* is generally considered to be a serum-sensitive pathogen, but it has also developed strategies to inhibit complement mediated lysis (53). For example, various LOS components, e.g. *lytC*, *lex2B* and *losA*, have been found to affect serum resistance (72-75).

M. catarrhalis

Adhesion. Several macromolecules contribute to *M. catarrhalis* adhesion, i.e. UspA, MID/Hag, McaP, OMP CD and surface exposed structures such as type IV pili and LOS structures (for review, see (76)).

Invasion. A macropinocytosis-like mechanism of cellular invasion in different epithelial cell types, as described for *H. influenzae*, was also observed for *M. catarrhalis* (77,78). Once intracellular, the bacteria were found to reside in vacuolar structures. Furthermore, UV-killed bacteria were used to demonstrate that *M. catarrhalis* actively invade the epithelial cells, as no structural changes in the epithelial membrane were observed with UV-killed bacteria and no bacterial structures were found inside cells (77,78).

Immune evasion. Resistance to complement-mediated killing is an important aspect of the *M. catarrhalis* pathogenicity, with almost all isolates recovered from OM or COPD patients being resistant to the bactericidal effect of normal human serum (79). UspA2, OMP CD, OMP E, CopB and LOS are examples of important factors responsible for complement evasion by *M. catarrhalis* (76).

Biofilm formation and polymicrobial infection

Biofilms are organizationally structured and specialized communities of adherent microorganisms embedded in a complex extracellular substance, which provides a protective life style (80). The capacity of *S. pneumoniae*, *H. influenzae* and/or *M. catarrhalis* to form biofilms has been implicated by *in vitro* assays *(*81-84), and has been found to be present *in vivo* on the middle ear mucosa of children with OM (85). Biofilms may contribute to the persistence of pathogens and the resistance of OM to antibiotic treatment (85,86). Although the occurrence of the OM pathogens in biofilms is generally accepted, there is still debate about the definition of a biofilm, and consequently, whether all OM pathogens fulfill all criteria to be called 'biofilm producer' (87). However, detailed elucidation of the relevance of biofilms in the pathogenesis of OM is considered to be very important in the

development of new approaches to treat and prevent OM (88).

Bacterial-viral co-infection

The synergistic effect of viral upper respiratory tract infections on bacterial super-infection is well recognized (89). Rhinovirus, adenovirus, enterovirus, influenza and parainfluenzavirus, as well as respiratory syncytial virus, human coronavirus, human metapneumovirus and human bocavirus are pathogens, which are considered to play a causal role in upper respiratory tract infections and OM and are known to facilitate bacterial super-infections (16). Viruses are considered to cause Eustachian tube dysfunction, to increase adherence of bacteria to epithelial cells resulting in a rise in bacterial colonization of the nasopharynx, and to modulate the host's immune function (52). Detection of viral pathogens is primarily performed in clinical studies rather than applied for diagnostic purposes, since viral detection does not affect treatment policy at present. As a result of detection difficulties using viral culture, the presence of viruses have been underestimated in the past. With the introduction of the (multiplex) polymerase chain reaction (PCR) amplification technology, the detection of viruses improved significantly. Importantly, one should realize that viral components may be vanished before OM becomes manifest due to bacterial super-infection, and consequently, their involvement in OM might be underestimated.

Immunology

The innate immune system offers the first line of defence to microbial pathogens. Epithelial surfaces, mucins and digestive enzymes, i.e. lysozyme, lactoferrin, β-defensins, collectins and surfact proteins A and D, form the first barrier against microorganisms (90). In addition, when microbes do penetrate the body, innate defence systems capable of distinguishing self from non-self structures are required. A set of pattern recognition receptors (PRRs) expressed by a wide variety of human cells recognize pathogen associated molecular patterns (PAMPs), in a pathogen-specific manner. The PRRs are expressed on a wide variety of cells of the innate immune system, including polymorphonuclear phagocytes, monocytes/macrophages, dendritic cells, natural killer cells and to some extent epithelial or endothelial cells. Also part of innate immunity is the complement system, comprising over 30 serum and membrane proteins which, when activated, form a cascade of reactions contributing to the elimination of invading microorganisms (63). Activation of the complement system (i.e. the classical, alternative and mannose-binding lectin pathways) will establish opsonization of the pathogens, chemotaxis and activation of leukocytes, and direct killing of pathogens. Recognition of the pathogens by immune cells within the respira-

tory tract generates an array of pro-inflammatory and anti-inflammatory cytokines (91). For example, the cytokines TNF-a, IL-1β, IL-6, IL-8 and IL-10 play a pivotal role mediating the inflammatory response during the process of immune activation in the middle ear. In addition, CD14, initially characterized as the LPS receptor, is involved in responses to components of both gram positive and negative bacteria as well as mycobacteria, fungi and possibly viruses. CD14 is suggested to play a central role in the innate immune defence against many upper respiratory tract pathogens (52).

Adaptive immunity mainly depends on antibody mediated phagocytosis through complement- and Fc-receptors expressed on neutrophils and monocytes/macrophages. In children with recurrent OM both increased as normal serum levels of IgA, IgM, IgG and IgG1 are detected, for IgG2 both normal and decreased levels have been found (52,92). More recently, it has been described that otitis-prone children have suboptimal circulating functional T-helper memory and reduced IgG responses to *S. pneumoniae* or *H. influenzae* upon colonization and AOM. This immune dysfunction is considered to cause susceptibility to recurrent AOM infections (93).

Animal models

In order to study in molecular detail the microbial pathogenesis and host response during OM at an experimental level, animal models are warranted. Multiple animal models have been developed to study various aspects of the OM disease process, to increase our understanding of OM pathogenesis, and to design and improve preventive and treatment strategies (94). Models using mice (94-97), rats (98-101), gerbils, guinea pigs, chinchillas (102-104), and monkeys (105) have been applied over the past decades. Each animal model has its specific advantages. For example, chinchillas have relatively large middle ear cavities, are often used in case large amounts of middle ear fluid are necessary (106). For genetic studies, well characterized rats and mice are primarily used (106). Due to the increasing availability of knockouts and transgenics, mice are increasingly becoming the model of choice (97). Importantly, a plethora of data indicate that human disease is very accurately modeled in the mouse. Consequently, insight gained in murine studies can be translated to humans in many cases. One of the limitations of the experimental models currently used to study the bacterial pathogenesis of OM is the artificial 'invasiveness' of the procedures, i.e. direct inoculation of pathogens into the middle ear cavity, and hence, bypassing the natural route of infection.

Study aim and outline of the thesis

In order to study the role of bacterial and viral pathogens and the host response during rAOM and OME, a prospective clinical cohort study was performed. In addition, a mouse model was developed, which allowed us to study the OM pathogenesis in molecular detail. The aim of this project was to increase the understanding of the underlying mechanisms of OM disease, and consequently, to support future management strategies.

To gain novel insight in the epidemiology of OM, in particular rAOM and OME, we performed a prospective clinical cohort study, and investigated whether the microbial profiles of middle ear fluid obtained from these children could be used to differentiate between rAOM and OME (**Chapter 2**). We also studied the effect of bacteria and viruses present in middle ear fluid in both rAOM and OME patients on the local inflammatory cytokine response (**Chapter 3**). Subsequently, we determined the protein specific humoral immune responses in serum and MEF of these patients in order to investigate the immunogenicity of putative vaccine candidates of *M. catarrhalis* and *S. pneumoniae* (**Chapter 4**). In **Chapter 5** non-typeable *H. influenzae* isolates obtained from the middle ear and the nasopharynx of our clinical study population were investigated in further immunological detail, in particular at the level of complement resistance. We investigated whether increased serum resistance of NTHi was related to the development of OM, and importantly, which molecular microbiological mechanisms contributed to serum resistance.

In order to study pneumococcal pathogenesis in an experimental setting, we developed a novel, non-invasive murine OM model (**Chapter 6**). Subsequently, the contribution of the *S. pneumoniae* proteins Streptococcal lipoprotein rotamase A (SlrA) and the Putative protease maturation protein A (PpmA) to OM pathogenesis was investigated. These two proteins were previously shown to play a pivotal role in i.e. colonization and adherence. The contribution of the *S. pneumoniae* DHH family proteins in experimental pneumococcal disease and their immune protective potential was investigated in **Chapter 7**. In **Chapter 8**, the involvement of the Pneumococcal serine rich repeat protein (PsrP) in biofilm formation was studied extensively. Finally, **Chapter 9** discusses the major findings in a summarizing fashion.

References

1. Plasschaert AI, Rovers MM, Schilder AG, Verheij TJ, Hak E. Trends in doctor consultations, antibiotic prescription, and specialist referrals for otitis media in children: 1995-2003. Pediatrics 2006; 117(6): 1879-86.
2. Gonzales R, Malone DC, Maselli JH, Sande MA. Excessive antibiotic use for acute respiratory infections in the United States. Clin Infect Dis 2001; 33(6): 757-62.
3. Freid VM, Makuc DM, Rooks RN. Ambulatory health care visits by children: principal diagnosis and place of visit. Vital Health Stat 13 1998; (137): 1-23.
4. Rovers MM, Schilder AG, Zielhuis GA, Rosenfeld RM. Otitis media. Lancet 2004; 363(9407): 465-73.
5. Uijen JH, Bindels PJ, Schellevis FG, van der Wouden JC. ENT problems in Dutch children: trends in incidence rates, antibiotic prescribing and referrals 2002-2008. Scand J Prim Health Care 2011; 29(2): 75-9.
6. Coco AS. Cost-effectiveness analysis of treatment options for acute otitis media. Ann Fam Med 2007; 5(1): 29-38.
7. Klein JO. The burden of otitis media. *Vaccine* 2000; 19 Suppl 1:S2-8.: S2-S8.
8. Cripps AW, Otczyk DC, Kyd JM. Bacterial otitis media: a vaccine preventable disease? Vaccine 2005; 23(17-18): 2304-10.
9. Marchisio P, Claut L, Rognoni A, et al. Differences in nasopharyngeal bacterial flora in children with nonsevere recurrent acute otitis media and chronic otitis media with effusion: implications for management. Pediatr Infect Dis J 2003; 22(3): 262-8.
10. Gates GA, Klein JO, Lim DJ, et al. Recent advances in otitis media. 1. Definitions, terminology, and classification of otitis media. Ann Otol Rhinol Laryngol Suppl 2002; 188:8-18.: 8-18.
11. Faden H, Duffy L, Boeve M. Otitis media: back to basics. Pediatr Infect Dis J 1998; 17(12): 1105-12.
12. Damoiseaux RA, Van Balen FA, Leenheer WAM, Kolnaar BGM. [Performance of family practitioners according to the guideline otitis media acuta of the Dutch College of Family Practitioners]. Ned Tijdschr Geneeskd 2006; 137(42): 2139-44.
13. Emonts M, Wiertsema SP, Veenhoven RH, et al. The 4G/4G plasminogen activator inhibitor-1 genotype is associated with frequent recurrence of acute otitis media. Pediatrics 2007; 120(2): e317-e23.
14. Emonts M, Veenhoven R, JJ H-D, et al. Genetic polymorphisms in immune response genes TNFA, IL6, IL10 and TLR4 are associated with recurrent acute otitis media.; 2006.
15. Recent advances in otitis media. Report of the Eighth Research Conference. June 3-7, 2003. Fort Lauderdale, Florida, USA. Ann Otol Rhinol Laryngol Suppl 2005; 194:6-160.: 6-160.
16. Heikkinen T, Chonmaitree T. Importance of respiratory viruses in acute otitis media. Clin Microbiol Rev 2003; 16(2): 230-41.
17. Damoiseaux RA, Rovers MM, Van Balen FA, Hoes AW, de Melker RA. Long-term prognosis of acute otitis media in infancy: determinants of recurrent acute otitis media and

persistent middle ear effusion. Fam Pract 2006; 23(1): 40-5.
18. Gravel JS, Karma P, Casselbrant ML, et al. Recent advances in otitis media. 7. Diagnosis and screening. Ann Otol Rhinol Laryngol Suppl 2005; 194:104-13.: 104-13.
19. Jung TT, Hunter LL, Alper CM, et al. Recent advances in otitis media. 9. Complications and sequelae. Ann Otol Rhinol Laryngol Suppl 2005; 194:140-60.: 140-60.
20. Cummings CW, Flint PW, Haughey BH, et al. Otolaryngology head and neck surgery. Philedelphia, USA: Mosby Elsevier; 2010.
21. Kontiokari T, Koivunen P, Niemela M, Pokka T, Uhari M. Symptoms of acute otitis media. Pediatr Infect Dis J 1998; 17(8): 676-9.
22. Diagnosis and management of acute otitis media. *Pediatrics* 2004; 113(5): 1451-65.
23. Akkerman AE, Kuyvenhoven MM, van der Wouden JC, Verheij TJ. Determinants of antibiotic overprescribing in respiratory tract infections in general practice. The Journal of antimicrobial chemotherapy 2005; 56(5): 930-6.
24. Vernacchio L, Vezina RM, Mitchell AA. Management of acute otitis media by primary care physicians: trends since the release of the 2004 American Academy of Pediatrics/American Academy of Family Physicians clinical practice guideline. Pediatrics 2007; 120(2): 281-7.
25. American Academy of Family P, American Academy of O-H, Neck S, American Academy of Pediatrics Subcommittee on Otitis Media With E. Otitis media with effusion. Pediatrics 2004; 113(5): 1412-29.
26. Kalu SU, Hall MC. A study of clinician adherence to treatment guidelines for otitis media with effusion. WMJ : official publication of the State Medical Society of Wisconsin 2010; 109(1): 15-20.
27. Pellman H. Thoughts on the American Academy of Pediatrics/American Academy of Family Physicians clinical practice guideline on acute otitis media: a different perspective. Pediatrics 2005; 115(5): 1443-4; author reply 4-5.
28. van den Aardweg MT, Schilder AG, Herkert E, Boonacker CW, Rovers MM. Adenoidectomy for otitis media in children. Cochrane Database Syst Rev 2010; %20;(1): CD007810.
29. Browning GG, Rovers MM, Williamson I, Lous J, Burton MJ. Grommets (ventilation tubes) for hearing loss associated with otitis media with effusion in children. Cochrane Database Syst Rev 2010; (10): CD001801.
30. Van Den Akker EH, Hoes AW, Burton MJ, Schilder AG. Large international differences in (adeno)tonsillectomy rates. Clin Otolaryngol Allied Sci 2004; 29(2): 161-4.
31. Wiertsema SP, Kirkham LA, Corscadden KJ, et al. Predominance of nontypeable Haemophilus influenzae in children with otitis media following introduction of a 3+0 pneumococcal conjugate vaccine schedule. Vaccine 2011; 29(32): 5163-70.
32. Eskola J, Kilpi T, Palmu A, et al. Efficacy of a pneumococcal conjugate vaccine against acute otitis media. N Engl J Med 2001; 344(6): 403-9.
33. Fireman B, Black SB, Shinefield HR, Lee J, Lewis E, Ray P. Impact of the pneumococcal conjugate vaccine on otitis media. Pediatr Infect Dis J 2003; 22(1): 10-6.
34. Straetemans M, Sanders EA, Veenhoven RH, Schilder AG, Damoiseaux RA, Zielhuis GA. Pneumococcal vaccines for preventing otitis media. Cochrane Database Syst Rev 2002; (2): CD001480.
35. Palmu AA, Verho J, Jokinen J, Karma P, Kilpi TM. The seven-valent pneumococcal conjugate vaccine reduces tympanostomy tube placement in children. Pediatr Infect Dis J

2004; 23(8): 732-8.
36. Veenhoven R, Bogaert D, Uiterwaal C, et al. Effect of conjugate pneumococcal vaccine followed by polysaccharide pneumococcal vaccine on recurrent acute otitis media: a randomised study. Lancet 2003; 361(9376): 2189-95.
37. Rozenbaum MH, Sanders EA, van Hoek AJ, et al. Cost effectiveness of pneumococcal vaccination among Dutch infants: economic analysis of the seven valent pneumococcal conjugated vaccine and forecast for the 10 valent and 13 valent vaccines. BMJ 2010; 340:c2509. doi: 10.1136/bmj.c2509.: c2509.
38. http://www.rivm.nl/Bibliotheek/Algemeen_Actueel/Nieuwsberichten/2011/Nieuw_pneumokokkenvaccin_voor_baby_s. RIVM website, 9/29/2011, 2011. (accessed.
39. Jefferies JM, Macdonald E, Faust SN, Clarke SC. 13-valent pneumococcal conjugate vaccine (PCV13). Hum Vaccin 2011; 7(10).).
40. Prymula R, Peeters P, Chrobok V, et al. Pneumococcal capsular polysaccharides conjugated to protein D for prevention of acute otitis media caused by both Streptococcus pneumoniae and non-typable *Haemophilus influenzae*: a randomised double-blind efficacy study. Lancet 2006; 367(9512): 740-8.
41. Briles DE, Tart RC, Swiatlo E, et al. Pneumococcal diversity: considerations for new vaccine strategies with emphasis on pneumococcal surface protein A (PspA). Clin Microbiol Rev 1998; 11(4): 645-57.
42. Pichichero ME. Short course antibiotic therapy for respiratory infections: a review of the evidence. Pediatr Infect Dis J 2000; 19(9): 929-37.
43. St GJ, III. The pathogenesis of nontypable *Haemophilus influenzae* otitis media. Vaccine 2000; 19 Suppl 1:S41-50.: S41-S50.
44. Labout JA, Duijts L, Arends LR, et al. Factors associated with pneumococcal carriage in healthy Dutch infants: the generation R study. J Pediatr 2008; 153(6): 771-6.
45. Barenkamp SJ, Kurono Y, Ogra PL, et al. Recent advances in otitis media. 5. Microbiology and immunology. Ann Otol Rhinol Laryngol Suppl 2005; 194:60-85.: 60-85.
46. Faden H, Duffy L, Wasielewski R, Wolf J, Krystofik D, Tung Y. Relationship between nasopharyngeal colonization and the development of otitis media in children. Tonawanda/Williamsville Pediatrics. J Infect Dis 1997; 175(6): 1440-5.
47. Labout JA, Duijts L, Lebon A, et al. Risk factors for otitis media in children with special emphasis on the role of colonization with bacterial airway pathogens: the Generation R study. Eur J Epidemiol 2011; 26(1): 61-6.
48. Bogaert D, Engelen MN, Timmers-Reker AJ, et al. Pneumococcal carriage in children in The Netherlands: a molecular epidemiological study. J Clin Microbiol 2001; 39(9): 3316-20.
49. Faden H, Waz MJ, Bernstein JM, Brodsky L, Stanievich J, Ogra PL. Nasopharyngeal flora in the first three years of life in normal and otitis-prone children. Ann Otol Rhinol Laryngol 1991; 100(8): 612-5.
50. Faden H, Stanievich J, Brodsky L, Bernstein J, Ogra PL. Changes in nasopharyngeal flora during otitis media of childhood. Pediatr Infect Dis J 1990; 9(9): 623-6.
51. Donlan RM, Costerton JW. Biofilms: survival mechanisms of clinically relevant microorganisms. Clin Microbiol Rev 2002; 15(2): 167-93.
52. Wiertsema SP, Veenhoven RH, Sanders EA, Rijkers GT. Immunologic screening of children with recurrent otitis media. Curr Allergy Asthma Rep 2005; 5(4): 302-7.
53. Hallstrom T, Nordstrom T, Tan TT, et al. Immune evasion of *Moraxella catarrhalis* involves

ubiquitous surface protein A-dependent C3d binding. J Immunol 2011; 186(5): 3120-9.
54. McAllister LJ, Tseng HJ, Ogunniyi AD, Jennings MP, McEwan AG, Paton JC. Molecular analysis of the psa permease complex of *Streptococcus pneumoniae*. Mol Microbiol 2004; 53(3): 889-901.
55. Tong HH, Blue LE, James MA, DeMaria TF. Evaluation of the virulence of a *Streptococcus pneumoniae* neuraminidase-deficient mutant in nasopharyngeal colonization and development of otitis media in the chinchilla model. Infect Immun 2000; 68(2): 921-4.
56. Pracht D, Elm C, Gerber J, et al. PavA of *Streptococcus pneumoniae* modulates adherence, invasion, and meningeal inflammation. Infect Immun 2005; 73(5): 2680-9.
57. Weiser JN, Bae D, Fasching C, Scamurra RW, Ratner AJ, Janoff EN. Antibody-enhanced pneumococcal adherence requires IgA1 protease. Proc Natl Acad Sci U S A 2003; 100(7): 4215-20.
58. Kerr AR, Adrian PV, Estevao S, et al. The Ami-AliA/AliB permease of *Streptococcus pneumoniae* is involved in nasopharyngeal colonization but not in invasive disease. Infect Immun 2004; 72(7): 3902-6.
59. Ogunniyi AD, Lemessurier KS, Graham RM, et al. Contributions of pneumolysin, pneumococcal surface protein A (PspA), and PspC to pathogenicity of *Streptococcus pneumoniae* D39 in a mouse model. Infect Immun 2007; 75(4): 1843-51.
60. Luke NR, Jurcisek JA, Bakaletz LO, Campagnari AA. Contribution of *Moraxella catarrhalis* Type-IV Pili to Nasopharyngeal Colonization and Biofilm Formation. Infect Immun 2007; .
61. Bakaletz LO, Baker BD, Jurcisek JA, et al. Demonstration of Type IV pilus expression and a twitching phenotype by *Haemophilus influenzae*. Infect Immun 2005; 73(3): 1635-43.
62. Cundell DR, Gerard NP, Gerard C, Idanpaan-Heikkila I, Tuomanen EI. *Streptococcus pneumoniae* anchor to activated human cells by the receptor for platelet-activating factor. Nature 1995; 377(6548): 435-8.
63. Hammerschmidt S, Wolff S, Hocke A, Rosseau S, Muller E, Rohde M. Illustration of pneumococcal polysaccharide capsule during adherence and invasion of epithelial cells. Infect Immun 2005; 73(8): 4653-67.
64. Nelson AL, Roche AM, Gould JM, Chim K, Ratner AJ, Weiser JN. Capsule enhances pneumococcal colonization by limiting mucus-mediated clearance. Infect Immun 2007; 75(1): 83-90.
65. Weiser JN, Austrian R, Sreenivasan PK, Masure HR. Phase variation in pneumococcal opacity: relationship between colonial morphology and nasopharyngeal colonization. Infect Immun 1994; 62(6): 2582-9.
66. Hyams C, Yuste J, Bax K, Camberlein E, Weiser JN, Brown JS. *Streptococcus pneumoniae* resistance to complement-mediated immunity is dependent on the capsular serotype. Infect Immun 2010; 78(2): 716-25.
67. St GJ, III. Molecular and cellular determinants of non-typeable *Haemophilus influenzae* adherence and invasion. Cell Microbiol 2002; 4(4): 191-200.
68. Heiniger N, Spaniol V, Troller R, Vischer M, Aebi C. A reservoir of *Moraxella catarrhalis* in human pharyngeal lymphoid tissue. J Infect Dis 2007; 196(7): 1080-7.
69. Forsgren J, Samuelson A, Ahlin A, Jonasson J, Rynnel-Dagoo B, Lindberg A. *Haemophilus influenzae* resides and multiplies intracellularly in human adenoid tissue as demonstrated by in situ hybridization and bacterial viability assay. Infect Immun 1994; 62(2): 673-9.
70. Ketterer MR, Shao JQ, Hornick DB, Buscher B, Bandi VK, Apicella MA. Infection of pri-

mary human bronchial epithelial cells by *Haemophilus influenzae*: macropinocytosis as a mechanism of airway epithelial cell entry. Infect Immun 1999; 67(8): 4161-70.
71. Pittman M. Variation and type specificity in the bacterial species *Haemophilus influenzae*. J Exp Med 1931; 53(4): 471-92.
72. Jenkins GA, Figueira M, Kumar GA, et al. Sialic acid mediated transcriptional modulation of a highly conserved sialometabolism gene cluster in *Haemophilus influenzae* and its effect on virulence. BMC Microbiol 2010; 10:48.: 48.
73. Severi E, Randle G, Kivlin P, et al. Sialic acid transport in *Haemophilus influenzae* is essential for lipopolysaccharide sialylation and serum resistance and is dependent on a novel tripartite ATP-independent periplasmic transporter. Mol Microbiol 2005; 58(4): 1173-85.
74. Griffin R, Cox AD, Makepeace K, Richards JC, Moxon ER, Hood DW. Elucidation of the monoclonal antibody 5G8-reactive, virulence-associated lipopolysaccharide epitope of *Haemophilus influenzae* and its role in bacterial resistance to complement-mediated killing. Infect Immun 2005; 73(4): 2213-21.
75. Ho DK, Ram S, Nelson KL, Bonthuis PJ, Smith AL. lgtC expression modulates resistance to C4b deposition on an invasive nontypeable *Haemophilus influenzae*. J Immunol 2007; 178(2): 1002-12.
76. de Vries SP, Bootsma HJ, Hays JP, Hermans PW. Molecular aspects of *Moraxella catarrhalis* pathogenesis. Microbiol Mol Biol Rev 2009; 73(3): 389-406, Table.
77. Slevogt H, Schmeck B, Jonatat C, et al. *Moraxella catarrhalis* induces inflammatory response of bronchial epithelial cells via MAPK and NF-kappaB activation and histone deacetylase activity reduction. Am J Physiol Lung Cell Mol Physiol 2006; 290(5): L818-L26.
78. Slevogt H, Seybold J, Tiwari KN, et al. Moraxella catarrhalis is internalized in respiratory epithelial cells by a trigger-like mechanism and initiates a. Cell Microbiol 2007; 9(3): 694-707.
79. Verhaegh SJ, Streefland A, Dewnarain JK, Farrell DJ, van BA, Hays JP. Age-related genotypic and phenotypic differences in *Moraxella catarrhalis* isolates from children and adults presenting with respiratory disease in 2001-2002. Microbiology 2008; 154(Pt 4): 1178-84.
80. Hall-Stoodley L, Costerton JW, Stoodley P. Bacterial biofilms: from the natural environment to infectious diseases. Nat Rev Microbiol 2004; 2(2): 95-108.
81. Budhani RK, Struthers JK. Interaction of *Streptococcus pneumoniae* and *Moraxella catarrhalis*: investigation of the indirect pathogenic role of beta-lactamase-producing moraxellae by use of a continuous-culture biofilm system. Antimicrob Agents Chemother 1998; 42(10): 2521-6.
82. Murphy TF, Kirkham C. Biofilm formation by nontypeable *Haemophilus influenzae*: strain variability, outer membrane antigen expression and role of pili. BMC Microbiol 2002; 2:7.: 7.
83. Pearson MM, Lafontaine ER, Wagner NJ, St GJ, III, Hansen EJ. A hag mutant of *Moraxella catarrhalis* strain O35E is deficient in hemagglutination, autoagglutination, and immunoglobulin D-binding activities. Infect Immun 2002; 70(8): 4523-33.
84. Maestre JR, Mateo M, Mendez ML, et al. In vitro interference of beta-lactams with biofilm development by prevalent community respiratory tract isolates. Int J Antimicrob Agents 2010; 35(3): 274-7.
85. Hall-Stoodley L, Hu FZ, Gieseke A, et al. Direct detection of bacterial biofilms on the

middle-ear mucosa of children with chronic otitis media. *JAMA* 2006; 296(2): 202-11.
86. Nistico L, Kreft R, Gieseke A, et al. An Adenoid Reservoir for Pathogenic Biofilm Bacteria. J Clin Microbiol 2011.
87. Moxon ER, Sweetman WA, Deadman ME, Ferguson DJ, Hood DW. *Haemophilus influenzae* biofilms: hypothesis or fact? Trends Microbiol 2008; 16(3): 95-100.
88. Murphy TF, Faden H, Bakaletz LO, et al. Nontypeable *Haemophilus influenzae* as a pathogen in children. Pediatr Infect Dis J 2009; 28(1): 43-8.
89. Casselbrant ML, Mandel EM. Genetic susceptibility to otitis media. Curr Opin Allergy Clin Immunol 2005; 5(1): 1-4.
90. Lim DJ, Chun YM, Lee HY, et al. Cell biology of tubotympanum in relation to pathogenesis of otitis media - a review. Vaccine 2000; 19 Suppl 1:S17-25.: S17-S25.
91. van der PT, Opal SM. Pathogenesis, treatment, and prevention of pneumococcal pneumonia. Lancet 2009; 374(9700): 1543-56.
92. Veenhoven R, Rijkers G, Schilder A, et al. Immunoglobulins in otitis-prone children. Pediatr Res 2004; 55(1): 159-62.
93. Sharma SK, Casey JR, Pichichero ME. Reduced Memory CD4+ T-Cell Generation in the Circulation of Young Children May Contribute to the Otitis-Prone Condition. J Infect Dis 2011; 204(4): 645-53.
94. MacArthur CJ, Trune DR. Mouse models of otitis media. Curr Opin Otolaryngol Head Neck Surg 2006; 14(5): 341-6.
95. Krekorian TD, Keithley EM, Takahashi M, Fierer J, Harris JP. Endotoxin-induced otitis media with effusion in the mouse. Immunohistochemical analysis. Acta Otolaryngol 1990; 109(3-4): 288-99.
96. Ryan AF, Ebmeyer J, Furukawa M, et al. Mouse models of induced otitis media. Brain Res 2006; 1091(1): 3-8.
97. Sabirov A, Metzger DW. Mouse models for the study of mucosal vaccination against otitis media. Vaccine 2008; 26(12): 1501-24.
98. Melhus A, Ryan AF. A mouse model for acute otitis media. *APMIS* 2003; 111(10): 989-94.
99. van der Ven LT, van den Dobbelsteen GP, Nagarajah B, et al. A new rat model of otitis media caused by *Streptococcus pneumoniae*: conditions and application in immunization protocols. Infect Immun 1999; 67(11): 6098-103.
100. Fogle-Ansson M, White P, Hermansson A, Melhus A. Otomicroscopic findings and systemic interleukin-6 levels in relation to etiologic agent during experimental acute otitis media. APMIS 2006; 114(4): 285-91.
101. Tonnaer EL, Sanders EA, Curfs JH. Bacterial otitis media: a new non-invasive rat model. Vaccine 2003; 21(31): 4539-44.
102. Giebink GS, Berzins IK, Marker SC, Schiffman G. Experimental otitis media after nasal inoculation of *Streptococcus pneumoniae* and influenza A virus in chinchillas. Infect Immun 1980; 30(2): 445-50.
103. Ehrlich GD, Veeh R, Wang X, et al. Mucosal biofilm formation on middle-ear mucosa in the chinchilla model of otitis media. JAMA 2002; 287(13): 1710-5.
104. Fulghum RS, Marrow HG. Experimental otitis media with *Moraxella* (*Branhamella*) *catarrhalis*. Ann Otol Rhinol Laryngol 1996; 105(3): 234-41.
105. Alper CM, Swarts JD, Doyle WJ. Prevention of otitis media with effusion by repeated air inflation in a monkey model. Arch Otolaryngol Head Neck Surg 2000; 126(5): 609-14.

106. Lim DJ, Hermansson A, Hellstrom SO, et al. Recent advances in otitis media. 3. Animal models; anatomy and pathology; pathogenesis; cell biology and genetics. Ann Otol Rhinol Laryngol Suppl 2005; 194:31-41.: 31-41.

Microbial profiling does not differentiate between childhood recurrent acute otitis media and chronic otitis media with effusion

K. Stol [‡], S.J.C. Verhaegh [‡], K. Graamans, J.A.M. Engel, P.D.J. Sturm, W.J.G. Melchers, J.F. Meis, A. Warris, J.P. Hays and P.W.M. Hermans.

[‡] These authors contributed equally to this study

International Journal of Pediatric Otorhinolaryngology 2013, 77(4):488-93

Abstract

Objectives

Otitis media (OM) is one of the most frequent diseases of childhood, with a minority of children suffering from recurrent acute otitis media (rAOM) or chronic otitis media with effusion (COME), both of which are associated with significant morbidity. We investigated whether the microbiological profiling could be used to differentiate between these two conditions.

Methods

Children up to five years of age, with rAOM ($n=45$) or COME ($n=129$) and scheduled for tympanostomy tube insertion were enrolled in a prospective study between 2008 and 2009. Middle ear fluids ($n=119$) and nasopharyngeal samples ($n=173$) were collected during surgery for bacterial culture and PCR analysis to identify *Streptococcus pneumoniae*, *Haemophilus influenzae* and *Moraxella catarrhalis*, and to detect 15 distinct respiratory viruses.

Results

The occurrence of bacterial and viral pathogens in middle ear fluids did not significantly differ between patients suffering from rAOM and COME. In both patient cohorts, *H. influenzae* and rhinovirus were the predominant pathogens in the middle ear and nasopharynx. Nasopharyngeal carriage with two or three bacterial pathogens was associated with the presence of bacteria in middle ear fluid ($P=0.04$). The great majority of the bacteria isolated from middle ear fluid were genetically identical to nasopharyngeal isolates from the same patient.

Conclusions

Based on these results, we propose that the common perception that rAOM is associated with recurrent episodes of microbiologically-mediated AOM, whereas COME is generally a sterile inflammation, should be reconsidered.

Introduction

Otitis media (OM) is one of the most frequent diseases during childhood and the most common reason for young children to visit a physician. In many countries, it is the most common reason for children to receive antibiotics or to undergo surgery (1-3).

OM is a common denominator for a variety of middle ear diseases that can be divided into various categories, including acute otitis media (AOM) and otitis media with effusion (OME) (4). AOM is defined as the presence of middle ear effusion accompanied by signs of acute inflammation of the middle ear, such as otalgia, otorrhea, fever, and malaise or irritability of the child (3,5). OME, on the other hand, can either develop as a sequel to AOM, or develop *de novo*, the primary symptom being hearing loss due to the presence of middle ear fluid in the middle ear cavity (but in the absence of signs of acute inflammation) (6). Albeit often self-limiting, in 10-20% of the cases OM can result in chronic OME (COME) or recurrent AOM (rAOM) disease (7).

Although there is currently no universal standard for OM management, several options are available to the clinician, namely: watchful waiting, antibiotic treatment, adenoidectomy, ventilation tube insertion, or vaccination. AOM management generally involves adequate analgesics with an optional observation period for 48-72 hours (5). Thereafter, antibiotic treatment or, in the case of recurrent infections, antibiotic prophylaxis or ventilation tube insertion are considered (5,8,9). In contrast, for OME disease, medical intervention is appropriate only if persistent clinical benefits can be achieved in the absence of spontaneous resolution. Therefore, healthy children with OME are observed for at least 3 months before medical intervention is considered, in which case surgical treatment involving the insertion of ventilation tubes or adenoidectomy is feasible (3,10). Vaccination against OM diseases is currently very limited, being directed against very few bacterial OM pathogens, and only one of the viral OM pathogens, i.e. the influenza vaccine. The heptavalent pneumococcal conjugate vaccine is primarily directed against pneumococcal invasive disease, whereas the introduction of vaccination only reduced the overall OM incidence by 6-9% due to serotype or pathogen replacement (11). However, herd immunity may induce a further decline in OM incidence, in line with nasopharyngeal colonization studies 3 years after the introduction of the vaccine (12,13).

A key element in the pathogenesis of OM is the nasopharynx, as this niche is the reservoir for bacterial pathogens involved in middle ear infections (4). Colonization of the nasopharynx with *Streptococcus pneumoniae*, *Haemophilus influenzae* or *Moraxella catarrh-*

alis (the three most important bacterial pathogens associated with OM disease) at an early stage, has been shown to predispose children for development of rAOM (14). In addition, OM-prone children have increased carriage rates of these bacterial pathogens compared to healthy controls (15,16). In AOM, *S. pneumoniae* is the most frequently detected pathogen in middle ear fluid, followed by non-typeable *H. influenzae* and *M. catarrhalis* (17-19). However, *H. influenzae* tends to predominate in COME, followed in a lesser extent by *S. pneumoniae* and *M. catarrhalis* (20). In general, bacteria have been found less frequently in the middle ear of children suffering from COME compared to AOM (approximately 30% versus 70%, respectively) (17).

In addition, many studies over the past decades have shown a close association between AOM and respiratory viral infections (21-24). Viral upper respiratory tract infections (URI) predispose children to AOM, as infection may cause Eustachian tube dysfunction, and facilitate an increase in adherence of bacteria to epithelial cells, resulting in a rise in bacterial colonization of the nasopharynx and a modulation of the host's immune function (25-27). Nevertheless, studies describing specific associations between respiratory viruses and bacteria in rAOM and COME are scarce.

In this study, we investigated bacterial and viral colonization and infection in the middle ear and nasopharynx of children diagnosed with rAOM or COME. In particular, the contribution of 3 major bacterial pathogens (*S. pneumoniae*, *H. influenzae* and *M. catarrhalis*) in the absence or presence of 15 distinct respiratory viruses was studied in relation to rAOM and COME disease.

Materials & Methods

Study design

A cohort of children up to five years of age who suffered from rAOM or COME was examined in this prospective clinical study. The cohort was enrolled at a secondary and a tertiary care hospital in Nijmegen, the Netherlands, from April 1st 2008 to July 1st 2009, and included children suffering from rAOM or COME who underwent surgery for the insertion of ventilation tubes. Recurrent AOM was defined as 3 or more episodes of AOM in the last 6 months or 4 episodes in the last 12 months (28). The COME patient population consisted of children who had experienced a period of persistent OM with effusion lasting longer than 3 months. RAOM or COME diagnosis was made by an otolaryngologist in routine clinical practice based upon signs, symptoms, otoscopy and audiometry including tympanometry. Patients with a history of malignancy, organ transplantation or immune deficiency were excluded from participation, as well as patients with recent elective ear surgery or systemic infectious diseases. Children with AOM and/or fever ($T \geq 38°C$) at the time of ventilation tube insertion were rescheduled for the procedure. Adenoidectomy performed in the same surgical setting was not considered to be an exclusion criterion. Patient characteristics and risk factors were acquired using a questionnaire, collected at the day of ventilation tube insertion. Ethical permission was obtained from the Committee on Research Involving Human Subjects in January 2008 (CMO 2007/239, international trial register number: NCT00847756).

Clinical samples

Per child, one middle ear fluid sample and one nasopharyngeal sample was collected. Middle ear fluid was collected during surgery using a middle ear fluid aspiration system (Kuijpers Instruments, Groesbeek, The Netherlands) (29), nasopharyngeal samples, taken through the nose, were obtained using a cotton wool swab (192C, Copan, Brescia, Italy). Middle ear fluid was suspended in 2 ml saline and divided into aliquots for bacterial culture, bacterial PCR, and viral multiplex PCR. The nasopharyngeal samples were used for bacterial culture and thereafter stored at -80°C in 1 ml of 80% glycerol for subsequent viral analysis.

Microbiology

Middle ear fluid and nasopharyngeal samples were cultured directly after collection according to standard laboratory procedures (14) to determine the presence of *S. pneumoniae, H. influenzae* and *M. catarrhalis*. Thereafter, bacteria were stored at -80°C in appropriate media containing an additional 15% (*S. pneumoniae*, *H. influenzae*) or 50% glycerol (*M. catarrhalis*). The less frequently described otopathogens *Staphylococcus aureus*, *Streptococcus pyogenes*, *Haemophilus parainfluenzae*, *Pseudomonas aeruginosa* and *Alloicoccus otitidis* were also included in the analysis if detected during bacterial culture.

To further characterize the bacterial isolates, all *S. pneumoniae* and *H. influenzae* isolates were cultured overnight on, respectively, blood agar and chocolate agar plates at 37°C supplemented with 5% CO_2. Pneumococcal isolates were serotyped using the Quellung reaction (Statens Serum Institute, Copenhagen, Denmark) and multiplex PCR as described previously (30). *H. influenzae* isolates were serotyped using slide agglutination according to the manufacturer's instructions (Becton Dickinson, Breda, The Netherlands) (31).

S. pneumoniae, *H. influenzae* or *M. catarrhalis* obtained from middle ear fluid, as well as the equivalent pathogen isolated from the nasopharynx of the same patient, were further analyzed using multilocus sequence typing (MLST). Genomic DNA was isolated using a Qiagen Genomic-tip 20/G Kit (Venlo, The Netherlands) according to the manufacturer's instructions. DNA amplification of the MLST loci and sequencing was performed as described previously (32-35). Quantitative DNA analysis of *S. pneumoniae*, *H. influenzae* and *M. catarrhalis* by real-time PCR was performed as previously described. The respective genes chosen for bacterial quantification were the *S. pneumoniae ply* gene (36), *H. influenzae* 16S rRNA gene (37) and the *M. catarrhalis ompJ* gene (38).

Virology

Middle ear fluid and nasopharyngeal samples were analyzed by multiplex PCR as previously described (39). Briefly, upon thawing, nucleic acids were extracted from each sample using the MagNA Pure LC System and the MagNA Pure LC Total Nucleic Acid Isolation Kit (Roche Applied Science, Almere, The Netherlands) according to manufacturer's instructions. A multiplex real-time PCR assay targeting 15 different viral pathogens was used. This assay was designed for the detection of the specific viral genomes of influenza virus (IV) type A and B, coronavirus (CoV) 229E and OC43, human bocavirus (hBoV), enterovirus (EV), adenovirus (AdV), parechovirus (PeV), parainfluenza virus (PIV) types 1-4, human metapneumovirus (hMPV), rhinovirus (RV) and respiratory syncytial virus (RSV). An internal control consisting of phocine herpesvirus (PhPV, IC DNA control) and equine arthritis virus (EAV, IC RNA control) was included in the assay. RNA was reverse transcribed to cDNA

using the TaqMan Reverse Transcription Reagents kit (Applied Biosystems, Nieuwekerk aan de IJssel, The Netherlands) in a 50 μl reaction mix containing 20 μl of nucleic acid isolate and random hexamers as primers (2.5μM), according to the manufacturer's instructions. PCRs were performed on the LightCycler 480 instrument using LightCycler 480 Probes Master Mix (Roche Diagnostics). Validated primer/probe-mixes were purchased from Diagenode (Liège, Belgium) and used according to the manufacturer's instructions. Cycling conditions were 95°C for 5 minutes, followed by 50 cycles of 95°C for 15 seconds and 55°C for 15 seconds and 72C for 20 seconds.

Statistical analysis

Statistical analyses were performed using the Statistical Package of Social Sciences version 17.0 (SPSS Inc., Chicago, IL, USA). The chi-square test or Mann-Whitney *U*-test was used when appropriate to calculate the statistical differences between patient baseline characteristics. The chi-square test was used in the analysis of categorical data obtained from bacterial culture, bacterial PCR and viral PCR. A *P*-value < 0.05 was considered statistically significant.

Table 1. Characteristics of the pediatric study population.

	rAOM *n*=25 (%)	COME *n*=94 (%)	*P*-value
Male sex	17/25 (69)	52/94 (55)	0.09
Mean age, years [SD]	3.3 [1.69]	4.02 [1.43]	0.10
< 2 years of age	7 (28)	13 (14)	0.09
Presence of middle ear fluid (MEF) [1]	25/25 (100)	94/94 (100)	-
≥ 4 URTI in the preceding year [2]	8/22 (36)	21/86 (24)	0.26
Recent antibiotic use	**9/25 (36)**	**9/94 (10)**	**< 0.01**
History of ENT surgery	8/18 (44)	37/67 (55)	0.42
Asthma/wheezing	2/23 (87)	7/87 (8)	0.92
Allergic rhinitis	2/22 (9)	4/86 (5)	0.42
Eczema	3/23 (13)	11/86 (13)	0.97
Birth weight, mean, (g, [SD])	3291 [624]	3308 [791]	0.82
Breast feeding < 3 months	15/23 (65)	51/87 (59)	0.57
PCV7 immunization [3]	**11/25 (44)**	**20/94 (21)**	**0.02**
Tobacco smoke exposure	8/21 (38)	26/84 (31)	0.53
Older siblings	11/18 (61)	47/74 (64)	0.85
Day care attendance	10/22 (46)	40/84 (48)	0.86

Significant differences are marked in **bold**.

[1]The MEF of 4 patients could not be collected for bacterial culture.

[2]Upper respiratory tract infections.

[3]The **PCV7** vaccine was introduced in Dutch National Immunization Program for children born after 01-04-2006.

Results

rAOM and COME cannot be differentiated based on bacterial infection

A total of 176 children were enrolled in the study. Selected demographic and clinical characteristics of the cohort are shown in Table 1. Recurrent AOM was mostly diagnosed at a younger age, while the prevalence of COME increased with age (rAOM 75% during the first year of life vs. 17% at 5 years of age; COME 25% during the first year of life vs. 83% at 5 years of age). A middle ear fluid specimen was collected from 69% of the children ($n=119$), with a significant difference in the presence of middle ear fluid and OM diagnosis (rAOM $n=26$ (58%) vs. COME $n=97$ (75%), $P=0.02$). Children suffering from rAOM presented with less ENT-related surgery in their medical history when compared to children suffering from COME, but received significantly more antibiotics in the year prior to surgery.

Microbial profiling does not differentiate between rAOM and COME

The frequency of *S. pneumoniae*, *H. influenzae* and *M. catarrhalis* in middle ear fluid and the nasopharynx is shown in Table 2. In total, 117 samples were screened for bacterial presence by both, bacterial culture and PCR. Not surprisingly, PCR detected bacterial DNA in a statistically significant percentage of culture-negative middle ear effusions: *S. pneumoniae* in 4.1% (NS), *H. influenzae* in 16.5% ($P<0.01$) and *M. catarrhalis* in 19% ($P<0.01$).

Importantly, the presence of each specific pathogen, measured using conventional culture techniques or PCR, was not significantly different between the rAOM and COME cohorts (Table 2).

The presence of multiple bacterial species of middle ear fluid was sporadic

The presence of multiple bacterial species within middle ear fluids (based on bacterial culture) was sporadic: co-infection by *S. pneumoniae* and *H. influenzae* was observed in a single patient only, as was co-infection by *H. influenzae* and *M. catarrhalis*.

Based on the PCR results, the presence of multiple bacterial pathogens was sporadic and similar in rAOM (10%) and COME (15%). In rAOM *S. pneumoniae* and *M. catarrhalis* were both detetected in 1 child (4%), *H. influenzae* and *M. catarrhalis* in 2 children (8%), and all 3 pathogens in 1 child (4%). In children suffering from COME, *S. pneumoniae* and *M. catarrhalis* were both detected in 3 children (3%), *M. catarrhalis* and *H. influenzae* in 5 children (5%), and *S. pneumoniae* and *H. influenzae* in 2 children (2%).

Table 2. Frequency of *S. pneumoniae*, *H. influenzae* and *M. cattarrhalis* in middle ear fluid (MEF) and the nasopharynx of children suffering from rAOM and COME

	Bacterial culture MEF		Bacterial PCR MEF		Bacterial culture nasopharynx	
	rAOM	COME	rAOM	COME	rAOM	COME
	n=25	*n*=94	*n*=24	*n*=93	*n*=25[1]	*n*=94[1]
No bacteria,*n*(%)	18 (72)	64 (68)	9 (38)	45 (48)	2 (8)	9 (10)
S. pneumoniae,*n*(%)	0 (0)	5 (5)	3 (13)	6 (7)	11 (44)	57 (61)
H. influenzae,*n*(%)	6 (24)	18 (19)	10 (42)	30 (32)	17 (68)	66 (70)
M. catarrhalis,*n*(%)	1 (4)	9 (10)	7 (29)	22 (24)	12 (48)	40 (43)

[1]MEF positive patients only.

Bacterial nasopharyngeal carriage is associated with bacterial presence in the middle ear

H. influenzae was the most frequently detected bacterial pathogen in the nasopharynx and was equally present in both the rAOM and COME cohort (68% versus 70%, respectively, Table 2). Colonization of the nasopharynx by *S. pneumoniae* occurred in 44% of the rAOM patients, compared to 61% of COME patients, while *M. catarrhalis* was detected in the nasopharynx of 48% of the rAOM and 43% of the COME patients. Eight percent and 10% of the children were culture negative for nasopharyngeal carriage in rAOM and COME disease, respectively (Table 2). Of note, co-colonization of two or more bacterial pathogens in the nasopharynx was significantly associated with the presence of bacteria in middle ear fluid (P=0.04).

Bacteria in the nasopharynx and middle ear are often genetically identical.

The presence of *S. pneumoniae* or *H. influenzae* in middle ear fluid correlated positively with the presence of the same species in the nasopharynx (*S. pneumoniae*, P=0.05; *H. influenzae*, P=0.04). *M. catarrhalis* was found in the nasopharynx of 42% of the children, with simultaneous occurrence of *M. catarrhalis* in the middle ear in 8% of the children; this latter association was not significant.

Serotype analysis of the 5 *S. pneumoniae* isolates cultured from middle ear fluid revealed the following serotypes: 23A (n=1), 23F (n=1), 6B (n=1), 19A (n=1) and 7F (n=1). In all cases, the corresponding serotype was also found in the nasopharynx. No statistically significant differences were observed between the 68 nasopharyngeal *S. pneu-*

moniae isolates, regarding pneumococcal vaccine types (i.e. those present in heptavalent Pneumococcal Conjugate Vaccine) and non-vaccine types (NVT, rAOM 72%; COME, 69%), nor between typeable and non-typeable (NT) pneumococcal strains (NT: rAOM 9%; COME 2%) when comparing rAOM and COME cohorts.

Twenty-two of the *H. influenzae* isolates cultured from the middle ear were non-typeable (rAOM 83%; COME 100%), compared to 80 non-typeable isolates cultured from the nasopharynx (rAOM 95%; COME 94%). Serotype E was detected in 4% of the middle ear fluid and 4% of the nasopharynx specimens. Serotype B was detected in 1 nasopharyngeal specimen.

MLST analysis revealed that the majority of nasopharyngeal and middle ear fluid isolates obtained from the same child were genetically identical (*S. pneumoniae* and *M. catarrhalis* 100%; *H. influenzae* 80%). Further, no clonal relationships were observed for any of the 3 bacterial pathogens, i.e. there was no evidence to suggest that isolates originated from a single "founder" isolate spreading throughout the community when the respective isolates were compared to their pathogen-specific databases.

Rhinovirus dominates in both rAOM and COME and contributes to bacterial colonization

Rhinovirus was the most frequently detected virus in middle ear fluids in both patient cohorts, followed by enterovirus, coronavirus and parainfluenza viruses (Table 3). The presence of enterovirus in middle ear fluids was associated with the presence of rhinovirus, as 8 out of the 9 enterovirus-positive middle ears were also positive for rhinovirus ($P=0.01$). Nevertheless, in the vast majority of the virus-positive samples only a single virus was detected.

Rhinovirus was also the most frequently detected virus in the nasopharynx, followed by enterovirus, parainfluenza viruses 1-4 and coronavirus (Table 3). Nasopharyngeal colonization with enterovirus was significantly more frequent in rAOM patients than in COME patients ($P=0.04$). In contrast to the results obtained from middle ear fluids, no association between rhinovirus and enterovirus could be found in the nasopharynx. Similar to middle ear fluid, in the majority of the virus-positive nasopharyngeal samples only a single virus was detected (74%).

Interestingly, a significant association was observed for bacterial-viral co-occurrence in the nasopharynx. In more detail, the presence of a virus was accompanied by the presence of a bacterium in 92% of the virus positive nasopharyngeal samples, whereas virus was present in 74% of the bacterial positive nasopharyngeal samples ($P=0.02$). More specifically, the presence of *S. pneumoniae* and *H. influenzae* was significantly associated with the presence of rhinovirus ($P=0.05$ and $P<0.01$, respectively), and the presence

of *M. catarrhalis* was significantly associated with the presence of enterovirus ($P=0.02$). However, no significant difference in bacterial-viral co-colonization of the nasopharynx was detected between children with rAOM or COME.

Table 3. Presence of viruses in middle ear fluid and the nasopharynx of children suffering from rAOM and COME

	Middle ear fluid		Nasopharynx	
	rAOM	COME	rAOM [1]	COME [1]
	n=25(%)	*n*=86[2](%)	*n*=22[3](%)	*n*=81[3](%)
no viruses detected, *n* (%)	10 (40)	40 (47)	5 (23)	23 (28)
Rhinovirus, *n* (%)	11 (44)	38 (44)	11 (50)	43 (53)
Enterovirus, *n* (%)	2 (8)	7 (8)	**5 (23)**	**6 (7)**
Coronavirus, *n* (%)	2 (8)	2 (2)	1 (5)	3 (4)
Parainfluenzavirus, 1-4, *n* (%)	1 (4)	1 (1)	2 (9)	8 (10)
Others, *n* (%)[4]	0 (0)	7 (8)	4 (18)	15 (19)

Significant differences are shown in **bold**. $P=0.04$.

[1]MEF positive patients.

[2]The MEF of 8 COME patients could not be collected for viral PCR.

[3]The nasopharyngeal swab of respectively 3 rAOM and 13 COME patients could not be used for viral PCR.

[4]Adenovirus, influenzavirus type A and B, hMPV, hPeV, hBV, RSV.

Discussion

In this prospective study, we investigated whether the clinical signs and symptoms specific for rAOM and COME could be microbiologically differentiated by the presence of bacteria and viruses in middle ear fluid. The results of our study show that the most predominant bacterial pathogen associated with middle ear fluids obtained from children suffering from rAOM and COME is non-typeable *H. influenzae*, and that the presence of *S. pneumoniae*, *H. influenzae* or *M. catarrhalis* is not significantly different between children with rAOM or COME. With respect to the nasopharynx (and similar to the results obtained using middle ear fluids), the most frequent bacterial pathogen detected within both patient cohorts was non-typeable *H. influenzae*. The predominance of *H. influenzae* in the middle ear and nasopharynx of rAOM and COME patients is similar to other otitis media studies performed elsewhere (40,41).

MLST analysis of the isolates indicated that the pathogens present in the nasopharynx and middle ear were genetically identical within the same child. The *S. pneumoniae*, *H. influenzae* and *M. catarrhalis* genotypes isolated from the total cohort of children comprised a genetically heterogeneous population structure, i.e. the isolates were genetically highly diverse, even though they all originated from a relatively restricted geographical region of The Netherlands. Importantly, the bacterial pathogens that were detected in the middle ear fluids of our cohorts tended to be genetically identical (using MLST) to those isolates cultured from the nasopharynx (80% to 100%), a finding that correlates with previously published data. Studies investigating the genetic relatedness of bacteria obtained from different locations of the upper respiratory tract, and within a single patient are scarce. Various approaches to determine the genetic relatedness of nasopharyngeal and OM isolates have been described, however MLST was only used once, a technique that is considered to be the gold standard regarding bacterial genotyping (42-44).

Rhinoviruses have been implicated in the pathogenesis of OM (45,46) and showed to be the most frequently found virus in the nasopharynx and middle ear of both COME and rAOM patients. Co-infection of rhinovirus and enterovirus was found in the middle ear, but not in the nasopharynx. Co-occurrence of these viruses has been previously described by Rezes *et al.*, who found rhinovirus in middle ear fluid in 4.8% of the 17 children, enterovirus in 23.8% and both rhino- and enterovirus in 14.3% (46). Nevertheless, in our study the co-occurrence of multiple viruses in middle ear fluid or in the nasopharynx was rare. In the nasopharynx of our OM patients we found a single virus in 46% and 2 viruses in

9%, in contrast to healthy children as described by Bogaert *et al*. (47). They found two or more viruses in the majority of the virus positive nasopharyngeal samples, in 96 children up to two years of age (47). In our cohort only 15% of the children under the age of 2 had maximal two viruses in the nasopharynx. This finding suggests that in symptomatic children suffering from OM one virus is predominant in the nasopharynx, whereas in healthy children more viruses can be present without clinical significance.

The ability of upper respiratory tract viruses to facilitate secondary bacterial infection in AOM has been described extensively in the literature (27,48,49). Influenza A and *S. pneumoniae*, RSV and *H. influenzae* are two examples of viral-bacterial interaction investigated in both animal models and human studies (50). To our knowledge this is the first report describing a highly significant association for the co-occurrence of bacteria and virus in the nasopharynx of rAOM and COME patients. More specifically, nasopharyngeal co-colonization of rhinoviruses with either *S. pneumoniae*, or *H. influenzae*, was statistically significant. Pitkaranta *et al.* observed a positive correlation between the presence of *S. pneumoniae* or *M. catarrhalis* and rhinovirus in the nasopharynx, but not of *H. influenzae* and rhinovirus (45). However, the authors focused on nasopharyngeal samples of OM-prone children, and exclusion criteria for their study were either recent or expected ventilation tube insertion and COME diagnosis (45). In the present study, no association between the co-occurrence of these viruses and bacteria was observed in middle ear fluids for both rAOM and COME cohorts, likely caused by the relatively low number of bacteria detected in middle ear fluid. In addition, since viruses can predispose to bacterial super-infection, it is possible that they are already cleared from the middle ear cavity at the time of surgery.

There are a few limitations of this study. First, the number of children with rAOM enrolled in this study is limited. Second, although we used internationally accepted definitions for rAOM and COME, the timing of clinical sampling in relation to the exact onset of OM is unknown. Finally, while bacteria can colonize and persist in the human respiratory tract for months, infection with respiratory viruses results in acute viral replication, which is cleared within days to weeks. As a consequence, the persistence of bacterial DNA probably exceeds that of viruses.

In conclusion, we performed a prospective cohort study to investigate the frequency and types of bacterial and viral pathogens in the middle ear and nasopharynx of children suffering from rAOM or COME. Our results show that the same pathogenic bacterial species and viruses are implicated in the pathogenesis of both rAOM and COME disease. Further, our findings do not support the general assumption that the microbial profile is pathognomonic for either rAOM or COME, or that COME is merely a consequence of persistent sterile inflammation in the middle ear.

Acknowledgments

The authors would like to thank all of the children and parents who participated in this study. We are grateful to the staff of the departments ORL and Medical Microbiology of the Canisius Wilhelmina Hospital and the Radboud University Nijmegen Medical Centre for their commitment to the study, in particular M. de Bruyn (CWZ), C. Bartels and K. Teuwen (RUNMC) for excellent coordination. E.R. Simonetti and C. de Jongh-van der Gaast are acknowledged for technical assistance. We thank H.J. Bootsma and S. van Selm for critical reading of the manuscript. This project was funded by a European Union Sixth Framework Program (Project Title: OMVac. Project No. 037653).

References

1. Gonzales R, Malone DC, Maselli JH, Sande MA. Excessive antibiotic use for acute respiratory infections in the United States. Clin Infect Dis 2001; 33(6): 757-62.
2. Freid VM, Makuc DM, Rooks RN. Ambulatory health care visits by children: principal diagnosis and place of visit. Vital Health Stat 13 1998; (137): 1-23.
3. Rovers MM, Schilder AG, Zielhuis GA, Rosenfeld RM. Otitis media. Lancet 2004; 363(9407): 465-73.
4. Marchisio P, Claut L, Rognoni A, et al. Differences in nasopharyngeal bacterial flora in children with nonsevere recurrent acute otitis media and chronic otitis media with effusion: implications for management. Pediatr Infect Dis J 2003; 22(3): 262-8.
5. Diagnosis and management of acute otitis media. *Pediatrics* 2004; 113(5): 1451-65.
6. Gates GA, Klein JO, Lim DJ, et al. Recent advances in otitis media. 1. Definitions, terminology, and classification of otitis media. Ann Otol Rhinol Laryngol Suppl 2002; 188:8-18.: 8-18.
7. Berman S. Otitis media in children. *N Engl J Med* 1995; 332(23): 1560-5.
8. Damoiseaux RA, Rovers MM. AOM in children. Clinical evidence 2011; 2011.
9. McDonald S, Langton Hewer CD, Nunez DA. Grommets (ventilation tubes) for recurrent acute otitis media in children. Cochrane Database Syst Rev 2008; (4): CD004741.
10. Browning GG, Rovers MM, Williamson I, Lous J, Burton MJ. Grommets (ventilation tubes) for hearing loss associated with otitis media with effusion in children. Cochrane Database Syst Rev 2010; (10): CD001801.
11. Eskola J, Kilpi T, Palmu A, et al. Efficacy of a pneumococcal conjugate vaccine against acute otitis media. N Engl J Med 2001; 344(6): 403-9.
12. Spijkerman J, van Gils EJ, Veenhoven RH, et al. Carriage of Streptococcus pneumoniae 3 years after start of vaccination program, the Netherlands. Emerg Infect Dis 2011; 17(4): 584-91.
13. Taylor S, Marchisio P, Vergison A, Harriague J, Hausdorff WP, Haggard M. Impact of pneumococcal conjugate vaccination on otitis media: a systematic review. Clin Infect Dis 2012; 54(12): 1765-73.
14. Faden H, Duffy L, Wasielewski R, Wolf J, Krystofik D, Tung Y. Relationship between nasopharyngeal colonization and the development of otitis media in children. Tonawanda/Williamsville Pediatrics. J Infect Dis 1997; 175(6): 1440-5.
15. Bogaert D, Engelen MN, Timmers-Reker AJ, et al. Pneumococcal carriage in children in The Netherlands: a molecular epidemiological study. J Clin Microbiol 2001; 39(9): 3316-20.
16. Faden H, Waz MJ, Bernstein JM, Brodsky L, Stanievich J, Ogra PL. Nasopharyngeal flora in the first three years of life in normal and otitis-prone children. Ann Otol Rhinol Laryngol 1991; 100(8): 612-5.
17. Ruohola A, Meurman O, Nikkari S, et al. Microbiology of acute otitis media in children with tympanostomy tubes: prevalences of bacteria and viruses. Clin Infect Dis 2006; 43(11): 1417-22.
18. Heslop A, Ovesen T. Severe acute middle ear infections: microbiology and treatment. Int J

Pediatr Otorhinolaryngol 2006; 70(10): 1811-6.
19. Faden H, Duffy L, Boeve M. Otitis media: back to basics. Pediatr Infect Dis J 1998; 17(12): 1105-12.
20. Bluestone CD, Stephenson JS, Martin LM. Ten-year review of otitis media pathogens. Pediatr Infect Dis J 1992; 11(8 Suppl): S7-11.
21. Chonmaitree T, Howie VM, Truant AL. Presence of respiratory viruses in middle ear fluids and nasal wash specimens from children with acute otitis media. Pediatrics 1986; 77(5): 698-702.
22. Chonmaitree T, Ruohola A, Hendley JO. Presence of viral nucleic acids in the middle ear: acute otitis media pathogen or bystander? Pediatr Infect Dis J 2012; 31(4): 325-30.
23. Heikkinen T, Thint M, Chonmaitree T. Prevalence of various respiratory viruses in the middle ear during acute otitis media. N Engl J Med 1999; 340(4): 260-4.
24. Kleemola M, Nokso-Koivisto J, Herva E, et al. Is there any specific association between respiratory viruses and bacteria in acute otitis media of young children? J Infect 2006; 52(3): 181-7.
25. Chonmaitree T, Revai K, Grady JJ, et al. Viral upper respiratory tract infection and otitis media complication in young children. Clin Infect Dis 2008; 46(6): 815-23.
26. Chonmaitree T, Heikkinen T. Viruses and acute otitis media. Pediatr Infect Dis J 2000; 19(10): 1005-7.
27. Heikkinen T, Chonmaitree T. Importance of respiratory viruses in acute otitis media. Clin Microbiol Rev 2003; 16(2): 230-41.
28. Veenhoven R, Bogaert D, Uiterwaal C, et al. Effect of conjugate pneumococcal vaccine followed by polysaccharide pneumococcal vaccine on recurrent acute otitis media: a randomised study. Lancet 2003; 361(9376): 2189-95.
29. van Heerbeek N, Straetemans M, Wiertsema SP, et al. Effect of combined pneumococcal conjugate and polysaccharide vaccination on recurrent otitis media with effusion. Pediatrics 2006; 117(3): 603-8.
30. Rivera-Olivero IA, Blommaart M, Bogaert D, Hermans PW, de Waard JH. Multiplex PCR reveals a high rate of nasopharyngeal pneumococcal 7-valent conjugate vaccine serotypes co-colonizing indigenous Warao children in Venezuela. Journal of medical microbiology 2009; 58(Pt 5): 584-7.
31. Satola SW, Collins JT, Napier R, Farley MM. Capsule gene analysis of invasive *Haemophilus influenzae*: accuracy of serotyping and prevalence of IS1016 among nontypeable isolates. J Clin Microbiol 2007; 45(10): 3230-8.
32. Meats E, Feil EJ, Stringer S, et al. Characterization of encapsulated and noncapsulated *Haemophilus influenzae* and determination of phylogenetic relationships by multilocus sequence typing. J Clin Microbiol 2003; 41(4): 1623-36.
33. Enright MC, Spratt BG. A multilocus sequence typing scheme for *Streptococcus pneumoniae*: identification of clones associated with serious invasive disease. Microbiology 1998; 144(Pt 11): 3049-60.
34. Maiden MC, Bygraves JA, Feil E, et al. Multilocus sequence typing: a portable approach to the identification of clones within populations of pathogenic microorganisms. Proc Natl Acad Sci U S A 1998; 95(6): 3140-5.
35. Thomas JC, Pettigrew MM. Multilocus sequence typing and pulsed field gel electrophoresis of otitis media causing pathogens. Methods Mol Biol 2009; 493:179-90.: 179-90.

36. Kais M, Spindler C, Kalin M, Ortqvist A, Giske CG. Quantitative detection of *Streptococcus pneumoniae*, *Haemophilus influenzae*, and *Moraxella catarrhalis* in lower respiratory tract samples by real-time PCR. Diagn Microbiol Infect Dis 2006; 55(3): 169-78.
37. Hall-Stoodley L, Hu FZ, Gieseke A, et al. Direct detection of bacterial biofilms on the middle-ear mucosa of children with chronic otitis media. JAMA 2006; 296(2): 202-11.
38. Hays JP, van SS, Hoogenboezem T, et al. Identification and characterization of a novel outer membrane protein (OMP J) of Moraxella catarrhalis that exists in two major forms. J Bacteriol 2005; 187(23): 7977-84.
39. Templeton KE, Scheltinga SA, Beersma MF, Kroes AC, Claas EC. Rapid and sensitive method using multiplex real-time PCR for diagnosis of infections by influenza a and influenza B viruses, respiratory syncytial virus, and parainfluenza viruses 1, 2, 3, and 4. J Clin Microbiol 2004; 42(4): 1564-9.
40. Brake MK, Jewer K, Flowerdew G, Cavanagh JP, Cron C, Hong P. Tympanocentesis results of a Canadian pediatric myringotomy population, 2008 to 2010. Journal of otolaryngology - head & neck surgery = Le Journal d'oto-rhino-laryngologie et de chirurgie cervico-faciale 2012; 41(4): 282-7.
41. Wiertsema SP, Kirkham LA, Corscadden KJ, et al. Predominance of nontypeable *Haemophilus influenzae* in children with otitis media following introduction of a 3+0 pneumococcal conjugate vaccine schedule. Vaccine 2011; 29(32): 5163-70.
42. Arai J, Hotomi M, Hollingshead SK, Ueno Y, Briles DE, Yamanaka N. *Streptococcus pneumoniae* isolated from middle ear fluid and nasopharynx of children with acute otitis media exhibit phase variation. J Clin Microbiol 2011.
43. Brygge K, Sorensen CH, Colding H, Ejlertsen T, Hojbjerg T, Bruun B. Ribotyping of strains of *Moraxella (Branhamella) catarrhalis* cultured from the nasopharynx and middle ear of children with otitis media. Acta Otolaryngol 1998; 118(3): 381-5.
44. Kaur R, Chang A, Xu Q, Casey JR, Pichichero ME. Phylogenetic relatedness and diversity of non-typable *Haemophilus influenzae* in the nasopharynx and middle ear fluid of children with acute otitis media. Journal of medical microbiology 2011; 60(Pt 12): 1841-8.
45. Pitkaranta A, Roivainen M, Blomgren K, et al. Presence of viral and bacterial pathogens in the nasopharynx of otitis-prone children. A prospective study. Int J Pediatr Otorhinolaryngol 2006; 70(4): 647-54.
46. Rezes S, Soderlund-Venermo M, Roivainen M, et al. Human bocavirus and rhino-enteroviruses in childhood otitis media with effusion. J Clin Virol 2009; 46(3): 234-7.
47. Bogaert D, Keijser B, Huse S, et al. Variability and diversity of nasopharyngeal microbiota in children: a metagenomic analysis. *PLoS ONE* 2011; 6(2): e17035.
48. Nokso-Koivisto J, Hovi T, Pitkaranta A. Viral upper respiratory tract infections in young children with emphasis on acute otitis media. Int J Pediatr Otorhinolaryngol 2006; 70(8): 1333-42.
49. Nokso-Koivisto J, Raty R, Blomqvist S, et al. Presence of specific viruses in the middle ear fluids and respiratory secretions of young children with acute otitis media. J Med Virol 2004; 72(2): 241-8.
50. Bakaletz LO. Immunopathogenesis of polymicrobial otitis media. J Leukoc Biol 2010; 87(2): 213-22.

Inflammation in the middle ear of children with recurrent or chronic otitis media is associated with bacterial load

K. Stol, D.A. Diavatopoulos, K. Graamans, J.A.M. Engel, W.J.G. Melchers, H.F.J. Savelkoul, J.P. Hays, A. Warris and P.W.M. Hermans

The Pediatric Infectious Disease Journal 2012, 31(11):1128-34

Abstract

Background

Viral upper respiratory tract infections have been described as an important factor in the development of otitis media (OM), although it is unclear whether they facilitate bacterial OM or can directly cause OM. To clarify the role of viral infections in otitis media, we compared the relative contribution of viruses and bacteria with the induction of inflammatory cytokine responses in the middle ear of children suffering from OM.

Methods

Children up to 5 years of age, with recurrent or chronic episodes of OM and scheduled for ventilation tube insertion were enrolled in a prospective study. Middle ear fluids (MEFs, $n = 116$) were collected during surgery, and quantitative PCR was performed to detect bacterial and viral otopathogens, i.e. *Streptococcus pneumoniae, Haemophilus influenzae, Moraxella catarrhalis* and 15 respiratory viruses. Finally, concentrations of the inflammatory mediators IL-1β, IL-6, IL-8, IL-10, IL-17a and TNF-α were determined.

Results

MEFs were clustered into four groups, based on the detection of viruses (28%), bacteria (27%), both bacteria and viruses (27%) or no otopathogens (19%). Bacterial detection was associated with significantly elevated concentrations of cytokines compared to MEF without bacteria ($P < 0.001$ for all cytokines tested) in a bacterial load- and species-dependent manner. In contrast, the presence of viruses was not associated with changes in cytokine values, and no synergistic effect between viral-bacterial co-infections was observed.

Conclusions

The presence of bacteria, but not viruses, is associated with an increased inflammatory response in the middle ear of children with recurrent or chronic OM.

Introduction

Many studies over the past decades have demonstrated that respiratory viral infections can directly cause acute otitis media (AOM) (1,2). However, respiratory viruses may also indirectly facilitate AOM by inducing migration of bacterial otopathogens up the Eustachian tube and bacterial replication in the middle ear cavity. For example, synergistic relationships between bacterial and viral pathogens have been described for *S. pneumoniae* and both respiratory syncytial virus (RSV) and influenza A virus (3,4). Although the exact mechanisms underlying these relationships are currently not fully understood, increased bacterial adherence in the nasopharynx, serous exudates and reduced ciliary activity in the Eustachian tube as a result of viral infection have all been suggested to play a role in OM. Importantly, whilst epidemiological data and animal studies suggest that bacterial, viral as well as bacterial-viral co-infections may all play a role in AOM, their relative contribution to the induction of inflammation and the development of OM, particularly in patients with more chronic forms of OM, remains largely unknown.

Cytokines play a pivotal role in mediating the inflammatory response during OM. For example, IL-1β and TNF-α, primarily produced by macrophages, initiate the acute inflammatory response and have been shown to contribute to pathological changes in the middle ear, including mucosal damage, bone erosion, fibrosis and sensorineural hearing loss (5-8). Another important cytokine in the context of OM is IL-8. It is secreted by several cell types and is an important chemotactic attractant for neutrophils (9). Two other cytokines, IL-6 and IL-10, have both been shown to play an important role during chronic OM (8,10,11). IL-6 plays a role in the activation of cytotoxic T cells, B-cell maturation and the induction of bone resorption. Whilst the anti-inflammatory cytokine IL-10 prevents excessive inflammation and damage to the host by suppressing the immune response (8), strong IL-10 responses can also increase susceptibility to bacterial infections, as has been described for *S. pneumoniae* (12). Another cytokine that may play a role in OM is IL-17a, which is produced by activated Th17-cells. IL-17a can stimulate the expression of IL-6, but can also activate neutrophils and enhance the production of nitric oxide (NO) (13), and is known to play an important role in the response against extracellular bacterial pathogens. Although high levels of IL-17a have been associated with other chronic inflammatory diseases, such as allergic asthma and rheumatoid arthritis (13,14), its relevance in the context of OM has not been extensively studied.

In this study, we investigated the local cytokine response in recurrent and chronic

OM. In particular, we investigated whether the presence of viruses and bacteria in the middle ear was associated with an increased inflammatory response. An important question that we sought to address is whether viral infections can enhance middle ear inflammation during co-infection with bacterial pathogens.

Materials & Methods

Study design

This retrospective clinical study comprises a cohort of children up to five years of age, suffering from recurrent or chronic episodes of OM and scheduled for ventilation tube insertion. The cohort was enrolled at a secondary and a tertiary referral hospital in Nijmegen, the Netherlands, from April 1st 2008 to July 1st 2009. Recurrent AOM was defined as having had three or more episodes of AOM in the last six months or four episodes in the last 12 months (15). The COME patient population consisted of children who had experienced a period of persistent OM with effusion lasting longer than three months. Patients were diagnosed by an otolaryngologist based on signs, symptoms, otomicroscopy and audiometry including tympanometry. Patients with a history of malignancy, organ transplantation or immune deficiency were excluded from this study, as well as patients with recent elective ear surgery or systemic infectious diseases. Children with acute OM and/or fever ($T \geq 38.0^{\circ}C$) at the time of ventilation tube insertion were rescheduled for the procedure. Adenoidectomy performed in the same surgical setting was not considered to be an exclusion criterion. Patient characteristics and risk factors were acquired using a questionnaire. Ethical permission was obtained from the Committee on Research Involving Human Subjects in January 2008 (CMO 2007/239, international trial register number: NCT00847756).

Clinical samples

MEF was collected during surgery using a middle ear fluid aspiration system (Kuijpers Instruments, Groesbeek, The Netherlands) (16), suspended in 2 mL 0.9% NaCl and divided into aliquots for bacterial PCR, viral PCR and cytometric bead array. Aliquots were stored at -80°C until further use. Per child one MEF sample from one ear was obtained.

Microbiology

MEF was cultured according to standard laboratory procedures to determine the presence of *Streptoccus pneumoniae*, *Haemophilus influenzae* and *Moraxella catarrhalis*. To determine the amount of bacteria present in MEF, quantitative real-time PCR (qRT-PCR) was performed. PCR primers and probes were developed using Primer Express v3 software (Applied Biosystems). The respective genes chosen for the detection of specific bacterial species were pneumolysin (*ply*) for *S. pneumoniae* (17), 16S rRNA for *H. influenzae* (18) and outer membrane protein J (*ompJ*) for *M. catarrhalis* (19). For quantification pur-

poses, calibration curves were prepared and included in every qRT-PCR run, using a dilution series (10^8, 10^5 and 10^3 CFU/mL) of pooled *S. pneumoniae* TIGR4, non-typeable *H. influenzae* 86-028NP and *M. catarrhalis* RH4. All calibration pools were tested in triplicate in each qRT-PCR run and a new calibration curve was generated for every batch of MEF tested. Variation between the calibration curves was negligible and therefore considered to be suitable for standardization.

Genomic DNA was extracted from 50μL of MEF and from pooled calibration controls using the MagNaPure – LC system, according to the manufacturer's instructions (Roche Applied Sciences). DNA extract was resuspended in 100L of extraction buffer. Reaction mixtures for qRT-PCR contained 18 pmoles of each primer, 4 pmoles of probe, 1x TaqMan Fast Universal PCR Master Mix No AmpErase® UNG (2X) and 7L of extracted DNA in a final volume of 20μL. A "fast" real time PCR protocol was used for all PCRs, comprising a two-step PCR thermocycling program of 95°C for 3 seconds followed by 60°C for 30 seconds for a total of 40 PCR cycles.

Virology

DNA was extracted from 500μL of MEF using the MagNA Pure-LC System. A multiplex real-time PCR assay containing 15 different viral pathogens was used, which was designed to detect specific viral genes belonging to influenza virus (IV) type A and B, coronavirus (CoV) 229E and OC43, human bocavirus (hBoV), enterovirus (EV), adenovirus (AdV), parechovirus (PeV), parainfluenzavirus (PIV) types 1-4, human metapneumovirus (hMPV), rhinovirus (RV) and respiratory syncytial virus (RSV) (20). An internal control comprising phocine herpesvirus (PhPV, IC DNA control) and equine arthritis virus (EAV, IC RNA control) was included in each assay run. RNA was reverse transcribed to cDNA using the TaqMan Reverse Transcription Reagents kit (Applied Biosystems), according to the manufacturer's instructions. PCRs were performed on the LightCycler 480 instrument using LightCycler 480 Probes Master Mix (Roche Diagnostics). Validated primer/probe-mixes were purchased from Diagenode (Liege, Belgium) and used according to the manufacturer's instructions. Cycling conditions were 95°C for 5 minutes, followed by 50 cycles of 95°C for 15 seconds and 55°C for 15 seconds and 72°C for 20 seconds. The semi-quantitative amount of virus was determined based on the cycle threshold (Ct) value.

Detection of cytokines

Concentrations of IL-1β, IL-6, IL-8, IL-10, IL-17a and TNF-α cytokines in MEF were determined using commercially available cytometryc bead array (CBA) kits, according to the instructions of the manufacturer (Becton Dickinson, Breda, the Netherlands). All buffers

used in this protocol were obtained from the BD CBA Soluble Protein Master Buffer Kit (BD Pharmingen). The detection limit was 1.1 pg/mL for IL-1β, 0.7 pg/mL for TNF-α, 0.13 pg/mL for IL-10, 0.6 pg/mL for IL-6, 1.8 pg/mL for IL-8 and 0.3 pg/mL for IL-17. The samples were measured on a FACSCanto II, using FCAP software (BD Biosciences).

Statistical analysis

Statistical analysis was performed using SPSS 17.0 (SPSS Inc., Chicago, IL, USA) and GraphPad Prism 4 (GraphPad Software, La Jolla, CA, USA). The demographic characteristics of the study cohort were investigated using one-way ANOVA and the chi-square test. One-way ANOVA with the Bonferroni correction was performed on log-transformed cytokine levels (mean, 95% CI) in order to calculate the statistical significance between groups (presence of bacteria, viruses, viruses / bacteria or no pathogens, respectively). Spearman's rank correlation was used to calculate the correlation coefficient between cytokine levels with *H. influenzae* and *M. catarrhalis* bacterial loads. Univariate analysis of variance was used to compare cytokine levels and bacterial load of *H. influenzae* positive MEFs with *M. catarrhalis* positive MEFs (mean, 95% CI).

Results

PCR detection indicates that the majority of MEFs from chronic OM patients contain DNA from otopathogens

To determine the presence of otopathogens during chronic OM, qRT-PCR was performed on 116 MEF samples from a clinical cohort of children suffering from rAOM or COME. Specifically, we determined the presence of the bacterial pathogens *S. pneumoniae*, *H. influenzae* and *M. catarrhalis,* as well as 15 respiratory viruses associated with OM (Table 1). In order to investigate the middle ear fluids for the presence of bacteria and viruses we measured the volume of middle ear fluid collected and described the consistency of the MEF. Neither the amount of middle ear fluid, nor the consistency of the middle ear fluid was associated with the detection of bacteria or viruses (data not shown). Out of 116 patients, 32 (28%) tested positive only for viruses, 31 samples (27%) contained only bacteria, and 31 MEFs (27%) contained both bacteria and viruses. Although the vast majority of patients tested positive for at least one of the known otopathogens, a smaller but significant group (n=22, 19%) of patients tested PCR-negative for all of the otopathogens (Table 1). With regard to the demographic characteristics of the study cohort, children under the age of two (n=19) were significantly more often co-infected with both bacteria and virus when all four clustered groups of MEFs were compared (Chi-square test, p=0.03, Table 1), although the sample size is small.

Of the viral pathogens that were detected, rhinovirus was by far the most frequently detected respiratory virus (n=53, 44%), followed by enterovirus (n=9, 8%) and human coronavirus (n=4, 3%). For the bacterial pathogens, *H. influenzae* and *M. catarrhalis* were the predominate bacterial pathogens, with 37% (n=43) and 25% (n=32) of samples PCR-positive for either pathogen, respectively. Unexpectedly, *S. pneumoniae* was only detected in 8% (n=9) of the MEFs.

Cytokine responses are increased in the presence of bacteria but not viruses

To determine whether the presence of viruses and/or bacteria affected the cytokine response, levels of the primary cytokines IL-1β and TNF-α, the secondary cytokines IL-6 and IL-8, and the regulatory cytokines IL-10 and IL-17a were measured in MEFs. Invariably, cytokine levels were increased when bacteria were detected compared to samples without bacteria ($P<0.001$ for all cytokines tested). Conversely, the presence of virus in MEFs was not associated with an increase in cytokine levels compared to MEFs without pathogens

Table 1. Demographic characteristics of the study cohort.

	No pathogens *n* = 22 (19%)	Viruses only *n* = 32 (28%)	Bacteria only *n* = 31(27%)	Bacteria and viruses *n* = 31 (27%)	P-value[1]
Male sex, *n* (%)	11 (50)	20 (63)	14 (45)	19 (61)	0.45
Mean age (years [SD])	4.2[1.27]	4.04 [1.52]	4.17 [1.41]	3.27 [1.65]	0.08
< 2 years of age, *n* (%)	**2 (9)**	**5 (16)**	**2 (7)**	**10 (32)**	**0.03**
Diagnosis rAOM, *n* (%)	2 (9)	7 (22)	9 (29)	8 (26)	0.36
≥ 4 URTI in the preceding year, *n* (%)[2]	5 (24)	10 (32)	5 (18)	7 (25)	0.65
URTI in the last month, *n* (%)[2]	4 (18)	6 (19)	2 (7)	10 (32)	0.11
Recent OM antibiotic prescription, *n* (%)	1 (5)	1 (3)	4 (13)	2 (7)	0.45
History of tympanostomy tube insertion, *n* (%)	7 (32)	12 (38)	12 (39)	10 (32)	0.93
Asthma/wheezing, *n* (%)	3 (14)	1 (3)	2 (7)	3 (11)	0.55
Allergic rhinitis, *n* (%)	1 (5)	1 (4)	1 (4)	1 (7)	0.92
Eczema, *n* (%)	1 (5)	5 (16)	7 (25)	3 (11)	0.21
Birth weight, mean (g)	3265	3421	3290	3342	0.88
Breast feeding < 3 months, *n* (%)	14 (64)	20 (67)	14 (50)	16 (55)	0.57
Prevnar immunization, *n* (%)[3]	4 (18)	7 (22)	7 (23)	13 (42)	0.16
Tobacco smoke exposure, *n* (%)	4 (19)	15 (50)	7 (26)	7 (24)	0.06
Older siblings, *n* (%)	11 (61)	16 (62)	13 (52)	18 (75)	0.43
Day care attendance, *n* (%)	9 (45)	13 (42)	13 (48)	17 (59)	0.61

Significant differences are shown in bold.
[1] Chi-square test or One-Way ANOVA were used where appropriate. Posthoc analysis for the determinants mean age and birth weight were notsignificant.
[2] Upper respiratory tract infections.
[3] The Prevnar vaccine was introduced in Dutch National Immunization Program in 2006 for children born after 01-04-2006.

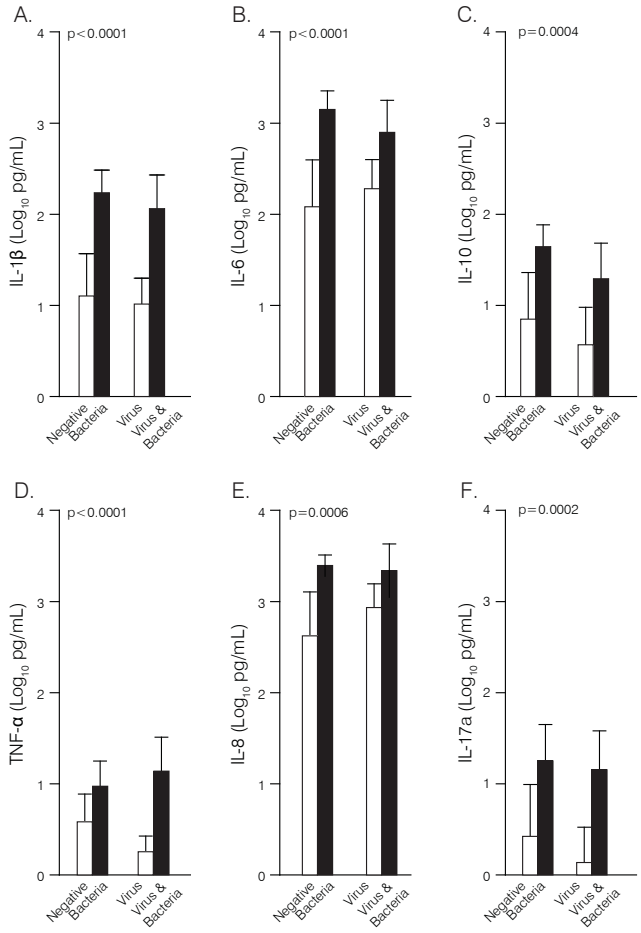

Figure 1. Effect of bacterial and viral pathogens on cytokine response in the middle ear. P values indicate between-group differences and are calculated using 1-way ANOVA on log-transformed cytokine levels (mean, 95% CI). ANOVA indicates analysis of variances; CI, confidence interval.

Table 2. *H. influenzae*-associated and *M. catarrhalis*-associated cytokine levels

Cytokine	Mean cytokine level (Log_{10} CFU/mL)		95% CI of difference[1]		P-value[2]
	H. influenzae	*M. catarrhalis*	Lower bound	Upper bound	
IL-1β	2.48	1.78	1.91	2.36	**0.003**
TNF-α	1.17	0.97	0.81	1.34	0.443
IL-6	3.28	2.80	2.86	3.29	**0.014**
IL-8	3.54	3.19	3.23	3.50	**0.014**
IL-10	1.78	1.20	1.27	1.71	**0.012**
IL-17a	1.28	1.09	0.86	1.51	0.564

Significant differences are shown in bold.
[1] CI, confidence interval.
[2] Univariate analysis of variance.

(Figure 1). Additionally, no significant changes were observed between samples containing only bacteria versus MEFs containing both bacteria and viruses, suggesting a more indirect role for viral infections.

Samples were screened for bacterial presence by both bacterial culture and PCR. Not surprisingly, PCR detected bacterial DNA in a significant percentage of culture negative effusions: *S. pneumoniae* in 4.1% (NS), *H. influenzae* in 16.5% ($P<0.001$) and *M. catarrhalis* in 19% ($P<0.001$). However, the effect of bacterial pathogens detected with bacterial culture did not significantly alter the results obtained by qPCR as shown in Figure 1.

As our clinical cohort contained both patients diagnosed with rAOM or COME, we also compared the cytokine profiles of these groups in response to the presence of either bacteria or viruses. Although the sample size is limited, we found no significant changes in MEF cytokine levels between rAOM and COME.

Cytokine levels correlate significantly with bacterial load

Having established that the presence of bacterial DNA corresponds to a general increase in cytokine levels, we then investigated whether this observation was dependent on the amount and the type of bacteria. First, MEFs positive for multiple bacterial species (12%) were excluded in order to facilitate analysis of the pathogen-specific cytokine response. Comparing cytokine levels to bacterial load showed a significant correlation for both *H. influenzae* and *M. catarrhalis* ($P<0.05$ for IL-1β, TNF-α, IL-6 and IL-8 for both pathogens; see Figure 2). Although a similar trend was observed for *S. pneumoniae,* no statistical significance was reached due to the small number of MEFs in which *S. pneumoniae* was detected ($n=9$). To investigate whether the cytokine response differed between the two dominant bacterial species, i.e. *H. influenzae* and *M. catarrhalis,* we also compared the cytokine levels and bacterial loads of these two groups. We found that the detection of *H. influenzae* was associated with significantly higher levels of IL-1β, IL-6, IL-8 and IL-10 as compared to *M. catarrhalis* (Table 2). Taken together, these data strongly suggest a direct role for bacterial but not viral pathogens in the inflammatory cytokine response during chronic OM. This effect is not only dependent on the bacterial load as measured by qRT-PCR, but is also affected by the bacterial species.

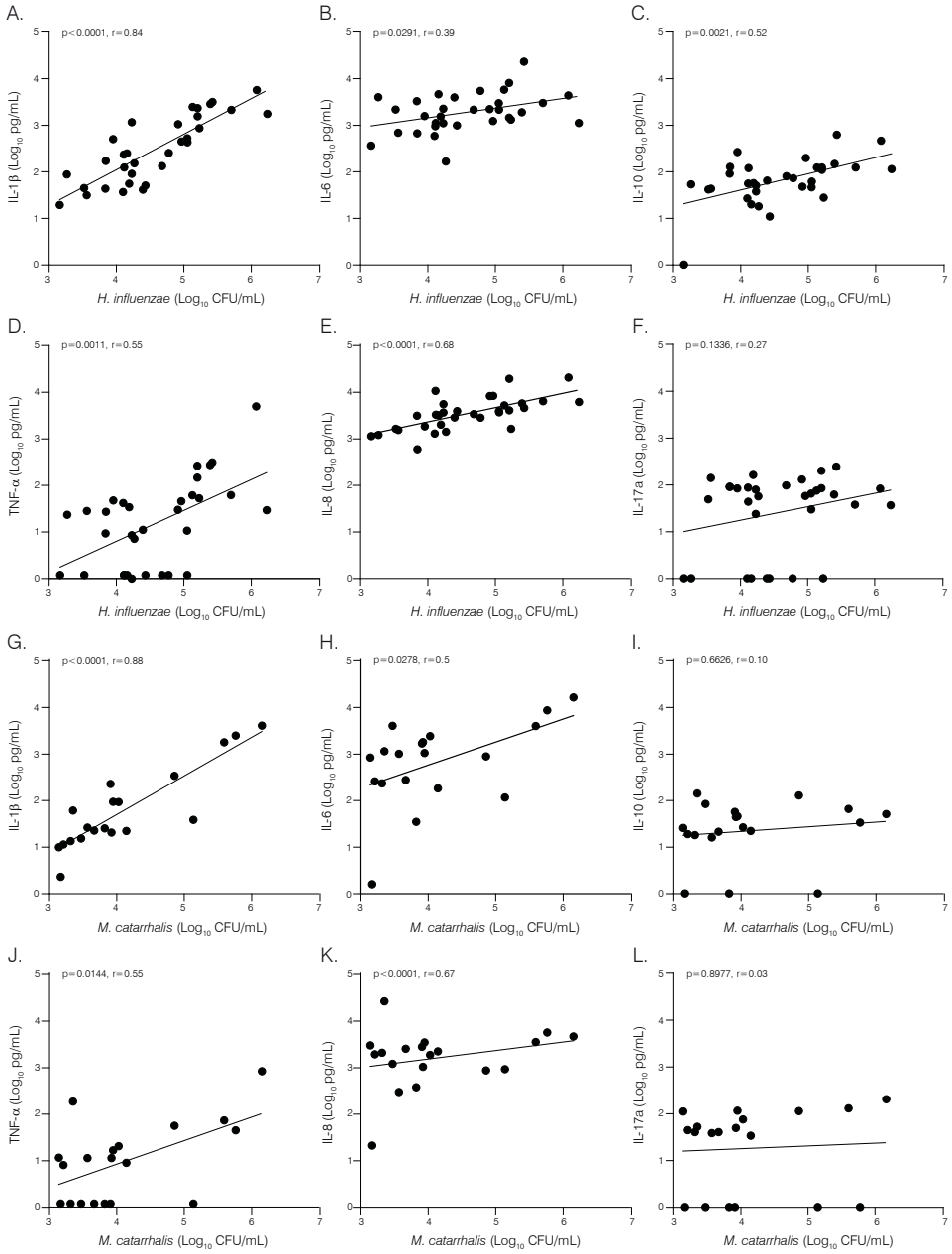

Figure 2. Cytokine responses are associated with bacterial load of H. *influenzae* (A-F) or M. *catarrhalis* (G-L). Cytokines (IL-1β, TNF-α, IL-6, IL-8, IL-10 and IL-17a) in the middle ear fluid of OM patients are plotted against the amount of bacteria, as derived from quantitative PCR. Each dot represents a single MEF sample. P values were calculated using Spearman rank correlation.

Discussion

In this study, we sought to investigate the respective contributions of bacterial and viral otopathogens to middle ear inflammation, one of the hallmarks of chronic OM. By relating the presence of pathogens to the cytokine response in the middle ear fluid of a cohort of patients suffering from recurrent acute OM and chronic OM, we show that the detection of bacteria by qRT-PCR is directly associated with an increase in inflammatory cytokines. In contrast to previous observations describing an association between cytokine response profiles and virus-induced acute otitis media (21,22), our data suggest that the MEF cytokine response is not significantly different when viruses are detected. These data suggest a more indirect role for virus infections in the inflammatory response, in particular for rhinovirus, during chronic OM.

OM comprises a spectrum of clinical manifestations, varying from acute otitis media (AOM) to recurrent (rAOM) and chronic (COME) episodes (23). Whereas (r)AOM is typically denoted by an acute onset, acute inflammation and the presence of middle ear fluid, COME is characterized by the presence of an asymptomatic middle-ear effusion (23,24). Whilst previous studies have reported a relatively low recovery of viable pathogens (30%) that are typically found in AOM, other studies using PCR detection techniques have shown a much higher detection rate of bacterial DNA (i.e. 77%). Although the detection of bacterial DNA does not necessarily reflect the presence of viable bacteria, these studies suggest that patients with chronic OM do not always have sterile effusions, as previously thought (25).

In this study, we found no significant differences in cytokine levels between rAOM and COME patients. This finding might partially be explained by the fact that at the time of surgery, children did not suffer from acute OM and/or fever, since acute inflammation is contra-indicative for ventilation tube insertion. Consequently, it may be expected that cytokine levels in rAOM are lower than during an episode of AOM. Nonetheless, these data suggest that the distinction between COME and rAOM patients cannot easily be made in the non-acute phase. An interesting finding was the observation that interestingly, even in OM patients with no detectable pathogens, cytokine levels in general were high (up to 1×10^4 pg/mL). As children enrolled in this study did not suffer from acute inflammation, this suggest that their inflammatory response remains elevated even in the absence of detectable pathogens. One potential explanation for the high cytokine levels in these patients may be the presence of bacterial or viral pathogens not included in this analysis.

In addition, bacteria in biofilms, intracellular persistence of bacteria or bacterial components undetectable by PCR may still provoke inflammation in the middle ear cavity (26,27).

We demonstrate that the detection of the three major bacterial OM pathogens is associated with a significantly elevated inflammatory cytokine response compared to MEFs without bacteria. Thus far, clinical data describing the innate immune response in the middle ear to otopathogens are scarcely available. Whilst most studies have focused on acute forms of OM, significantly less studies have addressed the cytokine response of children suffering from chronic forms of OM. Similar to our study, Skovsberg *et al.* compared the presence of viral and bacterial pathogens to the cytokine response. Although this study focused on children with acute OM in which the tympanic membrane ruptured spontaneously, it is important to note that they also found an association between the presence of bacteria and increased levels of cytokines (28). Thus, both their and our study point to an important role for bacteria in the inflammatory cytokine response during OM. In contrast to the study by Skovsberg, we also assessed the impact of bacterial load on the cytokine response. We found that the amount of bacteria was strongly associated with increased cytokine levels, in particular for *H. influenzae*, and to a lesser extent for *M. catarrhalis*. Previous studies have suggested that infection with *M. catarrhalis* results in less severe OM in comparison to other bacterial pathogens (29). Our data also support this hypothesis, as *M. catarrhalis* in general was associated with a weaker cytokine response compared to *H. influenzae*.

In parallel to the use of bacterial PCR, we also cultured the middle ear fluid to detect viable *S. pneumoniae*, *H. influenzae* and *M. catarrhalis*. Although PCR-based detection methods are much more sensitive compared to culture-based methods (25), we found that the use of data obtained with bacterial culture did not alter our results (data not shown).

In this study, rhinovirus was by far the most dominant respiratory virus, as 81% of all virus-containing MEFs were positive for rhinovirus. Rhinovirus has been shown to play an important role in lower respiratory tract pathology, where it can provoke exacerbations of cystic fibrosis, asthma and COPD (14,30-32). One mechanism by which rhinoviruses can induce inflammation during co-infection with bacterial pathogens is through the liberation of planktonic bacteria from biofilms. This in turn may cause increased recognition by the innate immune system, resulting in an increased cytokine response, as demonstrated in cystic fibrosis airway epithelial cells (31). In contrast to the established role of rhinovirus in lower respiratory tract infections, its role in disease pathogenesis of the upper respiratory tract, in particular during OM, remains enigmatic. For instance, rhinoviruses are commonly detected in subjects with mild symptoms or even from asymptomatic individuals (33,34).

In a study performed by Pitkaranta *et al.* in which rhinovirus RNA was detected by in situ hybridization, rhinovirus RNA was not found in any of the 18 middle ear biopsies of children with longstanding OME. In contrast, seven out of eight adenoid biopsies were positive for rhinovirus. These results show that children with longstanding OME do not have a rhinovirus infection in the middle ear mucosa, although the same children frequently harbor large amounts of rhinovirus RNA in their adenoid tissue (35). Nevertheless, some studies have suggested that rhinovirus may play a role in the development of chronic OM with effusion (COME) (36;37). The contribution of rhinovirus in the middle ear may be more indirect in that they facilitate bacterial replication, but do not trigger an inflammatory response themselves.

There are a number of limitations to this study. First, the appearance of a significant amount of fluid into the middle ear cavity is a pathological condition that is not apparent in healthy individuals. Consequently, it is not possible to include healthy controls. Furthermore, although we used internationally accepted definitions for rAOM and COME, the timing of clinical sampling in relation to the exact onset of OM infection is unknown. Moreover, whilst bacteria can colonize and persist in the human respiratory tract for weeks to months, infection with any of the 15 tested respiratory viruses results in acute viral replication, which is cleared within days to weeks. As a consequence, the persistence of bacterial DNA probably exceeds that of viruses (38,39).

Importantly, in 19% and 27% of the MEFs, no pathogens or only viral pathogens were detected, respectively. In these patients, cytokine responses were relatively low, as compared to those that contained bacteria. As such, subsequent destructive effects such as sensorineural hearing loss and bone erosion as induced by e.g. IL-1β may be limited in these patients. This raises the question whether it is valid to discriminate recurrent and chronic OM patients based on the detection of (bacterial) pathogens and/or cytokine profile in the middle ear. In addition to clinical presentation, measurement of bacterial load and cytokine levels may assist in the guidance of treatment to appropriately accommodate patients who are at risk to develop complications.

Acknowledgments

We thank all children and parents who participated in this study. We are grateful to the staff of the departments ORL and Medical Microbiology at Canisius Wilhelmina Hospital and Radboud University Nijmegen Medical Centre for their commitment to our study, in particular M. de Bruyn (CWZ) and C. Bartels and K. Teuwen (RUNMC) for excellent study coordination. E.R. Simonetti is acknowledged for technical assistance. We thank G.F. Borm for assistance in the statistical analysis.

References

1. Alper CM, Winther B, Mandel EM, Doyle WJ. Temporal Relationships for Cold-like Illnesses and Otitis Media in Sibling Pairs. Pediatr Infect Dis J 2007;26(9):778-81.
2. Nokso-Koivisto J, Raty R, Blomqvist S et al. Presence of specific viruses in the middle ear fluids and respiratory secretions of young children with acute otitis media. J Med Virol 2004;72(2):241-8.
3. Ogra PL. Respiratory syncytial virus: the virus, the disease and the immune response. Paediatr Respir Rev 2004;5 Suppl A:S119-26.:S119-S126.
4. Ruohola A, Meurman O, Nikkari S et al. Microbiology of acute otitis media in children with tympanostomy tubes: prevalences of bacteria and viruses. Clin Infect Dis 2006;43(11):1417-22.
5. Willett DN, Rezaee RP, Billy JM, Tighe MB, DeMaria TF. Relationship of endotoxin to tumor necrosis factor-alpha and interleukin-1 beta in children with otitis media with effusion. Ann Otol Rhinol Laryngol 1998;107(1):28-33.
6. Scharer G, Zaldivar F, Gonzalez G, Vargas-Shiraishi O, Singh J, Arrieta A. Systemic inflammatory responses in children with acute otitis media due to *Streptococcus pneumoniae* and the impact of treatment with clarithromycin. Clin Diagn Lab Immunol 2003;10(4):721-4.
7. Maeda K, Hirano T, Ichimiya I, Kurono Y, Suzuki M, Mogi G. Cytokine expression in experimental chronic otitis media with effusion in mice. Laryngoscope 2004;114(11):1967-72.
8. Skotnicka B, Hassmann E. Proinflammatory and immunoregulatory cytokines in the middle ear effusions. Int J Pediatr Otorhinolaryngol 2008;72(1):13-7.
9. Leibovitz E, Dagan R, Laver JH et al. Interleukin 8 in middle ear fluid during acute otitis media: correlation with aetiology and bacterial eradication. Arch Dis Child 2000;82(2):165-8.
10. Bikhazi P, Ryan AF. Expression of immunoregulatory cytokines during acute and chronic middle ear immune response. Laryngoscope 1995;105(6):629-34.
11. Smirnova MG, Birchall JP, Pearson JP. The immunoregulatory and allergy-associated cytokines in the aetiology of the otitis media with effusion. Mediators Inflamm 2004;13(2):75-88.
12. van der Sluijs KF, van Elden LJ, Nijhuis M et al. IL-10 is an important mediator of the enhanced susceptibility to pneumococcal pneumonia after influenza infection. J Immunol 2004;172(12):7603-9.
13. Besnard AG, Togbe D, Couillin I et al. Inflammasome - IL-1 - Th17 response in allergic lung inflammation. J Mol Cell Biol 2011.
14. Oliver BG, Lim S, Wark P et al. Rhinovirus exposure impairs immune responses to bacterial products in human alveolar macrophages. Thorax 2008;63(6):519-25.
15. Veenhoven R, Bogaert D, Uiterwaal C et al. Effect of conjugate pneumococcal vaccine followed by polysaccharide pneumococcal vaccine on recurrent acute otitis media: a randomised study. Lancet 2003;361(9376):2189-95.
16. van Heerbeek N, Straetemans M, Wiertsema SP et al. Effect of combined pneumococcal

conjugate and polysaccharide vaccination on recurrent otitis media with effusion. Pediatrics 2006;117(3):603-8.
17. Kais M, Spindler C, Kalin M, Ortqvist A, Giske CG. Quantitative detection of *Streptococcus pneumoniae*, *Haemophilus influenzae*, and *Moraxella catarrhalis* in lower respiratory tract samples by real-time PCR. Diagn Microbiol Infect Dis 2006;55(3):169-78.
18. Hall-Stoodley L, Hu FZ, Gieseke A et al. Direct detection of bacterial biofilms on the middle-ear mucosa of children with chronic otitis media. JAMA 2006;296(2):202-11.
19. Hays JP, van SS, Hoogenboezem T et al. Identification and characterization of a novel outer membrane protein (OMP J) of *Moraxella catarrhalis* that exists in two major forms. J Bacteriol 2005;187(23):7977-84.
20. Templeton KE, Scheltinga SA, Beersma MF, Kroes AC, Claas EC. Rapid and sensitive method using multiplex real-time PCR for diagnosis of infections by influenza a and influenza B viruses, respiratory syncytial virus, and parainfluenza viruses 1, 2, 3, and 4. J Clin Microbiol 2004;42(4):1564-9.
21. Patel JA, Nair S, Grady J et al. Systemic cytokine response profiles associated with respiratory virus-induced acute otitis media. Pediatr Infect Dis J 2009;28(5):407-11.
22. Patel JA, Nair S, Revai K, Grady J, Chonmaitree T. Nasopharyngeal acute phase cytokines in viral upper respiratory infection: impact on acute otitis media in children. Pediatr Infect Dis J 2009;28(11):1002-7.
23. Berman S. Otitis media in children. N Engl J Med 1995;332(23):1560-5.
24. Rovers MM, Schilder AG, Zielhuis GA, Rosenfeld RM. Otitis media. Lancet 2004;363(9407):465-73.
25. Post JC, Preston RA, Aul JJ et al. Molecular analysis of bacterial pathogens in otitis media with effusion. JAMA 1995;273(20):1598-604.
26. Coates H, Thornton R, Langlands J et al. The role of chronic infection in children with otitis media with effusion: evidence for intracellular persistence of bacteria. Otolaryngol Head Neck Surg 2008;138(6):778-81.
27. Hall-Stoodley L, Hu FZ, Gieseke A et al. Direct detection of bacterial biofilms on the middle-ear mucosa of children with chronic otitis media. JAMA 2006;296(2):202-11.
28. Skovbjerg S, Roos K, Nowrouzian F et al. High cytokine levels in perforated acute otitis media exudates containing live bacteria. Clin Microbiol Infect 2010;16(9):1382-8.
29. Rodriguez WJ, Schwartz RH. Streptococcus pneumoniae causes otitis media with higher fever and more redness of tympanic membranes than Haemophilus influenzae or Moraxella catarrhalis. Pediatr Infect Dis J 1999;18(10):942-4.
30. Message SD, Laza-Stanca V, Mallia P et al. Rhinovirus-induced lower respiratory illness is increased in asthma and related to virus load and Th1/2 cytokine and IL-10 production. Proc Natl Acad Sci U S A 2008;105(36):13562-7.
31. Chattoraj SS, Ganesan S, Jones AM et al. Rhinovirus infection liberates planktonic bacteria from biofilm and increases chemokine responses in cystic fibrosis airway epithelial cells. Thorax 2011;66(4):333-9.
32. Chantzi FM, Papadopoulos NG, Bairamis T et al. Human rhinoviruses in otitis media with effusion. Pediatr Allergy Immunol 2006;17(7):514-8.
33. Peltola V, Waris M, Osterback R, Susi P, Hyypia T, Ruuskanen O. Clinical effects of rhinovirus infections. J Clin Virol 2008;43(4):411-4.
34. Rezes S, Soderlund-Venermo M, Roivainen M et al. Human bocavirus and rhino-enterovi-

ruses in childhood otitis media with effusion. J Clin Virol 2009;46(3):234-7.
35. Pitkaranta A, Rihkanen H, Carpen O, Vaheri A. Rhinovirus RNA in children with longstanding otitis media with effusion. Int J Pediatr Otorhinolaryngol 2002;66(3):247-50.
36. Elkhatieb A, Hipskind G, Woerner D, Hayden FG. Middle ear abnormalities during natural rhinovirus colds in adults. J Infect Dis 1993;168(3):618-21.
37. Pitkaranta A, Jero J, Arruda E, Virolainen A, Hayden FG. Polymerase chain reaction-based detection of rhinovirus, respiratory syncytial virus, and coronavirus in otitis media with effusion. J Pediatr 1998;133(3):390-4.
38. Smith-Vaughan HC, McBroom J, Mathews JD. Modelling of endemic carriage of Haemophilus influenzae in Aboriginal infants in Northern Australia. FEMS Immunol Med Microbiol 2001;31(2):137-43.
39. Jartti T, Lee WM, Pappas T, Evans M, Lemanske RF, Jr., Gern JE. Serial viral infections in infants with recurrent respiratory illnesses. Eur Respir J 2008;32(2):314-20.

Comparative analysis of the humoral immune response to *Moraxella catarrhalis* and *Streptococcus pneumoniae* surface antigens in children suffering from rAOM and COME

S.J.C. Verhaegh‡, K. Stol‡, C.P. de Vogel, K. Riesbeck, E.R. Lafontaine, T.F. Murphy, A. van Belkum, P.W.M. Hermans, J.P. Hays

‡ These authors contributed equally to this study

Clinical Vaccine Immunology 2012, 19(6):914-8

Abstract

A prospective clinical cohort study was established to investigate the humoral immune response in middle ear fluids (MEF) and serum against bacterial surface proteins in children suffering from recurrent acute otitis media (rAOM) and chronic otitis media with effusion (COME), using Luminex xMAP technology. The association between the humoral immune response and the presence of *M. catarrhalis* and *S. pneumoniae* in the nasopharynx and middle ear was also studied.

The levels of antigen-specific IgG, IgA and IgM showed extensive inter-individual variation. No significant difference in anti-*M. catarrhalis* and *S. pneumoniae* serum and MEF MFI values (anti-*M. catarrhalis* and anti-pneumococcal IgG levels) was observed between the rAOM or COME groups for all antigens tested.

No significant difference was observed for *M. catarrhalis* and *S. pneumoniae* colonization and serum IgG levels against the Moraxella and pneumococcal antigens. Similar to the antibody response in serum, no significant difference in IgG, IgA and IgM levels in MEF was observed for all *M. catarrhalis* and *S. pneumoniae* antigens between OM *M. catarrhalis* or *S. pneumoniae* positive and OM *M. catarrhalis* or *S. pneumoniae* negative children suffering from either rAOM or COME. Finally, results indicated a strong correlation between antigen-specific serum and MEF IgG levels.

We observed no significant in vivo expressed anti-*M. catarrhalis* or anti-*S. pneumoniae* humoral immune responses using a range of putative vaccine candidate proteins. Other factors such as Eustachian-tube dysfunction, viral load, and genetic and environmental factors may play a more important role in the pathogenesis of OM, and in particular in the development of rAOM or COME.

Introduction

Otitis media (OM) is an important upper respiratory tract disease of early childhood and the primary reason for young children to visit a physician. The disease has a considerable negative impact on the quality of life during childhood and causes much concern to parents. OM encompasses a spectrum of conditions, including acute otitis media (AOM) and otitis media with effusion (OME), with approximately 80% of children having experienced an episode of AOM by the age of three years. Up to one-third of these children will have experienced recurrent infections, with many of these episodes being facilitated by a bacterial infection (3,37). In fact, bacteria may be isolated from the middle ear fluid (MEF) of approximately 80% of children with AOM, and 30-50% of chronic middle ear effusions obtained from children presenting with OME (12). In many countries, OM is a common reason to prescribe antibiotics or to undergo surgery for the insertion of ventilation tubes, resulting in a significant burden on healthcare systems (21,25,29). This means that the direct costs associated with OM are substantial (2), and that the prevention of OM disease via alternative methods such as vaccination offer a promising approach to reduce the burden of OM disease and its economic consequences.

Traditionally, *Streptococcus pneumoniae* has been reported to be the predominant bacterial species cultured in AOM disease, followed by *Haemophilus influenzae* and *Moraxella catarrhalis*. However, *H. influenzae* tends to predominate in OME disease, followed to a lesser extent by *S. pneumoniae* and *M. catarrhalis* (7,9,32). Further, although these common OM-related bacterial species may be cultured from the middle ear of children during OM episodes, either as single pathogens or as co-cultures (28), research has also shown the importance of (frequently culture negative) bacterial biofilm formation in the development of middle ear disease (22). Finally, the introduction of a conjugated heptavalent pneumococcal vaccine (PCV7) for use in children in the community has resulted in a significant reduction in the overall proportion of *S. pneumoniae* isolates and vaccine serotypes observed in AOM. Indeed, the success of vaccination against *S. pneumoniae* now means that *H. influenzae* is now becoming the predominant pathogen isolated from children suffering from persistent AOM disease (6,10).

Children are frequently colonized with bacterial pathogens at an early age and the pattern of nasopharyngeal colonization is an important determinant for OM disease (15-16). Further, research has also indicated that, as well as the presence of particular bacterial species, both the adaptive and innate immune systems, Eustachian-tube dysfunction,

viral load, and genetic and environmental factors all may be involved in the pathogenesis of OM (19,23,30-31,33,38).

The recent recognition of *M. catarrhalis* as an important human pathogen has stimulated active investigation into the molecular mechanisms of its pathogenesis. An essential step in colonization and infection is bacterial adherence to the mucosal epithelium of the respiratory tract. A growing number of adhesins have been identified in *M. catarrhalis* and most of these proteins are highly conserved, immunogenic and express distinct epitopes on the bacterial surface. This means that they may be suitable as potential *M. catarrhalis* vaccine candidates (27). However, relatively little is known regarding the development of the natural humoral immune response to these potential vaccine candidates in children. As yet, no licensed vaccine has been marketed against *M. catarrhalis,* and to date, none of the putative vaccine candidates so far described in the literature have actually progressed to clinical trials.

On the other hand, vaccination against *S. pneumoniae* infection is already established, for example via the introduction of the PCV7 vaccine. PCV7 was primarily used to prevent invasive pneumococcal disease (meningitis and other pneumococcal infections such as pneumonia) in children, with the introduction of PCV7 having lead to a noticeable reduction in the incidence of *S. pneumoniae* vaccine strains in the etiology of AOM (13). However, an increase in the carriage of non-vaccine serotypes has been reported, as well as a consequent increase in invasive disease by these non-vaccine serotypes, which could reduce, or even negate the benefits initially obtained through vaccination with PCV7 (11,26). In fact, *S. pneumoniae* serotype replacement and subsequent vaccine failure in PCV7 vaccinated children has become a serious concern in recent years, with most of these problems assigned to the serotype specific nature of the PCV7 vaccine. Currently, several pneumococcal surface proteins, either alone or in combinations, have been suggested as putative vaccine candidates (1,13,20), and could serve as more effective vaccines than those currently available, providing broad coverage against most pneumococcal serotypes. However, similar to the situation faced by vaccine candidates of *M. catarrhalis,* relatively little is known about the development of the humoral immune response to *S. pneumoniae* protein-based vaccine candidates in children.

With this study, we provide insights into the anti-*M. catarrhalis* and anti-pneumococcal humoral immune response in a cohort comprising Dutch children exhibiting recurrent (recurrent acute otitis media, rAOM) and chronic (chronic otitis media with effusion, COME) episodes of OM. Currently, there is a common perception that rAOM tends to be caused by recurrent episodes of AOM that are associated with bacteria and/or viral infections. In contrast, COME is generally considered a sterile inflammation. Studying the immune

response and the accompanying pathogens associated with rAOM and COME will allow us to better distinguish the types of bacterial and immune factors that are involved in the pathogenesis of rAOM and COME, and leading to a better understanding of the pathogenesis of these 2 clinical presentations of OM disease.

Materials & Methods

Study cohort

This study was performed as part of a prospective clinical cohort study set up at Radboud University Nijmegen Medical Centre (RUNMC), Nijmegen, The Netherlands, to determine the immune response to putative vaccine candidates of *M. catarrhalis* and *S. pneumoniae* in children suffering OM disease.

Patients were enrolled in two hospitals in Nijmegen, The Netherlands, from April 1st 2008 to July 1st 2009, with ages ranging from birth up to 5 years of age, and all suffering from rAOM or COME (for which tympanostomy tube insertion was indicated). Recurrent OM was defined as 3 or more episodes of AOM in the last 6 months or 4 episodes in the last 12 months. The COME patient population consisted of children who experienced a period of persistent OM lasting longer than 3 months. Diagnosis was made by an otolaryngologist based upon signs, symptoms, otoscopy and audiometry including tympanometry. Patient characteristics and risk factors were identified using a questionnaire. Permission was obtained from the Committee on Research Involving Human Subjects in January 2008 (CMO 2007/239, international trial register number NCT00847756).

Clinical materials and detection of bacterial pathogens

Middle ear fluid, a nasopharyngeal swab and serum were collected during surgery. Nasopharyngeal swabs were cultured according to standard laboratory procedures in order to determine the presence of *M. catarrhalis* and *S. pneumoniae*. Quantitative real-time PCR (Q-PCR) was performed in order to determine the presence of *M. catarrhalis* and *S. pneumoniae* in MEF.

Moraxella catarrhalis antigens

The previously described *M. catarrhalis* recombinant proteins used in this study comprised: ubiquitous surface proteins A (UspA1$^{557\text{-}704}$ (aa 557–704 of UspA1) and UspA2$^{165\text{-}318}$), two fragments of *Moraxella* immunoglobulin D-binding protein (MID$^{764\text{-}913}$ and MID$^{962\text{-}1200}$), human erythrocyte agglutinin (Hag$^{385\text{-}863}$), *M. catarrhalis* hemagglutinin-like proteins (MhaB and MhaC) and *M. catarrhalis* adherence protein (McaP$^{51\text{-}333}$). Orf238 and orf296 are hypothetical proteins that share homology with lipoprotein family A proteins and with an *M. osloensis* disulfide isomerase gene virulence factor, respectively. These 10 recombinant proteins (from 8 different OMPs) represented the majority of published *M. catarrhalis* immunogenic

proteins discovered at the time that the study was initiated, and are derived from the reference *M. catarrhalis* strains Bc5 (UspA1$^{557-704}$, UspA2$^{165-318}$, MID$^{764-913}$ and MID$^{962-1200}$) and O35E (MhaB, MhaC, McaP$^{51-333}$ and Hag$^{385-863}$) (5, 24, 34-35).

Streptococcus pneumoniae antigens

The previously described *S. pneumoniae* recombinant proteins used in this study comprised: choline binding protein A (PspC/CbpA), α-enolase (Eno), hyaluronidase (Hyl), immunoglobulin A1 (IgA-1) protease, neuraminidase (NanA), pneumolysin (PLY), a double mutant of pneumolysin (PdbD), putative protease maturation protein A (PpmA), pneumococcal surface adhesin A (PsaA), pneumococcal surface protein A (PspA), the pneumococcal histidine triad (Pht) proteins (SP1003 (PhtD) and BVH-3 (PhtE)), streptococcal lipoprotein rotamase A (SlrA), *S. pneumoniae* proteins (SP proteins) SP0189 (hypothetical protein), SP0376 (response regulator, intracellular location), SP1651 (thiol peroxidase, intracellular location), and Pilus A (8, 20).

Multiplex *M. catarrhalis* and *S. pneumoniae* antibody assay

Recombinant proteins were coupled to carboxylated SeroMAP™ beads that were developed for serological application, as detailed by Verkaik *et al.* (39). Uncoupled beads were used as negative control to determine non-specific antibody binding. If non-specific binding was observed, then the median fluorescence intensity (MFI) values obtained from this non-specific binding were subtracted from the antigen-specific results.

The Luminex multiplex procedure was performed as described previously (39). Briefly, after validation of the assay (achieved by comparison of human pooled serum (HPS) MFI values obtained using the multiplex assay with HPS MFI values obtained using the singleplex assays), the different antigen-coupled microspheres were mixed to a working concentration of 4000 beads per color per well. Serum samples were diluted 1:100 in phosphate-buffered saline containing 1% bovine serum albumin (PBS-BN) for measurement of antigen-specific IgG. Fifty microliters per diluted sample were incubated with the microspheres in a 96-well filter microtiter plate (Millipore) for 35 min at room temperature on a Thermomixer plate shaker (Eppendorf). The plate was washed twice with assay buffer (PBS-BN) and aspirated using a vacuum manifold. The microspheres were suspended in 50 μl of assay buffer, and 50 μl of a 1:200 dilution of R-phycoerythrin (RPE)-conjugated AffiniPure goat anti-human IgG (Jackson Immuno Research) was added in separate wells. The plate was incubated for 35 min at room temperature and washed. The microspheres were suspended in 100 μl of assay buffer. Measurements were performed on the Luminex 100 instrument (BMD) using Luminex IS software (version 2.2). Tests were performed in

duplicate, and the MFI values, reflecting quantitative antibody levels, were averaged. The coefficient of variation was calculated for each serum sample and averaged per protein and antibody isotype. The procedure for MEF was identical to that outlined above, except that IgA and IgM were also measured. Briefly, MEF samples were diluted 1:100 in PBS-BN for measurement of antigen-specific IgG and 1:50 for measurement of IgA and IgM. Fifty microliters of a 1:100 dilution of RPE-conjugated AffiniPure goat anti-human IgG and IgA and 50 μl of a 1:200 dilution of RPE-conjugated donkey anti-human IgM were then added. For assay validation, MFI values obtained from pooled MEF (PMEF) using the multiplex assay were compared to MFI values obtained from PMEF obtained using the singleplex assay.

Statistical analysis

Statistical analyses were performed using SPSS PASW Statistics version 17. Correlations between antigen-specific IgG in serum and MEF were assessed using Spearman's correlation coefficient. The Mann-Whitney *U*-test was used to compare anti-*M. catarrhalis* and anti-pneumococcal immunoglobulin (Ig) levels between children diagnosed with rAOM and COME and to compare differences in Ig levels between colonized and non-colonized children. The Bonferroni correction was applied to correct for multiple testing. A *P*-value of $\leq$0.00064 was considered to be statistically significant.

Results

Correlation between anti-*M. catarrhalis* and anti-pneumococcal IgG levels in serum and MEF

To determine the correlation between the levels of anti-*Moraxella* and anti-pneumococcal IgG in serum compared to MEF, samples from 111 children who donated both blood and MEF at tympanostomy surgery were included. The mean IgG levels (reflected by MFI values) in these samples were calculated for each protein (figure 1). IgG levels in serum showed a strong correlation to IgG levels in MEF for both *M. catarrhalis* ($R^2 = 0.97$) as well as *S. pneumoniae* ($R^2 = 0.89$).

Dynamics of the anti-*M. catarrhalis* and anti-pneumococcal antibody response in children with recurrent and chronic otitis media disease

A total of 156 children were included in the analysis of the antibody response to *M. catarrhalis* and *S. pneumoniae* proteins in serum. Forty-two children were diagnosed with rAOM, whereas 114 children were diagnosed with COME. No significant difference in anti-*M. catarrhalis* and *S. pneumoniae* serum MFI values (anti-*M. catarrhalis* and anti-pneumococcal IgG levels) was observed between the rAOM or COME groups for all antigens tested.

A total of 121 children were included in the analysis of the antibody response to *M. catarrhalis* and *S. pneumoniae* proteins in MEF, with 25 children and 96 children diagnosed with rAOM and COME, respectively. No significant difference in anti-*M. catarrhalis* and anti-pneumococcal MEF IgG, IgA and IgM levels were found for all proteins tested.

Association between bacterial colonization and infection and anti-*M. catarrhalis* and anti-pneumococcal antibody levels in children with rAOM and COME

A total of 156 children were included in the analysis of the antibody IgG response to *M. catarrhalis* and *S. pneumoniae* antigens in serum. Forty-two children were diagnosed with rAOM, whereas 114 children were diagnosed with COME. No significant difference was observed for the presence of *M. catarrhalis* and *S. pneumoniae* and serum IgG levels against the *Moraxella* and pneumococcal antigens.

A total of 117 children were included in the analysis of the antibody response to *M. catarrhalis* and *S. pneumoniae* proteins in MEF, including 23 children suffering from rAOM and 94 children suffering from COME. Similar to the antibody response in serum, no significant difference in IgG, IgA and IgM levels in MEF was observed for all *M. catarrhalis* and

S. pneumoniae antigens between OM *M. catarrhalis* or *S. pneumoniae* positive and OM *M. catarrhalis* or *S. pneumoniae* negative children suffering from either rAOM or COME.

Figure 2 shows an example of the results obtained; specifically the figure shows a comparison of anti-pneumococcal IgA-1 protease IgA levels in COME-positive children in the presence and absence of *S. pneumoniae* in the middle ear.

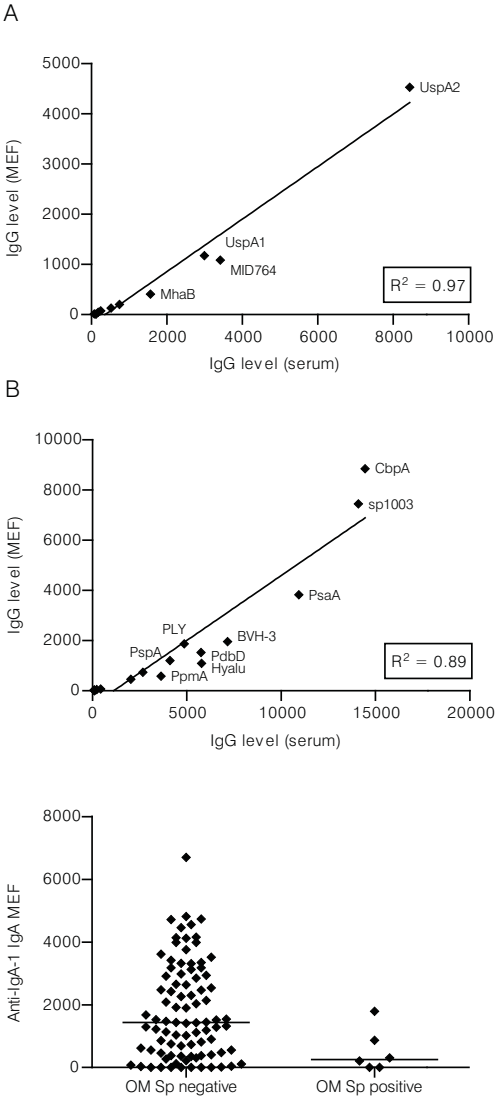

Figure 1. Correlation between IgG levels in serum and MEF. Mean IgG levels in serum and MEF were used to calculate the correlation statistics for each respective *M. catarrhalis* (A) or *S. pneumoniae* (B) protein (Spearman's correlation coefficient, R^2 = 0.97 and 0.89).

Figure 2. Example of the results obtained; specifically the figure shows a comparison of anti-pneumococcal IgA-1 protease IgA levels in COME-positive children in the presence and absence of *S. pneumoniae* in the middle ear.

Discussion

Studies have shown that *M. catarrhalis* and *S. pneumoniae* colonize the nasopharynx soon after birth and frequent colonization with *M. catarrhalis* and *S. pneumoniae* has been reported to increase the risk of OM (15). The adaptive immune system and the innate immune system are also important factors in the pathogenesis of OM (31). The immune response to pathogens develops rapidly during the first few years of life, as children become exposed to an increasing number of microbial species and strains. The high incidence and high rate of 'spontaneous' recovery from OM suggests that recovery is a natural phenomenon and part of the gradual maturation of the child's immune system, though a defective or immature antibody response to OM pathogens may explain the increased susceptibility of some children to OM (36).

Differences in the presence / absence and levels of pathogen-specific IgG and IgM at particular body sites may be one of the mechanisms by which OM pathogens are able to facilitate the development of OM disease. In this study, no significant difference in anti-*M. catarrhalis* and anti-*S. pneumoniae* serum and MEF IgG levels was observed between the rAOM or COME groups for all antigens tested, suggesting that differences in IgG levels between body sites does not play a significant role in the development of rAOM or COME disease. Interestingly however, a strong correlation was observed between IgG antibody levels in serum and IgG antibody levels in MEF, for both *M. catarrhalis* and pneumococcal proteins for the whole study cohort. This is an interesting finding, as it indicates that serum antibody levels are predictive of the presence of local (middle ear) IgG antibody (14,17), and raises the possibility that the measurement of OM pathogen-specific IgG antibodies in the middle ear may be achieved by simply measuring OM pathogen-specific serum IgG antibody levels in serum. At this moment in time however, it is not known whether OM pathogen-specific IgG is actually produced locally in the middle ear or transudes into the middle ear from the general circulation (4,14). From our results, it appears more likely that OM pathogen-specific IgG actually transudes into the middle ear rather than being locally produced, where it potentially provides some protection against OM disease. No significant difference in anti-*M. catarrhalis* and anti-*S. pneumoniae* MEF IgM levels was observed for either rAOM or COME cohort in this study.

The local production of secretory antibody is an important immunological defense at epithelial surfaces including the surfaces of the upper respiratory tract and middle ear. Secretory IgA has been shown to inhibit *S. pneumoniae* adherence and reduce naso-

pharyngeal bacterial colonization (18), and it is therefore possible that children with recurrent OM might lack OM pathogen-specific secretory IgA. In this study, the MFI levels of antigen-specific IgA showed extensive inter-individual variability over time, with IgA levels to all *M. catarrhalis* and *S. pneumoniae* OMPs being relatively low throughout the study period. However, though not significant, *S. pneumoniae*-negative / COME-positive children showed higher MEF IgA levels against the pneumococcal IgA-1 protease protein compared to *S. pneumoniae*-positive / COME-positive children. In fact, many mucosal pathogens, including *S. pneumoniae*, express an IgA-1 protease that cleaves IgA molecules, thereby circumventing the protective effects of IgA production (40). Our results suggest that IgA antibody directed against anti-IgA-1 protease may have a restorative effect by helping 'neutralizing' the effect of secreted anti-IgA-1 protease, thereby facilitating the binding of intact IgA to bacterial cells and promoting pathogen recognition and clearance by the immune response. However, it should be noted that the possibility exists that the differences in antibody levels observed in *S. pneumoniae* positive and negative COME MEFs are simply a product of antibody binding to *S. pneumoniae* bacterial cells, thereby making the antibodies inaccessible to measurement using our Luminex assay. Further research will be required in order to determine whether IgA-1 protease antibodies actually provide protection in patients suffering from OM disease.

Studying the immune response and pathogens associated with rAOM and COME disease indicated that COME is not in fact a sterile inflammation as is generally considered the case. Importantly, investigation into the immune response to potential vaccine candidates of *M. catarrhalis* and *S. pneumoniae* indicated that there may be a lack of a characteristic immune response profiles that will allow clinicians to distinguish between rAOM and COME. Our data correlate with the findings of Stol *et al.*, who investigated bacterial colonization and infection in the nasopharynx and middle ear of the same prospective cohort of children and found no clear-cut differences in the microbial flora present in middle ear fluids obtained during rAOM and COME disease.

In summary, the levels of antigen-specific serum IgG and MEF IgG / IgM / IgA showed extensive inter-individual variation in our rAOM and COME cohort of children, with no significant differences between the 2 groups. Both rAOM and COME children possessed a range of antibodies (IgG, IgA and IgM) against a variety of novel *M. catarrhalis* and *S. pneumoniae* recombinant proteins, and there were no distinguishing immune response profiles observed between the 2 groups. Factors such as Eustachian-tube dysfunction, viral load, and genetic and environmental factors may play a more important role in the pathogenesis of rAOM and COME disease than the humoral immune response to OM-associated bacterial pathogens.

Acknowledgments

The authors would like to thank all of the children and parents who participated in this study. We are grateful to the staff of the departments ORL and Medical Microbiology of the Canisius Wilhelmina Hospital and the Radboud University Nijmegen Medical Centre for their commitment to the study. The authors would like to thank Birgitta Henriques-Normark, and Timothy Mitchell for kindly supplying the *S. pneumoniae* proteins, and Nelianne J. Verkaik and Willem J. van Wamel for valuable discussions.

This work was supported by a European Union FP6 project grant [OMVac 037653].

References

1. American Academy of Pediatrics. 2000. Committee on Infectious Diseases. Policy statement: recommendations for the prevention of pneumococcal infections, including the use of pneumococcal conjugate vaccine (Prevnar), pneumococcal polysaccharide vaccine, and antibiotic prophylaxis. Pediatrics 106:362-366.
2. American Academy of Pediatrics Subcommittee on Management of Acute Otitis Media. 2004. Diagnosis and management of acute otitis media. Pediatrics 113:1451-1465.
3. Arguedas, A., K. Kvaerner, J. Liese, A. G. Schilder, and S. I. Pelton. 2010. Otitis media across nine countries: disease burden and management. Int. J. Pediatr. Otorhinolaryngol. 74:1419-1424.
4. Bakaletz, L. O., and K. A. Holmes. 1997. Evidence for transudation of specific antibody into the middle ears of parenterally immunized chinchillas after an upper respiratory tract infection with adenovirus. Clin. Diagn. Lab. Immunol. 4:223-225.
5. Balder, R., J. Hassel, S. Lipski, and E. R. Lafontaine. 2007. *Moraxella catarrhalis* strain O35E expresses two filamentous hemagglutinin-like proteins that mediate adherence to human epithelial cells. Infect. Immun. 75:2765-2775.
6. Block, S. L., J. Hedrick, C. J. Harrison, R. Tyler, A. Smith, R. Findlay, and E. Keegan. 2004. Community-wide vaccination with the heptavalent pneumococcal conjugate significantly alters the microbiology of acute otitis media. Pediatr Infect Dis J. 23:829-833.
7. Bluestone, C. D., J. S. Stephenson, and L. M. Martin. 1992. Ten-year review of otitis media pathogens. Pediatr. Infect. Dis. J. 11:S7-11.
8. Bogaert, D., P. W. Hermans, P. V. Adrian, H. C. Rumke, and R. de Groot. 2004. Pneumococcal vaccines: an update on current strategies. Vaccine 22:2209-2220.
9. Broides, A., R. Dagan, D. Greenberg, N. Givon-Lavi, and E. Leibovitz. 2009. Acute otitis media caused by *Moraxella catarrhalis*: epidemiologic and clinical characteristics. Clin. Infect. Dis. 49:1641-1647.
10. Casey, J. R., and M. E. Pichichero. 2004. Changes in frequency and pathogens causing acute otitis media in 1995-2003. Pediatr Infect Dis J. 23:824-828.
11. Chibuk, T. K., J. L. Robinson, and D. S. Hartfield. 2010. Pediatric complicated pneumonia and pneumococcal serotype replacement: trends in hospitalized children pre and post introduction of routine vaccination with Pneumococcal Conjugate Vaccine (PCV7). Eur. J. Pediatr. 169:1123-1128.
12. De Baere, T., M. Vaneechoutte, P. Deschaght, J. Huyghe, and I. Dhooge. 2010. The prevalence of middle ear pathogens in the outer ear canal and the nasopharyngeal cavity of healthy young adults. Clin. Microbiol. Infect. 16:1031-1035.
13. De Wals, P., S. Black, R. Borrow, and D. Pearce. 2009. Modeling the impact of a new vaccine on pneumococcal and nontypable *Haemophilus influenzae* diseases: a new simulation model. Clin. Ther. 31:2152-2169.
14. Faden, H., L. Brodsky, J. Bernstein, J. Stanievich, D. Krystofik, C. Shuff, J. J. Hong, and P. L. Ogra. 1989. Otitis media in children: local immune response to nontypeable *Haemophilus influenzae*. Infect. Immun. 57:3555-3559.

15. Faden, H., L. Duffy, R. Wasielewski, J. Wolf, D. Krystofik, and Y. Tung. 1997. Relationship between nasopharyngeal colonization and the development of otitis media in children. Tonawanda/Williamsville Pediatrics. J. Infect. Dis. 175:1440-1445.
16. Faden, H., M. J. Waz, J. M. Bernstein, L. Brodsky, J. Stanievich, and P. L. Ogra. 1991. Nasopharyngeal flora in the first three years of life in normal and otitis-prone children. Ann. Otol. Rhinol. Laryngol. 100:612-615.
17. Faden, H. S. 1997. Immunology of the middle ear: role of local and systemic antibodies in clearance of viruses and bacteria. Ann. N. Y. Acad. Sci. 830:49-60.
18. Fukuyama, Y., J. D. King, K. Kataoka, R. Kobayashi, R. S. Gilbert, K. Oishi, S. K. Hollingshead, D. E. Briles, and K. Fujihashi. 2010. Secretory-IgA antibodies play an important role in the immunity to *Streptococcus pneumoniae*. J. Immunol. 185:1755-1762.
19. Garcia-Rodriguez, J. A., and M. J. Fresnadillo Martinez. 2002. Dynamics of nasopharyngeal colonization by potential respiratory pathogens. J. Antimicrob. Chemother. 50 Suppl S2:59-73.
20. Giefing, C., A. L. Meinke, M. Hanner, T. Henics, M. D. Bui, D. Gelbmann, U. Lundberg, B. M. Senn, M. Schunn, A. Habel, B. Henriques-Normark, A. Ortqvist, M. Kalin, A. von Gabain, and E. Nagy. 2008. Discovery of a novel class of highly conserved vaccine antigens using genomic scale antigenic fingerprinting of pneumococcus with human antibodies. J. Exp. Med. 205:117-131.
21. Grevers, G., and E. N. T. M. G. First International Roundtable. 2010. Challenges in reducing the burden of otitis media disease: an ENT perspective on improving management and prospects for prevention. Int. J. Pediatr. Otorhinolaryngol. 74:572-577.
22. Hall-Stoodley, L., F. Z. Hu, A. Gieseke, L. Nistico, D. Nguyen, J. Hayes, M. Forbes, D. P. Greenberg, B. Dice, A. Burrows, P. A. Wackym, P. Stoodley, J. C. Post, G. D. Ehrlich, and J. E. Kerschner. 2006. Direct detection of bacterial biofilms on the middle-ear mucosa of children with chronic otitis media. JAMA 296:202-211.
23. Labout, J. A., L. Duijts, L. R. Arends, V. W. Jaddoe, A. Hofman, R. de Groot, H. A. Verbrugh, P. W. Hermans, and H. A. Moll. 2008. Factors associated with pneumococcal carriage in healthy Dutch infants: the Generation R Study. J. Pediatr. 153:771-776.
24. LaFontaine, E. R., L. E. Snipes, B. Bullard, A. L. Brauer, S. Sethi, and T. F. Murphy. 2009. Identification of domains of the Hag/MID surface protein recognized by systemic and mucosal antibodies in adults with chronic obstructive pulmonary disease following clearance of *Moraxella catarrhalis*. Clin Vaccine Immunol 16:653-659.
25. Leibovitz, E. 2003. Acute otitis media in pediatric medicine: current issues in epidemiology, diagnosis, and management. Paediatr Drugs 5 Suppl 1:1-12.
26. Melegaro, A., Y. H. Choi, R. George, W. J. Edmunds, E. Miller, and N. J. Gay. 2010. Dynamic models of pneumococcal carriage and the impact of the Heptavalent Pneumococcal Conjugate Vaccine on invasive pneumococcal disease. BMC Infect Dis 10:90.
27. Murphy, T. F., and G. I. Parameswaran. 2009. *Moraxella catarrhalis,* a human respiratory tract pathogen. Clin. Infect. Dis. 49:124-131.
28. Pettigrew, M. M., J. F. Gent, K. Revai, J. A. Patel, and T. Chonmaitree. 2008. Microbial interactions during upper respiratory tract infections. Emerg Infect Dis 14:1584-1591.
29. Plasschaert, A. I., M. M. Rovers, A. G. Schilder, T. J. Verheij, and E. Hak. 2006. Trends in doctor consultations, antibiotic prescription, and specialist referrals for otitis media in children: 1995-2003. Pediatrics 117:1879-1886.

30. Post, C. 2011. Genetics of otitis media. Adv. Otorhinolaryngol. 70:135-140.
31. Rovers, M. M., A. G. Schilder, G. A. Zielhuis, and R. M. Rosenfeld. 2004. Otitis media. Lancet 363:465-473.
32. Ruuskanen, O., and T. Heikkinen. 1994. Otitis media: etiology and diagnosis. Pediatr. Infect. Dis. J. 13:S23-26; discussion S50-24.
33. Rye, M. S., M. F. Bhutta, M. T. Cheeseman, D. Burgner, J. M. Blackwell, S. D. Brown, and S. E. Jamieson. 2011. Unraveling the genetics of otitis media: from mouse to human and back again. Mamm. Genome. 22:66-82.
34. Tan, T. T., J. J. Christensen, M. H. Dziegiel, A. Forsgren, and K. Riesbeck. 2006. Comparison of the serological responses to *Moraxella catarrhalis* immunoglobulin D-binding outer membrane protein and the ubiquitous surface proteins A1 and A2. Infect. Immun. 74:6377-6386.
35. Timpe, J. M., M. M. Holm, S. L. Vanlerberg, V. Basrur, and E. R. Lafontaine. 2003. Identification of a *Moraxella catarrhalis* outer membrane protein exhibiting both adhesin and lipolytic activities. Infect. Immun. 71:4341-4350.
36. Veenhoven, R., G. Rijkers, A. Schilder, J. Adelmeijer, C. Uiterwaal, W. Kuis, and E. Sanders. 2004. Immunoglobulins in otitis-prone children. Pediatr. Res. 55:159-162.
37. Vergison, A., R. Dagan, A. Arguedas, J. Bonhoeffer, R. Cohen, I. Dhooge, A. Hoberman, J. Liese, P. Marchisio, A. A. Palmu, G. T. Ray, E. A. Sanders, E. A. Simoes, M. Uhari, J. van Eldere, and S. I. Pelton. 2010. Otitis media and its consequences: beyond the earache. The Lancet infectious diseases 10:195-203.
38. Verhaegh, S. J., A. Lebon, J. A. Saarloos, H. A. Verbrugh, V. W. Jaddoe, A. Hofman, J. P. Hays, H. A. Moll, and A. van Belkum. 2010. Determinants of *Moraxella catarrhalis* colonization in healthy Dutch children during the first 14 months of life. Clin. Microbiol. Infect. 16:992-997.
39. Verkaik, N., E. Brouwer, H. Hooijkaas, A. van Belkum, and W. van Wamel. 2008. Comparison of carboxylated and Penta-His microspheres for semi-quantitative measurement of antibody responses to His-tagged proteins. J. Immunol. Methods 335:121-125.
40. Weiser, J. N., D. Bae, C. Fasching, R. W. Scamurra, A. J. Ratner, and E. N. Janoff. 2003. Antibody-enhanced pneumococcal adherence requires IgA1 protease. Proc. Natl. Acad. Sci. U. S. A. 100:4215-4220.

Modified lipooligosaccharide structure protects nontypeable *Haemophilus influenzae* from IgM-mediated complement killing in experimental otitis media

J.D. Langereis, K. Stol, E.K. Schweda, B. Twelkmeyer, H.J. Bootsma, S.P.W. de Vries, P. Burghout, D.A. Diavatopoulos and P.W.M. Hermans

MBio 2012, 3(4):e00079-12

Abstract

Nontypeable *Haemophilus influenzae* (NTHi) is a Gram-negative, human-restricted pathogen. Although this bacterium typically colonizes the nasopharynx in the absence of clinical symptoms, it is also one of the major pathogens causing otitis media (OM) in children. Complement represents an important aspect of the host defense against NTHi. In general, NTHi is efficiently killed by complement-mediated killing; however, various resistance mechanisms have also evolved. We measured the complement resistance of NTHi isolates isolated from the nasopharynx and the middle ear fluids of OM patients. Furthermore, we determined the molecular mechanism of NTHi complement resistance. Complement resistance was strongly increased in isolates from the middle ear, which correlated with decreased binding of IgM. We identified a crucial role for the R2866_0112 gene in complement resistance. Deletion of this gene altered the lipooligosaccharide (LOS) composition of the bacterium, which increased IgM binding and complement-mediated lysis. In a novel mouse model of coinfection with influenza virus, we demonstrate decreased virulence for the R2866_0112 deletion mutant. These findings identify a mechanism by which NTHi modifies its LOS structure to prevent recognition by IgM and activation of complement. Importantly, this mechanism plays a crucial role in the ability of NTHi to cause OM.

Importance

Nontypeable *Haemophilus influenzae* (NTHi) colonizes the nasopharynx of especially young children without any obvious symptoms. However, NTHi is also a major pathogen in otitis media (OM), one of the most common childhood infections. Although this pathogen is often associated with OM, the mechanism by which this bacterium is able to cause OM is largely unknown. Our study addresses a key biological question that is highly relevant for child health: what is the molecular mechanism that enables NTHi to cause OM? We show that isolates collected from the middle ear fluid exhibit increased complement resistance and that the lipooligosaccharide (LOS) structure determines IgM binding and complement activation. Modification of the LOS structure decreased NTHi virulence in a novel NTHi-influenza A virus coinfection OM mouse model. Our findings may also have important implications for other Gram-negative pathogens harboring LOS, such as *Neisseria meningitidis*, *Moraxella catarrhalis*, and *Bordetella pertussis*.

Introduction

Nontypeable *Haemophilus influenzae* (NTHi) is a Gram-negative bacterial pathogen that colonizes the upper respiratory tract of humans, generally in the absence of clinical symptoms. However, NTHi is also able to ascend the Eustachian tube to the middle ear and cause inflammation, resulting in otitis media (OM) (1). As such, NTHi accounts for almost 50% of all bacterial OM infections (2). Although acute OM is typically self-limiting, it can also lead to important sequelae such as meningitis and permanent hearing loss (3). Despite the fact that OM is one of the most common childhood diseases, the molecular processes underlying the migration of NTHi from the nasopharynx to the middle ear are poorly understood.

An important part of the innate immune system intended to clear pathogenic bacteria is the complement system. Activation of complement leads to a cascade of protein activation and deposition of complement factor C3b on the surface of bacteria, including NTHi (4), which may result in direct killing through the formation of the membrane-attack complex. NTHi strains are generally considered to be sensitive to complement-mediated lysis; however, studies have also shown that NTHi possesses complement resistance mechanisms, including variation and modifications in its lipooligosaccharide (LOS) composition (4). The LOS structure of NTHi consists of three parts: lipid A, an inner core comprised of a single 3-deoxy-d-manno-octulosonic acid (Kdo) linked to three heptoses, and an outer core containing a heteropolymer of mainly glucose and galactose moieties. Additional modifications have also been reported, including sialic acid, *N*-acetylgalactosamine, and phosphorylcholine (5,6). Variations in the composition of the LOS structure have previously been associated with decreased binding of antibodies and reduced complement deposition and have been suggested to contribute to the development of disease (7-11). Recently an important link between the presence of NTHi-specific IgM antibodies and colonization of the host was demonstrated (12). Although IgM binding and complement resistance were shown to play an important role in the lower respiratory tract during exacerbation of chronic obstructive pulmonary disease (COPD) by NTHi (10), it remains unclear whether similar immune evasion mechanisms are important during OM.

In this study, we investigated the contributions of IgM binding and complement-mediated killing of NTHi during OM. We show that NTHi strains isolated from the middle ear of children with OM are more complement resistant than are strains isolated from the nasopharynx. This decreased susceptibility correlated with decreased binding of IgM to

the bacterium. Expression of the R2866_0112 gene is essential for modifying the LOS structure, which prevents binding of IgM and confers bacterial resistance to complement-mediated killing, similar to our observation in clinical isolates. Finally, using a novel NTHi OM mouse model, we show that the R2866_0112 gene plays a crucial role in virulence.

Materials & Methods

Clinical isolates

Children up to 5 years of age who suffered from recurrent acute OM (rAOM) or chronic OM with effusion (COME) were enrolled in a retrospective clinical cohort study, which was approved by the Committee on Research Involving Human Subjects of the Radboud University Nijmegen Medical Centre (CMO 2007/239, international trial registration number NCT00847756). Legal guardians provided written informed consent. Middle ear fluid was collected during surgery using a middle ear fluid aspiration system (Kuijpers Instruments, Groesbeek, Netherlands), and nasopharyngeal samples were obtained using a cotton wool swab (Copan, Brescia, Italy). Middle ear fluid was mixed with 2 ml saline prior to bacterial culture and stored at −80°C. Isolates were serotyped using slide agglutination (BD Biosciences). All clinical isolates were minimally passaged *in vitro* (<4 passages).

Bacterial strains

Strains were grown with shaking at 225 rpm in brain heart infusion (BHI; BD Biosciences) supplemented with 10 μg/ml hemin (Sigma) and 2 μg/ml β-NAD (Merck), at 37°C and 5% CO_2. Live bacterial counts were determined by plating serial dilutions in phosphate-buffered saline (PBS) on BHI plates. For mutant libraries and gene deletion mutants, 150 μg/ml spectinomycin (Calbiochem) was added.

Generation of *H. influenzae* R2866 transposon mutant library

Genomic DNA was isolated with Genomic-tip 20/G (Qiagen) as described previously (29). The *H. influenzae marinerT7* transposon mutant library was generated as described previously for *S. pneumoniae* (13) with plasmid pGSF8 as a donor of the *marinerT7* transposon conferring spectinomycin resistance. Mutagenized genomic DNA was introduced into the bacterium with the M-IV transformation method (30).

Identifying genes involved in complement resistance

Genes involved in resistance to complement-mediated killing were identified by GAF (13,14). A volume of 0.1 ml (1×10^8 CFU/ml), containing approximately 30,000 unique mutants of the R2866 strain, was added to 0.4 ml of 50% normal human serum (NHS; GTI Diagnostics) or heat-inactivated (20 min, 56°C) NHS in phosphate-buffered saline (PBS) containing 0.1% gelatin (PBSG). Volumes of 100 μl were taken at 0, 30, and 60 min of

incubation at 37°C; diluted directly in 5 ml of supplemented BHI (sBHI); and cultured for 4.5 h. The GAF experiment was performed on two independent days in duplicate.

GAF readout was performed essentially as described previously, with some minor modifications (13). Chromosomal DNA was digested with HpyCH4V (New England Biolabs). Two micrograms of Cy3-labeled cDNA was hybridized to custom-made *H. influenzae* R2866 GAF Nimblegen microarrays. Probe signals were normalized using Analysis of NimbleGen Arrays Interface Suite (ANAIS) (31). Probes with >2.0-fold probe signal differences and a Bayesian *P* value of <0.001 (http://cybert.microarray.ics.uci.edu) were set as underrepresented following the challenge.

Generation of NTHi directed gene mutants

Targeted gene deletion mutants of NTHi were generated by allelic exchange of the target gene with an antibiotic resistance marker, as described previously for *S. pneumoniae* (14). DNA was introduced into the bacterium with the M-IV transformation method (30). All primers (Biolegio, Nijmegen, Netherlands) used in this study are listed in Table S1 in the supplemental material.

qRT-PCR

RNA was extracted from mid-log-phase-grown NTHi clinical isolates by using the RNeasy minikit (Qiagen) and was DNase treated (Ambion). One microgram of cDNA was synthesized using the SuperScript III reverse transcriptase kit (Invitrogen). Quantitative reverse transcription-PCR (qRT-PCR) was performed in a 20-μl reaction mixture with SYBR green PCR Master Mix (Applied Biosystems) on a 7500 Fast Real-Time PCR system (Applied Biosystems). The *gyrA*, *rpoA*, and *frdB* genes were used as the internal standard genes for GeNorm normalization (32).

R2866 expression microarray analysis

RNA was extracted from mid-log-phase-grown NTHi R2866 wild-type or R2866Δ0112 mutant cells by using the RNeasy minikit (Qiagen) and was DNase treated (Ambion). Cy3-labeled cDNA was obtained according to the Nimblegen array user's guide (http://www.nimblegen.com/products/lit/NG_Expression_Guide_v5p1.pdf). Two micrograms of Cy3-labeled cDNA was hybridized to custom-made *H. influenzae* R2866 expression Nimblegen microarrays. Probe signals were normalized using Analysis of NimbleGen Arrays Interface Suite (ANAIS) (31). Genes with a >2.5-fold signal difference and a Bayesian *P* value of <0.001 (http://cybert.microarray.ics.uci.edu) were selected to be significantly regulated.

Flow cytometric analysis

Hanks' buffered salt solution (HBSS) without Ca^{2+}/Mg^{2+}, containing 5% (vol/vol) heat-inactivated fetal calf serum, was used for all dilutions and washes. Surface opsonization with serum was performed by incubating bacteria in 5% heat-inactivated pooled human serum for 1 h at 37°C with 5% CO_2. Bacteria were fixed in 2% paraformaldehyde, and surface-bound IgM or IgG was detected using anti-human IgG- or IgM-fluorescein isothiocyanate (FITC)-conjugated antibodies (Sigma) by flow cytometry using a FACSCalibur cytometer (BD Biosciences). Data were analyzed using FlowJo version 7.6.3.

Serum IgM depletion

Five milliliters of 20% NHS was incubated with 500 μl of PBS-washed Sepharose beads coupled to anti-human IgM antibody (Sigma). After 2 h of incubation on a rotating wheel at 4°C, Sepharose beads were removed by centrifugation, and sera were diluted to 10% with PBS and immediately stored at −80°C.

Complement resistance assays

All experiments were conducted with the same batch of pooled human serum obtained from GTI Diagnostics (catalogue no. PHS-N100). Complement resistance of the NPS and MEF isolates was determined with 5% NHS or heat-inactivated NHS as described previously (10). The complement resistance of NTHi R2866, 3655, 86-028NP, Rd, 1521062, Δ*lgtC* mutant, and Δ*0112*mutant strains was determined as described previously (15). To determine the contribution of IgM, complement resistance was determined in 5% IgM-depleted serum. For competition experiments, wild-type and mutant bacteria were mixed in a 1:1 ratio, and serum was added as described above. The competitive index (CI) score was calculated by dividing the output ratio of the CFU counts of the mutant to those of the wild type by the input ratio of the mutant to the wild-type bacteria.

LOS analysis by Tris-Tricine SDS-PAGE

LOS was prepared by the proteinase K-ethanol precipitation method as described previously (33). LOS samples were separated on a Tris-Tricine SDS-PAGE gel in a Protean II XI cell electrophoresis system (Bio-Rad) and visualized by silver staining (34) or transferred to nitrocellulose for Western blotting. Membranes were blocked with 5% bovine serum albumin (BSA) in PBS, incubated for 2 h with 2% NHS in PBS, and subsequently incubated with goat anti-human IgM coupled to horseradish peroxidase (HRP) in PBS (1:5,000). The intensity of IgM binding to LOS bands was calculated using ImageJ software (35).

Structural characterization of LOS glycoforms by mass spectrometry

LOS was extracted from lyophilized bacteria using phenol-chloroform-light petroleum as described previously (36). LOS preparations and LC-ESI-MS experiments were performed as described previously (37,38) on a Waters 2690 high-pressure liquid chromatography (HPLC) system (Waters, Milford, MA) coupled to a Finnigan LCQ ion trap mass spectrometer (Finnigan-MAT, San Jose, CA). A microbore C_{18} column [Phenomenex Luna; 5-μm C18(2) column; 150 by 0.5 mm; Torrance, CA] was used with an eluent gradient consisting of 0.1 mM sodium acetate and 1% acetic acid in methanol as eluent A and 0.1 mM sodium acetate and 1% acetic acid in H_2O. Gradient elution was conducted as follows: 50% A at 0 min, 54% A at 15 min, 100% A at 35 min, 54% A at 55 min, and 50% A at 65 to 75 min. The flow rate was 0.018 ml/min. Average mass units were used for calculation of molecular weight values providing the basis for proposed compositions: hexose (Hex), 162.14; *N*-acetyl-hexosamine (HexNAc), 203.19; heptose (Hep), 192.17; reduced anhydro-Kdo (AnKdo-ol), 222.20; Me, 14.03; Na, 22.99. Relative abundance was estimated from the height of the ion peaks relative to the total (expressed as percent).

Influenza virus-NTHi coinfection mouse model

Six- to 8-week-old female, specific-pathogen-free (SPF) BALB/c mice (Harlan, Netherlands) were infected intranasally (i.n.) with $10^{4.5}$ PFU of egg-grown influenza virus strain A/Udorn/302/72 in a volume of 10 μl or a similar dilution of naive allantoic fluid (17). Three days later, mice were challenged with 5×10^7 CFU in 10 μl PBS of either the wild-type 1521062 strain alone or a 1:1 mixture of 1521062 wild-type and mutant strains. At 48 and 96 h following challenge with NTHi, mice were euthanized and perfused with PBS by intracardiac injection. The entire bulla from each ear was dissected, after which a nasopharyngeal lavage was performed. Bullae were immediately homogenized (T10 basic Ultra-turrax; IKA), and serial dilutions of bulla homogenates and nasopharyngeal lavages were prepared in PBS and cultured on sBHI agar with or without 150 μg/ml of spectinomycin (Calbiochem) (39). The CI score was calculated as described above. All animal experiments were approved by the Animal Ethics Committee of the Radboud University Nijmegen Medical Centre (RU-DEC2-11-246).

Statistical analysis

All statistical analyses were performed in GraphPad Prism version 4.0 for Windows (GraphPad Software, San Diego, CA), where $P < 0.05$ was considered significant.

Results

NTHi isolates from MEF display increased complement resistance

NTHi isolates were obtained from middle ear fluid (MEF) and nasopharyngeal swab (NPS) samples collected from children with OM. Isolates collected from MEF (n = 22) were significantly more resistant to complement-mediated killing than were isolates collected from the nasopharynx (n = 24) (Fig. 1A). To rule out potential attenuation by in vitro culture, we passaged complement-resistant isolates for 5 generations in the absence of serum. Subsequent analysis of complement resistance showed no significant changes, suggesting that the phenotype of these minimally passaged strains reflects their in vivo phenotype (data not shown).

To investigate the mechanism by which NTHi was killed by serum, we measured surface binding of IgM and IgG. We found that serum-sensitive isolates (<10% survival) showed increased IgM binding compared to complement-resistant isolates (>10% survival) (Fig. 1B). This difference was not observed for the binding of IgG (Fig. 1B). The amount of IgM binding correlated with the ability of serum to kill the NTHi isolates (Fig. 1C), implying an important role for IgM in activating the classical complement pathway.

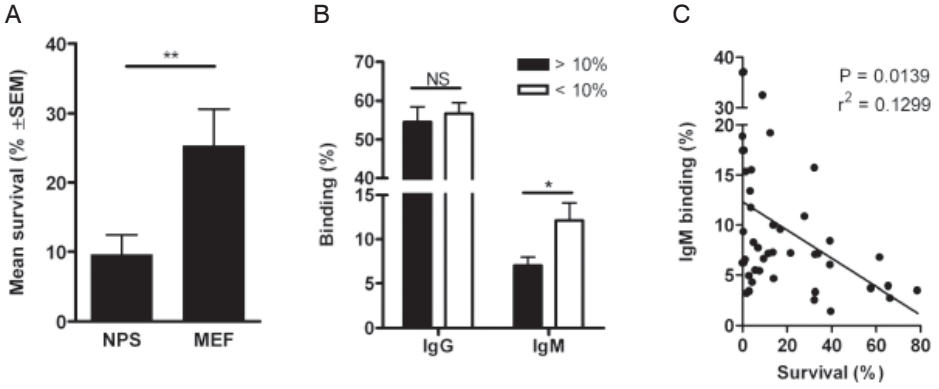

Figure 1. Determination of the complement resistance and IgM binding of clinical NTHi isolates. (A) Survival of MEF (n = 22) and NPS (n = 24) isolates was determined in 5% normal human serum and expressed as percent survival compared to that in 5% heat-inactivated human serum for 60 min. (B) Serum IgG and IgM binding on 25 serum-sensitive and 21 complement-resistant NTHi isolates was determined by flow cytometry. Statistical significance was determined with an unpaired t test with Welch's correction. *, $P < 0.05$; **, $P < 0.01$. (C) Correlation between complement resistance and IgM binding.

Table 1. Top list of genes identified in the serum resistance GAF screen at 30 min

Fold difference	Bayes, P	R2866 gene name	R2866 locus tag	R2866 annotation
−194.5	<1.00E−16		R2866_0112	Conserved hypothetical protein
−83.2	<1.00E−16	*lpsA2*	R2866_1629	Lipooligosaccharide glucosyltransferase LpsA
−16.0	<1.00E−16	*lic2A*	R2866_0033	Lipooligosaccharide biosynthesis protein Lic2A
−12.3	<1.00E−16	*galE*	R2866_0222	UDP-glucose 4-epimerase
–10.6	1.11E−16		R2866_0369	Conserved hypothetical protein
−9.6	3.35E−11	*bolA*	R2866_0424	Morphology-related protein BolA
			R2866_0425	Lipoprotein, putative
−9.4	<1.00E−16	*lgtF*	R2866_1822	UDP-glucose-lipooligosaccharide beta 1-4 glucosyltransferase
−9.2	<1.00E−16	*lgtc*	R2866_0326	1,4-Alpha-galactosyltransferase (LgtC)
−8.5	2.83E−06		R2866_1530	Hypothetical protein
−6.2	7.52E−07	*rfbB*	R2866_1509	dTDP-glucose 4,6-dehydratase
−4.9	<1.00E−16	*galU*	R2866_1581	Glucose-1-phosphate uridylyltransferase
−4.3	3.14E−09	*rfaD*	R2866_1286	ADP-L-glycero-D-mannoheptose-6-epimerase
−4.0	3.04E−13	*tex*	R2866_0016	Probable transcription accessory protein Tex
−3.9	2.44E−15	*lpt6*	R2866_0303	PE-tn-6–lipooligosaccharide phosphorylethanolamine transferase
−3.9	5.78E−07	*waaQ*	R2866_0055	ADP-heptose–lipooligosaccharide heptosyltransferase III
−3.9	9.28E−09	*hgpB*	R2866_1813	Hemoglobin and hemoglobin-haptoglobin binding protein B
−3.9	1.60E−07	*licA*	R2866_1070	Phosphorylcholine kinase LicA
−3.8	<1.00E−16	*ICE_orf31*	R2866_0596	Conserved hypothetical protein p31
−3.6	1.78E−15		R2866_1296	Conserved hypothetical protein
−3.6	1.11E−16	*accA*	R2866_0167	Acetyl coenzyme A carboxylase, subunit alpha

The R2866_0112 gene affects NTHi complement resistance

In order to identify genes affecting IgM binding and complement resistance, the negative genome-wide screen genomic array footprinting (GAF) was performed (13,14). For this screen, the sequenced complement-resistant strain R2866 was used (15). In total, 57 transposon mutants showed an attenuated phenotype, of which the top 20 most attenuated mutants are listed in Table 1. Functional class enrichment analysis showed that the majority of the identified genes were involved in LOS biosynthesis (Table 2). The R2866_0112 gene, coding for a conserved hypothetical protein, showed the most prominent phenotype, and transcriptional analysis indicated that expression of this gene was increased in complement-resistant isolates (Fig. 2A).

To validate a role for R2866_0112 gene expression in complement resistance, we determined survival of the R2866 wild type, the R2866Δ0112 mutant, and the R2866Δ*lgtC* strain as a control because the *lgtC* gene has previously been shown to confer complement resistance (8). Furthermore, we included the R2866Δ*licA* mutant because it showed a minor phenotype in the GAF screen. The Δ*0112* mutant was extremely sensitive to complement-mediated killing compared to the wild-type, Δ*licA* mutant, or Δ*lgtC* mutant strain (Fig. 2B). Heat inactivation of serum abrogated killing of the Δ*0112* mutant, which showed that the bactericidal activity was dependent on the action of the complement pathway (Fig. 2B). A polar effect of the R2866_0112 gene deletion was excluded by microarray data analysis of the R2866 wild type and the Δ*0112* mutant (Table 3). Besides the expression of R2866_0112 (251-fold decrease), a minor decrease in expression was observed for the hemoglobin and hemoglobin-haptoglobin binding protein B gene (*hgpB*), as was an increase in expression of gene locus R2866_1095—R2866_1101. However, the altered

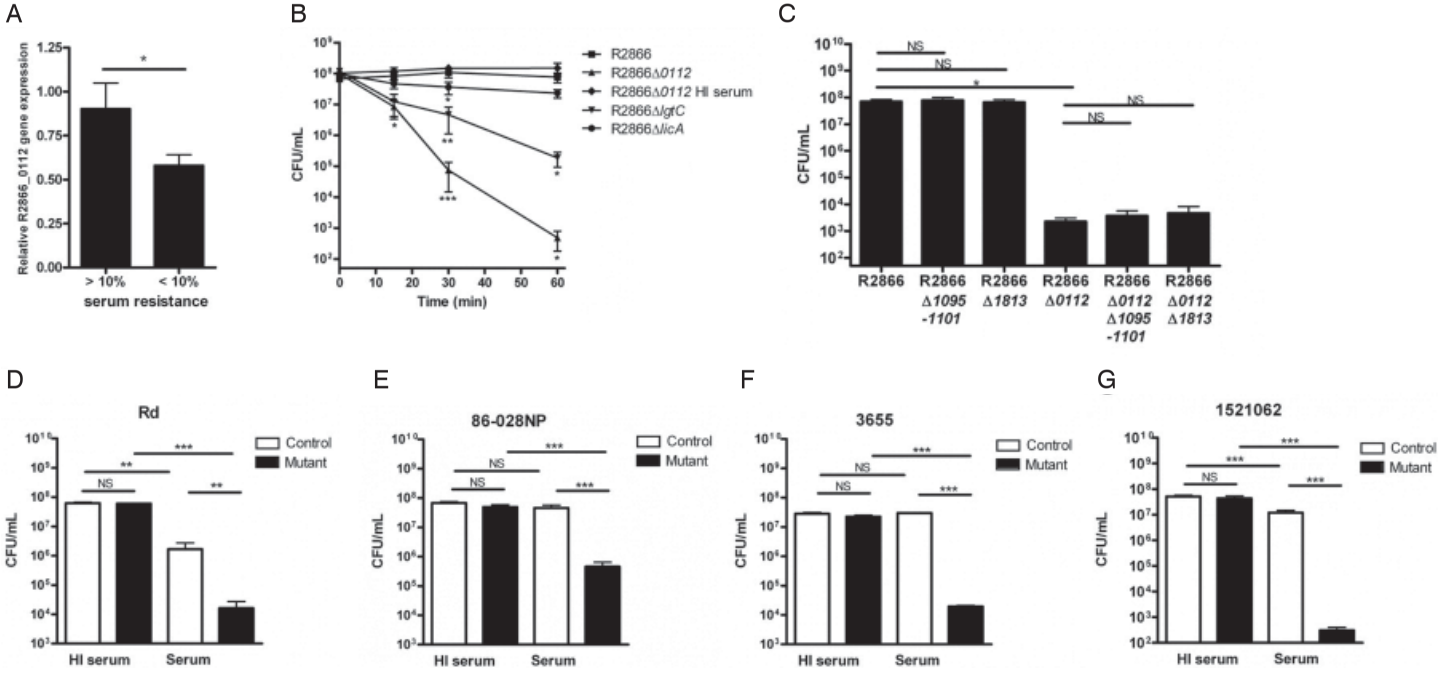

Figure 2. The R2866_0112 gene deletion mutant exhibits decreased complement resistance. (A) Relative expression of R2866_112 mRNA was analyzed by qRT-PCR in 25 serum-sensitive and 21 complement-resistant clinical isolates Statistical significance was determined with an unpaired *t* test with Welch's correction. (B) Complement resistance of R2866, Δ*0112* mutant, and Δ*lgtC* mutant ($n = 4$) was determined with 40% NHS or 40% heat-inactivated NHS. Statistical significance was determined with a two-way analysis of variance and the Bonferroni *post hoc* test. (C) Complement resistance of R2866, Δ*0112* mutant, Δ*1813* mutant, Δ*1095-1101* mutant, Δ*0112*/Δ*1813* mutant, and Δ*0112*/Δ*1095-1101* mutant was determined in 40% NHS ($n = 4$). Statistical significance was determined with a one-way analysis of variance and the Tukey *post hoc* test. (D to G) Complement resistance of Rd (HI0461) (D), 86-028NP (NTHI0592) (E), 3655 (CGSHi3655_02894) (F), and 1521062 (G) was determined with 10% (Rd), 20% (3655), or 40% (86-028NP and 1521062) serum, respectively ($n = 3$). Statistical significance was determined on $\log_{10}$-transformed data with a one-way analysis of variance and the Tukey *post hoc* test. *, $P < 0.05$; **, $P < 0.01$; ***, $P < 0.001$; NS, not significant.

Table 2. Database for annotation, visualization, and integrated discovery (DAVID) analysis

Functional annotation	*P value*	*Fold enrichment*
Lipopolysaccharide biosynthesis	*2.40E−05*	*27.4*
Cell outer membrane	*7.09E−04*	*11.9*
Glycosyltransferase	*1.00E−05*	*10.1*
Signal	*9.74E−05*	*5.9*
Cell membrane	*1.96E−04*	*2.8*
Membrane	*0.001*	*2.5*
Transferase	*0.007*	*2.2*

Table 3. R2866 and R2866Δ*0112* mutant gene expression array results[a]

R2866 locus tag	R2866 annotation	R2866 wild-type array signal	R2866Δ*0112* array signal	Bayes, *P*	Fold difference
R2866_0112	Conserved hypothetical protein	5,345	21	<1.00E−16	−251.3
R2866_1813	Hemoglobin and hemoglobin-haptoglobin binding protein B	5,312	1,249	<1.00E−16	−4.3
R2866_1095	Putative TPR[b] protein	302	4,685	<1.00E−16	15.3
R2866_1096	Hypothetical protein	302	6,706	<1.00E−16	21.9
R2866_1097	Putative TPR protein	604	10,290	<1.00E−16	16.7
R2866_1098	Hypothetical protein	308	6,610	<1.00E−16	21.3
R2866_1099	Putative TPR protein	200	9,008	<1.00E−16	44.4
R2866_1100	Hypothetical protein	309	6,792	<1.00E−16	21.7
R2866_1101	Putative TPR protein	297	9,918	<1.00E−16	32.7

[a] Genes regulated 2.5-fold with *P* values of <0.001 are included in the table.
[b] TPR, tetratricopeptide repeat.

expression of *hgpB* and gene locus R2866_1095—R2866_1101 was not involved in complement resistance because deletion did not alter the complement-sensitive phenotype of the Δ*0112* mutant (Fig. 2C). To confirm the importance of this gene for complement resistance in other NTHi strains, we also deleted the R2866_0112-homologous gene from NTHi Rd, 3655, 86-028NP, and 1521062. All mutant strains showed strongly reduced complement resistance compared to their respective parental strain, albeit complement resistance levels varied extensively (Fig. 2D to G).

R2866_0112 gene expression alters the LOS structure

As our results (Table 2), as well as previous reports, suggested an important role for LOS in complement resistance, we determined whether deletion of the R2866_0112 gene affected the LOS composition. As a control, the Δ*lgtC* mutant was included because previous reports showed an altered LOS structure for this mutant in the R2866 strain (8, 16). The Δ*0112* mutant showed a different LOS migration pattern than did the R2866 wild type and Δ*lgtC* mutant (Fig. 3A), suggesting that the R2866_0112 gene affects LOS biosynthesis. Deletion of the R2866_0112-homologous gene from NTHi Rd, 3655, 86-028NP, and 1521062 also altered the LOS migration pattern, which confirms a conserved function for this gene.

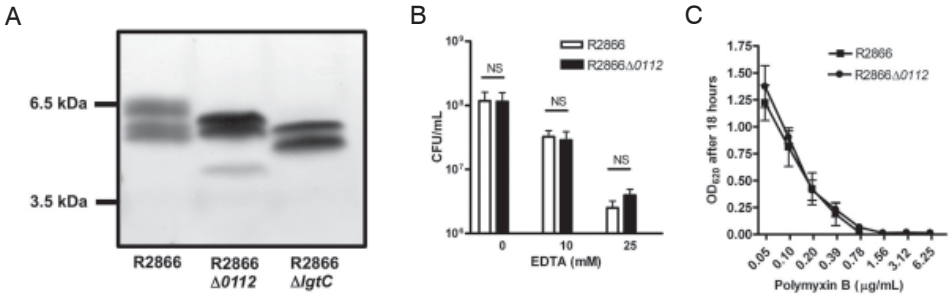

Figure 3. The R2866_0112 gene deletion mutant expresses an altered LOS structure. (A) LOS analysis of R2866, Δ*0112* mutant, and Δ*lgtC* mutant strains by Tris-Tricine SDS-PAGE and silver staining. (B and C) Outer membrane stability of R2866 wild type and mutant as determined by sensitivity to EDTA (n = 5) (B) or polymyxin B (n = 8) (C). Statistical significance was determined with a one-way analysis of variance and the Tukey *post hoc* test or a with a two-way analysis of variance and the Bonferroni *post hoc* test, respectively. OD_{620}, optical density at 620 nm; NS, not significant.

Table 4. Positive-ion ESI-MS data and proposed compositions for glycoforms in dephosphorylated and permethylated oligosaccharide derived from NTHi strains R2866 and R2866Δ*0112*[a]

	Relative Abundance (%)		
[M + Na^+]	R2866	R2866Δ*0112*	Proposed composition
2,736	*Tr*[b]		Hex7 · Hep4 · AnKdo-ol
2,369	*9*		HexNAc · Hex4 · Hep4 · AnKdo-ol
2,166		*8*	HexNAc · Hex3 · Hep4 · AnKdo-ol
2,124	19		Hex4 · Hep4 · AnKdo-ol
2,080	*10*	*9*	Hex5 · Hep3 · AnKdo-ol
1,920	*13*	*5*	Hex3 · Hep4 · AnKdo-ol
1,876	21	*7*	Hex4 · Hep3 · AnKdo-ol
1,716	*9*		Hex2 · Hep4 · AnKdo-ol
1,672	*6*	*6*	Hex3 · Hep3 · AnKdo-ol
1,521	*8*	27	Hex1 · Hep4 · AnKdo-ol
1,468		*5*	Hex2 · Hep3 · AnKdo-ol
1,265	*5*	35	Hex1 · Hep3 · AnKdo-ol

[a] The major ions are depicted in bold. All glycoforms contain Hep3 · AnKdo-ol. Points of elongation appear from HexI and/or HepIII in the following structure:

HexI-HepI-AnKdo-ol
|
HepII
|
HepIII

[b] Tr, traces.

Although changes in LOS structure may directly affect complement resistance by changing membrane stability, this was not the case for the Δ*0112* mutant because the mutant and wild-type strains showed similar sensitivities to EDTA (Fig. 3B), which interrupts intermolecular associations between LOS phosphate groups (10). Also, sensitivity to polymyxin B, which increases membrane permeability, was equal for the R2866 wild-type and Δ*0112* mutant strains (Fig. 3C). Liquid chromatography-electrospray ionization-mass spectrometry (LC-ESI-MS) analysis of the LOS showed that both the R2866 wild-type and Δ*0112* mutant strains contained a conserved inner-core triheptosyl moiety and belong to a group of NTHi strains expressing a heptose (HepIV) in the outer core (5). The R2866 wild-type LOS showed major ions at *m/z* 2124 and 1876, whereas the spectrum of the Δ*0112* mutant showed smaller major ions at *m/z* 1521 and 1265 (Table 4). In conclusion, the LOS structure of the Δ*0112* mutant strain showed various truncations, a finding which corresponds to the altered migration pattern (Fig. 3A).

Complement activation is dependent on direct binding of IgM to NTHi LOS

Because our primary observation in clinical isolates showed a correlation between IgM binding and complement resistance, we also determined IgG and IgM binding to the R2866 wild type and the Δ*0112* mutant. No significant change in IgG binding was observed. However, the Δ*0112* mutant showed a ~2-fold increase in IgM binding (Fig. 4A). Binding of IgM to the bacterial surface was essential for killing the Δ*0112* mutant, as depletion of IgM from serum completely prevented killing (Fig. 4B). The reduced killing of the Δ*0112*mutant with IgM-depleted serum was not due to decreased bactericidal activity, because an NTHi strain dependent on C-reactive protein (CRP)-mediated complement activation was killed equally as well with normal serum as with IgM-depleted serum (data not shown). Sera with different levels of IgM showed a strong correlation between IgM binding and killing of the bacteria, confirming the essentiality of IgM in complement-mediated killing of the Δ*0112* mutant (Fig. 4C).

To determine whether IgM directly recognizes the LOS of NTHi, Western blot experiments were performed. While IgM predominately binds to the lower band of the wild-type LOS, IgM also binds strongly to the truncated LOS band of the Δ*0112* mutant (Fig. 4D). The Δ*0112* mutant LOS bound ~2-fold-more IgM than did the R2866 wild-type LOS (Fig. 4E), which corresponds to the flow cytometry results (Fig. 4A). Also, the Δ*lgtC* mutant showed an increase in IgM binding, although not significant (Fig. 4E). Furthermore, we determined IgM binding to 4 complement-resistant and 4 complement-sensitive isolates. In accordance with the data for the complement-sensitive Δ*0112* mutant, LOS from complement-sensitive isolates bound significantly more IgM than did LOS from complement-resistant isolates (Fig. 4F and G).

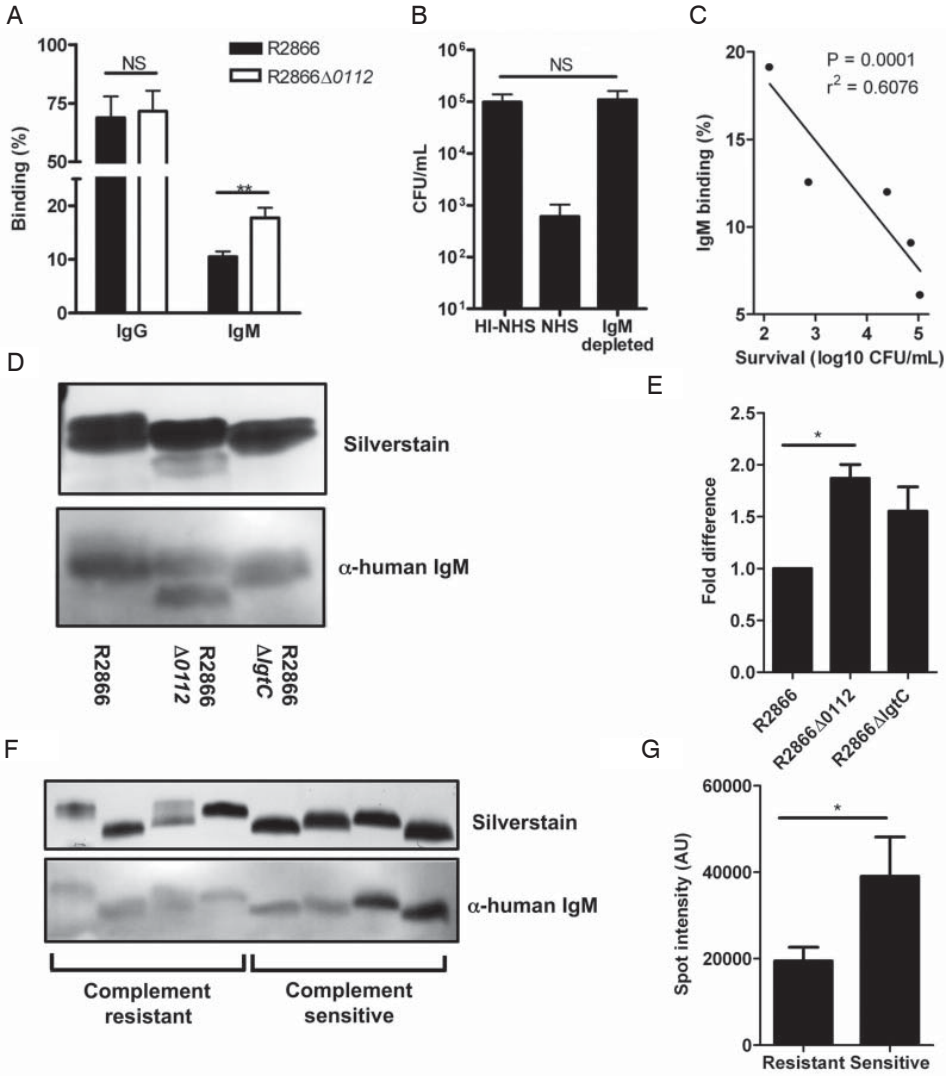

Figure 4. IgM binds R2866Δ0112 mutant LOS directly. (A) Serum IgG and IgM binding on R2866 and *Δ0112* mutant as determined by flow cytometry ($n = 9$). Statistical significance was determined with an unpaired *t* test with Welch's correction. (B) Complement resistance of R2866 and *Δ0112* mutant strains was determined in heat-inactivated NHS (HI-NHS), NHS, or IgM-depleted serum ($n = 4$). Statistical significance was determined with a one-way analysis of variance and the Tukey post hoc test. (C) Correlation between Δ0112 mutant serum survival and IgM binding. (D and F) Direct binding of IgM to LOS was analyzed by silver staining (loading control) and Western blotting. (E) Relative IgM binding to LOS of R2866, *Δ0112*, and *ΔlgtC* mutant was calculated ($n = 3$). (G) Signal intensities in arbitrary units (AU) of IgM binding to LOS of clinical isolates were calculated ($n = 4$). Statistical significance was determined with a one-way analysis of variance and the Tukey *post hoc* test or with an unpaired t test. *, $P < 0.05$; **, $P < 0.01$; NS, not significant.

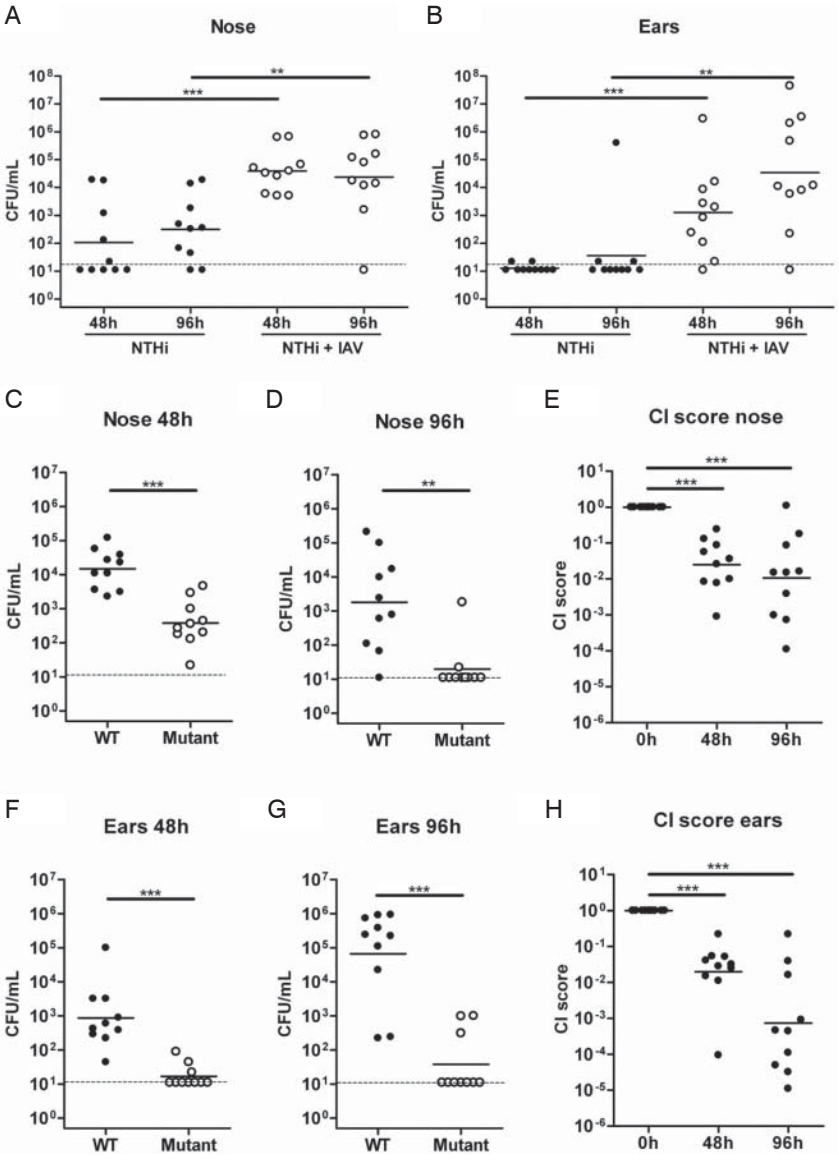

Figure 5. The R2866_0112 gene mutant shows decreased virulence in a murine coinfection otitis media model. Mice were inoculated with $10^{4.5}$ PFU of influenza A virus (IAV) or mock treated 3 days before intranasal infection with 5×10^7 CFU of NTHi. (A and B) CFU counts in the nose (A) or the middle ears (B) were determined 48 and 96 h postinfection ($n = 10$). (C, D, F, and G) Mice were infected with $10^{4.5}$ PFU of IAV 3 days before intranasal infection with a 1:1 ratio of NTHi 1521062 wild type (WT) and the R2866_0112 mutant (5×10^7 CFU total). CFU counts in the nose (C and D) or the middle ears (F and G) were determined 48 and 96 h postinfection ($n = 10$). Statistical significance was determined with a Mann-Whitney test. (E and H) CI scores were calculated. Statistical significance was determined with a one-way analysis of variance and the Tukey *post hoc* test. **, $P < 0.01$; ***, $P < 0.001$.

Deletion of the R2866_0112 gene attenuates colonization and otitis media

Although the *Δ0112*mutant was significantly less resistant to complement-mediated lysis, the consequences with regard to host colonization and/or OM remain uncertain. Because NTHi by itself does not infect mice efficiently, we adapted our previously described murine model of influenza A virus (IAV)-*Streptococcus pneumoniae* coinfection (17). In these experiments, mice are primed first with influenza virus or mock treated and subsequently challenged with NTHi. For these experiments, we used NTHi strain 1521062, which we had previously used in animal experiments. Infection of mice with IAV significantly increased the number of NTHi bacteria in the nose at both 48 h and 96 h postchallenge (Fig. 5A). Importantly, IAV infection also facilitated replication of NTHi in the middle ears (Fig. 5B).

Similar to R2866, deletion of the R2866_0112 gene from the NTHi 1521062 strain (designated the 1521062 mutant) attenuated complement resistance. IAV-NTHi coinfection experiments with a 1:1 mixture of the wild type and the mutant strain showed that the mutant was strongly outcompeted by the wild type. The mutant strain was attenuated in the nasopharynx as well as the middle ears, both at 48 h and at 96 h (Fig. 5C to H), suggesting that clearance of the mutant strain already occurs early during infection. Interestingly, although the CFU counts of the wild type in the nose decreased slightly from 48 h to 96 h, the CFU counts in the middle ears increased, suggesting that there is local bacterial replication in the middle ear cavity. In summary, these data demonstrate an important *in vivo* role for the R2866_0112 gene in complement resistance and bacterial pathogenesis.

Discussion

Although NTHi is generally sensitive to complement-mediated killing, some strains have developed immune evasion mechanisms that aid in colonization and disease. Previous data from animal models suggest that the complement system comprises an important aspect of the host defense against NTHi. For instance, depletion of complement by cobra venom resulted in the development of otitis media in chinchillas by "avirulent" NTHi strains (18). Recently, it was shown that NTHi isolates from the lower respiratory tract exhibit increased complement resistance compared to colonizing strains (10). Here, we provide strong evidence that NTHi strains isolated from the middle ears of children suffering from otitis media are more resistant to complement-mediated killing than are nasopharyngeal isolates.

The observation that bacterial isolates from the middle ear cavity show increased complement resistance may be explained by at least two mechanisms. One explanation is that the local inflammatory environment determines the bacterial phenotype of OM strains. Evidence to support this mechanism is the observation that serial passage of a serum-sensitive NTHi strain in the presence of active complement increased its complement resistance (10). This is particularly relevant in the context of OM, since large quantities of complement factors are present in the middle ears during inflammation of the middle ear (19,20). An alternative hypothesis is that only complement-resistant NTHi isolates are able to cause OM, which implies the existence of "colonizing" and "otitis media" genotypes. Despite a very high level of genetic heterogeneity among NTHi strains, especially for LOS synthesis-related genes (5), clinical isolates causing inflammatory diseases, including OM, display a distinct genetic profile that confers increased complement resistance (21). Future experiments that investigate whether these OM isolates are equally efficient at colonizing the mucosal surfaces of the nasopharynx, and whether this changes in the presence of inflammation (e.g., due to a viral infection), may shed more light into when and how NTHi requires complement resistance. Various modifications in the NTHi LOS structure have previously been described to contribute to complement resistance. Modification of LOS by the phase-variable LOS synthesis gene *lgtC* has been shown to delay C4b deposition on the bacterium, resulting in increased complement resistance (8). Another strategy used by NTHi is the incorporation of sialic acid in LOS, which also confers protection against complement attack (9) and leads to prolonged survival in the middle ear cavity in a chinchilla model (22). In this study, we identified a complement evasion mechanism,

which is dependent on the R2866_0112 gene. This gene was also identified in a complement resistance screen by Nakamura et al. (10), and transposon mutants of Rd showed decreased growth or survival in the mouse lungs (23). The R2866_0112 gene is highly conserved in all NTHi strains sequenced to date, and deletion of the homologous genes from all NTHi strains that we tested resulted in a dramatic decrease in complement resistance. Here, we demonstrate a role for the R2866_0112 gene in LOS structure synthesis. The high number of truncated glycoforms in LOS of mutant strains lacking this gene, together with the absence of one dominant LOS glycoform, suggests that the R2866_0112 gene is not a transferase involved in LOS synthesis directly. Identifying the specific function of this gene remains the subject of ongoing investigation.

Interestingly, the R2866_0112 gene mutant showed an increase in IgM binding, which was essential for complement-mediated killing. This was also observed for the clinical isolates, in which IgM binding correlated with complement resistance. Another study focusing on COPD also reported decreased binding of IgM to complement-resistant NTHi isolates from the lower respiratory tract (10), and recently, Micol et al. showed that patients with hyper-IgM syndrome were protected from NTHi colonization but not from other respiratory pathogens (12). Our results and these studies both point to an essential function for IgM in the recognition of NTHi. Consequently, increasing the level of bactericidal IgM antibodies, either by therapeutic administration or by vaccination, may effectively reduce NTHi colonization as well as disease. Such a strategy may be highly effective, as an initial study using a detoxified NTHi LOS protein conjugate vaccine already showed protection in a chinchilla and mouse model of OM (24, 25).

To assess the importance of the R2866_0112 gene for *in vivo* virulence, we made use of a novel murine IAV-NTHi coinfection model. Here, we show that coinfection of mice with IAV and NTHi results in enhanced bacterial colonization and progression to OM, similar to *S. pneumoniae* (17,26,27). A competition experiment between a wild-type strain and a mutant strain lacking the R2866_0112 gene resulted in a strong attenuation of the mutant in both colonization and survival in the middle ears at 48 h and 96 h. The exact mechanism by which mice clear NTHi is currently unclear. Because we used naive mice, polyspecific natural IgM antibodies may play an important role in this bactericidal effect. A similar effect of natural IgM was observed by Zola et al. (28), who found a role for these antibodies in limiting NTHi colonization in mice. Interestingly, in our study, the mutant was attenuated not only in the middle ears but also in the nasopharynx, implying similar clearance mechanisms in the middle ears and the nasopharynx. One possibility is that the primary infection with IAV allows for abundant complement components to be present at the mucosal surface of the nasopharynx, thereby providing selective pressure. Although the

exact mechanism by which IAV allows NTHi to replicate in either the nasopharynx or the middle ear cavity remains currently unclear, these data point to an important *in vivo* role for the R2866_0112 gene in complement resistance and the development of OM.

Acknowledgements

We thank Aldert Zomer for bioinformatics assistance and Fred van Opzeeland for technical support with the animal experiments. We also thank Derek W. Hood for the fruitful scientific discussions.

This work was supported by the Zentrum für Innovation und Technologie GmbH, Vienna Spot of Excellence (ZIT-VSOE-2007, ID337956).

References

1. Cripps AW, Otczyk DC, Kyd JM. 2005. Bacterial otitis media: a vaccine preventable disease? Vaccine 23:2304–2310.
2. Broides A, Dagan R, Greenberg D, Givon-Lavi N, Leibovitz E. 2009. Acute otitis media caused by *Moraxella catarrhalis*: epidemiologic and clinical characteristics. Clin. Infect. Dis. 49:1641–1647.
3. Bakaletz LO. 2010. Immunopathogenesis of polymicrobial otitis media. J. Leukoc. Biol. 87:213–222.
4. Hallström T, Riesbeck K. 2010. *Haemophilus influenzae* and the complement system. Trends Microbiol. 18:258–265.
5. Schweda EK, Richards JC, Hood DW, Moxon ER. 2007. Expression and structural diversity of the lipopolysaccharide of *Haemophilus influenzae*: implication in virulence. Int. J. Med. Microbiol. 297:297–306.
6. Swords WE, Jones PA, Apicella MA. 2003. The lipo-oligosaccharides of *Haemophilus influenzae*: an interesting array of characters. J. Endotoxin Res.9:131–144.
7. Griffin R, et al. 2005. Elucidation of the monoclonal antibody 5G8-reactive, virulence-associated lipopolysaccharide epitope of *Haemophilus influenzae* and its role in bacterial resistance to complement-mediated killing.Infect. Immun. 73:2213–2221.
8. Ho DK, Ram S, Nelson KL, Bonthuis PJ, Smith AL. 2007. lgtC expression modulates resistance to C4b deposition on an invasive nontypeable *Haemophilus influenzae*. J. Immunol. 178:1002–1012.
9. Jenkins GA, et al. 2010. Sialic acid mediated transcriptional modulation of a highly conserved sialometabolism gene cluster in *Haemophilus influenzae* and its effect on virulence. BMC Microbiol. 10:48.
10. Nakamura S, et al. 2011. Molecular basis of increased serum resistance among pulmonary isolates of non-typeable *Haemophilus influenzae*. PLoS Pathog. 7:e1001247.
11. Severi E, et al. 2005. Sialic acid transport in *Haemophilus influenzae* is essential for lipopolysaccharide sialylation and serum resistance and is dependent on a novel tripartite ATP-independent periplasmic transporter. Mol. Microbiol. 58:1173–1185.
12. Micol R, et al. 2012. Protective effect of IgM against colonization of the respiratory tract by nontypeable *Haemophilus influenzae* in patients with hypogammaglobulinemia. J. Allergy Clin. Immunol. 129:770–777.
13. Bijlsma JJ, et al. 2007. Development of genomic array footprinting for identification of conditionally essential genes in *Streptococcus pneumoniae*. Appl. Environ. Microbiol. 73:1514–1524.
14. Burghout P, et al. 2007. Search for genes essential for pneumococcal transformation: the RADA DNA repair protein plays a role in genomic recombination of donor DNA. J. Bacteriol. 189:6540–6550.
15. Williams BJ, Morlin G, Valentine N, Smith AL. 2001. Serum resistance in an invasive, nontypeable *Haemophilus influenzae* strain. Infect. Immun. 69:695–705.
16. Erwin AL, et al. 2006. Role of lgtC in resistance of nontypeable *Haemophilus influenzae*

strain R2866 to human serum. Infect. Immun.74:6226–6235.
17. Short KR, et al. 2011. Influenza virus induces bacterial and nonbacterial otitis media. J. Infect. Dis. 204:1857–1865.
18. Figueira MA, et al. 2007. Role of complement in defense of the middle ear revealed by restoring the virulence of nontypeable *Haemophilus influenzae* siaB mutants. Infect. Immun. 75:325–333.
19. Närkiö-Mäkelä M, Meri S. 2001. Cytolytic complement activity in otitis media with effusion. Clin. Exp. Immunol. 124:369–376.
20. Rezes S, Késmárki K, Sipka S, Sziklai I. 2007. Characterization of otitis media with effusion based on the ratio of albumin and immunoglobulin G concentrations in the effusion. Otol. Neurotol. 28:663–667.
21. Martí-Lliteras P, et al. 2011. Nontypable Haemophilus influenzae displays a prevalent surface structure molecular pattern in clinical isolates. PLoS One 6:e21133.
22. Bouchet V, et al. 2003. Host-derived sialic acid is incorporated into *Haemophilus influenzae* lipopolysaccharide and is a major virulence factor in experimental otitis media. Proc. Natl. Acad. Sci. U. S. A. 100:8898–8903.
23. Gawronski JD, Wong SM, Giannoukos G, Ward DV, Akerley BJ.2009. Tracking insertion mutants within libraries by deep sequencing and a genome-wide screen for Haemophilus genes required in the lung. Proc. Natl. Acad. Sci. U. S. A. 106:16422–16427.
24. Gu XX, et al. 1997. Detoxified lipooligosaccharide from nontypeable *Haemophilus influenzae* conjugated to proteins confers protection against otitis media in chinchillas. Infect. Immun. 65:4488–4493.
25. Sun J, et al. 2000. Biological activities of antibodies elicited by lipooligosaccharide based-conjugate vaccines of nontypeable *Haemophilus influenzae* in an otitis media model. Vaccine 18:1264–1272.
26. Diavatopoulos DA, et al. 2010. Influenza A virus facilitates *Streptococcus pneumoniae* transmission and disease. FASEB J. 24:1789–1798.
27. Short KR, et al. 2011. Using bioluminescent imaging to investigate synergism between *Streptococcus pneumoniae* and influenza A virus in infant mice. J. Vis. Exp. 50:pii:2357.
28. Zola TA, Lysenko ES, Weiser JN. 2009. Natural antibody to conserved targets of *Haemophilus influenzae* limits colonization of the murine nasopharynx. Infect. Immun. 77:3458–3465.
29. van Soolingen D, de Haas PE, Hermans PW, van Embden JD.1994. DNA fingerprinting of Mycobacterium tuberculosis. Methods Enzymol.235:196–205.
30. Herriott RM, Meyer EM, Vogt M. 1970. Defined nongrowth media for stage II development of competence in *Haemophilus influenzae*. J. Bacteriol.101:517–524.
31. Simon A, Biot E. 2010. ANAIS: analysis of NimbleGen arrays interface.Bioinformatics 26:2468–2469.
32. Vandesompele J, et al. 2002. Accurate normalization of real-time quantitative RT-PCR data by geometric averaging of multiple internal control genes. Genome Biol. 3:Research0034.
33. Jones PA, et al. 2002. *Haemophilus influenzae* type b strain A2 has multiple sialyltransferases involved in lipooligosaccharide sialylation. J. Biol. Chem. 277:14598–14611.
34. Tsai CM, Frasch CE. 1982. A sensitive silver stain for detecting lipopolysaccharides in polyacrylamide gels. Anal. Biochem. 119:115–119.
35. Rasband WS. 1997–2011. ImageJ. U.S. National Institutes of Health,Bethesda, MD.

36. Galanos C, Lüderitz O, Westphal O. 1969. A new method for the extraction of R lipopolysaccharides. Eur. J. Biochem. 9:245–249.
37. Engskog MK, Deadman M, Li J, Hood DW, Schweda EK. 2011.Detailed structural features of lipopolysaccharide glycoforms in nontypeable *Haemophilus influenzae* strain 2019. Carbohydr. Res. 346:1241–1249.
38. Lundström SL, et al. 2008. Application of capillary electrophoresis mass spectrometry and liquid chromatography multiple-step tandem electrospray mass spectrometry to profile glycoform expression during *Haemophilus influenzae* pathogenesis in the chinchilla model of experimental otitis media.Infect. Immun. 76:3255–3267.
39. Stol K, et al. 2009. Development of a non-invasive murine infection model for acute otitis media. Microbiology 155:4135–4144.

Development of a non-invasive murine infection model for acute otitis media

K. Stol, S. van Selm, S. van den Berg, H.J. Bootsma, W.A.M. Blokx, K. Graamans, E.L.G.M. Tonnaer and P.W.M. Hermans

Microbiology 2009, 155(12):4135-44

Abstract

Otitis Media (OM) is one of the most frequent diseases in childhood, and *Streptococcus pneumoniae* is among the main causative bacterial agents. Since current experimental models used to study the bacterial pathogenesis of OM have several limitations, such as the invasiveness of the experimental procedures, we developed a non-invasive murine OM model.

In our model, adapted from previously developed rat OM model, a pressure cabin is used in which a 40kPa pressure increase is applied to translocate pneumococci from the nasopharyngeal cavity into both mouse middle ears. Wild-type pneumococci were found to persist in the middle ear cavity for 144 hours after infection, with a maximum bacterial load at 96 hours. Inflammation was confirmed at 96 and 144 hours post infection by IL-1β and TNF-α cytokine analysis and histopathology. Subsequently, we investigated the contribution of two surface-associated pneumococcal proteins, the streptococcal lipoprotein rotamase A (SlrA) and the putative proteinase maturation protein A (*ppmA*) to experimental OM in our model. Pneumococci lacking the *slrA* gene, but not those lacking the *ppmA* gene, were significantly reduced in virulence in the OM model. Importantly, pneumococci lacking both genes were significantly more attenuated than the Δ*slrA* single mutant. This additive effect suggests that SlrA and PpmA exert complementary functions during experimental OM.

In conclusion, we have developed a highly reproducible and non-invasive murine infection model for pneumococcal OM using a pressure cabin, which is very suitable to study pneumococcal pathogenesis and virulence *in vivo*.

Introduction

In the first 3 years of life, otitis media (OM) affects 80% of the pediatric population (1). *Streptococcus pneumoniae*, together with non-typeable *Haemophilus influenzae* and *Moraxella catarrhalis*, is considered to be one of the three major bacterial pathogens involved in OM (2-5). OM is the most common reason for children to visit a physician, to receive antibiotics or to undergo surgery, which, consequently, results in a high disease burden for both children and their parents. Treatment with antibiotics remains controversial and is complicated by the rising numbers of isolates resistant to antibiotics (6,7). Despite the significant burden of OM on public health, the genetic basis of bacterial OM remains largely unclear (8).

Multiple animal models have been developed to study various aspects of the OM disease process, to increase our understanding of OM pathogenesis, and design or improve preventive and treatment strategies (9). Different methods are used to provoke middle ear inflammation in various animal species: models using mice (3,4,9,10), rats (11-14), gerbils , guinea pigs, chinchillas (15-17), and monkeys (18) have previously been described in literature. Among these, mice are increasingly becoming the model of choice in otitis media research. BALB/c mice are considered to be most susceptible to experimental AOM (3,11,19,20).

Acute otitis media (AOM) can be evoked by the introduction of live or heat-killed bacteria, as well as by inflammatory substances (3,4). In most animal models, AOM is induced by direct inoculation of live bacteria into the middle ear cavity, either via a transtympanic or a transbullar route. In the transtympanic model, application of the inoculum into the middle ear cavity is achieved by direct injection through the tympanic membrane. The transbullar approach consists of a ventral midline incision in the neck under sedation. The bulla is exposed after blunt dissection and the middle ear is infected with a bacterial suspension using a thin needle through the bony wall (3,5). Another possibility is intranasal inoculation, where initial bacterial colonization occurs in the nasopharynx, which is followed by invasion of the middle ear cavity by the pathogen in about 50% of the cases. This model resembles the natural route of infection in humans, and colonization of the nasopharynx is highly reproducible. However, development of OM after intranasal challenge is random and, consequently, reproducibility is low (3,4).

Reproducible induction of OM that maintains the physiological route of infection has been achieved successfully in rats by Tonnaer *et al.* (14). In their model, rats are inoculated

intranasally, after which pneumococci are transferred to the middle ear cavity via the Eustachian tube by an increase of atmospheric pressure. In the current study, we significantly adapted this model for mice, allowing us to study pneumococcal OM in reproducible and consistent fashion.

Furthermore, we explored our model to examine the contribution of two surface-associated pneumococcal proteins to otitis media: the streptococcal lipoprotein rotamase A (SlrA) and the putative proteinase maturation protein A (PpmA). SlrA and PpmA share homology with two dinstinct families of peptidyl-prolyl isomerases (PPIases). Both surface-associated proteins are known to play a key role during pneumococcal infection (21,22). Previous research has shown a pivotal role of SlrA in adherence, colonization and immune evasion, whereas PpmA is involved in invasive disease and colonization of the nasopharyngeal cavity (21-23).

Materials & Methods

Pneumococcal strains and growth conditions

The pneumococcal strains used in this study are listed in Table 1, and were kindly provided by B. Henriques-Normark (24). *S. pneumoniae* was routinely grown in Todd-Hewitt broth supplemented with 0.5% yeast extract or on Columbia blood agar (BA) plates at 37°C and 5% CO2. Prior to mouse infection experiments, bacteria were passaged in mice to maintain virulence as described previously (25). Cultures of mouse-passaged *S. pneumoniae* strains were grown to OD_{620} of 0.2 (mid-exponential phase) and stored in aliquots at -80°C in 15% glycerol. For *in vivo* challenges, aliquots were spun down and bacteria were resuspended in sterile PBS containing 1% methylcellulose, a viscous component, in order to minimize leakage of inoculum into the lungs (14). When indicated, antibiotics were used at the following concentrations: streptomycin, 100 μg/ml; trimethoprim, 25 μg/ml; and erythromycin, 4 μg/ml.

Construction of pneumococcal mutants

To obtain the streptomycin-resistant SME215::*rpsL*, the *rpsL* gene encoding a streptomycin-resistant mutant of the ribosomal protein S12 was amplified from D39::*rpsL* (21) with primer pair HB*rpsL*F (GTACAGGGACGTGCTGACAA) and HB*rpsL*R (CCCTTTCCTTATGCTTTTGG). The *rpsL*-PCR product was introduced into SME215 by CSP-1 induced trans-

Table 1. Pneumococcal strains and mutants used in this study.

Strain	Serotype	Relevant characteristics	Reference
S. pneumoniae			
D39	2	-	NCTC 7466
TIGR4(lux)	4	Tn*4001 luxABCDE* operon, Km^r	(42)
PJ1324(lux)	6B	Tn*4001 luxABCDE* operon, Km^r	(19)
SME215(lux)	19F	Tn*4001 luxABCDE* operon, Km^r	(19;23)
SME215(lux) strep	19F	SME215(lux) derivative, *rpsL*; Str^r	this study
SME215(lux) Δ*slrA*	19F	SME215(lux) derivative, Δ*slrA*; Ery^r	this study
SME215(lux) Δ*ppmA*	19F	SME215(lux) derivative, Δ*ppmA*; $Trim^r$	this study
SME215(lux) Δ*slrA* Δ*ppmA*	19F	SME215(lux) derivative, Δ*slrA* Δ*ppmA;* Ery^r $Trim^r$	this study

Km^r : Kanamycin resistance; Str^r: Streptomycin resistance; Ery^r Erythromycin resistance; $Trim^r$: Trimethoprim resistance; *slrA*: streptococcal lipoprotein rotamase A; *ppmA*: putatative proteinase maturation protein A.

formation and selection for streptomycin resistance. To delete the *slrA* gene from SME215, the Δ*slrA* region was amplified from D39Δ*slrA* (21) with primer pair HBslr*A*F (GTTCCCAAGCGAAATATGGA) and HBslr*A*R (TACACCAGGGCGCTTTATCT). The Δ*slrA*-PCR product was introduced into SME215 by CSP-1 induced transformation and selection for erythromycin resistance. To obtain the SME215Δ*ppmA* strain, a Δ*ppmA*-PCR region was amplified from D39Δ*ppmA* (26) with primer pair HB*ppmA*F1 (CTCTTGATGGCTGAACATGC) and HB*ppmA*R1 (GCAGCCTACAGCTAGCTTCC). The Δ*ppmA*-PCR product was introduced into SME215 by CSP-1 induced transformation, and trimethoprim-resistant transformants lacking the *ppmA* gene were selected (21,26). The Δ*slrA*Δ*ppmA* double mutants were constructed by transformation of the Δ*ppmA*-PCR product (amplified with primer pair HB*ppmA*F1 and HB*ppmA*R1) to each Δ*slrA* mutant and selecting for trimethoprim and erythromycin resistance. Deletion of *slrA* and *ppmA* in resulting transformants was confirmed by PCR and sequencing.

Mouse strain and disease monitoring

Experiments were conducted with 7-week old, female, specific pathogen free BALB/c mice (Harlan, Horst, the Netherlands) after approval was received from the Dutch animal protection legislation.

Pressure cabin

The pressure cabin consists of a perspex tube (l 30cm, Ø 15cm) with a fixed perspex wall. The perspex wall contains a manometer, an outlet valve, and a valve connected to a cylinder filled with compressed air. The removable front door is sealed with a rubber O-ring. Air pressure in the cabin can be increased stepwise (0-100 kPa) and monitored precisely (14).

Mouse otitis media model; single- and co-infection

Mice were lightly anesthetized with 2.5% (v/v) isoflurane over oxygen (1.5 liter min-1), and subsequently, a 10-μl suspension (containing 5×10^6 CFU bacteria or PBS/1% methylcellulose as control) was applied onto both nostrils in alternating fashion (single infection and co-infection). Mice were placed in supine position with an initial pressure rise set at 10 kPa. When the mice mice regained consciousness and the first swallowing movements occurred, pressure was raised 5 kPa / 15 seconds to 40 kPa in order to transfer the inoculum to the middle ear cavity. Thereafter, the pressure was lowered stepwise until atmospheric pressure was reached again. Pressure increase was evaluated using otomicroscopy and the tympanic membrane was scored for tympanic membrane perforation and for increased vascularization or bleeding.

For the single infection with respectively *S. pneumoniae* D39, TIGR4, SME215 and PJ1324, groups of 5-9 mice were sacrificed at 96 hours post-inoculation. For the single infection with *S. pneumoniae* SME215, groups of 5 mice were sacrificed at 1.5, 48, 96, and 144 hours post-inoculation. Blood was collected using orbital puncture. The bulla enclosing the right middle ear was dissected from the temporal bone and homogenized in the presence of 1 ml sterile PBS, as previously described (14,27). Thereafter bacteria were recovered from the nasopharynx by flushing the nose with 1 ml of sterile PBS per naris and collection at the controlateral side, a modified method from Wu *et al.* (28). Both lungs were extracted and homogenized in 2 ml sterile PBS. Viable counts were determined by serial 10-fold dilutions plated on BA plates.

For co-infection, a 10-μl inoculum containing a 1:1 ratio of streptomycin-resistant *S. pneumoniae* SME215 wild-type and either the Δ*slrA*, Δ*ppmA*, or Δ*slrA*Δ*ppmA* mutant (5×10^6 total CFU) was used to infect the mice intranasally as described above. Groups of 5 mice were sacrificed at 1.5, 12, 48 and 96 hours post-infection, whereupon samples from ear, lungs, nasopharynx, and blood were collected as described above. CFU counts were determined by plating serial dilutions of the specimens on BA plates and Columbia Agar plates supplemented with 5% (vol/vol) defribrinated sheep blood (Biotrading) containing the appropriate antibiotics.

Co-infection reduces variation between individual mice, inoculation preparation and distribution, and sample collection. Competitive index (CI) scores were calculated for the co-infection experiments as previously described (29). In short, the competitive index for each individual animal was calculated as the output ratio of mutant and wild-type divided by the input ratio of mutant to wild-type bacteria. For experiments in which no mutant bacteria were recovered from a particular mouse, the number 20 (lower limit of detection) was used as the numerator. Mice with neither mutant nor wild type bacteria in the middle ear were excluded from further analysis.

Histology

The skulls of all mice including both temporal bones, nose, and maxilla were removed and processed for histological analysis. The specimens were formalin fixed in 4% paraformaldehyde (Sigma Chemical Co. St. Louis, MO) in 0.1 M phosphate buffer (pH 7.4), decalcified using 10% EDTA (Serva, Heidelberg), and embedded in paraffin. Subsequently, all skulls were cut into 5 mm thick slices in an oblique direction. After deparaffinization through a series of xylene and graded ethanol baths sections were stained with haematoxilin-eosin (H&E). Sections were photographed with a microscope (Carl Zeiss Axioskop 2 plus) coupled to a computer (ProgRes Capturepro 2.1) at an original magnification of 25× and 200×.

IL-1β and TNF-α ELISA

Commercially available kits were used to measure the IL-1β (Becton Dickinson, Breda, the Netherlands) and TNF-α (U-cytech, Utrecht, the Netherlands) concentrations in murine middle ear homogenate and nasopharyngeal lavage.

Statistical analysis

All data were analyzed using SPSS 16.0 and GraphPad Prism version 4.0. For single infection a nonparametric test on log-transformed CFU-counts (mean, $p<0.05$) was used to calculate statistical significance. For co-infection the one sample *t*-test on log-transformed CI-scores (with an arbitrary mean of 0 and $p<0.01$) and comparative regression coefficients were used to calculate statistical significance.

Cytokine levels were calculated according to manufacturer's instructions. A nonparametric test (mean, standard error of the mean and $p<0.05$) was performed to calculate statistical significance between infected and PBS-infected mice at the corresponding time points.

Results

Development of a non-invasive murine OM model

The pathogenesis of pneumococcal OM involves bacterial translocation from the nasopharynx to the middle ear cavity through the Eustachian tube. In order to translocate bacteria in our model, we used a pressure cabin. First, we identified the appropriate pressure in our model with Evans blue dye. Pressure increase of 40kPa was sufficient to transfer Evans blue dye from the nasopharynx into the middle ear cavity of BALB/c mice, without causing damage to the tympanic membrane: otomicroscopy did not show rupture of the tympanic membrane, nor vascular dilatation of blood vessels present at the tympanic membrane (data not shown). Subsequently, the pressure cabin was used for bacterial infection with *S. pneumoniae* TIGR4 to test various doses and inoculum volumes. A dose of 5×10^6 CFU in a 10 μl volume resulted in reproducible infection, in line with the mouse colonization model used in our laboratory (23,30). To examine strain-specific behavior, mice were infected with the pneumococcal strains D39 (serotype 2), TIGR4 (serotype 4), PJ1324 (serotype 6B) and SME215 (serotype 19F). Ninety-six hours after infection mice were euthanized, whereupon ear- and lung-homogenates, nose lavage and blood were cultured. *S. pneumoniae* SME215 and PJ1324 induced a median bacterial load in the middle ear of 1×10^4 CFU and 5×10^2 CFU respectively, at 96 hours post-inoculation (Figure 1). OM induced by *S. pneumoniae* TIGR4 was complicated by pneumonia and sepsis (as confirmed by clinical scores and bacterial culture) and consequently excluded for further analysis. Bacterial counts in the middle ear and nasopharynx of *S. pneumoniae* D39 were significantly lower compared to *S. pneumoniae* SME215 (p-value 0.003) and PJ1324 (p-value 0.039). Therefore, *S. pneumoniae* PJ1324 and SME215 were considered most suitable for our model. No bacteria or signs of inflammation were detected in middle ears of mice inoculated with PBS, indicating that transfer of local nasopharyngeal flora does not occur in our model.

Since the bacterial load of *S. pneumoniae* SME215 in the middle ear was significantly higher than *S. pneumoniae* PJ1324 (p-value 0.015), SME215 was used to examine the bacterial kinetics in further detail at 1.5, 48, 96 and 144 hours after infection (Figure 2). Approximately 1×10^5 CFU were detected in the middle ear cavity at 1.5 hours post inoculation, this number declined 50-fold at 48 h post-inoculation. Wild-type pneumococci persisted in the middle ear cavity up to 96 h post infection (median 3×10^4 CFU). The bacterial load in the nasopharynx reached 1×10^6 CFU up to 96 h post-inoculation and 4×10^5 CFU at 144 h. The bacterial load initially detected in the lungs was high, 1×10^6

CFU, but declined rapidly over time with 5×10^2 CFU at 48 h and 6×10^1 CFU at 96 h post inoculation (Figure 2). No bacteria were recovered from blood (data not shown). Weight and temperature of the mice maintained within the normal range and importantly, mice did not show any signs of invasive disease; in particular no signs of pneumonia and sepsis were observed.

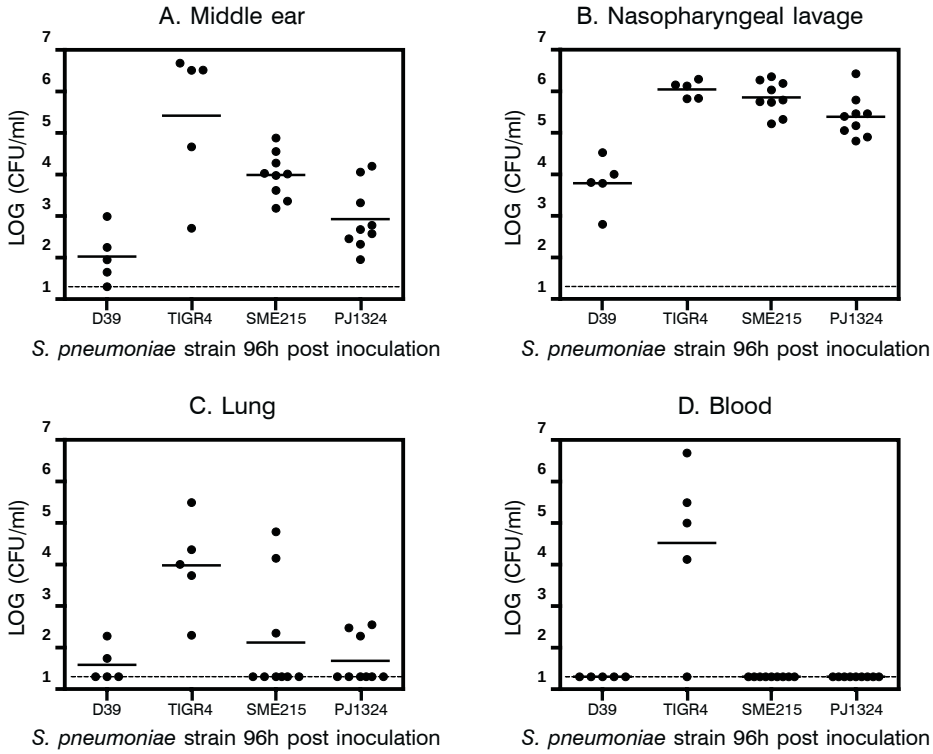

Figure 1. Bacterial load in the middle ear, nasopharyngeal lavage, lungs and blood 96 h after inoculation with *S. pneumoniae* D39 (serotype 2), TIGR4 (serotype 4), PJ1324 (serotype 6B) and SME215 (serotype 19F). Each dot represents a single mouse. Mean values are re-presented by horizontal bars. The lower limit of detection, 20 CFU, is indicated by a dashed line. (A), Bacterial counts in the middle ear; (B), Bacterial counts in the nasopharyngeal lavage; (C), Bacterial counts in lung homogenate; (D), Bacterial counts in blood.

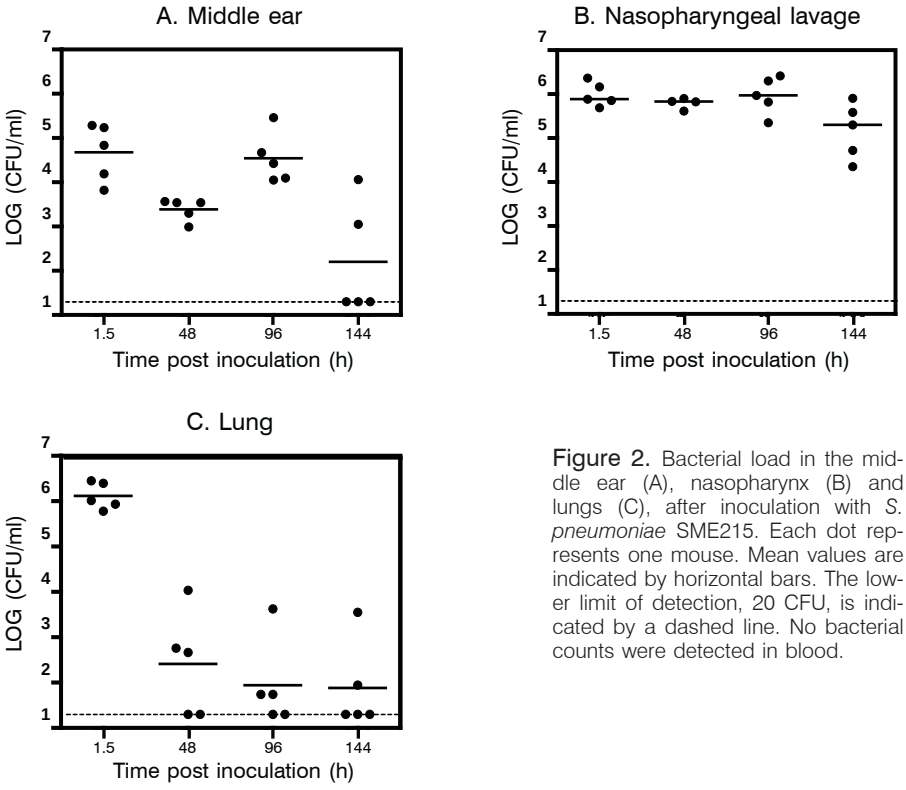

Figure 2. Bacterial load in the middle ear (A), nasopharynx (B) and lungs (C), after inoculation with *S. pneumoniae* SME215. Each dot represents one mouse. Mean values are indicated by horizontal bars. The lower limit of detection, 20 CFU, is indicated by a dashed line. No bacterial counts were detected in blood.

Immunology and histopathology

Both IL-1β and TNF-α levels in the middle ear were elevated throughout the course of infection. Importantly, levels in PBS-inoculated mice which were below the detection limit at 1,5, 48, 96 h post inoculation and marginal at 144 h post inoculation (TNF- α: 14,5 pg/ml; IL-1 β 24,4 pg/ml). The levels of TNF-α and IL-1β in the middle ear at 48 h and 96 h post-inoculation were significantly different from PBS-inoculated mice collected at the corresponding time points (Figure 3A and 3B). The TNF-α cytokine levels detected in the nasopharynx were 10-fold lower than the levels in the middle ear, and significantly different at 48, 96 and 144 h post inoculation when compared to PBS inoculated mice (Figure 3C). There was no significant difference between infected and PBS-infected mice concerning the IL-1β levels in the nasopharynx (Figure 3D).

Histopathological examination showed an increased inflammation over time (Figure 4). Neutrophils, lymphocytes and macrophages migrated into the ME cavity at 96 and 144 h post-inoculation (Figure 4 panel C and panel D). The mucous membrane, which is normally lined by a single layer of epithelium, by then is covered with a more irregular

and multiple layered epithelium (Figure 4 panel C, b + c and panel D, b + c). The loose connective tissue has expanded significantly, due to the presence of transient wandering immune cells that migrate from local blood vessels to the site of infection (Figure 4 panel C, b + c and panel D, b + c).

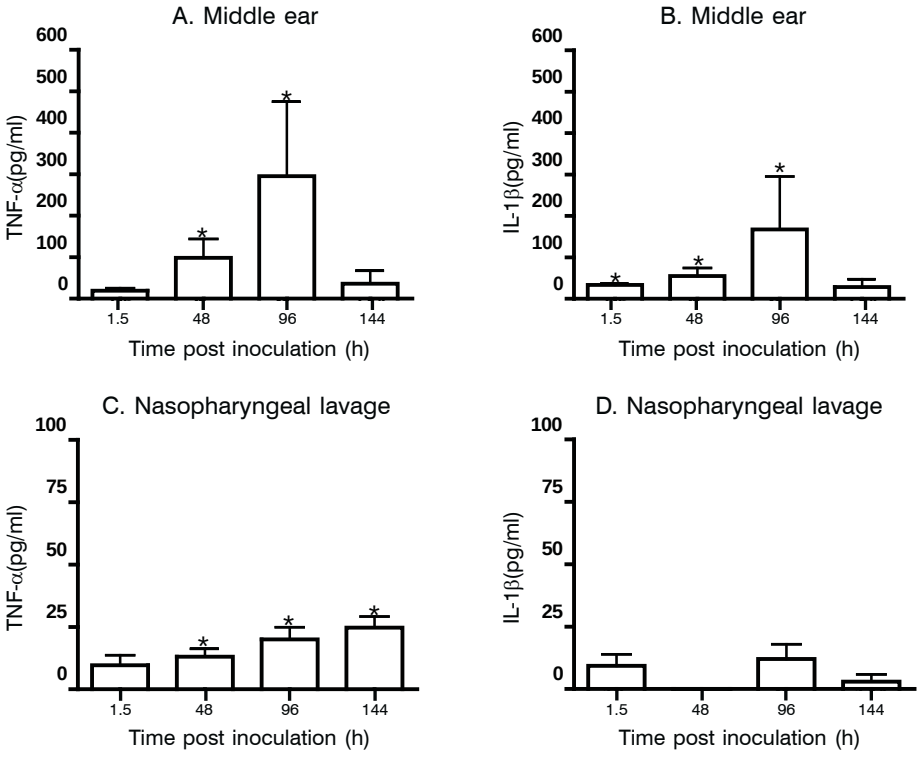

Figure 3. IL-1β and TNF-α cytokine levels in the middle ear and nasopharynynx. Each bar represents the mean value of 5 mice, error bars indicate the standard error of the means. (A) TNF-α in the middle ear; (B) IL-1β in the middle ear; (C) TNF-α in the nasopharyngeal lavage; (D) IL-1β in the nasopharyngeal lavage. Statistical significance was calculated between infected and mock-infected mice at the corresponding time point of collection. Significance with a $p<0.05$ is depicted with *.

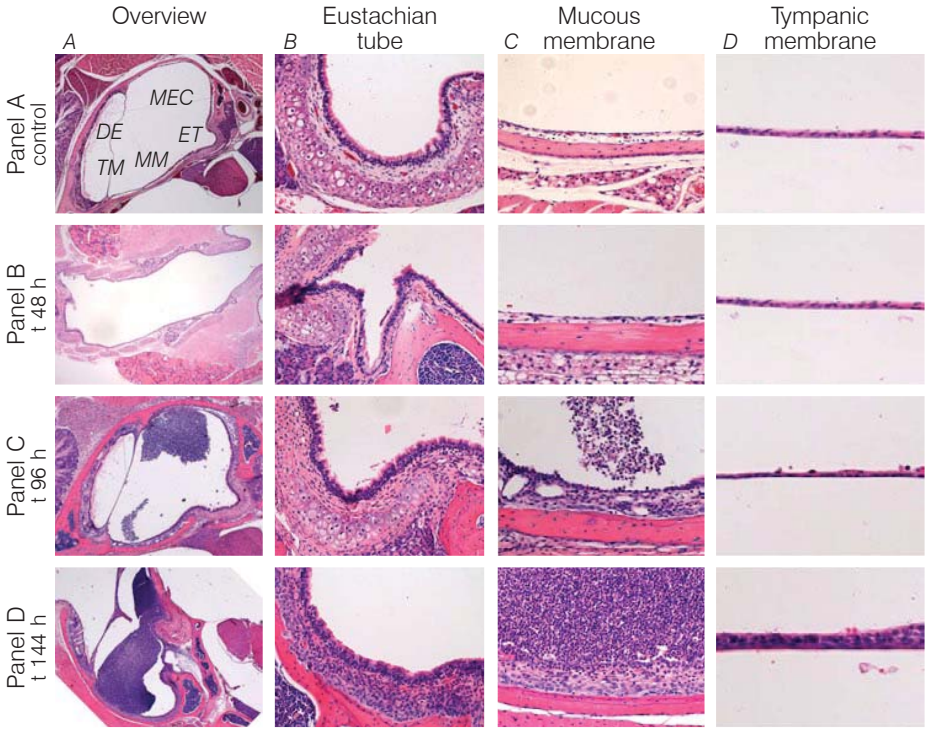

Figure 4. Histopathological changes in the middle ear. Sections were photographed at an original magnitude of 25× and 200× respectively. (panel A), Normal, non-infected middle ear; (panel B), 48 h after intranasal inoculation with *S. pneumoniae* SME215; (panel C), 96 h after intranasal inoculation with *S. pneumoniae* SME215; (panel D), 144 h after intranasal inoculation with *S. pneumoniae* SME215. The mucous membrane, which is normally lined by a single layer of epithelium (panel A, b + c), by then is covered with a more irregular and multiple layered epithelium (panel C, b + c and panel D, b + c). The loose connective tissue (panel A, b + c) has expanded significantly, due to the presence of transient wandering immune cells that migrate from local blood vessels to the site of infection (panel C, b + c and panel D, b + c). Abbreviations used in this figure: OE, Outer Ear; TM, tympanic membrane; MEC, middle ear cavity; MM, mucous membrane; ET, Eustachian tube.

Usefulness of the murine otitis media model to study pneumococcal virulence

To assess the role of the pneumococcal proteins SlrA and PpmA in OM, we inactivated the *slrA* and *ppmA* genes in strain SME215 by insertion deletion mutagenesis, and tested the wild-type and Δ*slrA*, Δ*ppmA*, or Δ*slrA*Δ*ppmA* mutants in a co-infection setup. Importantly, no differences in *in vitro* growth between the wild-type strains and the mutants were detected, indicating that differences in virulence did not originate from altered growth rates.

In the middle ear, the bacterial load of the Δ*slrA* mutant was significantly lower relative to the SME215 parent strain at 48 and 96 hours post-infection (mean CI 0.14 and 0.07 respectively, a 10-fold reduction) (Figure 5A). A significant difference between the wild-type and the Δ*ppmA* mutant was only found at 1.5 hours after infection, not at later time points (mean CI 0.47, a 5-fold reduction) (Figure 5C). Deletion of both *slrA* and *ppmA* resulted in a significant decrease in middle ear bacterial load compared to wild-type at all time points: the CI-score declined from 0.26 at 1.5 h post-inoculation to 0.003 at 96 h post-inoculation, representing a 3 to 300-fold reduction over time. In other words, the wild-type outcompeted the double knock out strain in a progressive and statistically significant fashion (Figure 5E). Interestingly, we observed an additive effect upon deletion of both genes, as the Δ*slrA*Δ*ppmA* mutant was significantly more attenuated in OM virulence than the Δ*slrA* or Δ*ppmA* single mutant (Figures 5A, C and E).

Colonization of the nasopharynx was highly reproducible, yielding approximately 5×10^5 CFU during all time points. Throughout the course of the experiment, the Δ*slrA*, Δ*ppmA* and Δ*slrA*Δ*ppmA* mutants were less able to colonize the nasopharynx in comparison to the parent strain (Figure 5B, D and F). Deletion of *slrA* resulted in a significant difference in colonization of the nasopharynx from wild-type at all time points (mean CI varying from 0.06-0.14, a 7 to 17-fold reduction) (Figure 5B). A significant difference between the wild-type and the Δ*ppmA*-mutant was seen at 12 (mean CI 0.70), 48 (mean CI 0.26) and 96 (mean CI 0.15) hours post-inoculation (Figure 5D). In line with the Δ*slrA*Δ*ppmA* mutant in the middle ear, outcompetition of the double mutant in the nasopharynx was progressive and statistically significant over time (CI 0.10 to 0.01, a 10 to 100-fold reduction) (Figure 5F). Again, the Δ*slrA*Δ*ppmA* mutant was significantly more attenuated in virulence than the Δ*slrA* or Δ*ppmA* single mutant (Figures 5B,D and F).

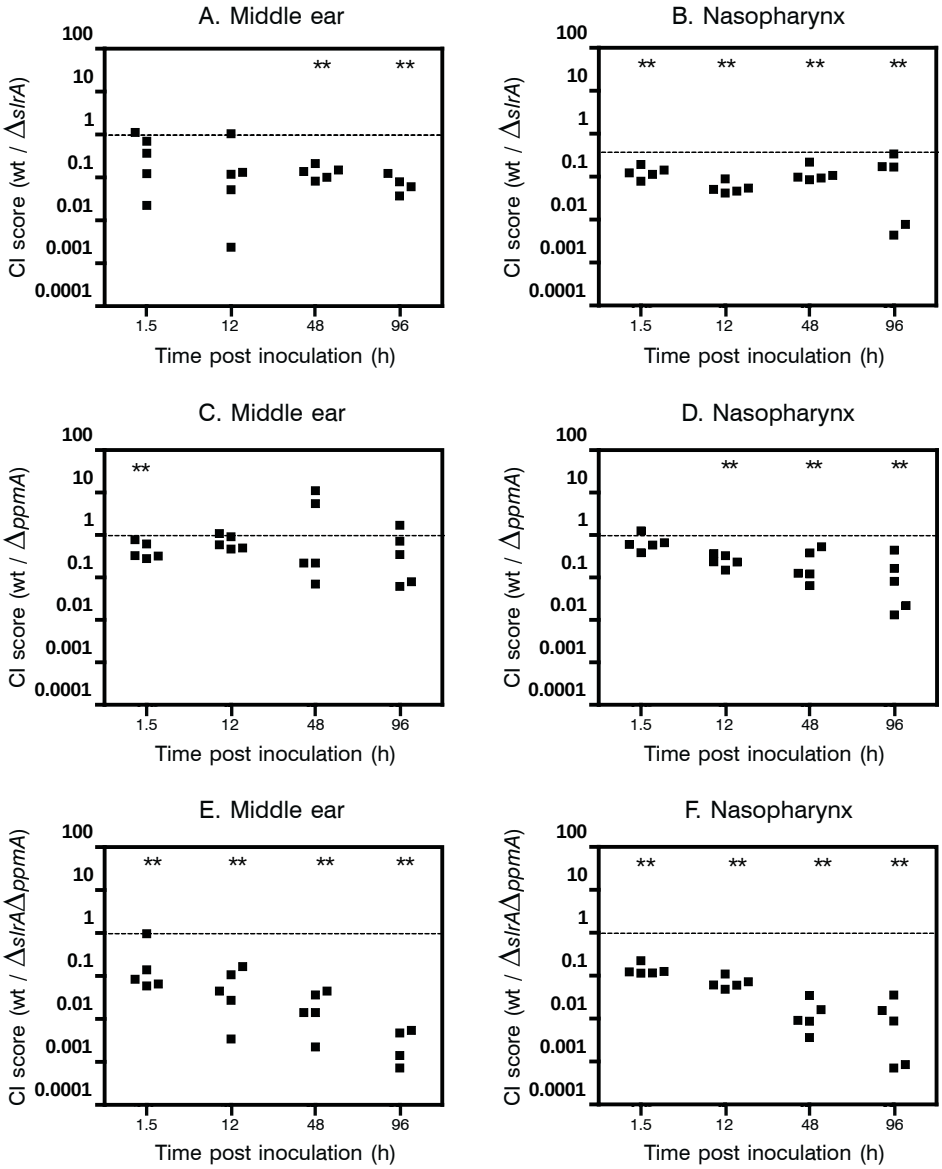

Figure 5. Competitive index (CI) in the middle (A,C,E) ear and nasopharynx (B,D,F) after co-infection, using the murine OM model. Female BALB/C mice were infected intranasally with a 1:1 mix of *S. pneumoniae* SME215 wild-type and *S. pneumoniae* SME215Δ*slrA* (A, B), *S. pneumoniae* SME215 wild-type and *S. pneumoniae* SME215Δ*ppmA* (C, D) and *S. pneumoniae* SME215 wild-type and *S. pneumoniae* SME215Δ*slrA*Δ*ppmA* (E, F). Each square represents one mouse. The CI score of 1 (i.e., no difference between wild-type and mutant) is indicated by a dashed line. Statistical significance of $p<0.01$ is depicted by **.

Discussion

In the present study we developed a novel non-invasive murine OM model with the use of a pressure cabin. The mouse affords many advantages for *in vivo* research, including ease of genetic manipulation, availability of inbred and transgenic strains and an extensively studied immune system. Moreover, experimental reagents for cellular and molecular studies are widely available (3,4,9,10). The model, which was adapted from a rat OM model described by Tonnaer and co-workers (14), was used to investigate OM caused by *S. pneumoniae* and the contribution of the pneumococcal proteins SlrA and PpmA to the pathogenesis of OM.

For various reasons, the pressure cabin model is an improvement over the experimental AOM models currently used. First, pressure elevation facilitates the ascending infection of pneumococci from the nasopharynx to the middle ear cavity via the Eustachian tube, resembling the natural route of infection in humans. In comparison to AOM models which rely on spontaneous OM development after nasopharyngeal colonization (4), the percentage of successful middle ear infections is 100% in our model. This is of major importance for future vaccination and challenge studies, since a 100% successful infection rate is warranted to monitor the efficiency of a vaccine, i.e. reduction of bacterial load. Secondly, dermal pathogens like *Staphylococcus epidermidis* will not influence experimental results, whereas with the widely used transtympanic or transbullar approaches, a connection between the middle ear and its surroundings is established. Third, an inflammatory response due to local manipulation is avoided. Among others, MacArthur *et al.* described signs of inflammation due to direct instillation of PBS in the middle ear that were equivalent to those induced by lower doses of heat killed bacteria. These inflammatory reactions were ascribed to the required tympanic membrane incision (10;19).

Of the pneumococcal strains tested, BALB/c mice were most susceptible to TIGR4 (serotype 4), followed by SME215 (serotype 19F), PJ1324 (serotype 6B) and D39 (serotype 2). These observations indicate pneumococcal strain-specific behaviour *in vivo* as described previously (31,32). *S. pneumoniae* SME215 and PJ1324 persisted in the middle ear cavity for at least 96 h. These two strains were therefore considered suitable for experimental otitis media studies *in vivo*, and subsequent experiments were performed using *S. pneumoniae* SME215 only. On the day of inoculation with *S. pneumoniae* SME215, bacteria were detected in the lungs, but they were cleared rapidly over time. We speculate that leakage to the lungs can be partially explained by the use of anesthetics and pressure

increase at the time of infection. Importantly, disease scores were low during this study, which implies absence of pneumonia or sepsis, and - as a result - moribund state or early loss did not occur. This is in contrast to current chinchilla OM models, which often record a moribund disease state (31). Since signs and symptoms of human OM mostly show a mild course of infection (7), we consider our model to be a clinical representative of OM in humans. Moreover infection with heat-inactivated bacteria to avoid systemic complications, as described in OM mouse models using direct tympanic membrane inoculation, was not necessary (19). Polymicrobial interactions between for instance, *S. pneumoniae*, (non-typeable) *H. influenzae* and *M. catarrhalis* or combined bacterial and viral infections are of interest for future studies (2,7,19,33).

The primary cytokines TNF-α and IL-1β were selected to monitor the initiation of the acute inflammatory response. TNF-α is produced mainly by macrophages or mast cells and is, among others, responsible for neutrophil migration (34). Along with various other functions, IL-1β contributes to permanent pathological changes in the middle ear, mucosal damage, bone erosion, fibrosis, and hearing loss. Higher concentrations of IL-1β were observed in purulent, acute, culture-positive effusions (34-36). Our results indicate a peak TNF-α and IL-1β response in the middle ear cavity at 96 h post-inoculation, whereas the maximum histopathological changes were shown at 144 h post-inoculation. These data confirm ongoing inflammation after onset of the inflammatory process by the primary cytokines: at 144 h, levels of both TNF-α and IL-1β were comparable to PBS-treated mice, most likely since the number of white blood cells were sufficient to eradicate *S. pneumoniae* from the middle ear cavity. Using a rat OM model Cripps *et al.* reported a maximum TNF-α level of 1.3×10^3 pg/ml at 24 h post infection, while IL-1β was not detectable. They also reported cytokine levels in a mouse pneumonia model of pneumococcal infection: a maximum TNF-α level around 3.0×10^2 pg/ml at 8 h post infection and maximum IL-1β level near 6.5×10^2 pg/ml at 24 h post-infection (37). However, as immune responses in *in vivo* experimental models are animal-specific, bacterial-strain specific, and infection-site specific, it is difficult to directly compare the results. Unlike the strong inflammation in the middle ear (38), there is a relative quiescent host response to colonizing pneumococci in the nasopharynx (8), underscored by the marginal levels of IL-1β and TNF-α detected in the nasopharyngeal lavage in our study.

Bacterial surface-exposed proteins often play an important role in the interaction between pathogens and their host. Identification of novel surface-exposed proteins that play an important role in virulence can improve our understanding of OM pathogenesis and will facilitate new preventive strategies such as vaccine development. Virulence studies described in literature have shown that most pneumococcal mutants display attenuated phenotypes in either colonization, pneumonia, or sepsis mouse models, thus indicat-

ing niche-specific involvement in virulence of the respective genes (6-8,8,21,29,38-41).

To our knowledge we report the first OM virulence study performed in mice. Only very few studies have investigated the role of virulence factors in OM models (8,36,41). Chen *et al*. very nicely demonstrated the first extensive search of genetic requirement for pneumococcal OM by using signature tagged mutagenesis in a chinchilla OM model and a murine colonization model (8). Since direct extrapolation from other models is problematic given the animal model specificity (8), we examined the contribution of two factors to OM and nasopharyngeal colonization directly. We showed that both single gene deletion of *slrA* and combined deletion of the *slrA* and *ppmA* genes significantly reduced the bacterial load during experimental AOM in both the nasopharynx and the middle ear compared to the wild-type strain. Pneumococci lacking the *slrA* gene, but not those lacking the *ppmA* gene were significantly reduced in virulence in the OM model. Interestingly, the virulence of the pneumococci lacking both genes was significantly decreased compared to the Δ*slrA* or Δ*ppmA* single mutant. This observation suggests complementary functions of SlrA and PpmA in both experimental OM and nasopharyngeal colonization, resulting in an additive decrease in virulence when both genes are absent. Previous studies have shown a role for both SlrA and PpmA in the early stage of infection, i.e. colonization (21,23). Our results, even in a different mouse background and with a different pneumococcal strain, confirmed these findings. SlrA is a functional PPI-ase involved in pneumococcal colonization, most likely by modulating the biological function of important virulence proteins, as described by Hermans et. al. (21). Although PpmA is a conserved surface protein with potential to elicit protective immune responses, the exact role of this protein is still unknown (22).

In summary, we developed an OM mouse model in which AOM can be established by various pneumococcal strains. This highly reproducible method is non-invasive, and infection is established in both ears. Consequently, multiple simultaneous applications are feasible, such as bacterial culture and histopathology. The model is highly valuable to study OM induced by *S. pneumoniae* and to study OM-related pneumococcal virulence. It is likely to be suitable to investigate the protective capacity of putative vaccine antigens against pneumococcal induced OM, since the route of infection does not bypass local immunity and the middle ear infection rate is 100%. Whether this model is also appropriate for other pathogens like *H. influenzae* and M. *catarrhalis* is currently under investigation.

Acknowledgements

This project was funded by the EC Sixth Framework Program. We thank B. Henriques Normark for providing the *S. pneumoniae* strains TIGR4, PJ1324 and SME215 and E. Simonetti and F. Hendriks for technical assistance. A. Maat is acknowledged for histological assistance.

References

1. Giebink GS. The prevention of pneumococcal disease in children. N Engl J Med 2001 October 18;345(16):1177-83.
2. Lysenko ES, Ratner AJ, Nelson AL, Weiser JN. The role of innate immune responses in the outcome of interspecies competition for colonization of mucosal surfaces. PLoS Pathog 2005 September;1(1):e1.
3. Ryan AF, Ebmeyer J, Furukawa M, Pak K, Melhus A, Wasserman SI et al. Mouse models of induced otitis media. Brain Res 2006 May 26;1091(1):3-8.
4. Sabirov A, Metzger DW. Mouse models for the study of mucosal vaccination against otitis media. Vaccine 2008 March 17;26(12):1501-24.
5. Sabirov A, Metzger DW. Intranasal vaccination of neonatal mice with polysaccharide conjugate vaccine for protection against pneumococcal otitis media. Vaccine 2006 July 7;24(27-28):5584-92.
6. Ogunniyi AD, Grabowicz M, Briles DE, Cook J, Paton JC. Development of a vaccine against invasive pneumococcal disease based on combinations of virulence proteins of *Streptococcus pneumoniae*. Infect Immun 2007 January;75(1):350-7.
7. Cripps AW, Otczyk DC, Kyd JM. Bacterial otitis media: a vaccine preventable disease? Vaccine 2005 March 18;23(17-18):2304-10.
8. Chen H, Ma Y, Yang J, O'Brien CJ, Lee SL, Mazurkiewicz JE et al. Genetic requirement for pneumococcal ear infection. PLoS ONE 2007 August 13;3(8):e2950.
9. MacArthur CJ, Trune DR. Mouse models of otitis media. Curr Opin Otolaryngol Head Neck Surg 2006 October;14(5):341-6.
10. Krekorian TD, Keithley EM, Takahashi M, Fierer J, Harris JP. Endotoxin-induced otitis media with effusion in the mouse. Immunohistochemical analysis. Acta Otolaryngol 1990 March;109(3-4):288-99.
11. Melhus A, Ryan AF. A mouse model for acute otitis media. APMIS 2003 October;111(10):989-94.
12. van der Ven LT, van den Dobbelsteen GP, Nagarajah B, van DH, Dortant PM, Vos JG et al. A new rat model of otitis media caused by *Streptococcus pneumoniae*: conditions and application in immunization protocols. Infect Immun 1999 November;67(11):6098-103.
13. Fogle-Ansson M, White P, Hermansson A, Melhus A. Otomicroscopic findings and systemic interleukin-6 levels in relation to etiologic agent during experimental acute otitis media. APMIS 2006 April;114(4):285-91.
14. Tonnaer EL, Sanders EA, Curfs JH. Bacterial otitis media: a new non-invasive rat model. Vaccine 2003 November 7;21(31):4539-44.
15. Giebink GS, Berzins IK, Marker SC, Schiffman G. Experimental otitis media after nasal inoculation of *Streptococcus pneumoniae* and influenza A virus in chinchillas. Infect Immun 1980 November;30(2):445-50.
16. Ehrlich GD, Veeh R, Wang X, Costerton JW, Hayes JD, Hu FZ et al. Mucosal biofilm formation on middle-ear mucosa in the chinchilla model of otitis media. JAMA 2002 April 3;287(13):1710-5.

17. Fulghum RS, Marrow HG. Experimental otitis media with *Moraxella* (*Branhamella*) *catarrhalis*. Ann Otol Rhinol Laryngol 1996 March;105(3):234-41.
18. Alper CM, Swarts JD, Doyle WJ. Prevention of otitis media with effusion by repeated air inflation in a monkey model. Arch Otolaryngol Head Neck Surg 2000 May;126(5):609-14.
19. MacArthur CJ, Hefeneider SH, Kempton JB, Parrish SK, McCoy SL, Trune DR. Evaluation of the mouse model for acute otitis media. Hear Res 2006 September;219(1-2):12-23.
20. Sandgren A, Albiger B, Orihuela CJ, Tuomanen E, Normark S, Henriques-Normark B. Virulence in mice of pneumococcal clonal types with known invasive disease potential in humans. J Infect Dis 2005 September 1;192(5):791-800.
21. Hermans PW, Adrian PV, Albert C, Estevao S, Hoogenboezem T, Luijendijk IH et al. The streptococcal lipoprotein rotamase A (SlrA) is a functional peptidyl-prolyl isomerase involved in pneumococcal colonization. J Biol Chem 2006 January 13;281(2):968-76.
22. Overweg K, Kerr A, Sluijter M, Jackson MH, Mitchell TJ, de Jong AP et al. The putative proteinase maturation protein A of *Streptococcus pneumoniae* is a conserved surface protein with potential to elicit protective immune responses. Infect Immun 2000 July;68(7):4180-8.
23. Cron LE, Bootsma HJ, Noske N, Burghout P, Hammerschmidt S, Hermans PW. Surface-associated lipoprotein PpmA of *Streptococcus pneumoniae* is involved in colonization in a strain-specific manner. Microbiology 2009 July;155(Pt 7):2401-10.
24. Albiger B, Sandgren A, Katsuragi H, Meyer-Hoffert U, Beiter K, Wartha F et al. Myeloid differentiation factor 88-dependent signalling controls bacterial growth during colonization and systemic pneumococcal disease in mice. Cell Microbiol 2005 November;7(11):1603-15.
25. Alexander JE, Lock RA, Peeters CC, Poolman JT, Andrew PW, Mitchell TJ et al. Immunization of mice with pneumolysin toxoid confers a significant degree of protection against at least nine serotypes of *Streptococcus pneumoniae*. Infect Immun 1994 December;62(12):5683-8.
26. Adrian PV, Thomson CJ, Klugman KP, Amyes SG. New gene cassettes for trimethoprim resistance, *dfr13*, and Streptomycin-spectinomycin resistance, *aadA4*, inserted on a class 1 integron. Antimicrob Agents Chemother 2000 February;44(2):355-61.
27. Kakiuchi M, Tsujigiwa H, Orita Y, Nagatsuka H, Yoshinobu J, Kariya S et al. Cyclooxygenase 2 expression in otitis media with effusion. Am J Otolaryngol 2006 March;27(2):81-5.
28. Wu HY, Virolainen A, Mathews B, King J, Russell MW, Briles DE. Establishment of a *Streptococcus pneumoniae* nasopharyngeal colonization model in adult mice. Microb Pathog 1997 September;23(3):127-37.
29. Hava DL, Camilli A. Large-scale identification of serotype 4 *Streptococcus pneumoniae* virulence factors. Mol Microbiol 2002 September;45(5):1389-406.
30. Hendriksen WT, Bootsma HJ, van DA, Estevao S, Kuipers OP, de GR et al. Strain-specific impact of PsaR of *Streptococcus pneumoniae* on global gene expression and virulence. Microbiology 2009 May;155(Pt 5):1569-79.
31. Forbes ML, Horsey E, Hiller NL, Buchinsky FJ, Hayes JD, Compliment JM et al. Strain-specific virulence phenotypes of *Streptococcus pneumoniae* assessed using the Chinchilla laniger model of otitis media. PLoS ONE 2008 April 9;3(4):e1969.
32. Briles DE, Crain MJ, Gray BM, Forman C, Yother J. Strong association between capsular type and virulence for mice among human isolates of *Streptococcus pneumoniae*. Infect Immun 1992 January;60(1):111-6.
33. Bakaletz LO. Developing animal models for polymicrobial diseases. Nat Rev Microbiol 2004

July;2(7):552-68.
34. Maeda K, Hirano T, Ichimiya I, Kurono Y, Suzuki M, Mogi G. Cytokine expression in experimental chronic otitis media with effusion in mice. Laryngoscope 2004 November;114(11):1967-72.
35. Skotnicka B, Hassmann E. Proinflammatory and immunoregulatory cytokines in the middle ear effusions. Int J Pediatr Otorhinolaryngol 2008 January;72(1):13-7.
36. Tong HH, Chen Y, Liu X, DeMaria TF. Differential expression of cytokine genes and iNOS induced by nonviable nontypeable *Haemophilus influenzae* or its LOS mutants during acute otitis media in the rat. Int J Pediatr Otorhinolaryngol 2008 August;72(8):1183-91.
37. Cripps AW, Kyd JM. Comparison of mucosal and parenteral immunisation in two animal models of pneumococcal infection: otitis media and acute pneumonia. Vaccine 2007 March 22;25(13):2471-7.
38. Tuomanen EI. Pathogenesis of pneumococcal inflammation: otitis media. Vaccine 2000 December 8;19 Suppl 1:S38-40.:S38-S40.
39. Hendriksen WT, Silva N, Bootsma HJ, Blue CE, Paterson GK, Kerr AR et al. Regulation of gene expression in *Streptococcus pneumoniae* by response regulator 09 is strain dependent. J Bacteriol 2007 February;189(4):1382-9.
40. Hendriksen WT, Kloosterman TG, Bootsma HJ, Estevao S, de GR, Kuipers OP et al. Site-specific contributions of glutamine-dependent regulator GlnR and GlnR-regulated genes to virulence of *Streptococcus pneumoniae*. Infect Immun 2008 March;76(3):1230-8.
41. Tong HH, Long JP, Li D, DeMaria TF. Alteration of gene expression in human middle ear epithelial cells induced by influenza A virus and its implication for the pathogenesis of otitis media. Microb Pathog 2004 October;37(4):193-20

Two DHH subfamily 1 proteins contribute to pneumococcal virulence and confer protection against pneumococcal disease

L.E. Cron, K. Stol, P. Burghout, S. van Selm, E.R. Simonetti, H.J. Bootsma, and P.W.M. Hermans

Infection and Immunity 2011, 79(9):3697-710

Abstract

Streptococcus pneumoniae is an important human bacterial pathogen, causing infections such as pneumonia, meningitis, septicemia, and otitis media. Current capsular polysaccharide-based conjugate vaccines protect against a fraction of the over 90 serotypes known, whereas vaccines based on conserved pneumococcal proteins are considered promising broad-range alternatives. The pneumococcal genome encodes two conserved proteins of an, as yet, unknown function, SP1298 and SP2205, classified as DHH subfamily 1 proteins. Here, we examined their contribution to pneumococcal pathogenesis using single and double knock-out mutants in three different strains: D39, TIGR4, and BHN100. Mutants lacking both SP1298 and SP2205 were severely impaired in adherence to human epithelial Detroit 562 cells. Importantly, the attenuated phenotypes were restored upon genetic complementation of the deleted genes. Single and mixed mouse models of colonization, otitis media, pneumonia, and bacteremia showed that bacterial loads in nasopharynx, middle ears, lungs, and blood of mice infected with the mutants were significantly reduced compared to wild-type-infected mice, with an apparent additive effect upon deletion of both genes. Minor strain-specific phenotypes were observed, i.e., deletion of SP1298 affected host-cell adherence in BHN100 only, and deletion of SP2205 significantly attenuated virulence in lungs and blood in D39 and BHN100, but not TIGR4. Finally, subcutaneous vaccination with a combination of both DHH subfamily 1 proteins conferred protection to nasopharynx, lungs, and blood of mice infected with TIGR4. We conclude that SP1298 and SP2205 play a significant role at several stages of pneumococcal infection, and, importantly, these proteins are potential candidates for a multicomponent protein vaccine.

Introduction

Streptococcus pneumoniae is a Gram positive bacterium causing serious invasive diseases such as pneumonia, septicemia, and meningitis. In addition, this human pathogen is the causative agent of less serious but highly prevalent mucosal infections such as otitis media (OM) and sinusitis. Young children under the age of 2 years, the elderly, and immunocompromised individuals account for the majority of pneumococcal morbidity and mortality observed worldwide (1). One of the main virulence factors of the pneumococcus is its polysaccharide capsule of which over 90 serotypes distinct in biochemical structure have been identified to date. The polysaccharide capsule contributes to protection against phagocytosis, enabling the pneumococcus to evade the immune system of the host (2,3). Current pneumococcal vaccines such as Pneumovax 23® (23-valent; Merck, USA), Synflorix™ (10-valent; GlaxoSmithKline, UK) and Prevnar® (7- and 13-valent; Pfizer, USA) target this polysaccharide capsule. While these vaccines do provide good immune protection, it is restricted to the serotypes included in the vaccine. As a result, serotype replacement is already occurring and the need for a serotype-independent vaccine is urgent (4;5).

A promising alternative vaccine approach explores the use of immunogenic, surface-exposed protective proteins. Pneumococci are estimated to express over 100 surface proteins, of which some are known to have a role in pathogenesis and virulence, but mostly their function is unknown (6). Among these surface proteins that are currently under investigation as vaccine candidates, are the pneumococcal surface proteins A and C (PspA and PspC), and the pneumococcal surface adhesin A (PsaA). The choline-binding proteins PspA and PspC are key virulence factors due to their ability to interfere with complement deposition. PspA is expressed by all pneumococci, is highly immunogenic, and is an inhibitor of C3 preventing opsonization and hence phagocytosis (7-9). PspC is a paralog of PspA which interacts with the complement-inhibitory factor H (10-12). PsaA is a metal-binding lipoprotein with specificity for Mn^{2+} and Zn^{2+} (13), both essential ions for pneumococcal growth and survival. One of the most well-studied proteins is pneumolysin (Ply). Although Ply is not a surface protein, it is an important virulence factor that is produced by all known clinical isolates of *S. pneumoniae*. Ply is a member of the cholesterol-dependent pore-forming toxin family that can directly damage epithelial surfaces and reduce the migration of phagocytic PMNs (14). Vaccination studies using the above-mentioned proteins have shown that they can protect mice from pneumococcal disease (15-23). In addition, these studies have clearly demonstrated that combinations of distinct

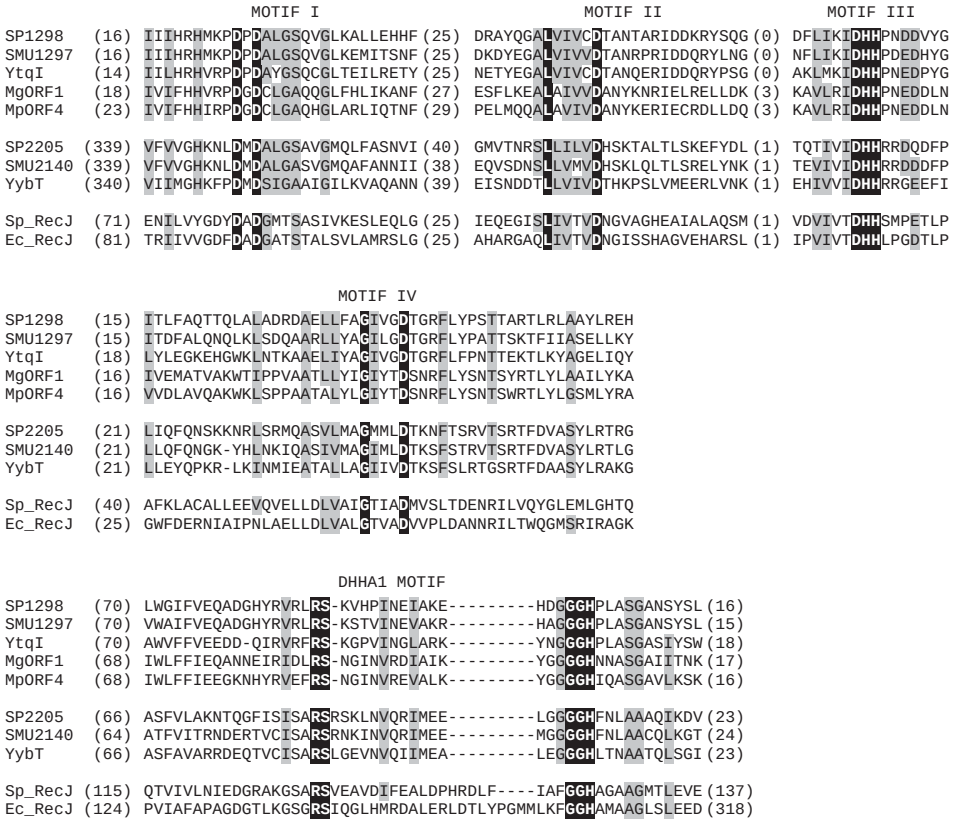

Figure 1. Sequence alignment of DHH motifs from selected bacterial DHH subfamily 1 proteins. The number of amino acids not shown in the alignment are depicted in parenthesis. Bold black shading indicates conserved residues, grey shading indicates similarity between residues. Dashes indicate gaps created to optimize alignment within motifs. Sequences are listed in order of similarity to sequence of SP1298. SP1298, *S. pneumoniae* TIGR4 SP1298; SMU1297, *S. mutans* AU159 SMU.1297; Ytql, *B. subtilis* Ytql; MgORF1, *M. genitalium* MG_190; MpORF4, *M. pneumoniae* MPN140; SP2205, *S. pneumoniae* TIGR4 SP2205; SMU2140, *S. mutans* AU159 SMU.2140c; YybT, *B. subtilis* Ytql; Sp_RecJ, *S. pneumoniae* TIGR4 SP0611 (RecJ); Ec_RecJ, *E. coli* RecJ.

pneumococcal proteins often enhance protection. Although these results are promising, there is still a need for additional protein targets to further improve existing experimental protein vaccine formulations.

Throughout the last decade, many genomic tools have been developed and used to identify potential protein vaccine targets, such as transcriptome analysis (24), differential fluorescence induction (25), and signature-tagged mutagenesis (STM) (26-28). We recently

developed Genomic Array Footprinting (GAF), a mutant library-based negative selection screen that uses microarrays to identify conditionally essential genes (29,30). We have applied the GAF technology to various *in vivo* animal models of pneumococcal disease, i.e. colonization, bacteremia and meningitis, to identify *S. pneumoniae* genes essential during infection (31-33). Interestingly, two pneumococcal proteins, SP1298 and SP2205, consisting of 311 and 657 amino acids, respectively, were consistently identified in all infection models. These two conserved proteins of an, as yet, unknown function are annotated as DHH subfamily 1 proteins in the pneumococcal genome. DHH family proteins belong to the superfamily of phosphoesterases (PE), and are named after their characteristic amino acid signature, Asp-His-His (DHH), found in a conserved N-terminal motif (i.e. motif III) (Figure 1). The DHH family can be divided further into two distinct subfamilies which share the four conserved N-terminal motifs, but have different C-terminal motifs. Subfamily 1 proteins are predominantly found in bacteria and archaea, while subfamily 2 proteins are also represented in eukaryotes. H-prune, the human homolog of *Drosophila* prune protein is an example of an eukaryotic DHH subfamily 2 protein suggested to be involved in cell migration (34). DHH domain proteins have been identified in a variety of prokaryotes, such as *Bacillus subtilis*, *Escherichia coli*, *Helicobacter pylori*, *Mycoplasma* species, and *Streptococcus gordonii* (35). RecJ of *E. coli* is one of the most well-known bacterial DHH subfamily 1 proteins possessing exonuclease activity (36,37). Recently, SMU.1297, a DHH-domain containing protein, has been described in another streptococcal species, *Streptococcus mutans* (38). Yet, little is known about DHH subfamily 1 proteins of *S. pneumoniae*.

In the current study, we examined the contribution of SP1298 and SP2205 to pneumococcal virulence using single and double knock-out mutants of three different strains of *S. pneumoniae*: D39, TIGR4, and BHN100 (serotypes 2, 4, 19F, respectively). We chose to examine the effect of both DHH subfamily 1 proteins in three pneumococcal strains as it has been shown that the genetic background can have a major influence on the contribution of proteins to virulence (39,40). Using four different murine models of single and mixed infections representing major phases of pneumococcal carriage and disease, we characterized the role of both DHH subfamily 1 proteins in the pneumococcal pathogenesis of colonization, otitis media, pneumonia, and bacteremia. We also assessed the contribution of both DHH subfamily 1 proteins to pneumococcal adherence *in vitro*. Finally, we provide evidence that vaccination with a combination of recombinant DHH subfamily 1 proteins can provide substantial protection against TIGR4-induced pneumonia in mice, and propose that these proteins should be considered as potential vaccine candidates.

Materials & Methods

Pneumococcal strains and growth conditions

Pneumococcal strains used in this study are shown in Table 1. *S. pneumoniae* was routinely grown in Todd-Hewitt broth supplemented with 5 g l^{-1} yeast extract (THY) or on Columbia blood agar (BA) plates (Oxoid) at 37°C and 5% CO_2. Prior to mouse infection experiments, bacteria were passaged in mice to maintain virulence as described previously (Kerr *et al.*, 2004). Cultures of mouse-passaged *S. pneumoniae* strains were grown to an optical density (OD) at 620 nm (OD_{620}) of 0.2 and aliquots were stored at -80°C in 15% glycerol. Prior to infection, defrosted aliquots were centrifuged, and bacteria were resuspended in sterile PBS to the desired concentration. When appropriate, antibiotics were used at the following concentrations: spectinomycin, 150 μg ml^{-1}, trimethoprim, 25 μg ml^{-1}, and kanamycin, 500 μg ml^{-1}. The number of CFU per ml in a particular sample was quantified by plating serial 10-fold dilutions in PBS on BA plates.

Construction of site-directed deletion mutants

All primers and plasmids used in this study are shown in Table 1. A megaprimer PCR method (30) was employed to replace target genes in the genome of the *S. pneumoniae* TIGR4, D39, and BHN100 strains with the spectinomycin resistance cassette amplified from plasmid pR412T7 (29). The resulting PCR products were introduced by competence stimulating peptide (CSP)-induced transformation into the corresponding strains using CSP-1 for D39 and BHN100 and CSP-2 for TIGR4. Transformants were selected on the basis of spectinomycin resistance and were checked by PCR for recombination at the desired location on the chromosome. In addition, a ΔSP1298ΔSP2205 double mutant was generated in each of the three pneumococcal strains. To this end, the SP1298 gene was inactivated by allelic replacement with a trimethoprim cassette and introduced into the respective ΔSP2205 strains (spectinomycin) by transformation.

Genetic complementation of DHH mutants

Genetic revertants of the SP1298 and SP2205 BHN100 single mutants were created using CEP, a chromosomal expression platform for ectopic, maltose-driven gene expression in *S. pneumoniae* (41). To this end, the genes were amplified with primer pairs HBSP1298atg/HBSP1298stop and HBSP2205atg/HBSP2205stop, respectively, using BHN100 chromosomal DNA as a template. After digestion by NcoI/BamHI, the SP1298 and SP2205

fragments were ligated with NcoI/ BamHI-digested plasmid pCEP. The resulting SP1298 and SP2205 ligation mixtures were used as donor in transformation of, respectively, strains BHN100ΔSP1298 and BHN100ΔSP2205, followed by selection for kanamycin-resistant transformants, thus generating the strains BHN100ΔSP1298 CEP^{SP1298} and BHN100ΔSP2205 CEP^{SP2205}. The complemented mutants were checked by PCR for integration at the desired location on the chromosome. A control $CEP^{Ø}$ strain lacking a gene insert was constructed by transforming BHN100 wild-type with HindIII-digested pCEP and selecting for kanamycin-resistant transformants. To examine SP1298 and SP2205 gene and protein expression levels, bacterial strains were grown to mid-log in THY medium without or with the addition of 0.4% maltose. Aliquots of these cultures were stored at -80°C with 15% glycerol for adherence assays.

Real-time PCR

Total RNA was extracted using the RNeasy Mini kit (Qiagen) after which contaminating genomic DNA was removed by treatment with DNase (DNAfree, Ambion). DNA-free total RNA (2.5 μg) was reverse transcribed using 300 ng of random hexamers and Superscript III reverse transcriptase (Invitrogen). To confirm the absence of genomic DNA, reactions without reverse transcriptase were carried out. Relative amounts of SP1298 and SP2205 transcripts were determined by quantitative real-time-PCR (qRT-PCR) using the SYBR Green technology on a 7500 Fast Real-Time PCR System (PE Applied Biosystems) according to the manufacturer's instructions. The relative quantification method was used to evaluate the quantitative variation between wild-type and complemented strains for each gene examined (42). The *gyrA* (SP1219) amplicon was used as an internal control for normalization of data.

Production of His-tagged SP1298 and SP2205 and generation of polyclonal rabbit antisera

The SP1298 and SP2205 genes of *S. pneumoniae* TIGR4 were PCR-amplified with oligonucleotide primer pairs LCSP1298AvrH6F/LCSP1298BamR, and LCSP2205AvrH6F/LCSP2205BamR, respectively. The amplicons were cloned into the pCR2.1 cloning vector of the TA cloning kit (Invitrogen) to obtain pLC1a (SP1298) and pLC2 (SP2205). Since sequence analysis showed that the AvrII site was not intact for SP1298, we PCR-amplified SP1298 from pLC1a using primer pair LCSP1298XbaF/LCSP1298BamR and subcloned the amplicon into pCR2.1 to obtain pLC1b. In the next step, the recombinant genes were excised with either XbaI/BamHI (SP1298) or AvrII/BamHI (SP2205) digestion and ligated to the BamHI/NheI-digested pET11c expression vector to obtain pLC1298 and pLC2205,

Table 1. Bacterial strains, primers, and plasmids used in this study

Strain, plasmid, or primer	Relevant characteristics[a]	Reference/source[b]
Species and strain		
S. pneumoniae		
D39	Wild-type (serotype 2)	NCTC 7466
TIGR4	Wild-type (serotype 4)	(73)
BHN100	Wild-type (serotype 19F)	(74)
ΔSP1298	Deletion mutant (Sp^r)	This study
ΔSP2205	Deletion mutant (Sp^r)	This study
ΔSP1298ΔSP2205	Deletion mutant (Sp^r/Tm^r)	This study
BHN100ΔSP1298 CEP^{SP1298}	BHN100ΔSP1298 with SP1298 ectopically expressed from CEP (Sp^r, Km^r)	This study
BHN100ΔSP2205 CEP^{SP2205}	BHN100ΔSP2205 with SP2205 ectopically expressed from CEP (Sp^r, Km^r)	This study
BHN100 $CEP^{\varnothing}$	BHN100 wild-type with empty CEP (Km^r)	This study
E. coli		
DH5α	Strain for DNA cloning	(75)
BL21	Strain for recombinant protein expression	Novagen
Plasmids		
pR412T7	Donor plasmid for Sp^r cassette	(29)
pKOT	Donor plasmid for Tm^r cassette	(44)
pCR2.1	Cloning vector (Ap^r, Km^r)	Invitrogen
pET11c	Expression vector (Ap^r)	Novagen
pLC1a	pCR2.1 containing SP1298 gene (BamHI)	This study
pCEP	pSC101 derivative; Sp^r, Km^r; carries the *S. pneumoniae* chromosomal expression platform, CEP	(41)
pLC1b	pCR2.1 containing SP1298 gene (XbaI and BamHI)	This study
pLC1298	pET11c containing rHisSP1298 gene	This study
pLC2	pCR2.1 containing SP2205 gene (AvrII and BamHI)	This study
pLC2205	pET11c containing rHisSP2205 gene	This study
Primers	Nucleotide sequence (5' to 3')	Target gene
CJsp1298_L1	CGTAGAAGGTATCTCCTGAG	SP1298; Left flank
CJsp1298_L2	CCACTAGTTCTAGAGCGGCGGGTCTGGTTTCATATGACG	SP1298; Left flank
CJsp1298_R1	CCTACAGATGAGTCTGGAAC	SP1298; Right flank
CJsp1298_R2	GCGTCAATTCGAGGGGTATCTAGCAAGTGGTGCTAATTC	SP1298; Right flank
CJsp1298_C	GATGTTCCAGCAAGGCTTTC	SP1298; control
HBsp1298_L2	GTCCAAGCTCACAAAAATCCGTGGGTCTGGTTTCATATGACG	SP1298; Left flank
HBsp1298_R2	CGTCTATGCGCGTCGTAACTAGCAAGTGGTGCTAATTC	SP1298; Right flank
CJsp2205_L1	CGCAGAAGATGTATCTCAAG	SP2205; Left flank
CJsp2205_L2	CCACTAGTTCTAGAGCGGCGTGGATAAGACTCCAAACGC	SP2205; Left flank
CJsp2205_R1	CGAATCGGAGCTTGTACTTG	SP2205; Right flank
CJsp2205_R2	GCGTCAATTCGAGGGGTATCGTAACCTTGTCAGAAGCAGG	SP2205; Right flank
CJsp2205_C	GCTGTCAAACTTTCTTCCGC	SP2205; control
PBpR412_L	GCCGCTCTAGAACTAGTGG	Sp cassette pR412
PBpR412_R	GATACCCCTCGAATTGACGC	Sp cassette pR412
PBMrTn9	CAATGGTTCAGATACGACGAC	Sp cassette; control
HBTmpFw	TCGGATTTTTGTGAGCTTGGAC	Tm cassette pKOT
HBTmpRv	GTTACGACGCGCATAGACG	Tm cassette pKOT
HBSP1298atg	GGgTATcc**ATG**GAGATTTGCCAACAAATTTTAG	SP1298
HBSP1298stop	GTTAAAAAACTTGCTTAAAAAC**TGA**TAggATcCTTGCCA	SP1298
HBSP2205atg	TTATGGTAccATGGGTGCCAAGAGGTTTTGA**ATG**	SP2205
HBSP2205stop	GGAAAAGGAGAAAGAAGAA**TGA**AAGgAtcCTTTcTAG	SP2205
HBgyrAF	AATGAACGGGAACCCTTGGT	*gyrA*, qRT-PCR
HBgyrAR	CCATCCCAACCGCGATAC	*gyrA*, qRT-PCR
HBSP2205F	GGGTCTGCTGCTTCAATCAAG	SP2205, qRT-PCR
HBSP2205R	ACACTCCGAATCTTATCTGAAATAGCT	SP2205, qRT-PCR
HBSP1298F	GATTACCCTATTTGCCCAAACAA	SP1298, qRT-PCR
HBSP1298R	ACAATTCCTGCAAAGAGCAACTC	SP1298, qRT-PCR
LCSP1298AvrH6F	CCCTAGGCATCACCATCACCATCACGAGATTTGCCAACAAATTTTAG	SP1298, AvrII
LCSP1298XbaF	CCCTAGGCATCACCATCACCATCACGAGATTTGCCAACAAATTTTAG	SP1298, XbaI
LCSP1298BamR	CGGATCCTCAGTTTTTAAGCAAGTTTTTTAAC	SP1298, BamHI
LCSP2205AvrH6F	CCCTAGGCATCACCATCACCATCACAAGAAACTGAGAGTGCATTATA	SP2205, AvrII
LCSP2205BamR	CGGATCCTCATTCTTCTTTCTCCTTTTCC	SP2205, BamHI

[a] Sp^r, spectinomycin resistant; Tm^r, trimethoprim resistant; Am^r, ampicillin resistant; Km^r, kanamycin resistant. Underlined sequences are complementary to primers used for amplification of antibiotic resistant cassettes. Small letters in the sequence indicate nucleotide changes to introduce convenient restriction sites. The start and stop codons of SP1298 and SP2205 are shown in bold.

[b] Left flak and right flank indicate positions relative to the target gene; qRT-PCR denotes primers used for real-time PCR; restriction sites introduced for cloning are indicated.

respectively. The nucleotide sequences of the SP1298 and SP2205 genes in pLC1298 and pLC2205 were confirmed by sequence analysis.

For the production of His-tagged SP1298 (rHisSP1298) and His-tagged SP2205 (rHisSP2205), an overnight culture of *E. coli* BL21 (pLC1298 or pLC2205) was diluted 50-fold in pre-warmed (37°C) 2 × LB supplemented with 0.5% glucose and 100 μg ml^{-1} ampicillin. At an OD_{600} between 0.6 and 0.8, 0.1 mM isopropyl-ß-D-thiogalactopyranoside (IPTG) was added to the culture. After 2 h, cells were placed on ice, pelleted by centrifugation, resuspended in ice-cold lysis buffer consisting of 20 mM sodium phosphate, 0.5 M sodium chloride, and 10 mM Imidazole (pH 7.4) to an equivalent of an OD_{600} of 100 and lysed by sonication. For pLC2205, 6 M urea, 1 mM phenylmethylsulfonyl fluoride (PMSF), and 0.1% Triton X-100 was added to the lysis buffer. For complete cell lysis of the pLC2205 culture, 6 M urea, 1 mM PMSF, and 0.1% Triton X-100 was first added to the lysis buffer and the suspension was frozen at -20°C. Subsequently, a defrosted cell suspension of pLC2205 was sonicated in the presence of 100 mM PMSF, 100 mM benzamidine (BZA), and lysozyme (100 mg ml^{-1}). Insoluble debris in both lysates was removed by ultracentrifugation (Sorvall WX Ultracentrifuge in a Ti70.1 Beckmann rotor) at 40,000 rpm for 1 h at 4°C. The resulting supernatants were loaded onto a 1 ml HiTrap Chelating HP column (Amersham Biosciences) preloaded with Ni^{2+}, washed with 10mM Imidazole phosphate buffer and eluted with 300 mM Imidazole phosphate buffer, and the fractions containing purified rHisSP1298 or rHisSP2205 were combined and dialyzed (Slide-A-Lyzer Dialysis Cassette 3500 MWO, 0.5-3 ml capacity; Pierce). Dialysis buffer for rHisSP1298 contained 10 mM HEPES, while rHisSP2205 was dialyzed against 10 mM HEPES, 6 M urea, and 0.1% Triton X-100. After dialysis, rHisSP1298 was lyophilized and rHisSP2205 was stored in the dialysis buffer; both stored at –20°C until further use. The identities of the purified proteins were confirmed by matrix-assisted laser desorption ionization-time-of-flight analysis, and their amounts were determined by the bicinchoninic acid (BCA) assay (Bio-Rad).

For the generation of anti-SP1298 and anti-SP2205 polyclonal rabbit antibodies, a total of 400 μg of each protein was used according to the Speedy program of Eurogentec.

Western blot analysis

Whole-cell bacterial lysates were used in Western blot analysis by separating 2.5 x 10^7 CFU/lane on SDS-PAGE gels (12.5%). After electrophoretic transfer onto a nitrocellulose membrane, transfer was visualized by staining membranes with Ponceau S (Sigma-Aldrich). Subsequently, membranes were blocked using PBS with 0.1% Tween 20, 2% skim milk powder, and 1% bovine serum albumin (BSA), and incubated with the primary antibodies (rabbit polyclonal α-SP1298 or α-SP2205) followed by horseradish peroxidase-

coupled secondary anti-rabbit antibody. Immunoblots were developed by enhanced chemiluminescence (Amersham).

Pneumococcal adherence assay

The human pharyngeal epithelial cell line Detroit 562 (ATCC number CCL-138) was routinely grown in RPMI 1640 medium without phenol red (Invitrogen, The Netherlands) supplemented with 1 mM sodium pyruvate and 10% (vol/vol) fetal calf serum (FCS). All cells were cultured at 37°C in a 5% CO_2 environment. For adherence assays, bacteria were resuspended in RPMI 1640 medium without phenol red supplemented with 1% FCS. For adherence experiments with complemented mutants, maltose was added to the medium to a concentration of 0.4%. Adherence of pneumococci to epithelial cells was performed as described previously (40,43). Briefly, Detroit 562 cells were seeded into 24-well plates and incubated for 48 h. Confluent monolayers were washed twice with 1 ml PBS and infected with 1×10^7 CFU ml^{-1} [multiplicity of infection (MOI) of 10 (bacteria/cells)] and pneumococci were allowed to adhere to the cells for 2 h at 37°C in a 5% CO_2 environment. Non-adherent bacteria were removed by 3 washes of 1 ml PBS, after which 200 μl of 0.05% trypsin, 1 mM EDTA was added to detach the cells, followed by 800 μl of ice-cold 0.025% Triton X-100 in PBS to lyse the cells. Samples were plated for CFU count, and corrected to account for small differences in the initial inoculum. All experiments were performed in triplicate and repeated at least three times. The adherence of the mutants is given as the percentage relative to the wild-type. All bacterial strains grew equally well in the tissue culture medium.

Mouse studies

Eight-week old female outbred CD-1 mice (Charles River Laboratories, Germany) were used for the colonization, pneumonia, and bacteremia models, while the OM experiments were performed with 7-week old female inbred specific pathogen free BALB/c mice (Harlan, The Netherlands). All mice were housed in filter-top cages and had access to food and water *ad libitum*. Mice were allowed to acclimate for a week prior to each experiment. All animal experiments were performed with approval of the Radboud University Nijmegen Medical Centre Committee for Animal Ethics.

Pneumonia model

Mice were lightly anesthetized with 2.5% (vol/vol) isoflurane over oxygen, and infected intranasally (i.n) by pipetting 50 μl of inoculum (5×10^6 CFU total) onto the nostrils of mice while held in an upright position. At predetermined times after infection, groups of mice

were sacrificed by injection anesthesia, and blood samples were taken by retro-orbital bleeding. Bacteria were recovered from the nasopharynx by flushing each nare with 1 ml sterile PBS (nasopharyngeal lavage, NPL) (44). A bronchoalveolar lavage (BAL) was performed by flushing the lungs with 2 ml sterile PBS, after which lungs were removed from the body and homogenized in 2 ml sterile PBS using a hand held homogenizer (Polytron PT 1200; Kinematica AG).

Colonization model

Mice were infected i.n. under anesthesia as mentioned above with a smaller volume of inoculum, 10 μl (5×10^6 CFU total). As described previously, nasal instillation of pneumococci with such a low volume does not cause a lethal infection in mice (40). Mice showed no visible signs of disease throughout the course of colonization and had less than 40 CFU in the lungs at the last time point. At predetermined time points after infection, NPL and lungs were collected as described above.

Otitis media model

Intranasal infection was performed as described above in the colonization model with the following exception: methylcellulose (1%) was added to the inoculum for all OM experiments in order to minimize leakage of inoculum to the lungs (45). Mice were placed in a supine position in the pressure cabin after infection as described previously (46). Briefly, an initial pressure rise was set at 10 kPa and when the mouse started to regain consciousness and the first swallowing movements occurred, pressure was raised at the rate of 5 kPa per 15 s until a pressure of 40 kPa was reached, enabling the inoculum to reach the middle ear cavity. Then the pressure was lowered gradually until atmospheric pressure was reached again. Groups of mice were sacrificed at 24, 48, and 96 h post-infection where mice were bled out by retro-orbital puncture, followed by cervical dislocation. The bullas enclosing the middle ears (ME) were dissected from the temporal bone and homogenized in the presence of 1 ml sterile PBS per ear, as previously described (45,46). Bacteria were also recovered from the nasopharynx by performing an NPL using 1 ml of sterile PBS and the lungs were extracted and homogenized in 2 ml sterile PBS.

Bacteremia model

Mice were infected via the tail vein with a 100 μl inoculum (10^6-10^7 CFU total). To confirm successful infection, blood was taken from a separate vein immediately after injection (t= 0 h). Subsequently, blood was recovered via a tail vein puncture from the same mouse at 12 and 24 h post-infection and by retro-orbital puncture at the last time point, 36 h.

Co-infection experiments

A 1:1 ratio of wild-type and its respective ΔSP1298, ΔSP2205, or ΔSP1298ΔSP2205 mutant was used to infect the mice as described in the above-mentioned infection models. This setup reduces variation between individual mice, inoculation preparation and distribution, and sample collection. Viable bacteria were quantified by plating serial dilutions on BA plates and BA plates supplemented with either spectinomycin or spectinomycin and trimethoprim. Subsequently, competitive index (CI) scores were calculated for each individual animal as the output ratio of mutant to wild-type divided by the input ratio of mutant to wild-type bacteria. A log CI score <0 indicates that the mutant is outcompeted by the wild-type. For samples in which no viable mutant bacteria were recovered, the lower limit of detection (20 CFU ml^{-1}) was substituted as the numerator. If in one particular sample neither wild-type nor mutant bacteria were detected, the data were excluded from further analysis.

Immunizations

Female CD-1 mice (6 weeks old) were subcutaneously immunized three times at 14-day intervals with a total of 50 μg protein in alum adjuvant (aluminum hydroxide gel; Sigma). Briefly, mice were either primed singly with rHisSP1298 or rHisSP2205, or with a combination of the two proteins. The negative control group consisted of mice given a 1:1 ratio of alum adjuvant and PBS. One tenth of the human dose of Prevnar® 7 was given to the positive control group. Blood samples from all mice were collected via tail vein puncture prior to any immunization, at the time of the third boost, and several days before infection. Mice were subsequently challenged i.n. with the TIGR4 wild-type strain (1×10^6 CFU total) three weeks after the last immunization in our pneumonia model and sampled 48 h post-infection as described above.

Detection of antigen-specific IgG by ELISA

IgG titers against SP1298 and SP2205 were determined by ELISA analysis. High binding-capacity microtitre plates (Greiner) were coated with 1 μg μl^{-1} purified rHisSP1298 or rHisSP2205 in 100 μl per well overnight at 4°C. Plates were washed with PBS with 0.05% Tween 20 (PBST) and then incubated for 1 h with PBST containing 2% BSA. Three-fold serial dilutions of sera were added to the plates and incubated for 1 h at 37°C. After washing, the alkaline phosphatase secondary antibody directed to mouse IgG-Fc (Sigma-Aldrich) was added for 1 h at 37°C using a 1:25,000 dilution. After washing, 100 μl per well of *p*-nitrophenyl phosphate (1 mg ml^{-1}) in substrate buffer (10 mM diethanolamine and 0.5 mM magnesium chloride, pH 9.5) was added and the absorbance was read at 405 nm.

Statistical analyses

For adherence assays, comparisons between wild-type and mutant pneumococcal strains were performed using Student's t-test (unpaired). The Mann-Whitney test was used for comparison of bacterial load in NPL, ME, BAL, lung homogenate, and blood between the wild-type- and their respective DHH mutant-infected mice in all infection models. For the co-infection data, a Wilcoxon test on log-transformed CI scores was used to determine if the median CI was statistically significantly different from 0 (i.e., no outcompetition). All statistical analyses were performed using GraphPad Prism version 4.0.

Results

DHH subfamily 1 proteins contribute to pneumococcal adherence *in vitro*

To assess the (strain-specific) contribution of the DHH subfamily 1 proteins SP1298 and SP2205 to pneumococcal pathogenesis, directed mutants were generated in three strains: D39, TIGR4, and BHN100. Western blot analysis of wild-type, ΔSP1298, ΔSP2205, and double mutant cell lysates using anti-SP1298 and anti-SP2205 rabbit serum confirmed that SP1298 and SP2205 were expressed in all three wild-type strains, but not in their respective single and double mutants (data not shown). Importantly, no differences in *in vitro* growth between the wild-type strains and the DHH subfamily 1 mutants were detected.

Adherence of pneumococci to respiratory epithelial cells is crucial for colonization of the nasopharynx. Therefore, we examined adherence of the three wild-type strains and their isogenic single and double DHH subfamily 1 mutants to human pharyngeal epithelial Detroit 562 cells. Wild-type adherence levels of TIGR4 ($\sim 6.5 \times 10^4$ adherent CFU) were statistically significantly higher than those of the wild types of the D39 or BHN100 strains by almost 1 log. Interestingly, no difference in adherence was observed upon deletion of the SP1298 gene in TIGR4 and D39, while adherence of BHN100ΔSP1298 was reduced by ~75%, suggesting that the contribution of SP1298 to adherence is strain-specific (Figure 2A). In contrast, all three SP2205 mutants showed a significant decrease in adherence compared to their wild types, ranging from 60 to 90% (Figure 2A). The ability of the double mutants in all three strains to adhere was drastically reduced by >80%, displaying an enhanced effect when both genes were deleted (Figure 2A).

To confirm that the observed phenotypes were indeed due to the deletion of the SP1298 and SP2205 genes, we generated genetically complemented mutants by ectopic expression of the respective genes from the maltose-inducible CEP site. Given that attenuated adherence of both single mutants was only observed in the BHN100 strain, we chose this background for the genetic complementation. As a control, we generated BHN100 $CEP^{\varnothing}$, containing the empty chromosomal expression platform. Real-time PCR and Western blot analysis of the genetic revertants showed that SP1298 gene and protein expression was restored to wild-type levels in normal medium, and was five-fold higher than wild-type upon addition of maltose (Figure 2B). For SP2205, both gene and protein expression was clearly restored in normal medium, but maltose-induction was required to reach wild-type levels (Figure 2B). Importantly, the ability of the complemented SP1298 mutant to adhere to Detroit cells was indistinguishable from wild-type when cells were grown without

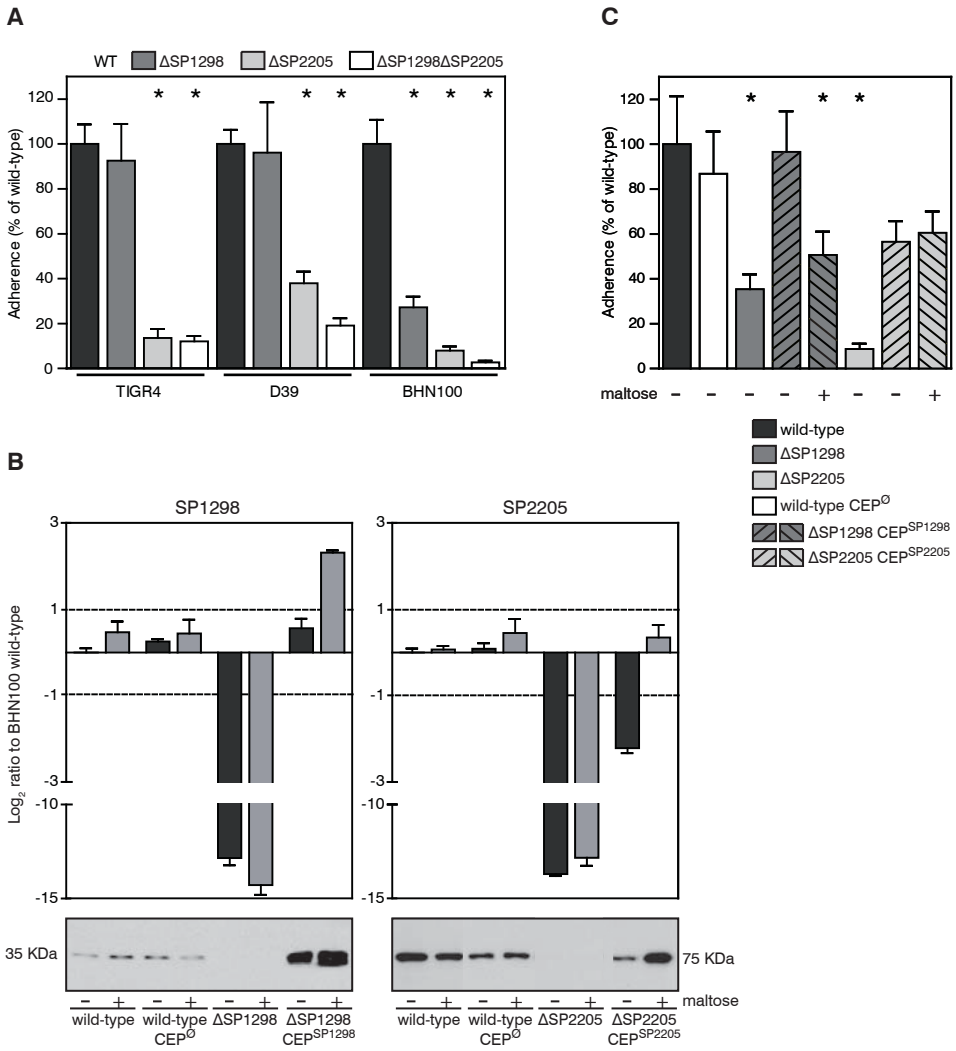

Figure 2. (A) *In vitro* adherence of pneumococcal strains to the human pharyngeal epithelial cell line Detroit 562. The adherence of the mutants is given as the percentage relative to the respective wild-type. (B) Real-time PCR (upper panels) and Western blot analysis (lower panels) of BHN100 complemented for SP1298 (left) or SP2205 (right) mutants. Real-time data are expressed as the $\log_2$ ratio of expression relative to that for the BHN100 wild-type grown without maltose. Strain names and presence of maltose in growth medium are indicated at the bottom. (C) *In vitro* adherence of BHN100 complemented mutants to Detroit 562 cells, given as the percentage relative to that for the BHN100 wild-type grown without maltose. Presence of maltose in growth medium is indicated at the bottom. All values are geometric means, and error bars represent SEM. *, $P<0.0001$.

maltose (Figure 2C), while the maltose-induced overexpression of SP1298 had a slight adverse effect on the adherence ability. Moreover, the adherence of the SP2205 mutant was also no longer significantly different from wild-type upon complementation, with or without maltose-induction. In all cases, BHN100 CEP$^{\varnothing}$ behaved the same as wild-type. Thus, the observed attenuated adherence phenotypes of the DHH mutants were not the result of an inadvertent mutation in a non-targeted gene.

DHH subfamily 1 proteins contribute to various stages of pneumococcal pathogenesis *in vivo*

(i) Colonization. Since colonization of the nasopharynx is a prerequisite for pneumococcal infection, we first compared all single and double SP1298 and SP2205 mutants to their isogenic parental wild types following intranasal infection in our established colonization model. All wild-type strains maintained an overall colonization level of approximately 10^5 CFU during the course of infection (Figures 3A, C, E). Even though all single and double SP1298 and SP2205 mutants were capable of colonizing the murine nasopharynx to varying degrees throughout infection, significant decreases in bacterial load were observed compared to their respective wild types over time. Interestingly, SP1298 and SP2205 mutants in a BHN100 background maintained a slightly higher level of colonization in the nasopharynx in comparison to the SP1298 and SP2205 mutants in the other two pneumococcal backgrounds. The most prominent phenotype was observed in the TIGR4 genetic background where all single and double SP1298 and SP2205 mutants were significantly attenuated at all time points from 24 h post-infection onwards (Figure 3A). The double mutants in all three strain backgrounds were significantly impaired in their ability to colonize the nasopharynx, but again the most severe attenuation was observed in the TIGR4 background with a 2,500-fold decrease compared to the wild-type after just 24 h ($p<0.005$) (Figure 3A). Since both single mutants in TIGR4 only showed a decrease of ~10-fold, this suggests an additive effect when both genes are absent. Mice infected with single and double SP1298 and SP2205 mutants of D39 (Figure 3C) and BHN100 (Figure 3E) also had lower bacterial loads than their respective wild-type-infected mice, especially at the later time-points.

To further characterize the potential role of these two DHH subfamily 1 proteins in pneumococcal colonization, we examined the phenotype of each mutant when in direct competition with its respective wild type, as minor differences between two bacterial strains can be unmasked with such a competitive setup. The TIGR4 and BHN100 wild types significantly outcompeted their respective single SP1298 and SP2205 mutants 96 h post-infection (900-7,000-fold; Figures 3B, F). Interestingly, although outcompetition of the

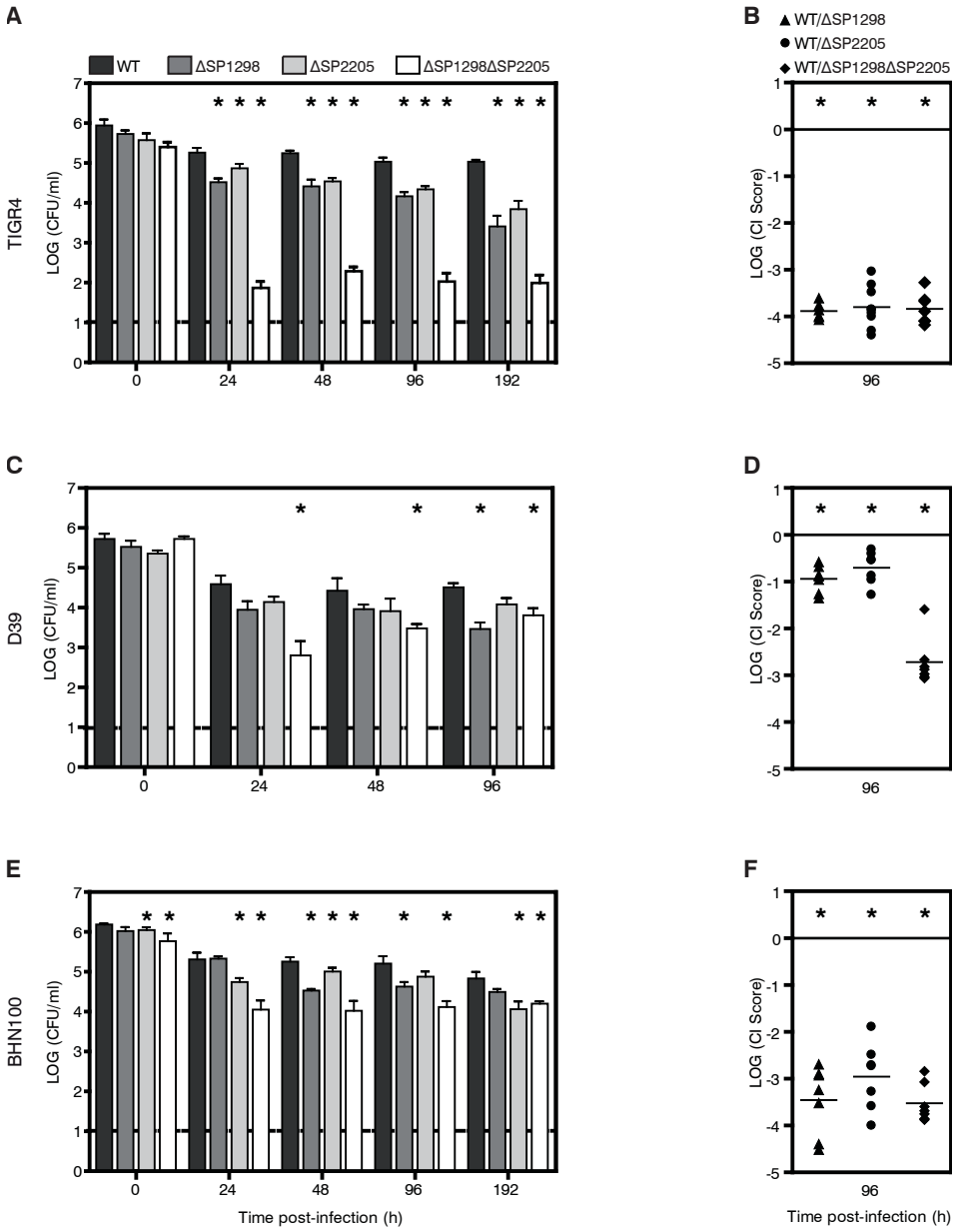

Figure 3. Bacterial load in the nasal lavage fluid of mice intranasally infected with 5×10^6 CFU of wild-type and/or the respective ΔSP1298, ΔSP2205, or ΔSP1298ΔSP2205 mutants. Strain data are depicted for TIGR4 (A and B), D39 (C and D), or BHN100 (E and F). Data from single-infection experiments are shown in panels A, C, and E; data from coinfection experiments are shown in panels B, D, and F. The horizontal line represents lower limit of detection, and error bars represent SEM. Each point in panels B, D, and F represents the log competitive index score from an individual mouse. Values <0 indicate attenuation of the mutant. Horizontal lines represent the mean. *, $P<0.05$.

D39 single mutants was significant but much less prominent (<10-fold; Figure 3D) than that for the other two strain backgrounds, the double mutants in all strains were outcompeted ~500-7,000-fold, suggestive of a strain-specific additive effect (Figures 3B, D, F). Especially for the TIGR4 strain, attenuation levels of mutants differed between single- and co-infection: both single mutants were outcompeted to the same extent as the double mutant in co-infection, whereas a 2-log difference in colonization levels was observed in single infection. This is most likely due to the enhanced sensitivity of the competitive setup, where both single mutants were already outcompeted to levels below our detection limit (20 CFU ml^{-1}).

(ii) Otitis media. The pathogenesis of pneumococcal OM involves translocation of the bacteria from the nasopharynx to the middle ear cavity through the Eustachian tube, accomplished by the use of a pressure cabin in the murine OM model recently described (46). We examined the contribution of the DHH subfamily 1 proteins to experimental OM using the mutants in TIGR4 and BHN100 since it has been established that these two strains produce higher CFU counts in the middle ear in this model than D39 (46). Colonization levels of the middle ear with BHN100 wild-type (>10^5 CFU ml^{-1}) were higher than the TIGR4 wild-type strain (~10^4 CFU ml^{-1}) throughout the course of OM infection (Figures 4A, C).

Attenuation of the BHN100 double mutant was observed at all time points post-infection (Figure 4A). Reduced bacterial loads of <10^3 CFU ml^{-1} were observed for BHN100ΔSP1298 throughout OM infection, albeit only statistically significant at the last two time points, while BHN100ΔSP2205 only appeared to be attenuated at 48 h (Figure 4A). In line with the BHN100 data, the TIGR4 double mutant was incapable of colonizing the middle ear at any of the time points (Figure 4C). A consistent reduction in bacterial load was observed for TIGR4ΔSP1298 and, to a lesser extent, TIGR4ΔSP2205 (Figure 4C), but this was not statistically significant except for TIGR4ΔSP1298 at 96 h due to large spread of the wild-type.

In the co-infection experiments, both wild types outcompeted their respective single and double SP1298 and SP2205 mutants in the middle ear by 20- to 350-fold (Figures 4B, D). These observations clearly confirmed the single infection data. Finally, nasopharyngeal colonization levels of wild-type and mutants in the OM model were similar to NPL data obtained with the colonization model (data not shown).

(iii) Pneumonia. Pneumococcal pneumonia can occur when bacteria are aspirated from the nasopharyngeal niche to the lungs. In the murine pneumonia model, infection was monitored at three sites: nasopharynx, lungs, and blood, allowing us to examine aspects of both colonization and invasive disease. Nasopharyngeal colonization in the

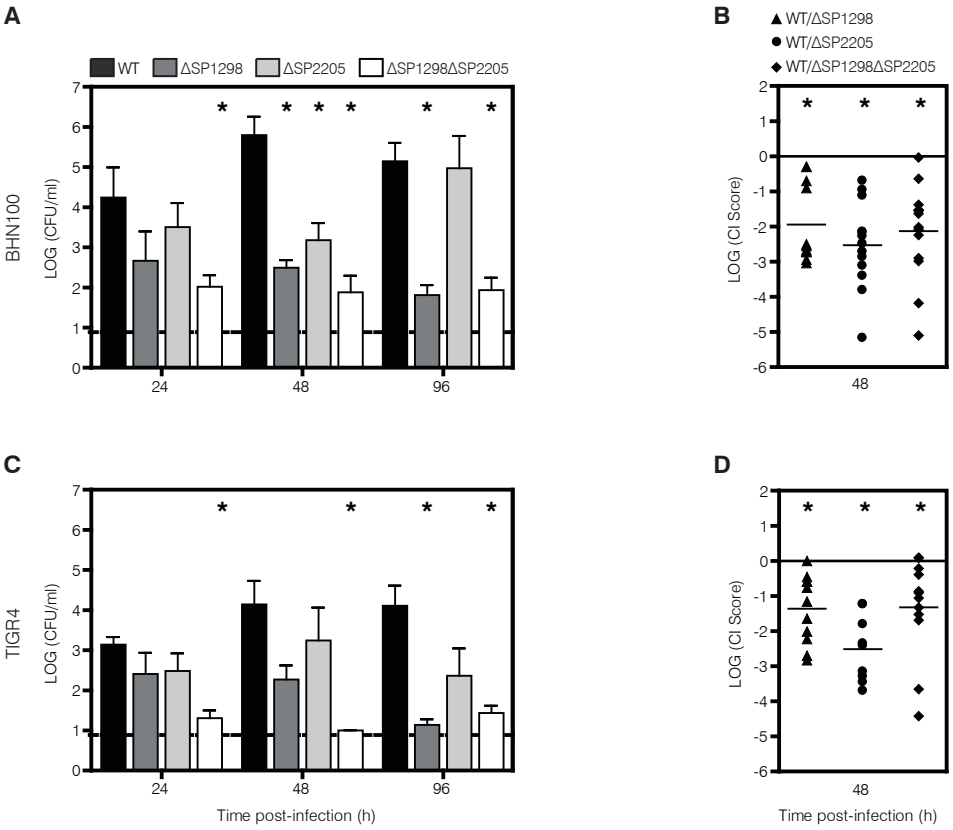

Figure 4. Bacterial load in the middle ear fluid of mice intranasally infected with 1×10^6 CFU of the wild-type and/or respective ΔSP1298, ΔSP2205, or ΔSP1298ΔSP2205 mutants. Strain data are depicted in panels A and B for BHN100 and in C and D for TIGR4. The single infections shown in panels A and C represent the sum of pneumococci in the left and right middle ear fluid. The horizontal line represents lower limit of detection and error bars represent SEM. Co-infection data are shown in panels B and D, where each point represents the log competitive index score from one mouse ear. Values <0 indicate attenuation of the mutant. Horizontal lines represent the mean. *, $P<0.05$.

pneumonia model was comparable to the results observed in the colonization and OM models (data not shown). Interestingly, similar to our observations in the NPL (Figure 3E), the number of BHN100 wild-type in the BAL fluid ($\sim 10^4$ CFU) was higher than that of the TIGR4 and D39 wild-type strains after 24 h post-infection (Figures 5B, E, H). A very pronounced phenotype was seen with the BHN100 single and double SP1298 and SP2205 mutants as they were all significantly attenuated ~2 logs in the lungs and BAL 24 and 48 h post-infection compared to the BHN100 wild-type (Figures 5G-H). In the lung tissue, we observed that the D39 double mutant was significantly attenuated at all time points;

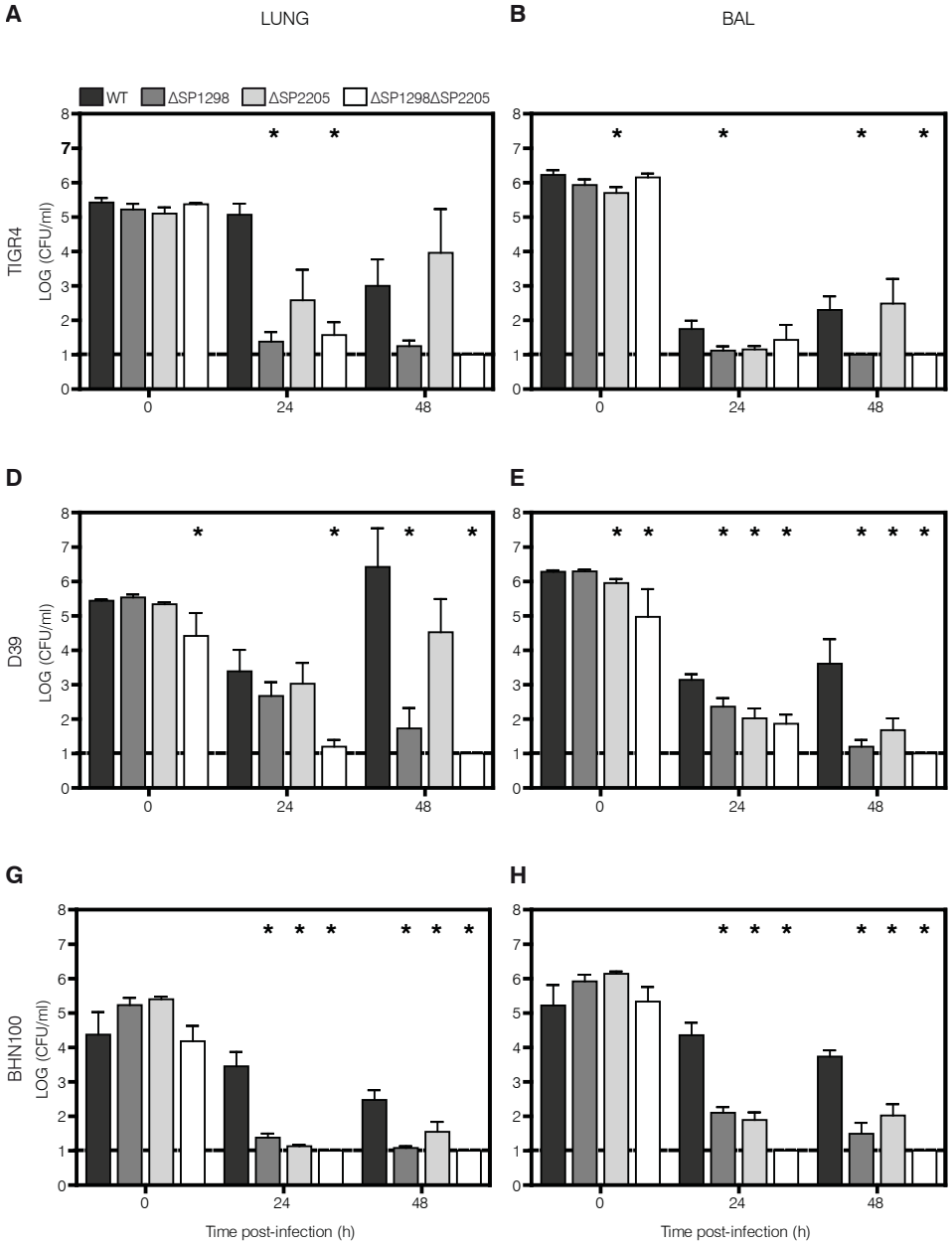

Figure 5. Bacterial load in the lung homogenate and bronchoalveolar lavage fluid of mice following intranasal infection with 5×10^6 CFU of the wild-type and/or respective ΔSP1298, ΔSP2205, or ΔSP1298ΔSP2205 mutants. Strain data for TIGR4 (A, B, and C), D39 (D, E, and F), or BHN100 (G, H, and I) are shown. Data from single-infection experiments are shown in panels A, B, D, E, G, and H, and data from coinfection experiments are shown in panels C, F, and I. The horizontal line represents the lower limit of detection, and error bars represent SEM. Each point depicted in panels C, F, I indicates the log competitive index score from an individual mouse. Values <0 indicate attenuation of the mutant. Horizontal lines represent the mean. *, $P<0.05$.

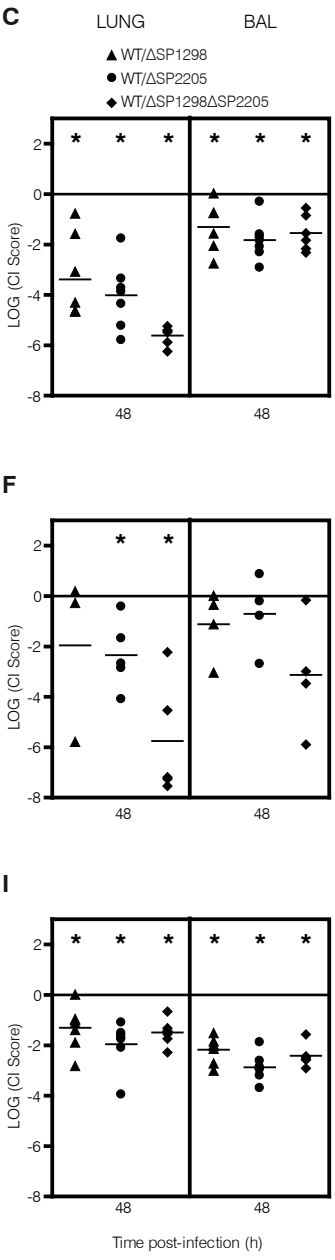

while only D39ΔSP1298 was attenuated at 48 h (Figure 5D). However, bacterial loads for all D39 single and double SP1298 and SP2205 mutants recovered in BAL at 24 and 48 h were significantly lower than wild-type loads (Figure 5E). For TIGR4, the single ΔSP1298 and the double mutant were also unable to cause infection in the lungs and BAL at 24 and 48 h (Figures 5A-B), albeit not always statistically significant due to a large spread of the wild-type. However, mice infected with TIGR4ΔSP2205 were capable of causing disease at wild-type levels 48 h post-infection (Figures 5A-B).

In the pneumonia coinfections, we observed that the TIGR4 and BHN100 wild types significantly outcompeted their respective SP1298 (20- to 2,200-fold) and SP2205 (70- to 10,000-fold) mutants at 48 h post-infection in the lung and BAL fluid (Figures 5C, I), while the D39 wild-type only significantly outcompeted the ΔSP2205 (200-fold) and ΔSP1298ΔSP2205 (50,000-fold) mutants only in the lung tissue (Figure 5F). Moreover, we observed that the TIGR4 and D39 wild types outcompeted their respective double mutants much more than their respective single DHH subfamily 1 mutants, displaying an enhanced effect when both genes were deleted (Figures 5C, F). For example, the TIGR4 double mutant was outcompeted by its wild-type 40,000-fold while the single SP1298 and SP2205 mutants were outcompeted by only 2,200-fold and 10,000-fold, respectively.

The TIGR4 and D39 strains and their respective mutants were all able to disseminate from lungs to blood, except for the SP1298 mutants for which no bacteria were detected at

any time-point. Once in the blood, the TIGR4 and D39 wild types and their respective ΔSP2205 mutants showed growth characteristics similar to those described in the bacteremia model below.

(iv) Bacteremia. Bacteremia is a severe complication which occurs in approximately 30% of pneumonia cases (47). To assess whether the DHH subfamily 1 proteins are required for survival of pneumococci once they have entered the bloodstream, we intravenously infected mice with wild-type and/or mutant pneumococci. Both wild types (TIGR4 and D39) had higher bacterial counts (7- to 25,000-fold more) in the blood compared to their respective SP1298 and SP2205 mutants throughout the course of the infection (Figures 6A, C), except for the TIGR4ΔSP2205 mutant. The fact that the TIGR4ΔSP2205 mutant behaved as the wild-type in this model is supported by corresponding blood data from the pneumonia model. The mice infected with TIGR4ΔSP1298 maintained significantly lower levels (~200-fold less) of bacteria after 12 h post-infection. In the case of D39, the single ΔSP1298 and double mutants were significantly attenuated at all time points, the ΔSP2205 mutant only at 32 h post-infection (Figure 6C). The BHN100 strain was not capable of surviving in the blood and was cleared from the bloodstream within 24 h after infection (data not shown). Furthermore, we observed that the TIGR4 and D39 wild types statistically outcompeted their respective double mutants up to 3 logs more than their respective single DHH subfamily 1 mutants, further signifying an additive effect when both genes were deleted (Figures 6B, D). Interestingly, the TIGR4ΔSP2205 mutant was only attenuated in blood in a co-infection setup, suggesting this mutant is only able to efficiently survive during bacteremia when it is not in direct competition with the wild-type.

DHH subfamily 1 proteins confer protection against pneumococcal pneumonia

To evaluate the protection elicited by immunization with recombinant rHisSP1298 and rHisSP2205 proteins either singly or in combination, CD-1 mice were immunized with these proteins and subsequently challenged with *S. pneumoniae* TIGR4. The individual IgG titers in sera of mice immunized with one or both DHH subfamily 1 proteins or with Prevnar® 7 were tested three weeks after the final immunization. Analysis showed antigen-specific antibody responses that were significantly higher compared to their respective negative pool pre-immune serum (data not shown). No difference in IgG titers was seen between the single or double vaccinated groups. At 48 h post-infection, protection was evaluated by quantifying bacterial load. As expected, mice that received Prevnar® 7 were protected (Figure 7), as capsular type 4 is included in this vaccine. While a minor reduction of bacteria in the nasopharynx ($p<0.013$) of rHisSP1298-vaccinated mice was observed (Figure 7A), mice receiving either rHisSP1298 or rHisSP2205 alone were not protected and suc-

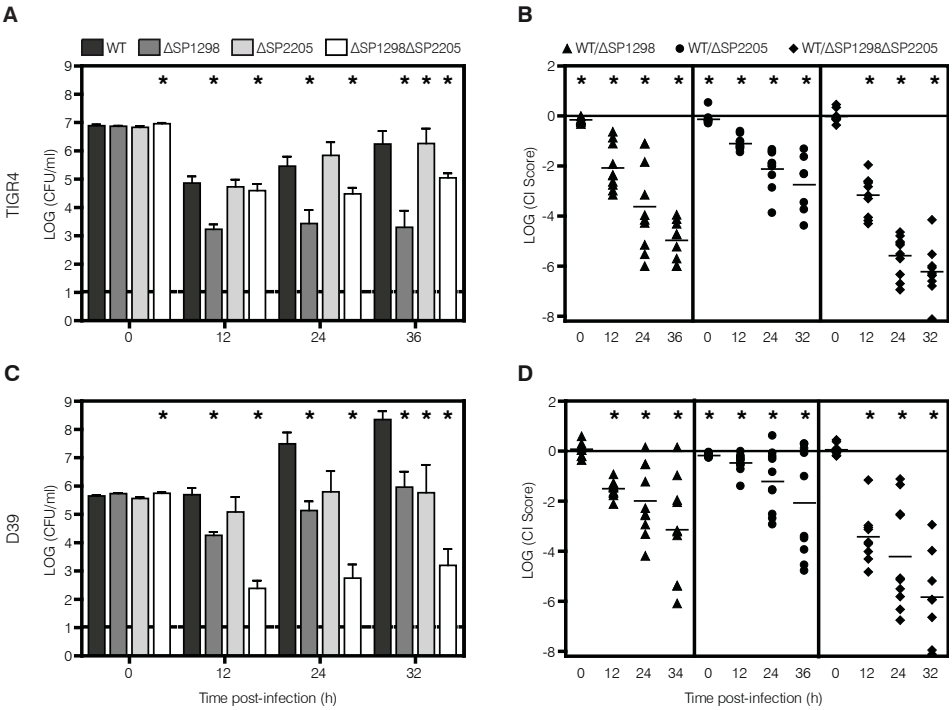

Figure 6. Bacterial load in the blood of mice over time following intravenous infection with $1 \times 10^{6/7}$ CFU of wild-type and/or respective ΔSP1298, ΔSP2205, or ΔSP1298ΔSP2205 mutants. Strain data for TIGR4 (A and B) or D39 (C and D) are depicted. Data from single-infection experiments are shown in panels A and C, and data from coinfection experiments are shown in B and D. The dotted horizontal line represents the lower limit of detection, and error bars represent SEM. Each point depicted in B and D indicates the log competitive index score from an individual mouse. Values <0 indicate attenuation of the mutant. Horizontal lines represent the mean. *, $P<0.05$.

cumbed to infection just as rapidly as mice receiving adjuvant only. Interestingly, protection was only seen with mice who received a combination of both DHH subfamily 1 antigens. Bacterial loads in the nasopharynx, blood, and lung of these mice were statistically significantly lower ($p<0.0001$, 0.013, 0.003, respectively) than those of mice receiving adjuvant only (Figures 7A, B, D) after subsequent challenge with TIGR4 wild-type. Sixty percent of these mice did not develop bacteremia and clinical signs of disease were minimal.

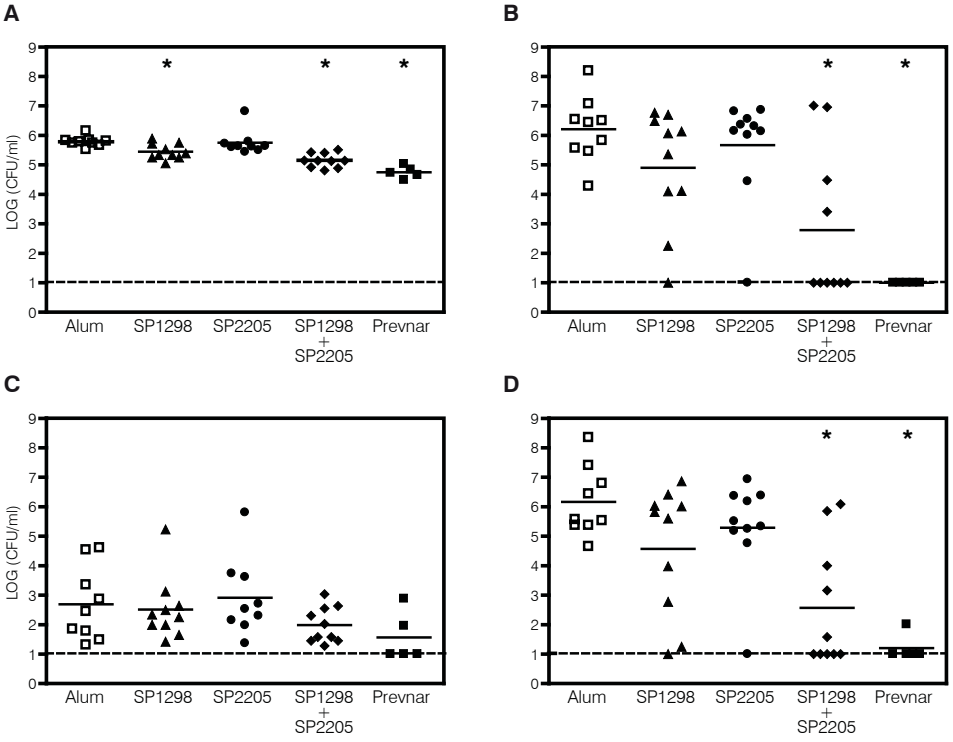

Figure 7. Protection against intranasal challenge with *S. pneumoniae* TIGR4. Mice subcutaneously immunized with alum (open squares), rHisSP1298 (filled triangles), rHisSP2205 (filled circles), a combination of rHisSP1298 and rHisSP2205 (filled diamonds), or Prevnar® 7 (filled squares) were subsequently challenged with TIGR4 wild type. Pneumococci were recovered 48 h postinfection from NPL (A), blood (B), BAL fluid (C), or lung homogenate (D). Each dot represents one mouse. The dotted horizontal line represents the lower limit of detection. *, $P<0.05$.

Discussion

Current polysaccharide conjugate vaccines targeting the respiratory tract pathogen *S. pneumoniae* provide excellent protection against invasive disease caused by vaccine serotypes, yet remain ineffective against circulating non-vaccine serotypes. Vaccines that include conserved (surface) proteins involved in pneumococcal virulence are considered promising alternatives. To identify such targets, we previously screened for genes essential during pneumococcal infection using the GAF technology (29,30,33). These *in vivo* GAF screens have led to the identification of the DHH subfamily 1 proteins SP1298 and SP2205. These two proteins have not been identified by previous STM or expression studies, and have consequently never been considered as virulence factors or vaccine leads in *S. pneumoniae*. This prompted us to examine their role in pneumococcal pathogenesis and protection in more detail.

Our *in vitro* and *in vivo* results clearly demonstrate that the two pneumococcal DHH subfamily 1 proteins are required for full pneumococcal virulence at several target sites of the host, e.g., nasopharynx, middle ear, lungs, and blood. Genetic complementation of the SP1298 and SP2205 genes in the BHN100 single mutants resulted in restoration of *in vitro* adherence to wild-type levels, indicating that our observed phenotypes are indeed the results of the gene deletions and not an inadvertent mutation in a non-targeted gene. Interestingly, an additive effect was observed *in vitro* and *in vivo* when both genes were deleted. These data suggest that SP1298 and SP2205 may functionally complement each other, rendering *S. pneumoniae* incapable of causing disease when both genes are absent. Additive or even synergistic reduction in virulence of pneumococcal mutants lacking multiple genes of complementary function has been described previously. For example, during their investigation of two iron ABC transporter systems, PiuA and PiaA, Brown *et al.* demonstrated that a single deletion of *piuA* or *piaA* resulted in only a moderate reduction in virulence, whereas a mutant strain lacking both genes displayed severe attenuation in both pulmonary and systemic models of infection (48). In another study individual Δ*aliA*, Δ*aliB*, and Δ*amiA* mutants of the Ami-AliA/AliB oligopeptide permease were only moderately impaired in nasopharyngeal colonization, while the triple knock-out *obl* mutant was severely attenuated (49).

Since the pneumococcal genetic background can have a significant impact on the contribution of individual genes to virulence, we performed our study using three genetically distinct strains. Adherence data showed that the ΔSP2205 and double mutants were

severely reduced in adherence to Detroit 562 cells in all three genetic backgrounds compared to their respective wild types, whereas the ΔSP1298 mutant showed diminished adherence only in a BHN100 background. Conversely, *in vivo* data of all infection models demonstrated that the ΔSP1298 and double mutants in all three strain backgrounds were significantly attenuated, while the TIGR4ΔSP2205 mutant displayed wild-type levels of virulence in lungs and blood in single infection. Attenuation of TIGR4ΔSP2205 was observed only in co-infection experiments, specifically in the pneumonia and bacteremia models. These data suggest that not only strain-specific but also host site-specific features of strains and their respective mutants can occur. An obvious explanation for strain-specific phenotypes of mutants is the presence or absence of other virulence genes (in) directly contributing to observed phenotypes. For instance, the type I pilus that has been described to be involved in pneumococcal adherence and colonization (50), is encoded by the genomes of the TIGR4 and BHN100 strains but not by that of D39. It does not appear to be responsible for the strain-specific adherence observed in our study, though, since the D39 and TIGR4 mutants showed similar phenotypes. Strain-specificity has also been described for virulence factors present in all strains; for example, the contribution of PspC to pneumococcal virulence has been shown to vary between strains, both at the level of virulence during pneumonia and bacteremia and at the level of factor H binding (51,52), and we have demonstrated that the putative proteinase maturation protein A (PpmA) contributes to adherence in a strain-specific manner (40). Finally, transcriptional response regulators (RR), such as RR04 and RR09, have also been shown to affect both virulence and gene expression in a strain-specific manner (39,53,54).

A reasonable explanation for the observed phenotypes of the DHH subfamily 1 mutants may be associated with the cellular localization of the DHH subfamily 1 proteins. SP2205 is predicted to be surface-exposed by virtue of N-terminal transmembrane helices, which suggests that its observed contribution to adherence may well be a direct effect, since the protein may act as an adhesin. A significant reduction in invasive disease was attributed to the deletion of SP1298, which may be the result of an indirect effect, since this protein is predicted to be cytoplasmic. SP1298 does not contain known signal sequences or typical motifs required for membrane anchoring. However, the presence of known export signals is not necessarily a prerequisite for surface exposure, as exemplified by two other pneumococcal virulence factors: the plasmin(ogen) binding proteins enolase (Eno) and GAPDH (glyceraldehyde-3-phosphate dehydrogenase) (55,56). Binding of human plasmin(ogen) by pneumococcal Eno and GAPDH enhances bacterial virulence by capturing surface-associated proteolytic activity, thus promoting penetration of bacteria through reconstituted basement membranes (55,57,58). Even though these proteins are

predicted to be cytoplasmic based on their amino acid sequence, immunoelectron microscopy and immunoblot analysis have clearly showed that both of these glycolytic enzymes are present in the cytoplasm as well as on the bacterial cell surface (55,58). Ply is also a signal peptide-lacking protein localized in the cytoplasm that, in addition to formation of pores, can activate complement and stimulate host cell apoptosis once released from the bacterium (59-61). Interestingly, unlike the SP1298 and SP2205 mutants, a *ply*-negative mutant could be complemented by the presence of the wild-type strain upon co-infection (62). This suggests that while Ply acts at distance from the pneumococcus, the DHH subfamily 1 proteins exert their effects in connection with or very close to the cell. Whether the cellular localization of SP1298 and SP2205 is the cell surface, cytoplasm or both, remains to be investigated, since preliminary fluorescense-activated cell sorter (FACS) analysis using the polyclonal antisera was inconclusive (data not shown).

Even though the exact function of SP1298 and SP2205 in *S. pneumoniae* is unknown at present, their DHH domain(s) (Figure 1) may shed some light on their putative role in pneumococcal pathogenesis. The N-terminal motifs I-IV of DHH family proteins contain the residues required for core catalytic activity, and the C-terminal, subfamily-specific motifs contribute to substrate specificity (35). In addition to the N-terminal DHH motifs, both SP1298 and SP2205 possess a DHHA1 domain, characteristic of members of the DHH subfamily 1. These domains are ~60 residues long and contain a conserved GGG motif located near the C-terminus (35). DHH domain proteins are known to function as phosphatases or phospho(di)esterases (PDE) capable of hydrolyzing a wide variety of substrates from inorganic pyrophosphate to single-stranded DNA (35). A well-studied bacterial example is RecJ of *E. coli*, an exonuclease involved in DNA repair and recombination systems (63), of which homologues are found in *S. pneumoniae* (Figure 1), and in *Bordetella pertussis*, *Haemophilus influenzae*, and *Neisseria meningitidis* (35,37). Some less-well characterized but interesting examples include two DHH proteins of *Mycoplasma genitalium* and *Mycoplasma pneumoniae*, located in operons encoding proteins required for adherence to the respiratory epithelium (64-66). Furthermore, SMU.1297, a DHH subfamily 1 protein of *S. mutans*, was recently found to be involved in superoxide stress tolerance by exposing wild-type and SMU.1297 mutant strains to menadione, a quinine compound that generates superoxide anions in bacteria (38). Analysis of the SMU.1297 sequence showed a high degree of homology to the *B. subtilis* YtqI protein, which possesses dual activities: oligoribonuclease (cleaves small RNAs less than 5-mers) and 3′-phosphoadenosine–5′-phosphate (pAp) phosphatase *in vitro* (67). Biochemical analysis of SMU.1297 demonstrated that it has pAp phosphatase but no oligoribonuclease activity (38). *B. subtilis* has another DHH/DHHA1 domain protein, YybT, which exhibits PDE activity toward cyclic

dinucleotides (68). Based on their amino acid sequence, SP1298 is ~68% identical to SMU.1297, while SP2205 shares 32% homology with YybT. SMU.1297 and YtqI consist of 310 and 313 amino acids, respectively, which is comparable to the size of SP1298, while the size of YybT (659 amino acids) is comparable to that off SP2205. Given these similarities, it is not unlikely that SP1298 and SP2205 may possess hydrolase and/or nuclease activity. Characterization of their biochemical function(s) will be subject of future studies.

The combination of both DHH subfamily 1 antigens SP1298 and SP2205 provided the best protection (60%) against pneumococcal infection, while immunization with the individual DHH subfamily 1 antigens did not confer significant protection. For more than a decade, the protective potential of various pneumococcal virulence factors, such as Ply, PspA, PspC, and PsaA, either as single proteins or in combination, has been examined (15,16,20,22,69-72). Two studies performed by Ogunniyi *et al*. have shown that in general, median survival times of mice immunized with different combinations of PspA, PsaA, PdB (a genetically detoxified derivative of Ply), and pneumococcal histidine triad (Pht) protein PhtB or PhtE were significantly longer upon pneumococcal challenge than survival times of mice immunized with single antigens (15,17). Briles *et al*. have shown that protection against pneumonia improved when mice were immunized with the combination of PspA and PdB compared to single-protein immunization (20). These studies have convincingly demonstrated that a combination protein vaccine improves the level of protection against pneumococcal disease in experimental mouse models. Our study also supports the paradigm that a multicomponent protein vaccine will confer protection against invasive disease and perhaps against carriage as well. In our opinion, future experimental protein vaccine studies should focus on vaccine formulations that comprise protein antigens sharing complementary functions or even combinations of functional protein families in order to determine whether the protection will be magnified.

In conclusion, we have demonstrated that the two conserved pneumococcal DHH subfamily 1 proteins, SP1298 and SP2205, play a significant role in four important stages of pneumococcal pathogenesis, i.e., colonization, otitis media, pneumonia, and bacteremia, and that vaccination with a combination of both proteins is able to confer protection against pneumococcal disease. While further research on these two proteins is needed to determine their cellular localization during pathogenesis and biochemical function and to evaluate the protective potential against other pneumococcal serotypes and genotypes, our data suggest that SP1298 and SP2205 are interesting candidates for future protein-based pneumococcal vaccines.

Acknowledgments

We thank Sofie van Erk, Marilyn Bok, Christa E. van der Gaast-de Jongh, and Marc Eleveld for their technical assistance. We thank Jean-Pierre Claverys (CNRS-Université Paul Sabatier, Toulouse, France) for kindly providing the pCEP plasmid. This work was financially supported by Pneumopath grant 222983 from the European Union Seventh Framework Program (FP7), EC Sixth Framework Program (FP6), and Horizon Breakthrough grant 93518023 from the Netherlands Genomics Initiative.

References

1. Bogaert D, de Groot R, Hermans PW. *Streptococcus pneumoniae* colonisation: the key to pneumococcal disease. Lancet Infect Dis 2004 March;4(3):144-54.
2. Fine DP. Pneumococcal type-associated variability in alternate complement pathway activation. Infect Immun 1975 October;12(4):772-8.
3. Giebink GS, Verhoef J, Peterson PK, Quie PG. Opsonic requirements for phagocytosis of *Streptococcus pneumoniae* types VI, XVIII, XXIII, and XXV. Infect Immun 1977 November;18(2):291-7.
4. Brueggemann AB, Pai R, Crook DW, Beall B. Vaccine escape recombinants emerge after pneumococcal vaccination in the United States. PLoS Pathog 2007 November;3(11):e168.
5. Leach AJ, Morris PS, McCallum GB, Wilson CA, Stubbs L, Beissbarth J et al. Emerging pneumococcal carriage serotypes in a high-risk population receiving universal 7-valent pneumococcal conjugate vaccine and 23-valent polysaccharide vaccine since 2001. BMC Infect Dis 2009 August 4;9:121.
6. Wizemann TM, Heinrichs JH, Adamou JE, Erwin AL, Kunsch C, Choi GH et al. Use of a whole genome approach to identify vaccine molecules affording protection against *Streptococcus pneumoniae* infection. Infect Immun 2001 March;69(3):1593-8.
7. Tu AH, Fulgham RL, McCrory MA, Briles DE, Szalai AJ. Pneumococcal surface protein A inhibits complement activation by *Streptococcus pneumoniae*. Infect Immun 1999 September;67(9):4720-4.
8. Ren B, Szalai AJ, Thomas O, Hollingshead SK, Briles DE. Both family 1 and family 2 PspA proteins can inhibit complement deposition and confer virulence to a capsular serotype 3 strain of *Streptococcus pneumoniae*. Infect Immun 2003 January;71(1):75-85.
9. Ren B, Szalai AJ, Hollingshead SK, Briles DE. Effects of PspA and antibodies to PspA on activation and deposition of complement on the pneumococcal surface. Infect Immun 2004 January;72(1):114-22.
10. Dave S, Pangburn MK, Pruitt C, McDaniel LS. Interaction of human factor H with PspC of *Streptococcus pneumoniae*. Indian J Med Res 2004 May;119 Suppl:66-73.:66-73.
11. Jarva H, Janulczyk R, Hellwage J, Zipfel PF, Bjorck L, Meri S. *Streptococcus pneumoniae* evades complement attack and opsonophagocytosis by expressing the pspC locus-encoded Hic protein that binds to short consensus repeats 8-11 of factor H. J Immunol 2002 February 15;168(4):1886-94.
12. Neeleman C, Geelen SP, Aerts PC, Daha MR, Mollnes TE, Roord JJ et al. Resistance to both complement activation and phagocytosis in type 3 pneumococci is mediated by the binding of complement regulatory protein factor H. Infect Immun 1999 September;67(9):4517-24.
13. Dintilhac A, Alloing G, Granadel C, Claverys JP. Competence and virulence of *Streptococcus pneumoniae*: Adc and PsaA mutants exhibit a requirement for Zn and Mn resulting from inactivation of putative ABC metal permeases. Mol Microbiol 1997 August;25(4):727-39.
14. Tilley SJ, Orlova EV, Gilbert RJ, Andrew PW, Saibil HR. Structural basis of pore formation

by the bacterial toxin pneumolysin. Cell 2005 April 22;121(2):247-56.
15. Ogunniyi AD, Folland RL, Briles DE, Hollingshead SK, Paton JC. Immunization of mice with combinations of pneumococcal virulence proteins elicits enhanced protection against challenge with *Streptococcus pneumoniae*. Infect Immun 2000 May;68(5):3028-33.
16. Ogunniyi AD, Woodrow MC, Poolman JT, Paton JC. Protection against *Streptococcus pneumoniae* elicited by immunization with pneumolysin and CbpA. Infect Immun 2001 October;69(10):5997-6003.
17. Ogunniyi AD, Grabowicz M, Briles DE, Cook J, Paton JC. Development of a vaccine against invasive pneumococcal disease based on combinations of virulence proteins of *Streptococcus pneumoniae*. Infect Immun 2007 January;75(1):350-7.
18. Ogunniyi AD, Lemessurier KS, Graham RM, Watt JM, Briles DE, Stroeher UH et al. Contributions of pneumolysin, pneumococcal surface protein A (PspA), and PspC to pathogenicity of *Streptococcus pneumoniae* D39 in a mouse model. Infect Immun 2007 April;75(4):1843-51.
19. Briles DE, Ades E, Paton JC, Sampson JS, Carlone GM, Huebner RC et al. Intranasal immunization of mice with a mixture of the pneumococcal proteins PsaA and PspA is highly protective against nasopharyngeal carriage of *Streptococcus pneumoniae*. Infect Immun 2000 February;68(2):796-800.
20. Briles DE, Hollingshead SK, Paton JC, Ades EW, Novak L, van Ginkel FW et al. Immunizations with pneumococcal surface protein A and pneumolysin are protective against pneumonia in a murine model of pulmonary infection with *Streptococcus pneumoniae*. J Infect Dis 2003 August 1;188(3):339-48.
21. McDaniel LS, Sheffield JS, Delucchi P, Briles DE. PspA, a surface protein of *Streptococcus pneumoniae*, is capable of eliciting protection against pneumococci of more than one capsular type. Infect Immun 1991 January;59(1):222-8.
22. Alexander JE, Lock RA, Peeters CC, Poolman JT, Andrew PW, Mitchell TJ et al. Immunization of mice with pneumolysin toxoid confers a significant degree of protection against at least nine serotypes of *Streptococcus pneumoniae*. Infect Immun 1994 December;62(12):5683-8.
23. Whaley MJ, Sampson JS, Johnson SE, Rajam G, Stinson-Parks A, Holder P et al. Concomitant administration of recombinant PsaA and PCV7 reduces *Streptococcus pneumoniae* serotype 19A colonization in a murine model. Vaccine 2010 April;28(18):3071-5.
24. Orihuela CJ, Radin JN, Sublett JE, Gao G, Kaushal D, Tuomanen EI. Microarray analysis of pneumococcal gene expression during invasive disease. Infect Immun 2004 October;72(10):5582-96.
25. Marra A, Asundi J, Bartilson M, Lawson S, Fang F, Christine J et al. Differential fluorescence induction analysis of *Streptococcus pneumoniae* identifies genes involved in pathogenesis. Infect Immun 2002 March;70(3):1422-33.
26. Hava DL, Camilli A. Large-scale identification of serotype 4 *Streptococcus pneumoniae* virulence factors. Mol Microbiol 2002 September;45(5):1389-406.
27. Lau GW, Haataja S, Lonetto M, Kensit SE, Marra A, Bryant AP et al. A functional genomic analysis of type 3 *Streptococcus pneumoniae* virulence. Mol Microbiol 2001 May;40(3):555-71.
28. Polissi A, Pontiggia A, Feger G, Altieri M, Mottl H, Ferrari L et al. Large-scale identification of virulence genes from *Streptococcus pneumoniae*. Infect Immun 1998 Decem-

ber;66(12):5620-9.
29. Bijlsma JJ, Burghout P, Kloosterman TG, Bootsma HJ, de Jong A, Hermans PW et al. Development of genomic array footprinting for identification of conditionally essential genes in *Streptococcus pneumoniae*. Appl Environ Microbiol 2007 March;73(5):1514-24.
30. Burghout P, Bootsma HJ, Kloosterman TG, Bijlsma JJ, de Jongh CE, Kuipers OP et al. Search for genes essential for pneumococcal transformation: the RadA DNA repair protein plays a role in genomic recombination of donor DNA. J Bacteriol 2007 September;189(18):6540-50.
31. Hermans PWM, Bootsma HJ, Burghout P, Bijlsma JJ, Kuipers OP, Kloosterman TG, inventors; New virulence factors of *Streptococcus pneumoniae*. The Netherlands patent PCT/NL2008/050191. 2008 Oct 23.
32. Hermans PWM, Bootsma HJ, Burghout P, Bijlsma JJ, Kuipers OP, Kloosterman TG, inventors; New virulence factors of *Streptococcus pneumoniae*. The Netherlands patent PCT/NL2009/050600. 2009 Oct 7.
33. Molzen TE, Burghout P, Bootsma HJ, Brandt CT, van der Gaast-de Jongh CE, Eleveld MJ et al. Genome-Wide Identification of *Streptococcus pneumoniae* Genes Essential for Bacterial Replication during Experimental Meningitis. Infect Immun 2011 January;79(1):288-97.
34. D'Angelo A, Garzia L, Andre A, Carotenuto P, Aglio V, Guardiola O et al. Prune cAMP phosphodiesterase binds nm23-H1 and promotes cancer metastasis. Cancer Cell 2004 February;5(2):137-49.
35. Aravind L, Koonin EV. A novel family of predicted phosphoesterases includes *Drosophila* prune protein and bacterial RecJ exonuclease. Trends Biochem Sci 1998 January;23(1):17-9.
36. Lovett ST, Kolodner RD. Identification and purification of a single-stranded-DNA-specific exonuclease encoded by the recJ gene of *Escherichia coli*. Proc Natl Acad Sci U S A 1989 April;86(8):2627-31.
37. Sutera VA, Jr., Han ES, Rajman LA, Lovett ST. Mutational analysis of the RecJ exonuclease of *Escherichia coli*: identification of phosphoesterase motifs. J Bacteriol 1999 October;181(19):6098-102.
38. Zhang J, Biswas I. 3'-Phosphoadenosine-5'-phosphate phosphatase activity is required for superoxide stress tolerance in *Streptococcus mutans*. J Bacteriol 2009 July;191(13):4330-40.
39. Blue CE, Mitchell TJ. Contribution of a response regulator to the virulence of *Streptococcus pneumoniae* is strain dependent. Infect Immun 2003 August;71(8):4405-13.
40. Cron LE, Bootsma HJ, Noske N, Burghout P, Hammerschmidt S, Hermans PW. Surface-associated lipoprotein PpmA of *Streptococcus pneumoniae* is involved in colonization in a strain-specific manner. Microbiology 2009 July;155(Pt 7):2401-10.
41. Guiral S, Henard V, Laaberki MH, Granadel C, Prudhomme M, Martin B et al. Construction and evaluation of a chromosomal expression platform (CEP) for ectopic, maltose-driven gene expression in *Streptococcus pneumoniae*. Microbiology 2006 February;152(Pt 2):343-9.
42. Livak KJ, Schmittgen TD. Analysis of relative gene expression data using real-time quantitative PCR and the 2(-Delta Delta C(T)) Method. Methods 2001 December;25(4):402-8.
43. Bootsma HJ, Egmont-Petersen M, Hermans PW. Analysis of the in vitro transcriptional response of human pharyngeal epithelial cells to adherent *Streptococcus pneumoniae*:

evidence for a distinct response to encapsulated strains. Infect Immun 2007 November;75(11):5489-99.
44. Hendriksen WT, Bootsma HJ, Estevao S, Hoogenboezem T, de Jong A, de Groot R et al. CodY of *Streptococcus pneumoniae*: link between nutritional gene regulation and colonization. J Bacteriol 2008 January;190(2):590-601.
45. Tonnaer EL, Sanders EA, Curfs JH. Bacterial otitis media: a new non-invasive rat model. Vaccine 2003 November 7;21(31):4539-44.
46. Stol K, van Selm S, van den Berg S, Bootsma HJ, Blokx WA, Graamans K et al. Development of a non-invasive murine infection model for acute otitis media. Microbiology 2009 December;155(Pt 12):4135-44.
47. Bouza E, Sousa D, Rodriguez-Creixems M, Lechuz JG, Munoz P. Is the volume of blood cultured still a significant factor in the diagnosis of bloodstream infections? J Clin Microbiol 2007 September;45(9):2765-9.
48. Brown JS, Gilliland SM, Holden DW. A *Streptococcus pneumoniae* pathogenicity island encoding an ABC transporter involved in iron uptake and virulence. Mol Microbiol 2001 May;40(3):572-85.
49. Kerr AR, Adrian PV, Estevao S, de Groot R, Alloing G, Claverys JP et al. The Ami-AliA/AliB permease of *Streptococcus pneumoniae* is involved in nasopharyngeal colonization but not in invasive disease. Infect Immun 2004 July;72(7):3902-6.
50. Barocchi MA, Ries J, Zogaj X, Hemsley C, Albiger B, Kanth A et al. A pneumococcal pilus influences virulence and host inflammatory responses. Proc Natl Acad Sci U S A 2006 February 21;103(8):2857-62.
51. Kerr AR, Paterson GK, McCluskey J, Iannelli F, Oggioni MR, Pozzi G et al. The contribution of PspC to pneumococcal virulence varies between strains and is accomplished by both complement evasion and complement-independent mechanisms. Infect Immun 2006 September;74(9):5319-24.
52. Yuste J, Khandavilli S, Ansari N, Muttardi K, Ismail L, Hyams C et al. The effects of PspC on complement-mediated immunity to *Streptococcus pneumoniae* vary with strain background and capsular serotype. Infect Immun 2010 January;78(1):283-92.
53. McCluskey J, Hinds J, Husain S, Witney A, Mitchell TJ. A two-component system that controls the expression of pneumococcal surface antigen A (PsaA) and regulates virulence and resistance to oxidative stress in *Streptococcus pneumoniae*. Mol Microbiol 2004 March;51(6):1661-75.
54. Hendriksen WT, Silva N, Bootsma HJ, Blue CE, Paterson GK, Kerr AR et al. Regulation of gene expression in *Streptococcus pneumoniae* by response regulator 09 is strain dependent. J Bacteriol 2007 February;189(4):1382-9.
55. Bergmann S, Rohde M, Chhatwal GS, Hammerschmidt S. alpha-Enolase of *Streptococcus pneumoniae* is a plasmin(ogen)-binding protein displayed on the bacterial cell surface. Mol Microbiol 2001 June;40(6):1273-87.
56. Pancholi V, Fischetti VA. A major surface protein on group A streptococci is a glyceraldehyde-3-phosphate-dehydrogenase with multiple binding activity. J Exp Med 1992 August 1;176(2):415-26.
57. Bergmann S, Wild D, Diekmann O, Frank R, Bracht D, Chhatwal GS et al. Identification of a novel plasmin(ogen)-binding motif in surface displayed alpha-enolase of *Streptococcus pneumoniae*. Mol Microbiol 2003 July;49(2):411-23.

58. Bergmann S, Rohde M, Hammerschmidt S. Glyceraldehyde-3-phosphate dehydrogenase of *Streptococcus pneumoniae* is a surface-displayed plasminogen-binding protein. Infect Immun 2004 April;72(4):2416-9.
59. Paton JC, Rowan-Kelly B, Ferrante A. Activation of human complement by the pneumococcal toxin pneumolysin. Infect Immun 1984 March;43(3):1085-7.
60. Paton JC, Andrew PW, Boulnois GJ, Mitchell TJ. Molecular analysis of the pathogenicity of *Streptococcus pneumoniae*: the role of pneumococcal proteins. Annu Rev Microbiol 1993;47:89-115.
61. Braun JS, Hoffmann O, Schickhaus M, Freyer D, Dagand E, Bermpohl D et al. Pneumolysin causes neuronal cell death through mitochondrial damage. Infect Immun 2007 September;75(9):4245-54.
62. Benton KA, Everson MP, Briles DE. A pneumolysin-negative mutant of *Streptococcus pneumoniae* causes chronic bacteremia rather than acute sepsis in mice. Infect Immun 1995 February;63(2):448-55.
63. Yamagata A, Kakuta Y, Masui R, Fukuyama K. The crystal structure of exonuclease RecJ bound to Mn2+ ion suggests how its characteristic motifs are involved in exonuclease activity. Proc Natl Acad Sci U S A 2002 April 30;99(9):5908-12.
64. Inamine JM, Loechel S, Collier AM, Barile MF, Hu PC. Nucleotide sequence of the *MgPa* (*mgp*) operon of *Mycoplasma genitalium* and comparison to the *P1* (*mpp*) operon of *Mycoplasma pneumoniae*. Gene 1989 October 30;82(2):259-67.
65. Krause DC. *Mycoplasma pneumoniae* cytadherence: unravelling the tie that binds. Mol Microbiol 1996 April;20(2):247-53.
66. Svenstrup HF, Nielsen PK, Drasbek M, Birkelund S, Christiansen G. Adhesion and inhibition assay of *Mycoplasma genitalium* and *M. pneumoniae* by immunofluorescence microscopy. J Med Microbiol 2002 May;51(5):361-73.
67. Mechold U, Fang G, Ngo S, Ogryzko V, Danchin A. YtqI from *Bacillus subtilis* has both oligoribonuclease and pAp-phosphatase activity. Nucleic Acids Res 2007;35(13):4552-61.
68. Rao F, See RY, Zhang D, Toh DC, Ji Q, Liang ZX. YybT is a signaling protein that contains a cyclic dinucleotide phosphodiesterase domain and a GGDEF domain with ATPase activity. J Biol Chem 2010 January 1;285(1):473-82.
69. Lock RA, Paton JC, Hansman D. Comparative efficacy of pneumococcal neuraminidase and pneumolysin as immunogens protective against *Streptococcus pneumoniae*. Microb Pathog 1988 December;5(6):461-7.
70. Lock RA, Hansman D, Paton JC. Comparative efficacy of autolysin and pneumolysin as immunogens protecting mice against infection by *Streptococcus pneumoniae*. Microb Pathog 1992 February;12(2):137-43.
71. Wu HY, Nahm MH, Guo Y, Russell MW, Briles DE. Intranasal immunization of mice with PspA (pneumococcal surface protein A) can prevent intranasal carriage, pulmonary infection, and sepsis with *Streptococcus pneumoniae*. J Infect Dis 1997 April;175(4):839-46.
72. Wu K, Zhang X, Shi J, Li N, Li D, Luo M et al. Immunization with a combination of three pneumococcal proteins confers additive and broad protection against *Streptococcus pneumoniae* Infections in Mice. Infect Immun 2010 March;78(3):1276-83.
73. Tettelin H, Nelson KE, Paulsen IT, Eisen JA, Read TD, Peterson S et al. Complete genome sequence of a virulent isolate of *Streptococcus pneumoniae*. Science 2001 July;293(5529):498-506.

74. Sandgren A, Albiger B, Orihuela CJ, Tuomanen E, Normark S, Henriques-Normark B. Virulence in mice of pneumococcal clonal types with known invasive disease potential in humans. J Infect Dis 2005 September 1;192(5):791-800.
75. Hanahan D. Studies on transformation of *Escherichia coli* with plasmids. J Mol Biol 1983 June 5;166(4):557-80.

The pneumococcal serine-rich repeat protein is an intra-species bacterial adhesin that promotes bacterial aggregation *in vivo* and in biofilms

C.J. Sanchez, P. Shivshankar, K. Stol, S. Trakhtenbroit, P.M. Sullam, K. Sauer, P.W.M. Hermans and C.J. Orihuela

PLoS Pathogens 2010, 6(8):e1001044

Abstract

The Pneumococcal serine-rich repeat protein (PsrP) is a pathogenicity island encoded adhesin that has been positively correlated with the ability of *Streptococcus pneumoniae* to cause invasive disease. Previous studies have shown that PsrP mediates bacterial attachment to Keratin 10 (K10) on the surface of lung cells through amino acids 273–341 located in the Basic Region (BR) domain. In this study we determined that the BR domain of PsrP also mediates an intra-species interaction that promotes the formation of large bacterial aggregates in the nasopharynx and lungs of infected mice as well as in continuous flow-through models of mature biofilms. Using numerous methods, including complementation of mutants with BR domain deficient constructs, fluorescent microscopy with Cy3-labeled recombinant (r)BR, Far Western blotting of bacterial lysates, co-immunoprecipitation with rBR, and growth of biofilms in the presence of antibodies and competitive peptides, we determined that the BR domain, in particular amino acids 122–166 of PsrP, promoted bacterial aggregation and that antibodies against the BR domain were neutralizing. Using similar methodologies, we also determined that SraP and GspB, the Serine-rich repeat proteins (SRRPs) of *Staphylococcus aureus* and *Streptococcus gordonii*, respectively, also promoted bacterial aggregation and that their Non-repeat domains bound to their respective SRRPs. This is the first report to show the presence of biofilm-like structures in the lungs of animals infected with *S. pneumoniae* and show that SRRPs have dual roles as host and bacterial adhesins. These studies suggest that recombinant Non-repeat domains of SRRPs (i.e. BR for *S. pneumoniae*) may be useful as vaccine antigens to protect against Gram-positive bacteria that cause infection.

Author Summary

Serine-rich repeat proteins (SRRPs) are a family of surface-expressed proteins found in numerous Gram-positive pathogens, including *Staphylococcus aureus, Streptococcus pneumoniae*, Group B streptococci, and the oral streptococci that cause infective endocarditis. For all of these bacteria, SRRPs have been demonstrated to play pivotal roles in adhesion to tissues and the development of invasive disease. It is now known that biofilm formation is an important step for bacterial pathogenesis. Bacteria in biofilms have been shown to have differences in metabolism, gene expression, and protein production that contribute to enhanced surface adhesion and the persistence of an infection. Herein we describe a novel role for PsrP, the *S. pneumoniae* SRRP, as an intra-species bacterial adhesin that promotes bacterial aggregation in the lungs of infected mice during pneumonia. *In vitro* we show that the Basic Region domain of PsrP promotes self-interactions that result in denser biofilms, greater biofilm biomass, and altered architectures of surface grown cultures; these interactions could be neutralized by antibodies to PsrP that are protective against pneumococcal infection. We also demonstrate that the SRRPs of *S. aureus* and *Streptococcus gordonii* also function as intra-species bacterial adhesins. Therefore we conclude that SRRPs have dual roles as host-cell and intra-species bacterial adhesins.

Introduction

Streptococcus pneumoniae is a leading cause of otitis media (OM), community-acquired pneumonia, sepsis and meningitis. Primarily a commensal, *S. pneumoniae* typically colonizes the nasopharynx asymptomatically, however in susceptible individuals such as infants, the elderly, persons who are immunocompromised, and those with sickle cell anemia, the pneumococcus is often able to cause opportunistic diseases (1-4). Worldwide, *S. pneumoniae* is responsible for up to 14.5 million episodes of invasive pneumococcal disease (IPD) and 11% of all deaths in children (5,6). In the elderly the mortality-rate associated with IPD can exceed 20% and for those in nursing homes may be as high as 40% (7). Thus, the pneumococcus has been and remains a major cause of morbidity and mortality.

psrP-secY2A2 is a *S. pneumoniae* pathogenicity island whose presence has been positively correlated with the ability to cause human disease (8). Analyses of the published *S. pneumoniae* genomes has demonstrated that *psrP-secY2A2* is present and conserved in a number of globally distributed invasive clones, in particular those belonging to serotypes not covered by the heptavalent conjugate vaccine (9). To date, numerous studies have shown that deletion of genes within *psrP-secY2A2* attenuated the ability of *S. pneumoniae* to cause disease in mice. *psrP-secY2A2* mutants were shown to be unable to attach to lung cells, establish lower respiratory tract infection, and were delayed in their ability to enter the bloodstream from the lungs. Importantly, the same studies found that *psrP-secY2A2* did not play an important role during nasopharyngeal colonization or during sepsis following intraperitoneal challenge(10-13). Thus *psrP-secY2A2* is currently understood to be a lung-specific virulence determinant.

In TIGR4, a virulent serotype 4 laboratory strain, *psrP-secY2A2* is 37-kb in length and encodes 18 proteins. These include the Pneumococcal serine-rich repeat protein (PsrP), which is a lung cell adhesin, 10 putative glycosyltranferases, and 7 proteins homologous to components of an accessory Sec translocase (14). To date, the latter 17 genes remain uncharacterized; however, based on their homology to genes found within the Serine-rich repeat protein (SRRP) locus of *Streptococcus gordonii*, the encoded proteins are putatively responsible for the intracellular glycosylation of PsrP and for its transport to the bacterial surface (8,15-18). PsrP in TIGR4 is composed of 4,776 amino acids, has been confirmed to be glycosylated, and separates at an apparent molecular mass of 2,300 kDa on an agarose gel (13). It is one of the largest bacterial proteins known. PsrP is organized into multiple domains including a cleavable N-terminal signal peptide, a small serine-rich repeat

region (SRR1), a unique non-repeat region (NR), followed by a second extremely long serine-rich region (SRR2), and a C-terminal cell wall anchor domain containing an LPXTG motif (Figure 1A). The SRR1 and SRR2 domains of PsrP are composed of 8 and 539 serine-rich repeats (SRR) of the amino acid sequence SAS[A/E/V]SAS[T/I], respectively, and are the domains believed to be glycosylated. The NR domain of PsrP has a predicted pI value of 9.9, for this reason it is called the Basic Region (BR) domain.

S. pneumoniae is surrounded by a polysaccharide capsule that protects the bacteria from phagocytosis but also inhibits adhesion to epithelial cells (19). Based on the size and domain organization of PsrP we have previously hypothesized that the extremely long SRR2 domain serves to extend the BR domain through the capsular polysaccharide to mediate lung cell adhesion (Figure 1B) (12,13). Consistent with this model, we have previously shown that PsrP is expressed on the bacterial surface, that the BR domain, in particular amino acids 273–341, was responsible for PsrP-mediated adhesion to Keratin 10 (K10) on lung cells, and that complementation of *psrP* deficient mutants with a truncated version of the protein (having only 33 SRRs in its SRR2 domain) restored the ability of uncapsulated but not capsulated PsrP mutants to adhere to A549 cells, a human type II pneumocyte cell line (13).

It is now recognized that biofilms play an important role during infectious diseases. Briefly, bacteria in biofilms are more resistant to host-defense mechanisms including phagocytosis and serve as a recalcitrant source of bacteria during antimicrobial therapy (20,21). For *S. pneumoniae*, pneumococcal biofilms have been shown to occur in the middle ears of children with chronic otitis media and is thought to contribute to its refractory nature (22). Likewise, biofilms have been detected in the nasopharynx of infected chinchillas (23). However, until now biofilm structures have not been described in the lungs during pneumococcal pneumonia. This is in contrast to other respiratory tract pathogens, such as *Pseudomonas aeruginosa* and *Bordatella pertussis*, for which *in vivo* biofilm production is now recognized to be an important pathogenic mechanism (21). Herein, we demonstrate for the first time that *S. pneumoniae* forms biofilm-like aggregates in the lungs. We show that this phenomenon is PsrP-dependent and mediated by its BR domain. Using recombinant protein and SRRP mutants, we show that the SRRPs of *S. gordonii* and *Staphylococcus aureus*, GspB and SraP, respectively, also promote bacterial aggregation, thus describing a previously unrecognized role for members of the SRRP family. Collectively, these findings suggest an important dual role for PsrP and other SRRPs during infection, host cell and intra-species bacterial adhesion, both of which may be targeted for intervention with antibodies against recombinant (r)NR.

A.

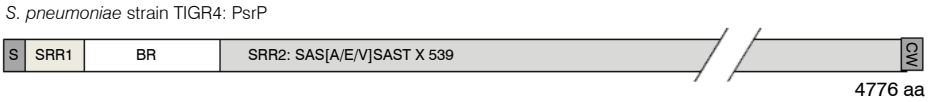

B.

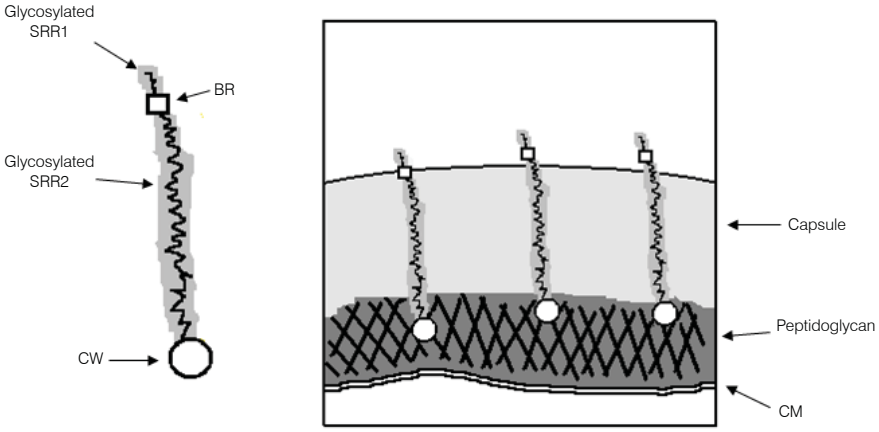

Figure 1. Hypothetical model of PsrP on the surface of *S. pneumoniae*.
A) Domain structure of PsrP: N-terminal signal peptide (S); serine-rich repeat motif 1 (SAS[A/E/V]SAST X 11) (SRR1); basic region (BR); serine-rich repeat motif 2 (SRR2); and the cell wall anchoring domain (CW) at the C-terminus.
B) Illustration of PsrP on the bacterial surface. Based on the structural organization of PsrP and studies demonstrating that the BR domain binds to K10 on lung cells [13], we propose that the CWAD attaches the protein to the cell wall, while the long glycosylated SRR2 domain serves to extend BR through the capsular polysaccharide to mediate interactions.

Materials & Methods

Bacterial strains and media

Wild type strains used in this study included *S. pneumoniae* strain TIGR4 and the previously described clinical isolates IPD-5, TNE-6012, and TBE-6050 (8,12,14). T4R is an unencapsulated derivative of TIGR4 (48). *S. aureus* ISP479C and *S. gordonii* M99 and their corresponding isogenic mutants ISP479C Δ*sraP*, and M99 Δ*gspB* have also been previously described (17,27). All of the *S. pneumoniae*mutants used in this study including T4 Δ*psrP*, T4 Ω*psrP-secY2A2*, T4 Ω*psrP*, and T4R Ω*psrP* have been shown not to have polar effects on upstream and downstream gene transcription (12,13). *S. pneumoniae* and *S. gordonii* were grown in Todd-Hewitt broth (THB) or on blood agar plates at 37°C in 5% CO_2. *S. aureus* were grown in Tryptic-Soy Broth (TSB) or on blood agar plates at 37°C. Stocks for the PsrP mutants were grown in media supplemented with 1 μg/mL of erythromycin, those complemented with the expression vector pNE1 were grown on media supplemented with 250 μg/mL of spectinomycin. SraP and GspB mutant stocks were grown in media supplemented with either 15 μg/mL of erythromycin or 5 μg/mL chloramphenicol respectively. *E. coli* strain DH5α (Invitrogen, Carlsbad CA) expressing recombinant PsrP constructs were grown with 50 μg/mL of kanamycin. Recombinant proteins were purified as previously described (13,26). To avoid stress effects on the bacteria, no antibiotics were added to the media during any of the experiments.

Infection of mice and collection of tissues

Female BALB/cJ mice, 5–6 weeks old, were obtained from The Jackson Laboratory (Bar Harbor, ME). Mice were anesthetized with 2.5% vaporized isoflurane prior to challenge. Exponential phase cultures of *S. pneumoniae* were centrifuged, washed, and suspended in sterile phosphate buffered saline (PBS). For each experimental cohort at least 6 mice were instilled with either 10^7 cfu of TIGR4 or T4 Δ*psrP* in 20 μL of PBS into the left nostril. After two days mice were sacrificed for tissue collection. For imaging experiments the intact lungs were collected and processed as described below. For enumeration of bacterial aggregates, nasal lavage fluid was collected from anesthetized mice by instillation and retraction of 20 μl PBS. The same mice were subsequently asphyxiated with compressed CO_2, and BAL fluid collected by flushing the lungs twice with 0.5 ml of PBS using a sterile catheter. All animal experimentation was conducted following the National Institutes for Health guidelines for housing and care of laboratory animals. Animal experiments were

reviewed and approved by the Institutional Animal Care and Use Committee at The University of Texas Health Science Center at San Antonio.

Scanning electron microscopy (SEM)

Lungs were cut in a sagital orientation, fixed for 2 hours with 2.5% glutaraldehyde in PBS, and then rinsed twice for 3 min in 0.1 M phosphate buffer (pH 7.4). Lungs were submerged in 1% osmium diluted in Zetterquist's Buffer for 30 minutes then washed with the same buffer for 2 minutes (49). This was followed by step-wise dehydration with ethanol (i.e. 70%, 95%, and 100%); the first two steps for 15 minutes, the last for 30 minutes. Samples were treated with hexamethyldisilizane for 5 minutes prior to drying in a desiccator overnight. The next day samples were sputter coated with gold palladium and viewed with a JEOL-6610 scanning electron microscope.

Visualization of bacterial aggregates *ex vivo*

From each mouse BAL and 1:10 PBS diluted nasopharyngeal lavage elutes were smeared onto glass slides, heat fixed, and Gram-stained. Since the nasopharyngeal samples were mucoid, dilution of the samples was warranted. Bacteria were visualized using a CKX41 Olympus microscope at 200× magnification. For each biological sample 100 CFU were randomly selected, taking note of the approximate number of diplococci composing each CFU, either 1, 2–10, or >10. Images of the bacteria were acquired at 400× magnification to better show the multiple bacteria composing the aggregates.

Fluorescent microscopy of tissue sections

Lung tissues were excised and frozen in Tissue Tek O.C.T. solution (Miles Scientific). 5 μm thick lung sections were cut at the University of Texas at San Antonio Histopathology Core and stored at −80° C. Bacteria in the lung sections were detected by immunofluorescence using antibody against the capsular polysaccharide. Sections were thawed, fixed with ice-cold acetone for 20 minutes, and then rehydrated with 70% ethyl alcohol and then PBS. Samples were permeabilized with 0.1% Triton-X-100 for 5 minutes then blocked with 10% fetal bovine serum (FBS) in F12 media for 1 hour. Sections were incubated with 1:1,000 rabbit anti-serotype 4 pneumococcus antiserum (Statens Serum Institut, Denmark) overnight at 4°C. After washing for three times with 0.5% Tween-PBS, sections were covered with FBS-F12 containing goat anti-rabbit FITC conjugated antibody (Invitrogen) at 1:2,000 and DAPI (5 μg/ml; for DNA) and the sections incubated for 1 hour at room temperature. Tissue sections were washed and mounted with FluorSave (Merck Biosciences). Images were acquired at 1,000× using a Nikon AX-70 fluorescent Microscope and images pro-

cessed with SimplePCI software.

Visualization of early and mature biofilms

Early biofilm formation was examined by measuring the ability of cells to adhere and accumulate biomass on the bottom of a 96-well (flat-bottom) polystyrene plates (Costar, Corning Incorporated, Lowell MA) (24). Microtiter wells with 200 μl THB were inoculated with 10^6 CFU of *S. pneumoniae* taken from cultures at mid-logarithmic phase growth (OD_{620} = 0.5). Plates were incubated at 37° C in 5% CO_2. *S. aureus* and *S. gordonii* biofilm formation on microtiter plates was done in a similar manner, with the exception that TSB was used for *S. aureus* (50,51). Bacteria were grown for 2, 4, 6, 8, 18, and 24 h, after which the biofilms were washed gently with PBS and stained with 100 μL of 0.1% CV. Biofilm biomass was subsequently quantified by image capture using an inverted microscope at 15× and 100× magnification and measuring the corresponding optical density (A_{540}) of the supernatant following washing of the bacteria and solubilization of CV in 200 μL of 95% ethanol.

Mature *S. pneumoniae* biofilms were grown under once through conditions in a glass slide chamber using a continuous-flow through reactor (25). The flow cell was constructed of anodized aluminum containing a chamber (4.0 mm by 1.3 cm by 5.0 cm) having two glass surfaces, one being a microscope slide and the other being a glass coverslip serving as the substratum. *S. pneumoniae* cells grown to mid-logarithmic phase served as the inoculum and were injected into a septum 4 cm upstream from the flow cell. Bacteria were allowed to attach to the glass substratum for 2 hours prior to initiating flow. The flow rate of the system was adjusted to 0.014 ml/min. Flow through the chamber was laminar, with a Reynolds number of $<$0.5, having a fluid residence time of 180 min. Biofilms were grown at 37°C in 5% CO_2 for 3 days under once through conditions. Biofilms were then visualized by confocal laser microscopy as described below.

Biofilms were also grown on the interior surface of a 1-meter long, size 16 Masterflex silicone tubing (0.89mm Internal Diameter, Cole Parmer Inc.) using once-through continuous flow conditions. The line was inoculated with 5 mL of a mid-logarithmic culture and the bacteria were allowed to attach for 2 hours. The flow rate of the system was adjusted to 0.035 ml/min and bacteria were grown for 3 days at 37°C in 5% CO_2. Bacterial cells were harvested from the interior surface by pinching the tube along its entire length, resulting in removal of the cell material from the lumen of the tubing. Following extraction, exudates were gently suspended in 1 ml of PBS and the optical density (OD_{620}) was measured. For light microscopy pictures, 50 μl of line exudate in saline was stained by the addition of 50 μL of 1% CV. A volume of 5 μl of stained line exudates was applied to glass slides, coverslipped, and images taken at 200× magnification using a light microscope. Viable cell

counts were determined by plating serial dilutions of exudates following the disruption of each sample by vortexing. Biofilm biomass was determined by measuring the total protein concentration of the exudates by BCA following the complete lysis of *S. pneumoniae* with saline containing 0.1% deoxycholate and 0.1% sodium-dodecyl sulfate, which activates the murein hydrolase autolysin, or use of French press for *S. gordonii* and *S. aureus* cultures. For studies testing whether antibodies or recombinant protein inhibited bacteria aggregation media was supplemented with BR antiserum at 1:1,000 or spiked with recombinant protein at a final concentration of 1.0 μM.

Confocal scanning laser microscopy and image acquisition

Confocal scanning laser microscopy was performed with an LSM 510 Meta inverted microscope (Zeiss, Heidelberg, Germany). Images were obtained with an LD-Apochrome 40×/0.6 lens and the LSM 510 Meta image acquisition software (Zeiss). To visualize the biofilm architecture of 3-day-old biofilms, biofilms were stained using the Live/Dead BacLight stain from Invitrogen (Carlsbad, CA). Quantitative analysis of epifluorescence microscopic images obtained from flow cell-grown biofilms at the 6-day time point was performed with COMSTAT image analysis software (52).

Far Western analysis of BR interactions

Recombinant full-length BR and truncated versions (BR.A, BR.B, BR.C) were expressed and purified from *E. coli* as previously described (13). Glycosylated $PsrP_{SRR2(33)\text{-}HIS}$ was purified in the same manner from TIGR4, with the exception that cultures were induced with 1% fucose and lysed with 1% SDS in PBS. Far Western analysis was carried out as described by Takamatsu *et al.* with minor modifications (53). Nitrocellulose membranes were spotted with either 1 μg of whole cell lysate of *S. pneumoniae*, *S. gordonii*, *S. aureus* or *E. coli* expressing various PsrP constructs or with purified recombinant proteins in PBS. Membranes were incubated overnight in PBS with 4% bovine serum albumin and 0.1% Tween 20 (T-PBS) at room temperature. The next day, membranes were washed with T-PBS three times for 5 minutes, and incubated overnight at 4°C on an orbital platform rocker with T-PBS containing 1% bovine serum albumin (TB-PBS) with 1 μg/mL of Gst-BR, $PsrP_{SRR2(33)\text{-}HIS}$, or the designated NR constructs from *S. gordonii* and *S. aureus*. Membranes were washed and incubated with monoclonal mouse anti-Gst antibody (1:5,000 dilution) (Proto-Tech) overnight at 4°C in TB-PBS. Antibody binding was detected by incubating the membranes for 1 h with HRP-conjugated anti-mouse IgG (1:10,000 dilution) (Sigma), followed by development with the Super Signal chemiluminescent detection system (Thermo Scientific). As a control for inadvertent interactions with the Gst tag, Far Western blots were

also performed using an unrelated Gst-tagged *Chlamydia trachomatis* protein (TC0109). No interactions were observed.

Co-immunoprecipitation of Gst-BR with rBR

Co-immunoprecipitation of Gst-BR with the truncated versions of rPsrP was carried out as previously described by Shivshankar *et al.* (13) Protein G Sepharose beads (Amersham) were incubated overnight at 4°C with mouse monoclonal penta-His antibody (1:50; Qiagen) in 500 ml of F12 media supplemented with 10% fetal bovine serum. Beads were incubated with 400 μl of whole bacterial lysates from *E. coli* expressing penta-His tagged recombinant versions of PsrP spiked with 200 μg of recombinant Gst-BR full length and incubated overnight at 4°C with gentle agitation. Beads were washed with RIPA buffer, then boiled in sample buffer for 10 min (54). Samples were separated on 12% SDS-PAGE gels and electrophoretically transferred to nitrocellulose membranes. Membranes were blocked with T-PBS containing 4% bovine serum for 30 min at room temperature. Membranes were then incubated overnight at 4°C with mouse anti-Gst (1:7500; Proto-tech) in blocking buffer. Following incubation, membranes were washed with T-PBS three times for 5 minutes. HRP-conjugated goat anti-rabbit Immunoglobulin G (1:10 000; Sigma) was used as the secondary antibody, followed by development with the Super Signal chemiluminescent detection system (Thermo Scientific).

Visualization of recombinant BR bound to TIGR4

For labeling of bacteria, TIGR4 and T4 Δ*psrP* were pelleted and suspended in 1 ml of carbonate buffer (pH 9.0) containing FITC (1 mg/ml) and incubated in the dark at room temperature with constant end-to-end tumbling. FITC-labeled bacteria were washed with PBS (pH 7.4) and centrifuged, until the supernatant became clear. rBR fragments were labeled using a FluorLink-Ab Cy3 labeling kit (Amersham) using the instructions provided by the manufacturer. Labeled bacteria were suspended in serum-free F12 media containing the labeled constructs for 1 hour and gently mixed. Subsequently, pneumococci were washed and suspended in F12 medium. Labeled bacteria and bound recombinant protein were visualized using an AX-70 fluorescent microscope and the images were captured at 0.1112–0.8886 ms exposure time for Cy2 and Cy3 filters. The magnification used for capture of digital images was 1000×. Captured images were processed using Simple PCI software.

Adhesion assays

A549 cells (human alveolar type II pneumocytes; ATCC CRL-185), were grown to 90% confluence on 24-well plates (~10^6 cells/well). Prior to use, cells were washed with cell F12 media to remove serum. For competitive inhibition binding assays, A549 cells were incubated with 1μM of either rBR, rBR.C, a synthesized peptide corresponding to AA 122–167, or BSA for 1 HR. Following incubation, cells were exposed to media that contained 10^7 cfu/mL of bacteria and incubated for 1 h at 37°C in 5% CO_2. Nonadhering bacteria were removed by washing the cells 3 times with T-PBS and the number of adhering bacteria was determined by lysis of the monolayer with 0.1% Triton X-100 and plating wells per experiment.

Opsonophagocytosis assay

Bacterial cultures were centrifuged and suspended in 0.1M sodium carbonate buffer (pH 8.0) at an OD_{620} of 0.2. Care was taken to cause minimal disruption of the biofilm aggregates. The diluted cultures were labeled with fluorescent isothiocyanate (1mg/ml) for 30 min at room temperature in the dark. Following labeling, cultures were gently washed three times with sterile PBS to remove free FITC and suspended in PBS. FITC-labeled bacteria were opsonized with 3% control rabbit serum for 30 minutes at 37°C with mild periodical tapping. Mouse J774.1, macrophage cultures maintained in 10% FBS containing DMEM were used for phagocytosis of the opsonized pneumococci. Macrophages were harvested, washed and diluted with opsonophagocytosis buffer (PBS containing 0.2% BSA). FITC-labeled bacteria in 100 μl were added to 10^6 macrophage cells in 400 μl and incubated for 1 hour at 37°C with periodic shaking. Afterwards, the macrophages were pelleted and washed twice in the assay buffer. Cells were suspended in 400μl of 2% paraformaldehyde until flow cytometric analysis. A2-Laser BD FACSCaliber Analyzer (Becton Dickinson, NJ; Institutional Flow Cytometry Core Facility at the Health Science Center) was employed to analyze percent phagocytic uptake of the labeled bacteria by the macrophages. A minimum of 20,000 events were counted for each sample at 480 nm excitation and 530nm detection wavelengths. Background fluorescence was nullified by subjecting negative control macrophages in assay buffer without any fluorescent bacteria to FACS analysis. Data were processed using CellQuest software.

Statistical analysis

For pair-wise comparisons of groups statistical analyses were performed using a Student's *t*-test. For multivariate analyses a 1-Way ANOVA followed by a post-priori test using Sigma Stat software was used.

Results

PsrP promotes pneumococcal aggregation *in vivo*

To test whether PsrP contributed to biofilm or microcolony formation *in vivo* mice were infected with TIGR4 and its isogenic *psrP* deficient mutant, T4 Δ*psrP*, and whole lung sections were examined using scanning electron microscopy (SEM). As would be expected for both wild type and the mutant, the majority of bacteria present were in the form of diplococci. However, for TIGR4 we also observed the presence of large bacterial aggregates attached to ciliated bronchial epithelial cells as well as to alveolar epithelial cells (Figure 2). For quantitative analysis of this phenomenon, nasal lavage fluid and bronchoalveolar lavage (BAL) fluid from mice was collected two days post-challenge. Aliquots from each biological sample were heat-fixed to glass slides, Gram-stained, and examined with a microscope (Figure 3A). In all, the number of bacterial aggregates composed of 2–9, and ≥10 diplococci were significantly greater for mice infected with TIGR4 than T4 Δ*psrP* in both the nasopharyngeal and BAL elute fluids (Figure 3B,C). Moreover, the largest aggregates, those composed of >100 bacteria, were observed only in mice infected with TIGR4. Fluorescent imaging of bacteria in frozen lung sections confirmed this phenotype; large bacterial aggregates were only detected in the lungs of TIGR4 infected mice. Thus we determined that PsrP promoted the formation of biofilm-like aggregates *in vivo*, including in the nasopharynx, a site previously shown not to require PsrP for bacterial colonization (12).

PsrP affects intimate bacteria to bacteria interactions

Given the previous results, moreover to develop an *in vitro* model that was amendable to manipulation, the ability of TIGR4 and T4 Δ*psrP* to form early biofilms was tested using microtiter plates (24). As shown in Figure 4A, no differences were observed between wild type and the mutant, suggesting that PsrP does not play a role in pneumococcal attachment to polystyrene or the formation of early biofilm structures, in particular the bacteria lawn. The role of PsrP was next tested in 3-day old mature biofilms using the once-through continuous flow cells as described previously by Allegrucci *et al.* (25). In this system, a stark difference in the architecture of TIGR4 and T4 Δ*psrP* biofilms was observed (Figure 4B). Wild type biofilms displayed a dense cloud-like morphology with extremely large aggregates that covered the glass surface. Closer inspection revealed that these aggregates were composed of tightly clustered pneumococci. In contrast, T4 Δ*psrP* biofilms displayed a less intimate phenotype characterized by smaller aggregates, gaps, and the formation

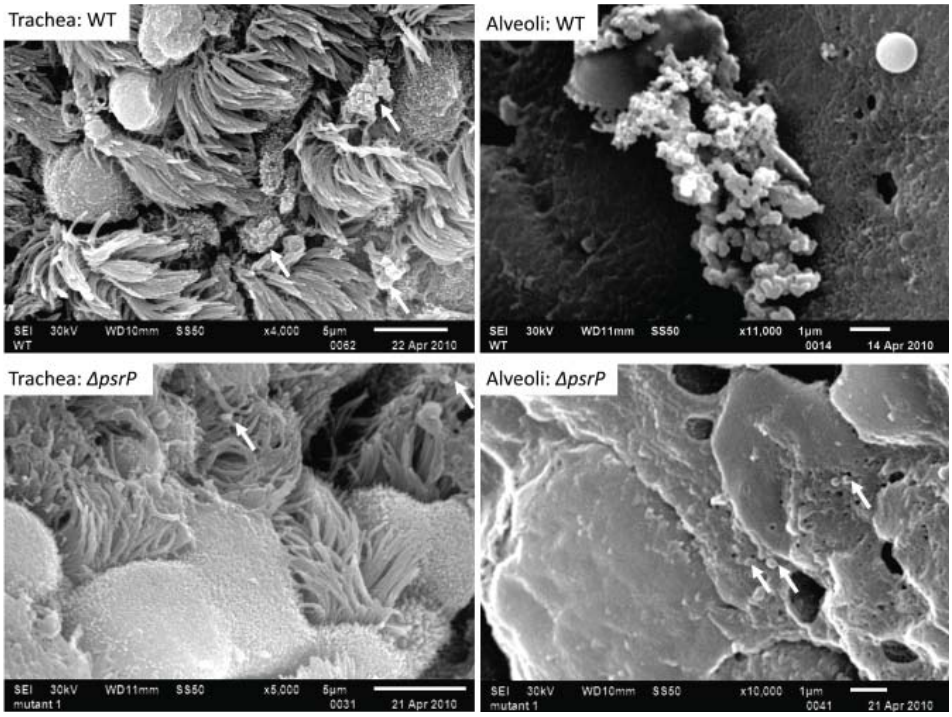

Figure 2. PsrP promotes the formation of bacterial aggregates *in vivo*.
SEM images of bronchial and alveolar epithelial cells following infection with TIGR4 (WT) and T4 Δ*psrP (ΔpsrP)*. White arrows point at attached bacteria. Note the presence of WT bacteria in large aggregates of various sizes.

of columns, resulting in an overall patchier phenotype. Quantitative analysis of the biofilm structures using COMSTAT software confirmed that TIGR4 biofilms had significantly greater total biomass and average thickness than those formed by the T4Δ*psrP* (Figure 4C). No differences in either the maximum thickness of the biofilms or the roughness coefficient (a measure of biofilm heterogeneity) were observed (Figure 4C; data not shown, respectively), indicating that T4 Δ*psrP* could still form biofilms, although with distinct architecture. Importantly, T4 Ω*psrP-secY2A2*, a mutant deficient in the entire *psrP-secY2A2* pathogenicity island, behaved identically to T4 Δ*psrP*, forming patchy biofilms with small aggregates and less intimate associated bacteria.

Bacterial biofilms were also grown under once through conditions in silicone tubing. After a designated time, the biofilms were extruded from the line and examined for biomass both visually and quantitatively. After 3 days of growth, differences between TIGR4

and T4 Δ*psrP* in opacity of the exudates were visible to the eye (Figure 5A) and could be confirmed using a spectrophotometer which showed a >3-fold difference in optical density (Figure 5B). Microscopic visualization of the line exudates following crystal violet (CV) staining revealed that TIGR4 had formed large aggregates whereas T4Δ*psrP* exudates were composed of small clusters or of individual diplococci (Figure 5C). Increased biofilm biomass was supported by measurement of total protein concentrations that showed TIGR4 biofilm exudates had 2–3 fold more protein than those corresponding to T4 Δ*psrP* (Figure 5D).

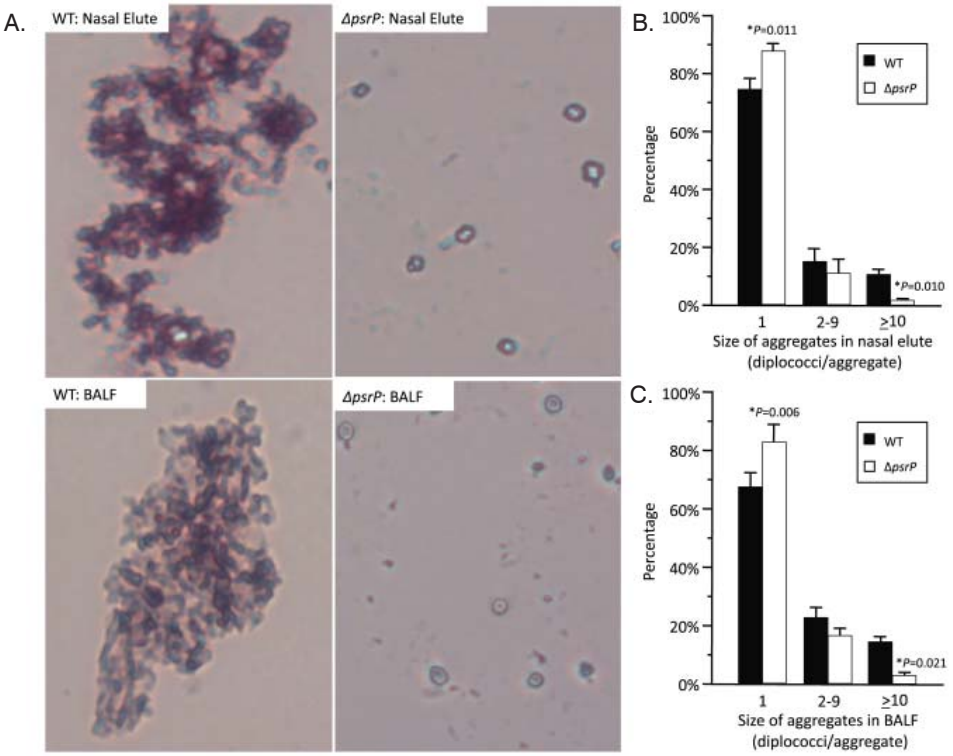

Figure 3. Frequency of bacterial aggregates in the nasopharynx and lungs.
A) Micrographs of TIGR4 (WT) and T4 Δ*psrP (ΔpsrP)* Gram-stained bacteria from either BAL or nasal lavage (IN) elutes. Images were taken at 400× magnification. Images are not representative of the total bacteria population, but instead are shown to demonstrate the typical pneumococcal aggregate containing at least 10 or more individual diplococci (10+).
B) Actual percentages of pneumococcal aggregate based on size in the nasopharynx and
C) lungs following counting of >100 randomly selected CFUs per biological replicate. Note that TIGR4 had significantly greater levels of 2–9 and 10+ aggregates compared to T4 Δ*psrP*. Furthermore, while 10+ aggregates were observed in mice infected with T4 Δ*psrP*, albeit infrequently, the largest of these aggregates were not comparable in size to those formed by TIGR4. Statistical analyses were performed using a Student's *t*-test.

Of note, during planktonic growth TIGR4, T4 Δ*psrP*, and T4 Ω*psrP-secy2A2* were indistinguishable, growing either as short chains or diplococci with a marked absence of aggregates (data not shown). This led us to examine *psrP* transcription using Real-Time PCR and the finding that TIGR4 expressed *psrP*at levels 47-fold greater during biofilm versus planktonic culture ($P = 0.04$ using a Student's *t*-test). Thus low expression of *psrP* may be one reason TIGR4 did not form aggregates during liquid culture.

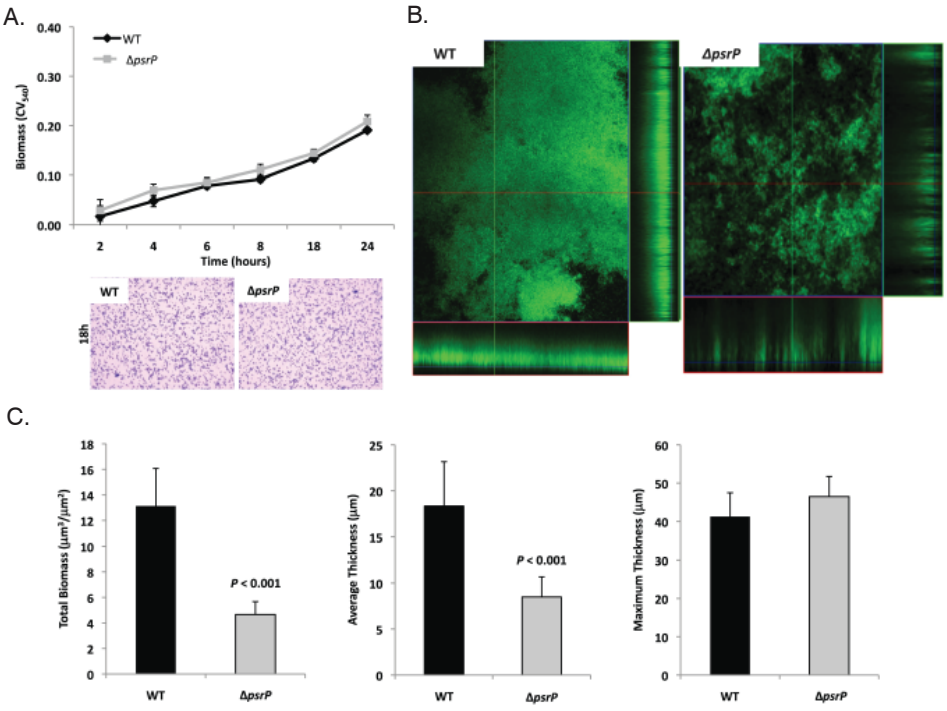

Figure 4. Deletion of *psrP* alters bacterial interactions in mature biofilms but not during early biofilm attachment.
A) Attachment of TIGR4 (WT) and T4 Δ*psrP (ΔpsrP)* to the bottom of 96-well polystyrene microtiter plate in an early biofilm model. Biofilm biomass was determined using crystal violet (CV_{540}) stain as described in the methods.
B) Micrographs of mature TIGR4 and T4 Δ*psrP* biofilms grown in a flow cell under once-through flow conditions for 3 days. Bacteria were visualized with Live/Dead BacLight stain using an inverted confocal laser scanning microscope at 400× magnification.
C) Quantitative analysis of the biofilms was performed using COMSTAT image analysis software. All experiments were performed in triplicate. Statistical analyses were performed using a two-tailed Student's *t*-test. For panel C error bars denote standard error.

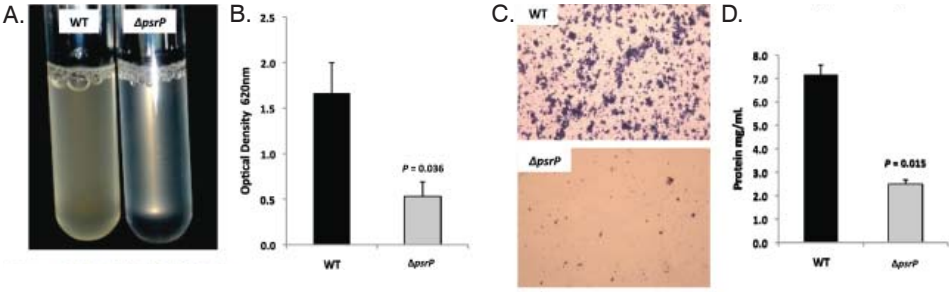

Figure 5. PsrP promotes bacterial aggregation in a line biofilm model.
Mid-logarithmic growth phase TIGR4 (WT) and T4 Δ*psrP (ΔpsrP)* were used to inoculate 1 meter of a 0.8 mm diameter silicone-lined plastic tubing. After 3 days, biofilms within the lines were extruded.
A) Representative photograph of the exudate suspension immediately following its collection.
B) Optical density (OD_{540}) of bacterial exudates.
C) Microscopic images of CV stained bacteria extracted from the lines. Note the formation of aggregates by TIGR4 but not T4 Δ*psrP*.
D) Levels of protein in bacteria line exudates as determined by bicinchoninic acid assay (BCA) following detergent lysis of the bacteria. Images are representative of at least 3 experiments. Statistical analyses were performed using a two-tailed Student's *t*-test. Error bars denote standard error.

The BR domain mediates intra-species bacterial interactions

To date a number of groups, including our own, have shown that SRRPs mediate bacterial adhesion to host cells primarily through their NR domain (13,26,27). For this reason we sought to test whether the BR domain of PsrP was also involved in biofilm/bacterial aggregation. To do this we first utilized a pre-existing collection (described in Figure S3) of encapsulated (T4 Ω*psrP*) and unencapsulated (T4RΩ*psrP*) *S. pneumoniae* mutants deficient in PsrP that either expressed a truncated version of PsrP with 33 SRRs in its SRR2 domain ($PsrP_{SRR2(33)}$), a similar truncated version lacking the BR domain ($PsrP_{SRR2(33)\text{-}BR}$), or carried the empty expression vector pNE1 (13). These strains were tested for their ability to form biofilms in silicone lines under once through conditions.

Complementation of T4 Ω*psrP* with $PsrP_{SRR2(33)}$, but not $PsrP_{SRR2(33)\text{-}BR}$ or the empty pNE1 vector, partially restored the ability of T4 Ω*psrP* to form large aggregates in the lines when examined microscopically (Figure 6A). However, measurement of other biofilm markers such as optical density and total protein concentration showed no differences between any of the complemented mutants and the negative controls (Figure 6B–C). Complementation of T4R Ω*psrP* with $PsrP_{SRR2(33)}$, also partially restored the ability of T4R Ω*psrP* to form aggregates (Figure 6A). In this instance, line exudates from T4R Ω*psrP* with $PsrP_{SRR2(33)}$ had significant more biofilm biomass than the negative controls (Figure 6B–C).

Importantly, the truncated version of PsrP lacking the BR domain failed to restore, even partially, T4 Ω*psrP* or T4R Ω*psrP* suggesting that the BR domain was responsible for the intra-species aggregation. This was subsequently confirmed by Far-Western blot analyses that showed that Gst-tagged recombinant BR (Gst-BR) bound only to *S. pneumoniae* cell lysates that contained a truncated PsrP with the BR domain (Figure 6D) and a control experiment showing that a Gst-tagged *Chlamydia trachomatis* protein did not interact with these lysates.

To further explore the role of the BR domain in the observed bacteria to bacteria interactions, the ability of His-tagged BR constructs (rBR; Figure 7A), purified from *Escherichia coli* and Cy3 labeled, were tested for their ability to bind to the surface of TIGR4 and T4 Δ*psrP*. Full-length rBR interacted with TIGR4 but not with T4 Δ*psrP* (Figure 7B), confirming not only that PsrP bound to pneumococci, but also suggesting that its ligand was another PsrP. Furthermore, only rBR.A retained the ability to attach to PsrP on the pneumococcal surface. This suggested that the binding domain of PsrP was possibly located within AA 122–166, the section not shared between rBR.A and rBR.B.

Hereafter, BR to BR interactions were tested for by Far Western and co-immunoprecipitation. Far Western blot experiments using assorted *E. coli* cell lysates from bacteria expressing assorted rBR constructs, confirmed that only lysates containing PsrP constructs with AA 122–166 bound successfully to Gst-BR (Figure 7C). This was also observed in co-immunoprecipitation experiments, whereby Gst-BR was tested for its ability to bind whole cell lysates from *E. coli* expressing versions of PsrP (Figure 7D). Far Western blots using purified proteins showed that Gst-BR had affinity to purified rBR, rBR.A, and a synthesized peptide corresponding to AA 122–166, but not rBR.B, BR.C, or the control his-tagged Streptolysin O (Figure 7E). Hence, using numerous assays it was determined that the BR domain, most likely AA 122–166, had self-interacting properties that might be responsible for the observed bacterial aggregation.

Of note, because the BR constructs were purified from *E. coli* and PsrP is normally glycosylated, the above observations may have been an artifact of the unglycosylated constructs used. To address this possibility a glycosyated truncated PsrP construct was purified from *S. pneumoniae* ($PsrP_{SRR2(33)\text{-}HIS}$) and tested for its ability to bind *S. pneumoniae* cell lysates containing either native PsrP or assorted constructs. As shown in Figure 7F, it was determined that a glycosylated PsrP probe maintained specificity for the BR domain even in the context of glycosylated recipient protein. A finding that supports the notion that PsrP to PsrP interactions occur in natural setting when PsrP is always glycosylated.

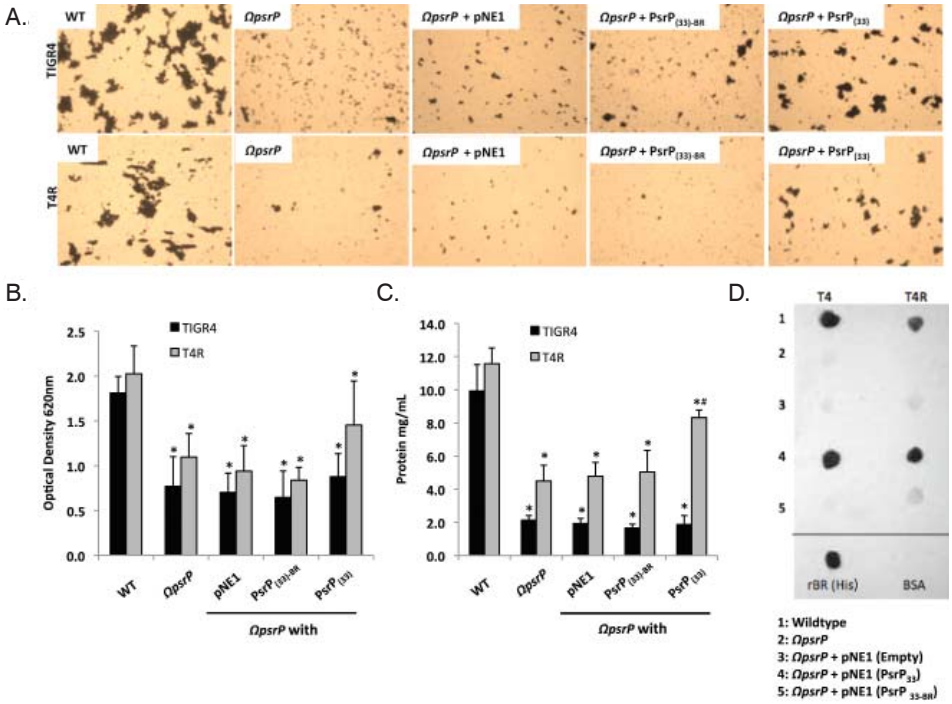

Figure 6. The BR domain of PsrP mediates intra-species bacterial interactions.
Encapsulated and unencapsulated mutants of TIGR4, lacking PsrP (T4 Ω*psrP*, T4R Ω*psrP*, respectively), were complemented with plasmids expressing: a truncated version of PsrP having only 33 SRR2 repeats ($PsrP_{(33)}$), the truncated version of PsrP missing the BR domain ($PsrP_{(33)-BR}$), or with the empty expression vector (pNE1).
A) Microscopic images of CV stained bacteria isolated from the line biofilm model.
B) Optical density (OD_{620}) of biofilm line exudates.
C) Biomass of the biofilms as determined by protein levels using the BCA assay.
D) Far Western analyses of recombinant BR interactions with membrane-bound truncated versions of PsrP expressed in *S. pneumoniae*.
All images are representative of at least 3 independent experiments. Statistical analyses were performed using 1-Way ANOVA analysis. Error bars denote standard error. For panel B and C asterisks denote statistical significance versus WT; hash sign denotes statistical significance versus the empty vector control.

The aggregation and K10-binding subdomains of BR are independent

To determine whether the BR aggregation (AA 122–167) and the K10 binding subdomains (AA 273–341) of BR had functionally independent roles, competitive inhibition assays were performed using rBR constructs. Bacterial adhesion to A549 cells was tested following incubation of cells with the AA 122–166 peptide, rBR, and rBR.C (Figure 8A). Pre-treatment of A549 cells with AA 122–167 had no impact on adhesion. In contrast and consistent with the location of the K10 binding domain within BR.C: 1) TIGR4 adhered significantly less

to cells treated with rBR or rBR.C, 2) TIGR4 adhered to BSA treated cells better than T4 Δ*psrP*. In complementary biofilm experiments the opposite result was observed. Addition of 1 μM peptide AA 122–167 to media reduced the aggregation phenotype observed for TIGR4 (Figure 8B) and modestly lowered the optical density of the biofilm exudate and the total biomass collected from the continuous flow lines versus addition of BR.C (Figure 8C–D). Thus these findings suggested that the aggregation and K10 subdomains of PsrP had distinct roles that did not overlap during host cell adhesion or biofilm formation.

Finally we sought to determine a biological effect for the aggregation phenotype. We observed that after 1 hour, 69±2% of J477 macrophages incubated with planktonically grown TIGR4 were associated with FITC-labeled bacteria whereas only 51±5% of macrophages mixed with biofilm grown TIGR4 were positive ($P = 0.024$). Macrophages exposed to biofilm grown TIGR4 also took up less bacteria than macrophages mixed with planktonic (74±1%; $P = <0.001$) and biofilm (60±1%; $P = <0.001$) cultures of T4 Δ*psrP*. Interestingly, a 10% reduction in macrophage uptake was observed for the biofilm versus planktonic grown T4 Δ*psrP* cultures ($P = 0.077$); and no difference was observed between macrophage uptake of TIGR4 and T4 Δ*psrP* when taken from planktonic cultures. These findings suggest, that in addition to PsrP, other bacterial factors expressed during growth in a biofilm also affect opsonophagoyctosis.

Antibodies to the BR domain, but not to the SASASAST motif, block bacterial aggregation

Previously we had shown that antibodies against the SRR1-BR domains of PsrP neutralized the ability of *S. pneumoniae* to attach to lung cells and that vaccination with rBR protected mice against pneumococcal challenge (1213). For this reason we tested the ability of polyclonal antiserum against rBR and against a SRR motif peptide to block bacterial aggregation in the biofilm line model. Todd Hewitt Broth (THB) supplemented with a 1:1000 dilution of antiserum against the BR domain inhibited the formation of bacterial aggregates as observed by microscopic visualization of the biofilm line exudates. In contrast, bacteria in media supplemented with antiserum to the SRR motif peptide or that from naïve animals, formed aggregates similar to wild type bacteria grown under serum free conditions (Figure 9A). Biofilm exudate optical density and protein concentrations supported these microscopic observations (Figure 9B–C). To determine whether the effect of the BR antiserum on biofilm formation was specific for TIGR4, we tested the ability of antibodies to the BR domain to block biofilm formation in unrelated clinical isolates. Antiserum against rBR from TIGR4 inhibited biofilm formation in two unrelated clinical isolates that carried PsrP. The same sera had no effect on biofilm formation by an invasive serotype

14 isolate that lacked PsrP. Therefore these studies confirmed previous observations that increased bacteria aggregation in biofilm models can occur independently of PsrP, but that if present, antiserum against BR can block the contribution of PsrP to these processes.

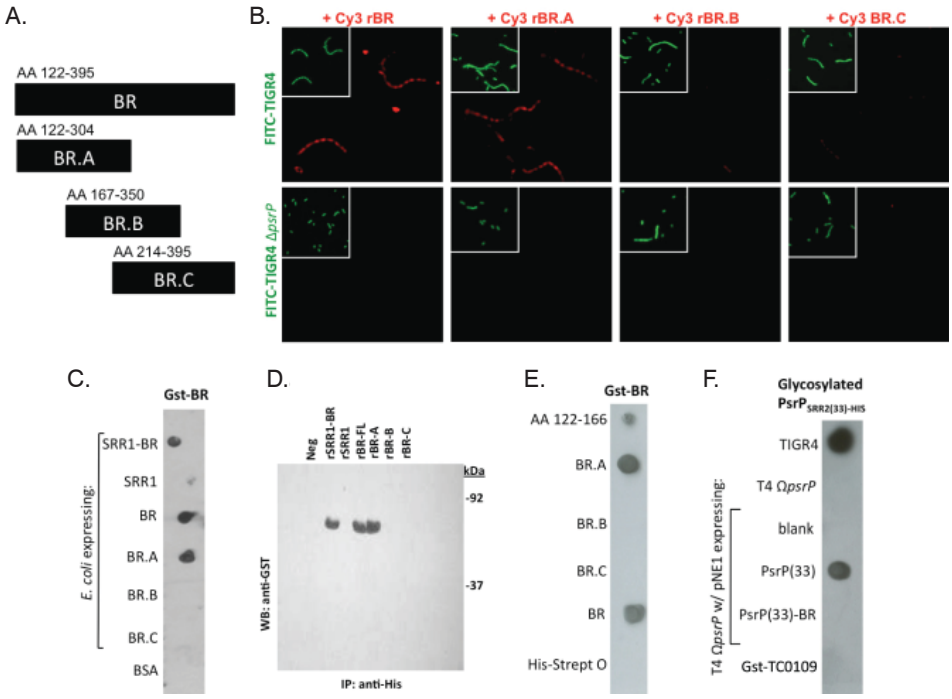

Figure 7. Recombinant BR interacts with pneumococci that carry amino acids 122–166 of PsrP.
A) The designated recombinant PsrP constructs were expressed and purified from *E. coli*.
B) Micrographs of FITC-labeled bacteria following their incubation with CY3-labeled rBR or the designated truncated versions. Note that only Cy3-labeled rBR and rBR.A bound to TIGR4. Moreover, neither bound to T4 Δ*psrP*. This suggests that recombinant BR binds to PsrP on the bacteria surface.
C) Far Western blot examining the interaction of Gst-BR with cell lysates from *E. coli* expressing assorted rBR constructs spotted on a membrane.
D) Co-immunoprecipitation of Gst-BR (65 kDa) from spiked *E. coli* lysates expressing His-tagged rBR constructs.
E) Far Western blot examining the interaction of Gst-BR with purified rBR constructs and a synthesized peptide corresponding to AA 122–166.
F) Far Western blot examining the interaction of a glycosylated PsrP construct purified from *S. pneumoniae*, $PsrP_{SRR2(33)-HIS}$ with glycosylated PsrP constructs expressed in TIGR4.

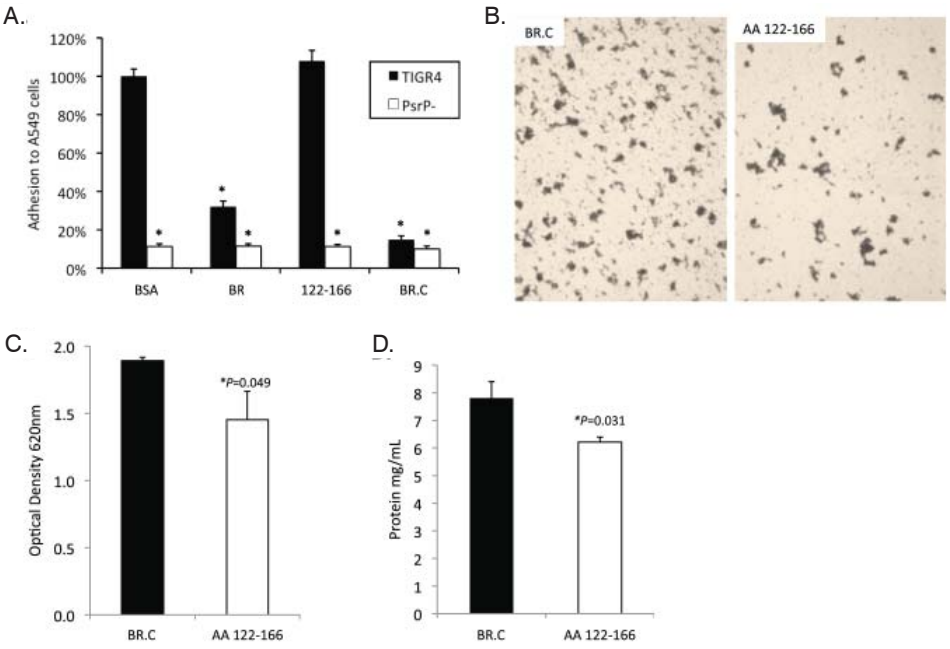

Figure 8. Incubation of bacteria with AA 122–166 impairs bacterial aggregation but not adhesion to cells.
A) Adhesion of TIGR4 following pre-incubation of A549 cells with media containing 1.0 μM of the designated rBR constructs. All values were normalized against cells incubated with BSA (163±4 bacteria/10^6 cells). TIGR4 in media containing 1 μM BR.C or the synthesized peptide 122–126 was used to inoculate and grow biofilms in the line biofilm model. After 3 days, biofilms within the lines were extruded.
B) Representative photograph of the exudate suspension immediately following its collection and staining with CV. Images are representative of at least 3 experiments.
C) Optical density (OD_{540}) of bacterial exudates.
D) Levels of protein in bacteria line exudates. Statistical analyses were performed using a Student's *t*-test. Error bars denote standard error.

SRRPs mediate intra-species adhesion in pathogenic bacteria

To determine whether other SRRPs also mediated intra-species aggregation we tested the effect of *gsp B*and *sraP* deletion on *S. gordonii* and *S. aureus* biofilm architecture, respectively. Deletion of *gspB* and *sraP* negatively impacted biofilm formation in the microtiter biofilm model at 24 hours (Figure 10A,B). Growth of wild type and mutant bacteria in the line models also demonstrated that both proteins contributed to the formation of large aggregates during surface attached growth; although this property was much more dramatic for *S. gordonii* than for *S. aureus* which did not show a significant difference in the optical densities of the exudates (Figure 10C,D). Of note, *S. aureus* biofilm experiments were stopped after 1 day due to bacteria overgrowth and blockage of the lines.

Subsequent Far Western analysis using Gst-BR from *S. pneumoniae* as well as recombinant SRR1-NR from SraP and recombinant NR from GspB showed that these proteins have affinity for cell lysates from their parent strain but not for cell lysates from isogenic SRRP deficient mutants (Figure 10E). This supports the notion that these proteins might be involved in intra-species aggregation. For PsrP BR from*S. pneumoniae*, no affinity was observed for cell lysates from either *S. gordonii* or *S. aureus* suggesting that PsrP does not play a role as an inter-species adhesin (Figure 10E). In contrast, the NR constructs from *S. aureus* and *S. gordonii* bound to cell lysates from the other bacteria, even in the absence of the SRRP (Figure 10E). The discrepancy between PsrP and the other SRRPs might be explained by the fact that certain SRRPs have been described to have lectin activity (26,27). In contrast PsrP adhesion has been shown to be independent of lectin-activity (13).

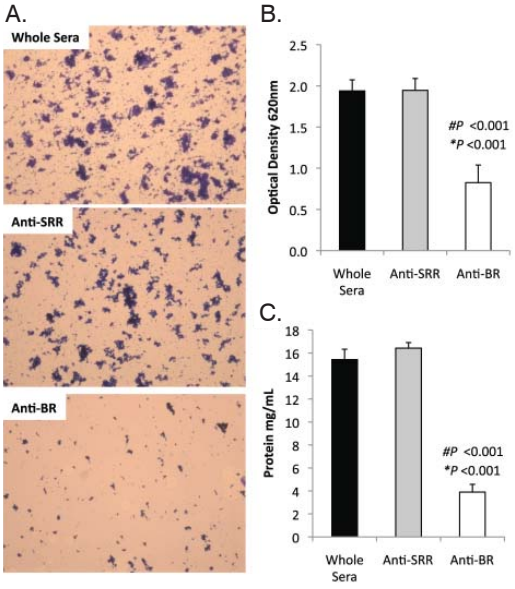

Figure 9. Antibodies to the BR domain but not the serine-rich motif block intra-species bacterial interactions.
THB was supplemented with either a 1:1000 dilution of naïve rabbit serum (control), rabbit antiserum from rabbits immunized with a SASASASTSASASAST peptide designed after the SRR motif, or rabbit antiserum to recombinant BR.
A) Micrographs of CV stained bacteria extruded from the biofilm lines.
B) Optical density of bacterial exudates.
C) Levels of protein in bacterial line exudates as determined by BCA analysis.
Images are representative of at least 3 independent experiments. Statistical analyses were performed using a two-tailed Student's *t*-test. Number sign denotes statistical significance versus whole serum. Asterisks denote statistical significance versus anti-SRR serum. Error bars denote standard error.

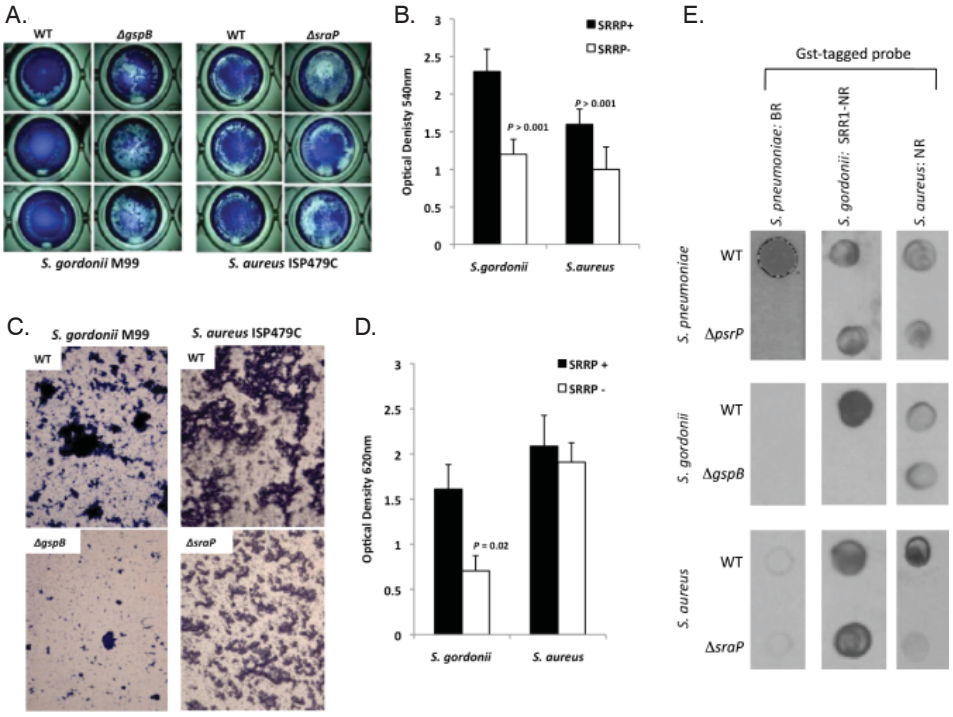

Figure 10. The SRRPs of *S. gordonii* and *S. aureus* promote bacterial aggregation.
Light microscopic images of CV stained
A) *S. gordonii M99* and
B) *S. aureus ISP479C* and their respective isogenic SRRP mutants following 24 hours of growth in a 96-well polystyrene microtiter plate early biofilm model. B) Average biomass of early biofilms as determined by CV_{540} analyses. Error bars denote standard deviation.
C) Microscopic images of bacteria extruded from the biofilm lines after 3 days for *S. gordonii* and 1 day for *S. aureus*.
D) Measurement of optical density of bacterial exudates collected from the biofilm lines. Error bars denote standard deviation.
E) Far-western examining the intra- and inter-species specificity of the NR domains of *S. pneumoniae*, *S. gordonii* and *S. aureus*.
Whole cell lysates from *S. gordonii*, *S. aureus*, and their respective isogenic SRRP mutants were spotted onto nitrocellulose membranes and probed with these GST-tagged proteins. Images are representative of three individual experiments. For panels B) and D) statistical analyses were performed using a Student's *t*-test.

Discussion

To date, SRRPs have been described in at least 9 Gram-positive bacteria and have been shown to function as adhesins that contribute to virulence. For example, deletion of *sraP* and *gspB* in *S. aureus* and *S. gordonii*, respectively, decreased the ability of these bacteria to bind to platelets and form vegetative plaques on heart valves of catheterized rats (27,28). Similarly, Srr-1 of *Streptococcus agalactiae* has been shown to bind human Keratin 4, mediate adherence to mucosal epithelial cells, and promote invasion of bacteria through human brain microvasculature endothelial cells (29,30). SRRPs also mediate acellular attachment, a role important for colonization of the dental surface by oral streptococci. Froelinger and Fives-Taylor showed that *Streptococcus parasanguis* containing mutations of Fap1 failed to attach to saliva-coated hydroxyapatite (31). Likewise, deletion of *srpA* significantly diminished the ability of *Streptococcus cristatus* to attach to glass slides (32). Thus, while it was well established that SRRPs play an important role in bacterial attachment to cells or surfaces, until this report their role as intra-species adhesins remained unrecognized.

A dual role, host and bacterial adhesin for bacterial surface proteins is not unprecedented. For example, in *Streptococcus pyogenes* and *S. agalactiae*, the pilus proteins mediate adhesion to epithelial cells and promote microtiter biofilm formation (33,34). Likewise, for *Neisseria meningitidis*, PilX, also a pilus-associated protein, mediates adhesion to epithelial cells and facilitates bacterial aggregation (35). For the pneumococcus, some evidence existed that bacterial adhesins may also have dual roles. In 2008, Munoz-Elias *et al.* found that the pneumococcal adhesins Choline binding protein A and the pilus protein RrgA were both required for robust biofilm formation on microtiter plates and efficient nasopharyngeal colonization (36). However, the attenuated biofilm phenotype was observed only with unencapsulated bacteria and encapsulated mutants formed biofilms normally. Other pneumococcal proteins shown to affect biofilm formation *in vitro* include Neuraminidase A, which possibly alters the extracellular matrix (37-39), competence proteins, which suggest an altered protein profile (40,41), and capsule synthesis enzymes, which were determined to be down regulated in biofilms (36,42,43). Unlike PsrP, which would be expected to bridge cells directly, these proteins most likely act indirectly by altering gene expression, the extracellular milieu, or the surface availability of other adhesins, including possibly RrgA and CbpA.

Our studies determined that the self-aggregating subdomain of PsrP was located in

the BR domain and involves amino acids 122–166. Recombinant BR constructs containing these amino acids were able to bind *S. pneumoniae* carrying PsrP, had an affinity for the BR domain in other PsrP constructs, and could modestly inhibit biofilm formation when added to media. Importantly, adhesion assays using pretreated cells and biofilm assays with rBR.C showed that the AA 122–166 was not responsible for adhesion to lung cells and that the K10 binding subdomain (AA 273–341) was not involved in bacterial aggregation. Thus these subdomains appeared to have independent roles during the conditions tested. Further studies are warranted to delineate the specific AAs responsible for these adhesive properties, also to determine the structure of the BR domain and clarify how these subdomains interact with PsrP on other pneumococci and K10 on lung cells.

GspB and SraP have been previously shown to bind platelets (27,28). While the ligand for SraP is unknown, it has been determined that GspB binds to Sialyl T-antigen on platelet membrane glycoprotein Ibα (26,27). The observation that the NR domains of GspB and SraP bound to cell lysates containing their respective SRRPs but not to their mutants and that the mutants had diminished aggregative properties suggests that SRRPs in other bacteria might also mediate aggregation *in vivo*. One could imagine that SraP on *S. aureus* or GspB on *S. gordonii* mediating attachment to platelets and cells in an endocarditic lesion while at the same time mediating adhesion of individual bacteria to each other. Similarly, one could envision a microcolony of the pneumococcus in the lungs with some bacteria attached to host cells via PsrP/K10 interactions and other bacteria attached to these bacteria through PsrP/PsrP interactions. Presumably, this is what was observed in the lungs of the infected mice. Interestingly, the finding that GspB and SraP NRs bound to cell lysates from other bacteria suggests that these proteins may also mediate inter-species biofilm formation. For *S. gordonii*, this would be relevant as the dental plaque is now recognized to be a multi-species biofilm. Importantly, neutralization of pneumococcal aggregation in biofilms with BR antiserum suggests that SRRPs might have utility as vaccine antigens. One caveat is that SRRPs would have to be one-component of a multi-valent vaccine because not all strains of *S. pneumoniae*, *S. aureus*, or the oral streptococci carry these proteins.

In previous studies we had found that the length of the SRR2 domain was important for adhesion to K10 when capsule was present. Consistent with these findings, the inability of truncated PsrP to fully complement capsulated mutants supports our hypothetical model that the SRR2 domain serves to extend the BR domain away from the cell to mediate bacterial interactions. This model is also indirectly supported by Munoz-Elias *et al.*, who showed that down-regulation of capsule allowed CbpA and RrgA to contribute to biofilm production (36). It is also noteworthy to state that Munoz-Elias *et al.* did not identify PsrP in

their screen for biofilm mutants although they used TIGR4 which carries PsrP. This can be explained by the fact that we observed no contribution for PsrP in the microtiter plate early biofilm model.

We observed that PsrP-mediated bacterial aggregation occurred in the nasopharynx, despite earlier studies demonstrating that K10 was absent from this site and that PsrP was not required for nasopharyngeal colonization. Aggregation of *S. pneumoniae* in the nasopharynx may serve as a mechanism to resist opsonophagocytosis as shown herein, or we speculate a way to resist desiccation during transmission of infectious particles. The observation that aggregates were present at an anatomical site that lacked K10, further supports an independent role for these PsrP subdomains. In regards to opsonophagoyctosis, one important consideration is that the pneumococcus most likely has different gene expression profiles in vivo as an aggregate attached to a cell versus in vitro as a biofilm (44). Thus caution is warranted in applying our vitro observations, such as resistance to opsonophagoyctosis or enhanced PsrP expression during biofilm growth, with events that occur in vivo.

Polyclonal antibodies against the BR domain, but not the SRR motif, neutralized the ability of TIGR4 and clinical isolates carrying PsrP to form aggregates in the line model. These findings were consistent with previous studies showing that antibodies against BR also neutralized its ability to mediate adhesion to host cells and protected mice against pneumonia (12,13). One possible reason that antibodies against the SRR motif peptide failed to have a neutralizing effect is that PsrP is glycosylated and antibodies against the peptide failed to recognize the native version of the protein. Alternatively, antibodies to the SRR motif may bind away from the BR domain and therefore do not inhibit the ability of the BR domain to self-interact. Interestingly, polyclonal antibodies to surface proteins often promote aggregation. This did not occur for unknown reasons. Finally, our finding that antibodies against rBR neutralized bacterial aggregation in the biofilm line model suggests that the same antibodies might also neutralize bacterial aggregation *in vivo*. This remains to be tested, however, the protection that was observed in mice following immunization with rBR (13), may have been in part due to inhibition of bacterial aggregation in addition to blocking interactions with K10.

Importantly, because rNR domains produced in *E. coli* are not glycosylated, yet for the tested SRRPs were able to aggregate, immunoprecipitate, and bind to native protein in cell lysates, it seems that the BR domain does not require glycosylation to function as a self-adhesin. This is supported by the observation that addition of antibodies against unglycosylated rBR and that synthetic peptide AA 122–166 both inhibited bacterial aggregation in the biofilm line. In contrast to the latter concept, Wu *et al.*demonstrated that

monoclonal antibodies specific for the glycan motifs of the serine-rich repeat motifs of Fap1 were capable of blocking attachment to saliva coated hydroxyapatite by *Streptococcus parasanguis* (45). Importantly, Fap1 is the most divergent of the SRRPs and has 2 NR domains. Fap1 adhesion to saliva coated hydroxyapatite is mediated by glyconjugates on the serine-rich repeat domain (46); as evidenced by the fact that inactivation of one of the glycosyltranferases known to modify the glycan moieties of Fap1, drastically altered the ability of *S. parasanguis* to form biofilms (45). Thus Fap1 is interesting because it suggests an NR-independent mechanism for SRRP adhesion, which is distinct from those discussed for GspB, SraP, or PsrP. Future studies need to further examine the differences between these diverse SRRPs and to determine if the two NRs of Fap1 play a role in bacterial aggregation. This is especially true given that the NR domain of SraP has a pI of 5.6, in contrast to the basic NRs of GspB (9.5 pI) and PsrP (9.9 pI) (47).

In summary, we have described for the first time the presence of a pneumococcal biofilm-like structure in the lungs of infected mice. We have determined that PsrP mediates a more intimate bacterium to bacterium interaction that contributes to the presence of large bacteria aggregates *in vivo* and increased biofilm biomass and aggregates *in vitro*. This property appears to be shared among other SRRPs including those of medically relevant bacteria such as *S. aureus* and *S. gordonii*, suggesting that it is a conserved function for this class of proteins. How these interactions contribute to pathogenesis remains to be fully determined, however, studies with other bacteria indicate that biofilms serve to inhibit phagocytosis, protect against defensin-mediated killing, and serve as a focal point of infection during early stages of disease. Future experiments will be required to determine the extent to which this may apply for SRRP-mediated aggregates *in vivo*.

Acknowlegdements

We would like to thank Jim Jorgenson for the gift of low-passage clinical isolates. Angela R. Boyd is acknowledged for her technical assistance with the animal experiments and protein purification.

References

1. (1999) Pneumococcal vaccines. WHO position paper. Wkly Epidemiol Rec 74: 177–183.
2. Lexau CA, Lynfield R, Danila R, Pilishvili T, Facklam R, et al. (2005) Changing epidemiology of invasive pneumococcal disease among older adults in the era of pediatric pneumococcal conjugate vaccine. JAMA 294: 2043–2051.
3. Overturf G, Powars D (1980) Infections in sickle cell anemia: pathogenesis and control. Tex Rep Biol Med 40: 283–292.
4. Wong WY, Overturf GD, Powars DR (1992) Infection caused by *Streptococcus pneumoniae* in children with sickle cell disease: epidemiology, immunologic mechanisms, prophylaxis, and vaccination. Clin Infect Dis 14: 1124–1136.
5. Roush SW, Murphy TV (2007) Historical comparisons of morbidity and mortality for vaccine-preventable diseases in the United States. JAMA 298: 2155–2163.
6. O'Brien KL, Wolfson LJ, Watt JP, Henkle E, Deloria-Knoll M, et al. (2009) Burden of disease caused by *Streptococcus pneumoniae* in children younger than 5 years: global estimates. Lancet 374: 893–902.
7. Maruyama T, Gabazza EC, Morser J, Takagi T, D'Alessandro-Gabazza C, et al. (2010) Community-acquired pneumonia and nursing home-acquired pneumonia in the very elderly patients. Respir Med 104: 584–592.
8. Obert C, Sublett J, Kaushal D, Hinojosa E, Barton T, et al. (2006) Identification of a candidate *Streptococcus pneumoniae* core genome and regions of diversity correlated with invasive pneumococcal disease. Infect Immun 74: 4766–4777.
9. Orihuela CJ (2009) Role played by *psrP-secY2A2* (accessory region 34) in the invasive disease potential of *Streptococcus pneumoniae*. J Infect Dis 200: 1180–1181; author reply 1181–1182.
10. Hava DL, Camilli A (2002) Large-scale identification of serotype 4 *Streptococcus pneumoniae* virulence factors. Mol Microbiol 45: 1389–1406.
11. Embry A, Hinojosa E, Orihuela CJ (2007) Regions of Diversity 8, 9 and 13 contribute to *Streptococcus pneumoniae* virulence. BMC Microbiol 7: 80.
12. Rose L, Shivshankar P, Hinojosa E, Rodriguez A, Sanchez CJ, et al. (2008) Antibodies against PsrP, a novel *Streptococcus pneumoniae* adhesin, block adhesion and protect mice against pneumococcal challenge. J Infect Dis 198: 375–383.
13. Shivshankar P, Sanchez C, Rose LF, Orihuela CJ (2009) The *Streptococcus pneumoniae* adhesin PsrP binds to Keratin 10 on lung cells. Mol Microbiol 73: 663–679.
14. Tettelin H, Nelson KE, Paulsen IT, Eisen JA, Read TD, et al. (2001) Complete genome sequence of a virulent isolate of *Streptococcus pneumoniae*. Science 293: 498–506.
15. Takamatsu D, Bensing BA, Sullam PM (2005) Two additional components of the accessory Sec system mediating export of the *Streptococcus gordonii* platelet-binding protein GspB. J Bacteriol 187: 3878–3883.
16. Takamatsu D, Bensing BA, Sullam PM (2004) Four proteins encoded in the *gspB-secY2A2* operon of *Streptococcus gordonii* mediate the intracellular glycosylation of the platelet-binding protein GspB. J Bacteriol 186: 7100–7111.

17. Bensing BA, Gibson BW, Sullam PM (2004) The *Streptococcus gordonii* platelet binding protein GspB undergoes glycosylation independently of export. J Bacteriol 186: 638–645.
18. Takamatsu D, Bensing BA, Sullam PM (2004) Genes in the accessory Sec locus of*Streptococcus gordonii* have three functionally distinct effects on the expression of the platelet-binding protein GspB. Mol Microbiol 52: 189–203.
19. Hammerschmidt S, Wolff S, Hocke A, Rosseau S, Muller E, et al. (2005) Illustration of pneumococcal polysaccharide capsule during adherence and invasion of epithelial cells. Infect Immun 73: 4653–4667.
20. Moscoso M, Garcia E, Lopez R (2009) Pneumococcal biofilms. Int Microbiol 12: 77–85.
21. Hall-Stoodley L, Stoodley P (2009) Evolving concepts in biofilm infections. Cell Microbiol 11: 1034–1043.
22. Hall-Stoodley L, Hu FZ, Gieseke A, Nistico L, Nguyen D, et al. (2006) Direct detection of bacterial biofilms on the middle-ear mucosa of children with chronic otitis media. JAMA 296: 202–211.
23. Reid SD, Hong W, Dew KE, Winn DR, Pang B, et al. (2009) *Streptococcus pneumoniae* forms surface-attached communities in the middle ear of experimentally infected chinchillas. J Infect Dis 199: 786–794.
24. Lizcano A, Chin T, Sauer K, Tuomanen EI, Orihuela CJ (2010) Early biofilm formation on microtiter plates is not correlated with the invasive disease potential of*Streptococcus pneumoniae*. Microb Pathog 48: 124–130.
25. Allegrucci M, Hu FZ, Shen K, Hayes J, Ehrlich GD, et al. (2006) Phenotypic characterization of *Streptococcus pneumoniae* biofilm development. J Bacteriol 188: 2325–2335.
26. Takamatsu D, Bensing BA, Cheng H, Jarvis GA, Siboo IR, et al. (2005) Binding of the*Streptococcus gordonii* surface glycoproteins GspB and Hsa to specific carbohydrate structures on platelet membrane glycoprotein Ibalpha. Mol Microbiol 58: 380–392.
27. Siboo IR, Chambers HF, Sullam PM (2005) Role of SraP, a Serine-Rich Surface Protein of *Staphylococcus aureus*, in binding to human platelets. Infect Immun 73: 2273–2280.
28. Xiong YQ, Bensing BA, Bayer AS, Chambers HF, Sullam PM (2008) Role of the serine-rich surface glycoprotein GspB of *Streptococcus gordonii* in the pathogenesis of infective endocarditis. Microb Pathog 45: 297–301.
29. Samen U, Eikmanns BJ, Reinscheid DJ, Borges F (2007) The surface protein Srr-1 of*Streptococcus agalactiae* binds human keratin 4 and promotes adherence to epithelial HEp-2 cells. Infect Immun 75: 5405–5414.
30. van Sorge NM, Quach D, Gurney MA, Sullam PM, Nizet V, et al. (2009) The Group B Streptococcal serine-rich repeat 1 glycoprotein mediates penetration of the blood-brain barrier. J Infect Dis 199: 1479–1487.
31. Froeliger EH, Fives-Taylor P (2001) *Streptococcus parasanguis* fimbria-associated adhesin Fap1 is required for biofilm formation. Infect Immun 69: 2512–2519.
32. Handley PS, Correia FF, Russell K, Rosan B, DiRienzo JM (2005) Association of a novel high molecular weight, serine-rich protein (SrpA) with fibril-mediated adhesion of the oral biofilm bacterium *Streptococcus cristatus*. Oral Microbiol Immunol 20: 131–140.
33. Konto-Ghiorghi Y, Mairey E, Mallet A, Dumenil G, Caliot E, et al. (2009) Dual role for pilus in adherence to epithelial cells and biofilm formation in *Streptococcus agalactiae*. PLoS Pathog 5: e1000422.
34. Manetti AG, Zingaretti C, Falugi F, Capo S, Bombaci M, et al. (2007) *Streptococcus*

pyogenes pili promote pharyngeal cell adhesion and biofilm formation. Mol Microbiol 64: 968–983.
35. Helaine S, Carbonnelle E, Prouvensier L, Beretti JL, Nassif X, et al. (2005) PilX, a pilus-associated protein essential for bacterial aggregation, is a key to pilus-facilitated attachment of *Neisseria meningitidis* to human cells. Mol Microbiol 55: 65–77.
36. Munoz-Elias EJ, Marcano J, Camilli A (2008) Isolation of *Streptococcus pneumoniae*biofilm mutants and their characterization during nasopharyngeal colonization. Infect Immun 76: 5049–5061.
37. Parker D, Soong G, Planet P, Brower J, Ratner AJ, et al. (2009) The NanA neuraminidase of *Streptococcus pneumoniae* is involved in biofilm formation. Infect Immun 77: 3722–3730.
38. Trappetti C, Kadioglu A, Carter M, Hayre J, Iannelli F, et al. (2009) Sialic acid: a preventable signal for pneumococcal biofilm formation, colonization, and invasion of the host. J Infect Dis 199: 1497–1505.
39. Soong G, Muir A, Gomez MI, Waks J, Reddy B, et al. (2006) Bacterial neuraminidase facilitates mucosal infection by participating in biofilm production. J Clin Invest 116: 2297–2305.
40. Oggioni MR, Trappetti C, Kadioglu A, Cassone M, Iannelli F, et al. (2006) Switch from planktonic to sessile life: a major event in pneumococcal pathogenesis. Mol Microbiol 61: 1196–1210.
41. Aspiras MB, Ellen RP, Cvitkovitch DG (2004) ComX activity of *Streptococcus mutans*growing in biofilms. FEMS Microbiol Lett 238: 167–174.
42. Allegrucci M, Sauer K (2007) Characterization of colony morphology variants isolated from *Streptococcus pneumoniae* biofilms. J Bacteriol 189: 2030–2038.
43. Moscoso M, Garcia E, Lopez R (2006) Biofilm formation by *Streptococcus pneumoniae*: Role of choline, extracellular DNA, and capsular polysaccharide in microbial accretion. J Bacteriol 188: 7785–7795.
44. Orihuela CJ, Radin JN, Sublett JE, Gao G, Kaushal D, et al. (2004) Microarray analysis of pneumococcal gene expression during invasive disease. Infect Immun 72: 5582–5596.
45. Wu H, Zeng M, Fives-Taylor P (2007) The glycan moieties and the N-terminal polypeptide backbone of a fimbria-associated adhesin, Fap1, play distinct roles in the biofilm development of *Streptococcus parasanguinis*. Infect Immun 75: 2181–2188.
46. Stephenson AE, Wu H, Novak J, Tomana M, Mintz K, et al. (2002) The Fap1 fimbrial adhesin is a glycoprotein: Antibodies specific for the glycan moiety block the adhesion of *Streptococcus parasanguis* in an *in vitro* tooth model. Mol Microbiol 43: 147–157.
47. Zhou M, Wu H (2009) Glycosylation and biogenesis of a family of serine-rich bacterial adhesins. Microbiology 155: 317–327.
48. Mann B, Orihuela C, Antikainen J, Gao G, Sublett J, et al. (2006) Multifunctional role of Choline binding protein G in pneumococcal pathogenesis. Infect Immun 74: 821–829.
49. Sheldon H, Zetterquist H (1955) Internal ultrastructure in granules of white blood cells of the mouse; a preliminary note. Bull Johns Hopkins Hosp 96: 135–139.
50. Izano EA, Amarante MA, Kher WB, Kaplan JB (2008) Differential roles of poly-*N*-acetylglucosamine surface polysaccharide and extracellular DNA in *Staphylococcus aureus* and *Staphylococcus epidermidis* biofilms. Appl Environ Microbiol 74: 470–476.
51. Loo CY, Corliss DA, Ganeshkumar N (2000) *Streptococcus gordonii* biofilm formation:

identification of genes that code for biofilm phenotypes. J Bacteriol 182: 1374–1382.
52. Heydorn A, Nielsen AT, Hentzer M, Sternberg C, Givskov M, et al. (2000) Quantification of biofilm structures by the novel computer program COMSTAT. Microbiology 146 (Pt 10): 2395–2407.
53. Takamatsu D, Bensing BA, Prakobphol A, Fisher SJ, Sullam PM (2006) Binding of the Streptococcal surface glycoproteins GspB and Hsa to human salivary proteins. Infect Immun 74: 1933–1940.
54. Ausubel FM, Brent R, Kingston RE, Moore DD, Seidman JG, et al., editors. (2008) Current Protocols in Molecular Biology. Hoboken, NJ: John Wiley & Sons, Inc.

Summarizing Discussion

Summarizing discussion

Acute otitis media (AOM) is one of the most frequent diseases in childhood. In developed countries 80% of all children suffer at least from one AOM episode before the age of three (1). Although AOM is self-limiting in the majority of the cases, there is a significant group of children suffering from recurrent acute otitis media (rAOM) or chronic otitis media with effusion (COME), which are both associated with significant morbidity.

Optimal treatment for rAOM and COME remains highly controversial. In order to understand the underlying mechanisms of OM disease, in particular the microbiology and immunology, and to support future treatment and prevention strategies, clinical and experimental studies are warranted. In this thesis a cohort of rAOM and COME patients was described, and the microbial profile in the middle ear and nasopharynx was investigated. In addition, the association between inflammation and bacterial load in the middle ear was demonstrated, as well as the humoral immune response to a selection of *Moraxella catarrhalis* and *Streptococcus pneumoniae* antigens. We demonstrated an increased serum resistance of non-typeable *Haemophilus influenzae* (NTHi) isolates in middle ear fluid. Furthermore, using a novel murine model of AOM infection, several pneumococcal proteins were investigated as to their contribution to OM pathogenesis, their protective potential against pneumococcal disease and their role in bacterial aggregation and biofilm formation.

Clinical microbiology

Bacteria, viruses and OM

We investigated whether the microbial profiling was useful to differentiate between rAOM and COME patients (**Chapter 2**). Children up to 5 years of age, suffering from rAOM or COME and scheduled for tympanostomy tube insertion were enrolled in a retrospective study between 2008 and 2009. Our results showed that the same pathogenic bacterial species and viruses are implicated in the pathogenesis of both rAOM and COME disease. In line with recent studies (2,3) these findings do not support the classical assumption that the microbial profile is pathognomic for either rAOM or COME, or that COME is merely a consequence of persistent sterile inflammation in the middle ear.

In children with rAOM and COME, *H. influenzae* and rhinovirus are the predominant pathogens in middle ear and nasopharynx (**Chapter 2**). Analysis of the middle ear fluid using bacterial culture typically revealed the presence of one predominant bacterial species per sample, i.e. in 98% of the middle ear fluids one bacterial species was detected. With the use of bacterial culture *S. pneumoniae*, *H. influenzae* and *M. catarrhalis* were detected in respectively 4%, 20% and 8% of the middle ear fluids. Bacterial PCR is a more sensitive method to detect (multiple) bacteria compared to detection by bacterial culture: *S. pneumoniae*, *H. influenzae* and *M. catarrhalis* were found in respectively 7%, 34% and 25% of the middle ear fluids. Co-infections in the middle ear were scarce: 14% of the children had multiple bacterial species in the middle ear based on PCR-analysis. In bacterial culture negative specimens *S. pneumoniae* was detected in 4.1% (NS), *H. influenzae* in 16.5% ($P<0.01$) and *M. catarrhalis* in 19% ($P<0.01$). Thus, in particular detection of *M. catarrhalis* increases with the use of PCR compared to culture.

S. pneumoniae, *H. influenzae* and *M. catarrhalis* isolates that were detected in the middle ear fluids of our cohorts were in the great majority genetically identical (80-100%) to those isolates cultured from the nasopharynx, as determined by multi-locus sequence typing (4,5) as the genotypes of the bacteria cultured from the middle ear comprised a heterogeneous population structure, even though they all originated from a relatively restricted geographical region of the Netherlands. Kaur et al. have investigated 165 NTHi isolates but were unable to identify predominant MLST-types among strains colonizing the nasopharynx versus those causing OM. They suggested that the progression from asymptomatic colonization to OM may not be dependent on the strain of NTHi but rather on quantitative or qualitative differences in the immune defense of the child. In addition,

other factors such as differential expression of specific adhesins might be also involved (5). Which bacterial factors contribute to the migration from nasopharynx to middle ear remains largely to be investigated.

Clinical immunology

Innate immune response and rAOM, COME

To further explore the contribution of bacteria and viruses to OM, we investigated the association of cytokine responses and the presence of bacteria and viruses in the middle ear of children with recurrent and chronic OM (**Chapter 3**). We demonstrated that bacterial detection was associated with significantly elevated levels of cytokines compared to MEF without bacteria in a bacterial load- and species-dependent manner. Cytokine responses for IL-1b, IL-6, IL-8 and IL-10 were significantly higher in MEFs positive for *H. influenzae* compared with MEFs positive for *M. catarrhalis*. OM caused by *M. catarrhalis* is generally believed to be mild in comparison with OM induced by other bacterial pathogens. OM caused by *M. catarrhalis* is characterized by a higher proportion of mixed infections, younger age at diagnosis, a lower proportion of spontaneous perforation of the tympanic membrane, and no mastoiditis (6). These results are supported by the current data.

The clinical implications for viruses such as rhinovirus are still of debate. In respectively 19% and 27% of the MEFs collected in our retrospective cohort study, no pathogens or only viral pathogens were detected. The presence of virus in MEFs was not associated with an increase in cytokine levels compared to MEFs without pathogens. Additionally, no significant changes were observed between samples containing only bacteria versus MEFs containing both bacteria and viruses, suggesting a more indirect role for viral infections.

Rhinovirus has been shown to play an important role in lower respiratory tract pathology, where it can provoke exacerbations of cystic fibrosis, asthma and COPD (7-10). Various factors might play a role, such as viruses triggering exacerbations by enhancing already existing inflammation in the lower airways. The mechanisms are not fully defined, but growing evidence supports the concept that viral modulation of epithelial function may initiate the inflammatory response (11). In that case, the role of rhinovirus is different in lower respiratory tract pathology compared to upper respiratory tract pathology (**Chapter 3**) (12). Another mechanism by which rhinoviruses can induce inflammation in lower respiratory tract infections is during co-infection with bacterial pathogens, through the liberation of planktonic bacteria from biofilms (8). Whether rhinovirus is involved in the liberation of planktonic bacteria from biofilms in the middle ear remains to be elucidated.

Importantly, in patients with only viral pathogens detected in their middle fluid and in patients without bacterial or viral pathogens in their middle ear fluid, cytokine responses

were relatively low and subsequent destructive effects such as sensorineural hearing loss and bone erosion as induced by e.g. IL-1β is expected to be limited (13-16). This raises the question whether it is valid to discriminate recurrent and chronic OM patients based on the detection of pathogens and/or cytokine profile as detected in MEF in order to guide treatment rather than based on their clinical presentation. Further research is required to optimize diagnostic measurements and treatment in order to accommodate the patients at risk for complications.

Humoral immune response and serum resistance

Chapter 4 describes the humoral immune response in middle ear fluids and serum to *M. catarrhalis* and *S. pneumoniae* surface antigens in children suffering from rAOM and COME, using Luminex xMAP technology. Similar to other studies (17), the levels of antigen-specific IgG, IgA and IgM showed extensive inter-individual variation, and no significant differences were found between the rAOM and COME cohort. A strong correlation between antigen-specific serum IgG and MEF IgG-levels per child was observed. It is still under debate whether antibodies are (in part) produced locally (18,19) or primarily transude from blood to the middle ear cavity (5,20). Based on the strong correlation between antigen-specific serum IgG and MEF IgG, our results support the latter.

Consistent with other studies (21,22), we did not find a correlation between the presence of protein-specific antibodies in serum and protection from nasopharyngeal colonization. Prevaes and colleagues showed that in a cohort of children tested at 12 and 24 months of age, anti-pneumococcal antibodies increased and the anti-staphylococcal antibodies declined, corresponding with the natural dynamics of colonization (22). Results from murine models suggest a CD4-Th17 mediated immunity rather than antibody mediated immunity to be the primary mechanism of protection against pneumococcal colonization, although this still needs to be confirmed in humans (23,24). In addition, other bacterial and host factors possibly play a more significant role, such as bacterial evasion, co-infection of various bacterial species or viral-bacterial co-infection, Eustachian tube dysfunction or genetic susceptibility.

The pathogenesis of many microorganisms relies on their capacity to avoid, resist, or neutralize the host defense, including the complement system. Therefore, many pathogens have evolved mechanisms to avoid complement-mediated killing (25). Recently, it was shown that NTHi isolates from the lower respiratory tract exhibit increased complement resistance compared to colonizing strains (26). Similarly, we provide strong evidence that NTHi OM isolates displayed increased serum resistance to complement-mediated killing

compared to isolates collected from the nasopharynx (**Chapter 5**). This decreased susceptibility correlated with decreased binding of IgM to the bacterium, which incited us to investigate the mechanisms underlying serum resistance. Deletion of this R2866_0112 gene decreased complement resistance, which coincided with an increased IgM binding. Expression of the R2866_0112 gene was increased in serum resistant NTHi isolates, which encoded a novel LOS biosynthesis gene.

Bacterial evasion of the immune system by NTHi is feasible due to various aspects of LOS: (i) LOS is very heterogeneous and contains a number of phase varying epitopes (ii) LOS can mimic human blood group antigens, the pk antigen and paragloboside and (iii) LOS sialylation in *H. influenzae* has been shown to affect its ability to evade the lytic effects of human serum. Although the LOS structure is very heterogeneous, the existence of bactericidal IgM to NTHi-LOS makes it worthwhile to pursue LOS as a vaccine target in the prevention of otitis media. Previous studies already suggested to use detoxified LOS as a vaccine component to prevent OM caused by NTHi (27-29). A detoxified NTHi LOS protein conjugate vaccine showed protection in a chinchilla and mouse model for OM (27,29). In these mice, there was an inverse correlation between the IgG/IgM antibody levels in MEF and the NTHi bacterial load in the middle ear (29). Importantly, another study performed by Gergova *et. al.* showed that an IgM monoclonal antibody raised against *M. catarrhalis* LOS cross-reacted with NTHi LOS (30). This suggests that in the development of a LOS-based vaccine against *M. catarrhalis*, immunization could result in immune response to epitopes conserved in other important respiratory pathogens, such as NTHi (30).

Microbial pathogenesis

Development of a murine model for OM infection

One of the limitations of the current experimental models used to study the bacterial pathogenesis of OM is the invasiveness of the experimental procedures. In most animal models, AOM is induced by direct inoculation of live bacteria into the middle ear cavity, either via a transtympanic or transbullar route (31,32). In order to investigate pneumococcal AOM pathogenesis in a non-invasive experimental setting, we developed a murine model for AOM infection (**Chapter 6**). With the use of a pressure cabin we were able to develop a highly reproducible and non-invasive murine infection method. In our model, pressure is applied to translocate pneumococci from the nasopharygeal cavity into both mouse middle ears. Wild-type pneumococci were found to persist in the middle ear cavity up to six days after infection. Inflammation was confirmed by IL-1β and TNF-α cytokine analysis and histopathology.

The use of a pressure cabin is an improvement over the experimental AOM models currently used for various reasons. First, pressure elevation facilitates the ascending infection of pneumococci from the nasopharynx to the middle ear cavity and thus resembles the natural route of infection in humans. Second, an inflammatory response due to local manipulation is avoided (33). Third, the percentage of successful infections is 100%. This is of importance, since a 100% successful infection is warranted to monitor the efficiency of a vaccine, i.e. the reduction of bacterial load. This is in contrast to intranasal inoculation, where bacterial colonization occurs in the nasopharynx, which is followed by 'spontaneous' invasion of the middle ear cavity by the pathogen in about 50% of the cases (31).

Recently, Short and colleagues also developed a non-invasive model of *S. pneumoniae* induced OM (34). Infant mice co-infected with *S. pneumoniae* and influenza A virus had a high bacterial load in the middle ear, middle ear inflammation and hearing loss. Due to viral-bacterial co-infection OM occurred spontaneously in almost all cases. Since viral infections may skew the immune system, both models are of interest to study bacterial pathogenesis and the host immune response.

NTHi is unable to cause AOM in mice, as this bacterial pathogen is cleared rapidly from the murine middle ear cavity. In parallel to co-infection of the nasopharynx with *S. pneumoniae* and influenza A virus, we developed an experimental model to investigate NTHi induced OM (**Chapter 5**). Mice were inoculated with influenza A virus or mock treated three days before intranasal infection with NTHi. Infection with influenza A virus signifi-

cantly increased the number of NTHi bacteria in the nasopharynx and middle ears, which resulted in 100% OM.

Identification of novel pneumococcal virulence factors in AOM

Bacterial surface-exposed proteins often play an important role in the interaction between pathogens and their host. Identification of novel surface-exposed proteins that play an important role in virulence can improve our understanding of OM pathogenesis and will facilitate new preventive strategies such as vaccine development. Virulence studies described in literature have shown that most pneumococcal mutants display attenuated phenotypes in either colonization, pneumonia, or sepsis mouse models, thus indicating niche-specific involvement in virulence of the respective genes (35-42).

We explored our AOM pressure cabin model to examine the contribution of two surface-associated pneumococcal proteins to otitis media: the streptococcal lipoprotein rotamase A (SlrA) and the putative proteinase maturation protein A (PpmA) (**Chapter 6**). Both proteins have the potential to elicit protective immune responses (43,44). Previous research has shown a pivotal role of SlrA in adherence, colonization and immune evasion (39). PpmA is a conserved protein involved in invasive disease and colonization of the nasopharyngeal cavity. Nevertheless, the exact function of this protein is still unknown (44,45).

We investigated the contribution of SlrA and PpmA to experimental OM in our model. Pneumococci lacking the gene encoding SlrA, but not PpmA, were significantly reduced in virulence in the otitis media model. Importantly, pneumococci lacking both genes were significantly more attenuated than the Δ*slrA* single mutant. This additive effect suggests that SlrA and PpmA exert complementary functions during experimental OM. As described by Audouy *et. al.*, intranasal immunization in mice with SlrA-IgA1p or SlrA-IgA1p-PpmA showed significant protection against fatal pneumonia in mice (46). Whether the SlrA protein has potential as a vaccine candidate directed against OM infection remains to be elucidated. We showed that our model is valuable to study OM induced by *S. pneumoniae* and to study OM related virulence.

The genomic array footprinting (GAF) technology is developed to screen for potential vaccine targets (47). GAF is a mutant library-based negative selection screen that uses microarrays to identify the virulence essential genes. Using the GAF technology, two pneumococcal proteins SP1298 and 2205, were consistently identified in mouse models of nasopharyngeal colonization, bacteremia and meningitis to be crucial for bacterial survival *in vivo*. SP1298 and 2205 are two conserved proteins of unknown function, classified as DHH subfamily 1 proteins. We examined the contribution of SP1298 and 2205 to pneu-

mococcal virulence in nasopharyngeal colonization, OM, pneumonia and bacteremia with various pneumococcal strains (**Chapter 7**). The OM mouse model showed that bacterial loads in the middle ears of mice infected with the mutants were reduced compared to wild-type-infected mice, with a significant reduction in bacterial load upon deletion of both genes at all time-points post infection. In co-infection experiments, both wild-types outcompeted their respective single and double SP1298 and 2205 mutants in the middle ear.

Site-specific variances were observed, i.e. the SP2205 mutant was attenuated in the nasopharynx and middle ears of mice, in contrast to the lungs and blood of mice, where the SP2205 mutant was as virulent as the wild-type. Importantly, in all four models an apparent additive effect was shown upon deletion of both genes.

As OM episodes are usually preceded by nasopharyngeal colonization, DHH proteins have potential as vaccine candidates also directed against OM infection. We showed that subcutaneous vaccination with (the recombinant forms of) SP1298 and 2205 conferred protection to pneumococcal disease in mice, including nasopharyngeal colonization, pneumonia and bacteremia. Thus, these proteins play a significant role at several stages of pneumococcal infection and are potential candidates for a multi-component protein vaccine.

Research is currently ongoing to determine the cellular localization during pathogenesis and biochemical function. Western blot analysis and 3D prediction modeling revealed that the SP1298 mutant is directly or indirectly involved in oxidative stress tolerance. Based on homology with proteins from other bacteria is 3'(2')-phosphoadenosine-5'-phosphate (pAp) activity a possible explanation for impaired growth of the SP1298 deletion mutant.

OM and biofilm formation

Serine-rich repeat proteins (SRRPs) are a family of surface-expressed proteins found in numerous Gram-positive pathogens, including *Staphylococcus aureus*, *S. pneumoniae*, Group B streptococci and oral streptococci. We described a novel role for the pneumococcal serine-rich repeat protein (PsrP), the SRRP of *S. pneumoniae* as an intra-bacterial adhesin that promotes bacterial aggregation during colonization and pneumonia in mice (**Chapter 8**). *In vitro* we showed that the basic region domain of PsrP promotes self-interactions that result in denser biofilms, greater biofilm biomass, and altered architectures of surface grown cultures; these interactions could be neutralized by antibodies to PsrP that are protective against pneumococcal infection. Thus, PsrP has a dual role as host-cell and intra-bacterial adhesin.

The exact role of PsrP in OM is under current investigation. Animals challenged with *S. pneumoniae* T4Δ*psrP* had a higher bacterial load and elevated levels of IL-1β, IL-6 and

TNFα versus TIGR4 infected controls. A similar finding has been described for NTHi *luxS* mutants (48,49). They found that LuxS promotes biofilm maturation and persistence of NTHi *in vivo*. Bacterial counts within middle-ear fluids and the severity of the host inflammatory response were increased in *luxS* mutants as compared with parental strains.

Although it is generally considered that over half of all bacterial infections are biofilm related (50), studies concerning virulence factors involved in biofilm formation related to OM are scarce. Experimental studies primarily use a chinchilla model of infection and found an association between biofilm formation and the pneumococcal virulence factors PcpA, PspA and PspC, all choline binding proteins (51). Bacterial factors important to NTHi biofilms include lipooligosaccharide (LOS), pili and double-stranded DNA (52). For future research on virulence factors potentially related to biofilm formation, the rat OM model for biofilm formation of Chaney et al. might be of additional value (53). Similar to our mouse model, a pressure cabin was used to translocate pneumococci from the nasopharynx to the middle ear. Whereas we used an acute OM model with singly infected mice, these authors repeatedly inoculated the rats every four to seven days, for up to seven months. Animals were sacrificed at various time points to monitor biofilm formation in the middle ear (53).

Concluding remarks

Taken together, the data described in this thesis showed that in children with recurrent or chronic OM, non-typeable *H. influenzae* and rhinovirus are the predominant pathogens in the middle ear and nasopharynx. MLST analysis showed that the micro-organisms from the nasopharynx and the middle ear per child are mostly genetically identical. Based on microbial profiling of the nasopharynx and middle ear fluid, no difference can be made between rAOM and COME diagnosis. We demonstrated that the cytokine response in the middle ear of these patients was associated with the presence of bacteria, but not viruses. In addition, we showed that non-typeable *H. influenzae* isolates obtained from the middle ear exhibit increased complement resistance and that the lipooligosaccharide (LOS) structure determines IgM binding and complement activation. In experimental studies, we provided insight into the role of several pneumococcal virulence factors in the molecular pathogenesis of *S. pneumoniae* induced OM.

There are a few limitations of the clinical studies described in this thesis. I will highlight the most important ones. First, the sample size is relatively small ($n=176$ patients) with patients enrolled in a limited region in the Netherlands. Second, the human immune system is a complex system which cannot be simulated *in vitro*. In order to test virulence factors and vaccine candidates the immune response, animal models, in our case mouse models, are an inevitable stepping stone towards understanding and unraveling the human immune response. Obviously, mice are not men and results can never fully be extrapolated to the human situation.

Future perspectives

Vaccine Development

Considerable data indicate that OM can be prevented by immunization (54-56). Vaccines effective in preventing acute OM will most likely have a large impact on the entire spectrum of middle ear disease, including rAOM and COME, since these entities arise from early AOM (57). To vaccinate only those children who already developed recurrent and chronic disease is unlikely to be effective, in particular because herd immunity will not be established (58,59).

There are several requirements for an effective vaccine: it should be save and protective in the target population, and it should elicit sustained protection, induce neutralizing antibodies and trigger protective T-cells. In addition there are practical considerations such as low costs, biological stability, ease of administration and limited side effects (60). Potential vaccine antigens should be non-toxic, conserved among strains and expressed *in vivo* without cross-reactivity. Furthermore, vaccine antigens should not be homologous to human factors. The ideal vaccine to prevent OM would cover the 3 bacterial pathogens: *S. pneumoniae* (59), *H. influenzae* (57) and *M. catarrhalis* (61). Vaccines with greater coverage based on proteins common to all serotypes, or addition of protein-based vaccines to the current PCV will be needed in the future (59).

In contrast to invasive diseases, such as pneumonia, meningitis and sepsis, otitis media typically affects the mucosa. It is therefore important to understand how middle ear pathogens stimulate the mucosal immunity in order to develop effective vaccines. There are various obstacles to overcome in vaccine development for mucosal diseases, i.e. the lack of appropriate correlates of protection for mucosal disease. The use of bactericidal assays, opsonophagocytotic killing assays and reduction of bacterial load in experimental models are explored, however, thus far a direct correlation between immune response and bacterial clearance in the middle ear has not been found.

References

1. Daly KA, Hoffman HJ, Kvaerner KJ, et al. Epidemiology, natural history, and risk factors: panel report from the Ninth International Research Conference on Otitis Media. International journal of pediatric otorhinolaryngology 2010; 74(3): 231-40.
2. Brake MK, Jewer K, Flowerdew G, Cavanagh JP, Cron C, Hong P. Tympanocentesis results of a Canadian pediatric myringotomy population, 2008 to 2010. Journal of otolaryngology - head & neck surgery = Le Journal d'oto-rhino-laryngologie et de chirurgie cervico-faciale 2012; 41(4): 282-7.
3. Wiertsema SP, Kirkham LA, Corscadden KJ, et al. Predominance of nontypeable *Haemophilus influenzae* in children with otitis media following introduction of a 3+0 pneumococcal conjugate vaccine schedule. Vaccine 2011; 29(32): 5163-70.
4. Kaur R, Kim T, Casey JR, Pichichero ME. Antibody in middle ear fluid of children originates predominantly from sera and nasopharyngeal secretions. Clinical and vaccine immunology : CVI 2012; 19(10): 1593-6.
5. Schumacher SK, Marchant CD, Loughlin AM, Bouchet V, Stevenson A, Pelton SI. Prevalence and genetic diversity of nontypeable *Haemophilus influenzae* in the respiratory tract of infants and primary caregivers. The Pediatric infectious disease journal 2012; 31(2): 145-9.
6. Broides A, Dagan R, Greenberg D, Givon-Lavi N, Leibovitz E. Acute otitis media caused by *Moraxella catarrhalis*: epidemiologic and clinical characteristics. Clinical infectious diseases : an official publication of the Infectious Diseases Society of America 2009; 49(11): 1641-7.
7. Chantzi FM, Papadopoulos NG, Bairamis T, et al. Human rhinoviruses in otitis media with effusion. Pediatric allergy and immunology : official publication of the European Society of Pediatric Allergy and Immunology 2006; 17(7): 514-8.
8. Chattoraj SS, Ganesan S, Jones AM, et al. Rhinovirus infection liberates planktonic bacteria from biofilm and increases chemokine responses in cystic fibrosis airway epithelial cells. Thorax 2011; 66(4): 333-9.
9. Message SD, Laza-Stanca V, Mallia P, et al. Rhinovirus-induced lower respiratory illness is increased in asthma and related to virus load and Th1/2 cytokine and IL-10 production. Proceedings of the National Academy of Sciences of the United States of America 2008; 105(36): 13562-7.
10. Oliver BG, Lim S, Wark P, et al. Rhinovirus exposure impairs immune responses to bacterial products in human alveolar macrophages. Thorax 2008; 63(6): 519-25.
11. Proud D. Upper airway viral infections. Pulmonary pharmacology & therapeutics 2008; 21(3): 468-73.
12. Skovbjerg S, Roos K, Nowrouzian F, et al. High cytokine levels in perforated acute otitis media exudates containing live bacteria. Clinical microbiology and infection : the official publication of the European Society of Clinical Microbiology and Infectious Diseases 2010; 16(9): 1382-8.
13. Maeda K, Hirano T, Ichimiya I, Kurono Y, Suzuki M, Mogi G. Cytokine expression in

experimental chronic otitis media with effusion in mice. The Laryngoscope 2004; 114(11): 1967-72.
14. Scharer G, Zaldivar F, Gonzalez G, Vargas-Shiraishi O, Singh J, Arrieta A. Systemic inflammatory responses in children with acute otitis media due to *Streptococcus pneumoniae* and the impact of treatment with clarithromycin. Clinical and diagnostic laboratory immunology 2003; 10(4): 721-4.
15. Skotnicka B, Hassmann E. Proinflammatory and immunoregulatory cytokines in the middle ear effusions. International journal of pediatric otorhinolaryngology 2008; 72(1): 13-7.
16. Willett DN, Rezaee RP, Billy JM, Tighe MB, DeMaria TF. Relationship of endotoxin to tumor necrosis factor-alpha and interleukin-1 beta in children with otitis media with effusion. The Annals of otology, rhinology, and laryngology 1998; 107(1): 28-33.
17. Pichichero ME, Kaur R, Casey JR, Xu Q, Almudevar A, Ochs M. Antibody response to *Streptococcus pneumoniae* proteins PhtD, LytB, PcpA, PhtE and Ply after nasopharyngeal colonization and acute otitis media in children. Human vaccines & immunotherapeutics 2012; 8(6): 799-805.
18. Faden H, Brodsky L, Bernstein J, et al. Otitis media in children: local immune response to nontypeable *Haemophilus influenzae*. Infection and immunity 1989; 57(11): 3555-9.
19. Faden HS. Immunology of the middle ear: role of local and systemic antibodies in clearance of viruses and bacteria. Annals of the New York Academy of Sciences 1997; 830: 49-60.
20. Bakaletz LO, Holmes KA. Evidence for transudation of specific antibody into the middle ears of parenterally immunized chinchillas after an upper respiratory tract infection with adenovirus. Clinical and diagnostic laboratory immunology 1997; 4(2): 223-5.
21. Lebon A, Verkaik NJ, Labout JA, et al. Natural antibodies against several pneumococcal virulence proteins in children during the pre-pneumococcal-vaccine era: the generation R study. Infection and immunity 2011; 79(4): 1680-7.
22. Prevaes SM, van Wamel WJ, de Vogel CP, et al. Nasopharyngeal colonization elicits antibody responses to staphylococcal and pneumococcal proteins that are not associated with a reduced risk of subsequent carriage. Infection and immunity 2012; 80(6): 2186-93.
23. Bogaert D, Weinberger D, Thompson C, Lipsitch M, Malley R. Impaired innate and adaptive immunity to *Streptococcus pneumoniae* and its effect on colonization in an infant mouse model. Infection and immunity 2009; 77(4): 1613-22.
24. Lu YJ, Gross J, Bogaert D, et al. Interleukin-17A mediates acquired immunity to pneumococcal colonization. PLoS pathogens 2008; 4(9): e1000159.
25. Hallstrom T, Resman F, Ristovski M, Riesbeck K. Binding of complement regulators to invasive nontypeable *Haemophilus influenzae* isolates is not increased compared to nasopharyngeal isolates, but serum resistance is linked to disease severity. Journal of clinical microbiology 2010; 48(3): 921-7.
26. Nakamura S, Shchepetov M, Dalia AB, et al. Molecular basis of increased serum resistance among pulmonary isolates of non-typeable *Haemophilus influenzae*. PLoS pathogens 2011; 7(1): e1001247.
27. Gu XX, Sun J, Jin S, et al. Detoxified lipooligosaccharide from nontypeable *Haemophilus influenzae* conjugated to proteins confers protection against otitis media in chinchillas. Infection and immunity 1997; 65(11): 4488-93.
28. Hong W, Peng D, Rivera M, Gu XX. Protection against nontypeable Haemophilus influen-

zae challenges by mucosal vaccination with a detoxified lipooligosaccharide conjugate in two chinchilla models. Microbes and infection / Institut Pasteur 2010; 12(1): 11-8.
29. Sun J, Chen J, Cheng Z, Robbins JB, Battey JF, Gu XX. Biological activities of antibodies elicited by lipooligosaccharide based-conjugate vaccines of nontypeable Haemophilus influenzae in an otitis media model. Vaccine 2000; 18(13): 1264-72.
30. Gergova RT, Iankov ID, Haralambieva IH, Mitov IG. Bactericidal monoclonal antibody against Moraxella catarrhalis lipooligosaccharide cross-reacts with Haemophilus Spp. Current microbiology 2007; 54(2): 85-90.
31. Ryan AF, Ebmeyer J, Furukawa M, et al. Mouse models of induced otitis media. Brain research 2006; 1091(1): 3-8.
32. Sabirov A, Metzger DW. Intranasal vaccination of neonatal mice with polysaccharide conjugate vaccine for protection against pneumococcal otitis media. Vaccine 2006; 24(27-28): 5584-92.
33. MacArthur CJ, Hefeneider SH, Kempton JB, Parrish SK, McCoy SL, Trune DR. Evaluation of the mouse model for acute otitis media. Hearing research 2006; 219(1-2): 12-23.
34. Short KR, Diavatopoulos DA, Thornton R, et al. Influenza virus induces bacterial and non-bacterial otitis media. The Journal of infectious diseases 2011; 204(12): 1857-65.
35. Chen H, Ma Y, Yang J, et al. Genetic requirement for pneumococcal ear infection. PloS one 2008; 3(8): e2950.
36. Cripps AW, Otczyk DC, Kyd JM. Bacterial otitis media: a vaccine preventable disease? Vaccine 2005; 23(17-18): 2304-10.
37. Hava DL, Camilli A. Large-scale identification of serotype 4 Streptococcus pneumoniae virulence factors. Molecular microbiology 2002; 45(5): 1389-406.
38. Hendriksen WT, Bootsma HJ, Estevao S, et al. CodY of *Streptococcus pneumoniae*: link between nutritional gene regulation and colonization. Journal of bacteriology 2008; 190(2): 590-601.
39. Hermans PW, Adrian PV, Albert C, et al. The streptococcal lipoprotein rotamase A (SlrA) is a functional peptidyl-prolyl isomerase involved in pneumococcal colonization. The Journal of biological chemistry 2006; 281(2): 968-76.
40. Ogunniyi AD, LeMessurier KS, Graham RM, et al. Contributions of pneumolysin, pneumococcal surface protein A (PspA), and PspC to pathogenicity of Streptococcus pneumoniae D39 in a mouse model. Infection and immunity 2007; 75(4): 1843-51.
41. Tong HH, Long JP, Li D, DeMaria TF. Alteration of gene expression in human middle ear epithelial cells induced by influenza A virus and its implication for the pathogenesis of otitis media. Microbial pathogenesis 2004; 37(4): 193-204.
42. Tuomanen EI. Pathogenesis of pneumococcal inflammation: otitis media. Vaccine 2000; 19 Suppl 1: S38-40.
43. Adrian PV, Bogaert D, Oprins M, et al. Development of antibodies against pneumococcal proteins alpha-enolase, immunoglobulin A1 protease, streptococcal lipoprotein rotamase A, and putative proteinase maturation protein A in relation to pneumococcal carriage and Otitis Media. Vaccine 2004; 22(21-22): 2737-42.
44. Overweg K, Kerr A, Sluijter M, et al. The putative proteinase maturation protein A of *Streptococcus pneumoniae* is a conserved surface protein with potential to elicit protective immune responses. Infection and immunity 2000; 68(7): 4180-8.
45. Cron LE, Bootsma HJ, Noske N, Burghout P, Hammerschmidt S, Hermans PW. Surface-

associated lipoprotein PpmA of *Streptococcus pneumoniae* is involved in colonization in a strain-specific manner. Microbiology (Reading, England) 2009; 155(Pt 7): 2401-10.
46. Audouy SA, van Selm S, van Roosmalen ML, et al. Development of lactococcal GEM-based pneumococcal vaccines. Vaccine 2007; 25(13): 2497-506.
47. Bijlsma JJ, Burghout P, Kloosterman TG, et al. Development of genomic array footprinting for identification of conditionally essential genes in *Streptococcus pneumoniae*. Applied and environmental microbiology 2007; 73(5): 1514-24.
48. Armbruster CE, Hong W, Pang B, et al. LuxS promotes biofilm maturation and persistence of nontypeable *Haemophilus influenzae* in vivo via modulation of lipooligosaccharides on the bacterial surface. Infection and immunity 2009; 77(9): 4081-91.
49. Daines DA, Bothwell M, Furrer J, et al. *Haemophilus influenzae* luxS mutants form a biofilm and have increased virulence. Microbial pathogenesis 2005; 39(3): 87-96.
50. Munoz-Elias EJ, Marcano J, Camilli A. Isolation of *Streptococcus pneumoniae* biofilm mutants and their characterization during nasopharyngeal colonization. Infection and immunity 2008; 76(11): 5049-61.
51. Reid SD, Hong W, Dew KE, et al. *Streptococcus pneumoniae* forms surface-attached communities in the middle ear of experimentally infected chinchillas. The Journal of infectious diseases 2009; 199(6): 786-94.
52. Juneau RA, Pang B, Weimer KE, Armbruster CE, Swords WE. Nontypeable *Haemophilus influenzae* initiates formation of neutrophil extracellular traps. Infection and immunity 2011; 79(1): 431-8.
53. Chaney EJ, Nguyen CT, Boppart SA. Novel method for non-invasive induction of a middle-ear biofilm in the rat. Vaccine 2011; 29(8): 1628-33.
54. Magnus MC, Vestrheim DF, Nystad W, et al. Decline in early childhood respiratory tract infections in the norwegian mother and child cohort study after introduction of pneumococcal conjugate vaccination. The Pediatric infectious disease journal 2012; 31(9): 951-5.
55. Mawas F, Ho MM, Corbel MJ. Current progress with *Moraxella catarrhalis* antigens as vaccine candidates. Expert review of vaccines 2009; 8(1): 77-90.
56. Prymula R, Kriz P, Kaliskova E, Pascal T, Poolman J, Schuerman L. Effect of vaccination with pneumococcal capsular polysaccharides conjugated to *Haemophilus influenzae*-derived protein D on nasopharyngeal carriage of *Streptococcus pneumoniae* and *H. influenzae* in children under 2 years of age. Vaccine 2009; 28(1): 71-8.
57. Giebink GS. Vaccination against middle-ear bacterial and viral pathogens. Annals of the New York Academy of Sciences 1997; 830: 330-52.
58. Fitzwater SP, Chandran A, Santosham M, Johnson HL. The worldwide impact of the seven-valent pneumococcal conjugate vaccine. The Pediatric infectious disease journal 2012; 31(5): 501-8.
59. Rodgers GL, Klugman KP. The future of pneumococcal disease prevention. Vaccine 2011; 29 Suppl 3: C43-8.
60. Janeway CA, Travers P, M. W, Shlomchik MJ. Immunobiology: the immune system in health and disease. 6th edition ed. New York: Garland Science Publishing; 2005.
61. Murphy TF, Faden H, Bakaletz LO, et al. Nontypeable *Haemophilus influenzae* as a pathogen in children. The Pediatric infectious disease journal 2009; 28(1): 43-8.

Nederlandse samenvatting

Nederlandse samenvatting

Acute middenoorontsteking (acute otitis media, AOM) is één van de meest voorkomende kinderziekten. In westerse landen heeft 80% van alle kinderen voor het derde levensjaar tenminste 1 episode met AOM doorgemaakt (1). Hoewel AOM in het merendeel van de gevallen vanzelf geneest, is er een grote groep kinderen waarbij de ontsteking regelmatig terugkeert (recidiverende AOM, rAOM) of waarbij gedurende langere tijd vocht in het middenoor aanwezig is (chronische otitis media met effusie, COME). Deze vormen van middenoorontsteking (otitis media, OM) gaan gepaard met een aanzienlijke ziektelast.

Middenoorontstekingen komen frequent voor bij kinderen, desalniettemin is het niet duidelijk wat de beste behandeling is voor rAOM en COME. Het ontwikkelen van effectieve behandelingen vraagt om een grondige kennis van de microbiologische en immunologische aspecten van OM. Derhalve zijn klinische en experimentele studies nodig om deze aspecten van OM te doorgronden. Zo wordt een beter inzicht verworven in de wijze waarop OM ontstaat en kunnen op basis daarvan nieuwe therapeutische en preventieve strategieën ontwikkeld worden.

In dit proefschrift zijn een aantal studies beschreven in een cohort kinderen met rAOM of COME. Allereerst is de aanwezigheid onderzocht van bacteriën en virussen in het middenoor. Vervolgens is de relatie tussen de mate van ontsteking en de hoeveelheid bacteriën in het middenoor bestudeerd, alsook de humorale immuunrespons gericht tegen een aantal geselecteerde oppervlakte eiwitten van 2 bacteriën die veel voorkomen bij OM: *Moraxella catarrhalis* en *Streptococcus pneumoniae* (de pneumokok). Daarnaast is de rol van resistentie tegen componenten van het afweersysteem in relatie met de ongekapselde *Haemophilus influenzae* bacterie (NTHi; de derde veel voorkomende bacterie bij OM) onderzocht. Middels een experimentele studie, met een door ons ontwikkeld nieuw muizenmodel voor AOM, is de rol bestudeerd van verschillende pneumokokken serotypes en specifieke pneumokokkeneiwitten in de pathogenese van OM. Tenslotte hebben we gekeken naar de rol van één specifiek pneumokokkeneiwit in bacteriële aggregatie en het vormen van biofilms.

Medische Microbiologie

Bacteriën, virussen en OM

We hebben bestudeerd of er op basis van de aanwezigheid van specifieke bacteriën en virussen een (microbiologisch) onderscheid tussen rAOM en COME gemaakt kan worden (**Hoofdstuk 2**). Kinderen in de leeftijd van 0-5 jaar met rAOM of COME die middenoorbuisjes geplaatst kregen, werden na toestemming van ouders, geïncludeerd in de OMVac-studie in de periode 2008-2009. De resultaten laten zien dat dezelfde bacteriën en virussen betrokken zijn bij de pathogenese van rAOM en COME. Daarnaast vonden wij evenals in eerder onderzoek (2,3) dat de veronderstelling dat bepaalde bacteriën en virussen specifiek betrokken zijn bij ofwel rAOM ofwel COME onjuist is, evenals de hypothese dat COME een gevolg is van een continue steriele ontsteking van het middenoor.

H. influenzae en rhinovirus zijn de voornaamste micro-organismen in het middenoor en in de neus-keelholte van kinderen met rAOM en COME (**Hoofdstuk 2**). Analyse van de middenoorvloeistof door middel van bacteriële kweken toonde met name mono-infecties aan. In 98% van de kweken werd slechts 1 bacteriële soort in het middenoor gedetecteerd. *S. pneumoniae*, *H. influenzae* en *M. catarrhalis* werden gekweekt in respectievelijk 4%, 20% en 8% van de middenoorvloeistoffen.

De polymerase kettingreactie (PCR) is in vergelijking met bacteriële kweek een gevoeliger methode om (meerdere) bacteriën aan te tonen. *S. pneumoniae*, *H. influenzae* en *M. catarrhalis* werden gedetecteerd in respectievelijk 7%, 34% en 25% van de middenoorvloeistoffen. Menginfecties in het middenoor werden beperkt gevonden: 14% van de kinderen hadden op basis van PCR-analyse meerdere micro-organismen in het middenoor. In de kweek negatieve middenoorvloeistoffen werd door middel van PCR *S. pneumoniae* aangetoond in 4.1% (NS), *H. influenzae* in 16.5% ($P<0.01$) en *M. catarrhalis* in 19% ($P<0.01$). Vooral de detectie van *M. catarrhalis* stijgt dus significant met het gebruik van PCR ten opzichte van bacteriële kweek.

Met behulp van multilocus sequence typing (MLST) hebben we de genetische variatie onderzocht van bacteriën uit het middenoor en de neus-keelholte binnen één patiënt. Daarnaast bestudeerden we eveneens de genetische variatie van bacteriën uit het middenoor en de neus-keelholte tussen verschillende patiënten. In dit onderzoek vonden we dat *S. pneumoniae*, *H. influenzae* en *M. catarrhalis* isolaten in het middenoor in het merendeel van de gevallen (80-100%) genetisch identiek waren aan isolaten die gekweekt werden uit de neus-keelholte. Conform andere klinische studies (4,5) tonen we aan dat de bacteriële

genotypen bij de verschillende patiënten heterogeen zijn, ook al betreft het een patiëntenpopulatie uit een relatief beperkte regio in Nederland. Kaur et al. hebben 165 NTHi isolaten bestudeerd, maar zij waren niet in staat om een dominant MLST type te identificeren. Ook kon aan de hand van het MLST type geen onderscheid gemaakt worden tussen stammen die resulteren in dragerschap in de neus-keelholte, versus stammen die naast dragerschap in de neus-keelholte tevens OM veroorzaken. De auteurs suggereren dat de progressie van asymptomatische kolonisatie naar OM niet zozeer afhankelijk is van de NTHi stam zelf, maar meer van de kwantitatieve en kwalitatieve verschillen in het afweersysteem van het kind. Verder zouden andere factoren zoals de expressie van specifieke adhesines, ook een rol kunnen spelen (4). De bijdrage van bacteriële factoren aan de migratie van neus-keelholte naar middenoor is een nog braak liggend onderzoeksterrein.

Immunologie

rAOM, COME en de aangeboren immuunrespons

Om de rol van de aangeboren immuunrespons in de pathogenese van OM te onderzoeken hebben we de cytokine respons bestudeerd in relatie tot de aanwezigheid van bacteriën en/of virussen in het middenoor van kinderen met rAOM of COME (**Hoofdstuk 3**). We tonen in dit proefschrift aan dat de aanwezigheid van bacteriën geassocieerd is met significant verhoogde cytokine concentraties in vergelijking met middenoorvloeistoffen waarin geen bacteriën aanwezig waren. De hoogte van de cytokine respons was gerelateerd aan de aanwezigheid van de hoeveelheid bacteriën in het middenoor. Een significante correlatie werd aangetoond tussen de aanwezigheid van *H. influenzae* en de cytokines IL-1β, TNF-α, IL-6 en IL-8. Eenzelfde significante correlatie vonden we tussen *M. catarrhalis* en deze cytokines. Voor *S. pneumoniae* en de cytokine respons werd een gelijke trend gezien. Echter, door het kleine aantal middenoorvloeistoffen waarin *S. pneumoniae* werd gedetecteerd, was dit verschil niet significant. De cytokine responsen voor IL-1β, IL-6, IL-8 en IL-10 waren significant hoger in de middenoorvloeistoffen waarin *H. influenzae* aanwezig was, in vergelijking met middenoorvloeistoffen die positief waren voor *M. catarrhalis*. OM veroorzaakt door *M. catarrhalis* is over het algemeen geassocieerd met een hoger percentage menginfecties, een lager percentage van perforatie en het uitblijven van mastoïditis, een gevreesde complicatie van OM (6).

De klinische implicaties van OM veroorzaakt door virussen, zoals het rhinovirus, zijn nog steeds onderwerp van discussie. In respectievelijk 19% en 27% van de middenoorvloeistoffen in ons klinische cohort waren geen micro-organismen aantoonbaar of alleen virussen aanwezig. De aanwezigheid van virussen in middenoorvloeistof was niet geassocieerd met verhoogde cytokine concentraties in vergelijking met middenoorvloeistoffen waarin geen micro-organismen aanwezig waren. Ook werden er geen significante verschillen in cytokine concentraties gezien tussen middenoorvloeistoffen met alleen bacteriën versus middenoorvloeistoffen waarin zowel bacteriën als virussen aanwezig waren. Dit suggereert een indirecte rol voor virale infecties in de pathogenese van OM.

Rhinovirus speelt een belangrijke rol in lagere luchtweginfecties: het kan exacerbaties van taaislijmziekte, astma en COPD veroorzaken (7-10). Verschillende factoren spelen hierbij een rol, zoals de versterking van een reeds aanwezige ontstekingsreactie hetgeen door de aanwezigheid van virussen leidt tot een exacerbatie. Het mechanisme hierachter wordt niet volledig begrepen, maar er zijn in toenemende mate aanwijzingen dat modulatie

van de functie van het epitheel door virussen een ontstekingsreactie uitlokt (11). In dat geval verschilt de rol van rhinovirussen in lagere luchtweginfecties ten opzichte van bovenste luchtweginfecties zoals OM (**Hoofdstuk 3**) (12). Een ander mechanisme waarbij rhinovirussen ontsteking kunnen induceren is tijdens co-infectie met bacteriële pathogenen, door stimulatie van de loslating van bacteriën uit een biofilm (8). Of rhinovirus betrokken is bij het losmaken van bacteriën uit de biofilm die zich in het middenoor kan vormen, is nog onbekend.

Het is van belang te beseffen dat bij kinderen met alleen virussen en bij patiënten zonder bacteriën of virussen in de middenoorvloeistof de cytokine concentraties relatief laag zijn en eventuele complicaties zoals gehoorschade of boterosie door IL-1β beperkt zijn (13-16). Het is daarom de vraag of rAOM en COME niet beter onderscheiden kunnen worden op basis van detectie van micro-organismen en/of het cytokineprofiel in de middenoorvloeistof dan op basis van klinische presentatie. Verder onderzoek is nodig om vroegdiagnostiek te ontwikkelen om kinderen met OM die een verhoogd risico hebben voor het ontwikkelen van complicaties in een vroeg stadium te detecteren.

Humorale immuunrespons en serumresistentie

Hoofdstuk 4 beschrijft, gebruikmakend van de Luminex xMAP technologie, de humorale immuunrespons in middenoorvloeistoffen en serum gericht tegen *M. catarrhalis* en *S. pneumoniae* oppervlakte antigenen van kinderen met rAOM en COME. In vergelijking met andere studies (17) laten de concentraties antigeen-specifiek IgG, IgA en IgM een grote inter-individuele variatie zien. Hierbij werden geen significante verschillen aangetoond tussen het rAOM en het COME cohort. Per patiënt werd een sterke correlatie gevonden tussen antigeen-specifiek serum IgG en IgG in de middenoorvloeistof. Het is nog onduidelijk of antilichamen (deels) lokaal geproduceerd worden (18,19) of diffunderen vanuit het bloed naar het middenoor (4,20). Gezien de sterke correlatie gevonden tussen antigeen-specifiek serum IgG en IgG in de middenoorvloeistof ondersteunen onze resultaten de laatstgenoemde hypothese.

Evenals in andere studies (21,22) vonden we geen correlatie tussen aanwezigheid van eiwit-specifieke antilichamen in serum en het voorkómen van nasofaryngeale bacteriële kolonisatie. Prevaes en collega's toonden aan dat in een cohort kinderen getest op de leeftijd van 12 en 24 maanden, antilichamen gericht tegen pneumokokken stegen en antilichamen gericht tegen stafylokokken daalden, hetgeen overeenkomt met de natuurlijke dynamiek van kolonisatie (22). Studies bij de muis suggereren dat een CD4-Th17 gemedieerde immuniteit een belangrijker rol speelt dan een antilichaam gemedieerde immuniteit als afweermechanisme tegen pneumokokken kolonisatie. Deze bevinding moet

echter nog wel bevestigd worden in de mens (23,24). Bovendien zouden andere bacteriële en gastheerfactoren een prominentere rol kunnen spelen, zoals bacteriële ontsnappingsmechanismen, co-infectie van verschillende bacteriële species of co-infectie van virussen en bacteriën, dysfunctie van de buis van Eustachius en genetische factoren van het kind.

De pathogenese van veel micro-organismen is gebaseerd op het vermogen om verschillende afweermechanismen te vermijden, te weerstaan of te neutraliseren. Veel micro-organismen hebben mechanismen ontwikkeld om complement-gemedieerde 'killing' te weerstaan (25). Recent is aangetoond dat NTHi isolaten uit de lage luchtwegen een grotere complement resistentie hebben in vergelijking met koloniserende stammen uit de neus-keelholte (26). Parallel hieraan hebben wij laten zien dat NTHi isolaten uit het middenoor meer complement resistent zijn dan isolaten uit de neus-keelholte (**Hoofdstuk 5**). Deze afgenomen gevoeligheid correleerde met afgenomen binding van IgM aan de bacterie. Deze bevinding gaf aanleiding om het onderliggende mechanisme van serumresistentie nader te onderzoeken. Hierbij bleek dat het R2866_0112 gen een belangrijke rol speelt. Expressie van het R2866_0112 gen was hoger in serum-resistente dan serum-gevoelige NTHi isolaten, en deletie van het R2866_0112 gen ging gepaard met een sterkere IgM binding. Dit gen codeert voor een nieuw lipooligosaccharide (LOS) biosynthese gen.

NTHi is in staat aan het immuunsysteem te ontsnappen door de verschillende karakteristieken van het LOS: (i) LOS is heterogeen en bevat een aantal epitopen die in staat zijn tot fasevariatie, (ii) LOS kan humane bloedgroep antigenen imiteren en (iii) sialysatie van LOS in NTHi beïnvloedt de mogelijkheid om de lytische effecten van humaan serum te omzeilen. Ook al is de structuur van LOS heterogeen, de bactericide capaciteit van IgM gericht tegen NTHi-LOS maakt het de moeite waard om LOS te onderzoeken als een potentieel vaccin kandidaat in het kader van preventie tegen OM. Voorgaande studies suggereerden reeds om gedetoxificeerd LOS te gebruiken als een vaccincomponent om OM veroorzaakt door NTHi te voorkomen (27-29). Een gedetoxificeerd NTHi LOS eiwit conjugaat vaccin is beschermend in een chinchilla model en in een muismodel voor OM (29). Nota bene, in een studie uitgevoerd door Gergova en collega's werd aangetoond dat een IgM monoklonaal antilichaam gericht tegen *M. catarrhalis*-LOS kruis reageerde met NTHi-LOS (30). Dit suggereert dat in de ontwikkeling van een LOS gebaseerd vaccin tegen *M. catarrhalis*, immunisatie kan resulteren in een immuunrespons tegen epitopen geconserveerd in andere belangrijke luchtweg pathogenen zoals NTHi (30).

Microbiële pathogenese

Ontwikkeling van een muismodel voor OM

Eén van de beperkingen van de huidige experimentele modellen voor de bestudering van de bacteriële pathogenese van AOM is de invasieve benadering van de experimentele procedures. In de meeste diermodellen wordt AOM geïnduceerd door directe inoculatie van levende bacteriën in de middenoorholte, ofwel via het benige gedeelte van het middenoor, ofwel via het trommelvlies (31,32). Om de pathogenese van AOM te onderzoeken op non-invasieve wijze werd door ons een muismodel ontwikkeld voor AOM veroorzaakt door *S. pneumoniae* (**Hoofdstuk 6**). In het model wordt drukverhoging gebruikt om pneumokokken vanuit de neus-keelholte te verplaatsen naar beide middenoren. Gebruikmakend van deze methode waren we in staat om op non-invasieve en reproduceerbare wijze AOM te induceren: wild-type pneumokokken bleven tot 6 dagen na infectie aanwezig in het middenoor en ontsteking van het middenoor werd aangetoond met IL-1β en IL-6 cytokine analyse en histopathologie.

Het gebruik van een druk cabine is een verbetering op de bestaande experimentele AOM modellen om verscheidene redenen: i) drukverhoging faciliteert de verplaatsing van pneumokokken vanuit de neus-keelholte naar de middenoorholte en komt dus overeen met de route van infectie bij de mens; ii) een ontstekingsreactie door lokale manipulatie van het middenoor wordt vermeden (33); iii) de succeskans is 100%. Laatstgenoemde is van essentieel belang om het effect van vaccinatie, namelijk reductie in de hoeveelheid bacteriën in het middenoor, te kunnen monitoren. Dit is een aanzienlijke verbetering ten opzichte van intranasale inoculatie zonder drukverhoging, waarbij na bacteriële kolonisatie van de neusholte, spontane invasie van het middenoor plaatsvindt in slechts ongeveer 50% van de gevallen (31).

Onlangs hebben Short en collega's een andere niet-invasieve AOM infectie methode in de muis beschreven (34). Co-infectie van babymuizen met *S. pneumoniae* en influenza A virus na intranasale inoculatie toonde een hoge hoeveelheid bacteriën in het middenoor, ontsteking van het middenoor en gehoorverlies. Door co-infectie van bacterie en virus ontstond OM spontaan in nagenoeg alle gevallen. Omdat virale infecties de immuunrespons kunnen beïnvloeden zijn beide modellen van belang om de bacteriële pathogenese en de immuunrespons van de gastheer te onderzoeken.

NTHi is niet in staat om AOM te induceren in muizen, omdat deze bacterie snel geklaard wordt uit het middenoor. Wij hebben analoog aan het intranasale *S. pneumo-*

niae – influenza A co-infectiemodel een experimenteel model ontwikkeld om OM geïnduceerd door NTHi te bestuderen (**Hoofdstuk 5**). Muizen werden geïnoculeerd met influenza A virus of placebo 3 dagen voorafgaand aan intranasale infectie met NTHi. Infectie met influenza A zorgde voor een significant grotere hoeveelheid NTHi bacteriën in de neus-keelholte en het middenoor in vergelijking met infectie met NTHi alleen, en resulteerde in OM in 100% van de gevallen.

Identificatie van nieuwe pneumokokken virulentiefactoren in AOM

Bacteriële oppervlakte eiwitten spelen een belangrijke rol in de interactie tussen gastheer en pathogeen. Identificatie van nieuwe oppervlakte eiwitten die een belangrijke rol spelen in virulentie kan het inzicht in OM pathogenese versterken en zo vaccinontwikkeling faciliteren. Verschillende virulentie studies hebben laten zien dat de meeste pneumokokkenmutanten een verzwakt fenotype hebben in ofwel kolonisatie, ofwel pneumonie, ofwel sepsis. De bijdrage aan virulentie van die verschillende pneumokokkencomponenten is afhankelijk van de aard en lokalisatie van de infectie (35-42).

We hebben het AOM druk cabine model gebruikt om de bijdrage van twee verwante oppervlakte eiwitten in OM te onderzoeken: het streptokokken lipoproteïne rotamase A (SlrA) en het vermeende proteïnase maturatie proteïne A (PpmA) (**Hoofdstuk 6**). Beide eiwitten hebben de potentie om een afweerreactie op te wekken (43,44). Eerder onderzoek toonde een cruciale rol aan voor SlrA in adherentie, kolonisatie en immuun evasie (39). PpmA is een geconserveerd oppervlakte eiwit en is betrokken bij kolonisatie van de neus-keelholte en bij invasieve ziekte. Desalniettemin is de exacte functie van dit eiwit nog steeds onbekend (44,45).

Wij hebben de bijdrage van SlrA en PpmA aan OM onderzocht in ons muismodel. Pneumokokken waarbij het coderende gen voor SlrA (maar niet voor PpmA) ontbrak, waren significant minder virulent in het OM model. Let wel: pneumokokken waarin beide genen ontbraken waren veel minder virulent dan mutanten die alleen het *slrA* gen misten. Dit additieve effect suggereert dat SlrA en PpmA een complementaire functie hebben in experimentele OM. Zoals beschreven door Audouy en collega's liet intranasale immunisatie van muizen met SlrA-IgA1p of SlrA-IgA1p-PpmA significante bescherming tegen pneumonie zien (46). Of het SlrA eiwit geschikt is als vaccin kandidaat voor bescherming tegen OM dient nog verder te worden onderzocht. We hebben aangetoond dat ons muismodel geschikt is om OM geïnduceerd door pneumokokken te bestuderen en dat met behulp van dit experimentele model ook pneumokokken virulentiestudies uitgevoerd kunnen worden.

De 'genomic array footprinting' (GAF) technologie is ontwikkeld in ons laboratorium om potentiële virulentiefactoren te identificeren (47). De technologie is gebaseerd op een selectieprocedure waarbij micro-arrays gebruikt worden om genen te identificeren die van cruciaal belang zijn tijdens verschillende stadia van het infectieproces. Met de GAF technologie werden twee pneumokokken eiwitten, SP1298 en SP2205, op consistente wijze geïdentificeerd in muismodellen voor kolonisatie van de neus-keelholte, bacteriëmie en meningitis. SP1298 en SP2205 zijn twee geconserveerde eiwitten met een nog onbekende functie, geclassificeerd als DHH subfamilie 1 eiwitten. We onderzochten de bijdrage van SP1298 en SP2205 aan kolonisatie van de neus-keelholte, OM, pneumonie en bacteriëmie (**Hoofdstuk 7**). Het aantal bacteriën in het middenoor van muizen geïnfecteerd met mutanten die beide genen misten, bleek verminderd ten opzichte van de wild-type geïnfecteerde muizen op alle onderzochte tijdspunten na infectie. In OM co-infectie experimenten was het wild-type virulenter dan zowel de SP1298 en SP2205 enkel mutanten als de dubbelmutant. Ook hier speelde de anatomische locatie van de infectie een rol: de SP2205 mutant bleek verzwakt in de neus-keelholte en middenoren van muizen, dit in tegenstelling tot de longen en het bloed waar de mutant net zo virulent was als het wild-type. Deletie van beide genen resulteerde in een verminderde virulentie zich uitend in een verminderde kolonisatie van de neus-keelholte en lagere aantallen bacteriën in het middenoor, de long en de bloedbaan.

Omdat OM episodes meestal voorafgegaan worden door kolonisatie van de neus-keelholte, hebben de DHH eiwitten potentie als vaccinkandidaten gericht tegen OM. We hebben aangetoond dat subcutane vaccinatie met SP1298 en SP2205 bescherming kan bieden tegen pneumokokkenziekte in muizen, inclusief nasofaryngeale kolonisatie, pneumonie en bacteriëmie. Deze eiwitten spelen dus een significante rol in verschillende stadia van infectie en zijn potentiële kandidaten voor een multi-component eiwitvaccin. Op dit moment onderzoeken wij de cellulaire lokalisatie tijdens pathogenese en proberen we de biochemische functie van beide eiwitten te achterhalen. Western blot analyse en 3D predictie modellering hebben aangetoond dat SP1298 direct of indirect betrokken is bij oxidatieve stresstolerantie. Op basis van homologie met eiwitten uit andere bacteriën zou SP1298 3'(2')-phosphoadenosine-5'-fosfaat (pAp) phospatase activiteit kunnen bevatten, waardoor de beperkte groei van de SP1298 deletiemutant mogelijk veroorzaakt wordt door ophoping van pAp.

OM en biofilm formatie

Serine-rijke repeat-eiwitten (SRRPs) behoren tot een familie van oppervlakte-eiwitten die worden aangetroffen in tal van gram-positieve bacteriën, inclusief *Staphylococcus aureus*,

S. pneumoniae, groep B streptokokken en orale streptokokken. We hebben een nieuwe rol voor het pneumokokken serine-rijke repeat eiwit (PsrP) beschreven, het SRRP van *S. pneumoniae,* als een intra-species bacterieel adhesine dat bacteriële aggregatie tijdens kolonisatie en pneumonie in muizen bevordert (**Hoofdstuk 8**). *In vitro* hebben we aangetoond dat de basale regio van PsrP eigen interacties bevordert, zich uitend in een toegenomen densiteit van de biofilms, een grotere massa van de biofilm en een veranderde architectuur van oppervlakte structuren. Deze interacties konden geneutraliseerd worden door antilichamen tegen PsrP. PsrP heeft derhalve een duale rol in zowel de interactie met cellen van de gastheer als wel de intra-bacteriële interactie.

De exacte rol van PsrP in OM wordt momenteel onderzocht. Muizen met *S. pneumoniae* TIGR4Δ*psrP* hebben een groter aantal bacteriën in het middenoor en verhoogde spiegels van IL-1β, IL-6 en TNF-α in vergelijking met wild-type TIGR4 geïnfecteerde controlemuizen. Een dergelijke bevinding is eerder beschreven voor NTHi *luxS* mutanten (48,49). De onderzoekers beschreven dat LuxS biofilm maturatie en persistentie voor NTHi *in vivo* bevordert. Ook hier waren bacteriële tellingen in middenoorvloeistoffen en de hoogte van de inflammatoire gastheerrespons toegenomen bij muizen geïnfecteerd met *luxS* mutanten in vergelijking met de wild-type stam.

In het algemeen wordt de helft van alle bacteriële infecties als biofilm gerelateerd beschouwd (50). Toch zijn studies over de rol van virulentiefactoren bij biofilm vorming in kader van OM schaars. Experimentele studies in het chinchilla infectie model voor OM laten een associatie zien tussen biofilm vorming en de pneumokokken virulentiefactoren PcpA, PspA en PspC, allen choline bindingseiwitten (51). Bacteriële factoren belangrijk voor NTHi biofilms zijn onder andere LOS, pili en dubbelstrengs DNA (52). Voor verder onderzoek met betrekking tot biofilm vorming is het ratten OM model van Chaney en collega's wellicht van toegevoegde waarde (53). Zoals ook in ons muismodel, werd een druk cabine gebruikt om pneumokokken te verplaatsen van de neus-keelholte naar het middenoor. Waar wij gebruik maakten van een AOM model met eenmalig geïnfecteerde muizen, inoculeerden deze onderzoekers de ratten elke 4-7 dagen gedurende 6 maanden. De ratten werden op verscheidene tijdspunten geofferd om zo biofilm vorming in het middenoor te monitoren.

Conclusie

In dit proefschrift wordt aangetoond dat *H. influenzae* en rhinovirus de voornaamste micro-organismen zijn in het middenoor en in de neus-keelholte van kinderen met rAOM of COME. MLST analyse toont aan dat de micro-organismen uit de neus-keelholte en het middenoor binnen één patiënt meestal genetisch identiek zijn. Het is in onze studie niet mogelijk een onderscheid te maken tussen rAOM en COME op basis van de microbiologische resultaten. We hebben aangetoond dat cytokine concentraties in het middenoor geassocieerd zijn met de aanwezigheid van bacteriën maar niet met die van virussen. Daarnaast laten we zien dat ongekapselde *H. influenzae* isolaten uit het middenoor een toegenomen complement resistentie hebben en dat de LOS structuur de mate van IgM binding en complementactivatie bepaalt. In experimentele studies hebben we het inzicht verdiept in de moleculaire pathogenese van pneumokokken virulentie factoren die een rol spelen bij de pathogenese van OM.

Er zijn een aantal kanttekeningen te plaatsen bij de studies beschreven in dit proefschrift. Allereerst is het klinisch cohort relatief klein (n = 176 patiënten) en heeft deze zich beperkt tot kinderen die allen woonachtig waren in één regio van Nederland. Ten tweede is het menselijk immuunsysteem een complex systeem, dat niet *in vitro* in al haar details gesimuleerd kan worden. Om virulentie- en vaccinkandidaten te testen zijn diermodellen, in onze studies een muizenmodel, onvermijdelijk om de menselijke immuunrespons op specifieke bacteriële componenten beter te ontrafelen en begrijpen. Het mag duidelijk zijn dat de muis geen mens is, en onze resultaten derhalve niet zondermeer geëxtrapoleerd kunnen worden naar de humane situatie.

Toekomstig onderzoek

Vaccinontwikkeling

Diverse studies laten zien dat vaccinatie OM kan voorkómen (54-56). Vaccinaties gericht op het reduceren van AOM zullen waarschijnlijk van invloed zijn op het complete spectrum van OM, inclusief rAOM en COME, aangezien deze in het merendeel van de gevallen een gevolg zijn van AOM. Echter, immunisatie van alleen kinderen met rAOM of COME lijkt niet effectief, met name omdat collectieve immuniteit niet wordt bewerkstelligd (57,58).

Er zijn verschillende vereisten voor een effectief vaccin: het moet veilig zijn en beschermen in de betreffende doelgroep, de bescherming dient langdurig te zijn en zowel antilichamen als beschermende T-cellen te activeren. Daarnaast zijn er ook praktische overwegingen zoals lage productiekosten, biologische stabiliteit, een gemakkelijke toedieningsroute en een gering aantal bijwerkingen (59). Potentiële vaccinantigenen mogen uiteraard niet toxisch zijn, moeten geconserveerd zijn binnen de bacteriesoort, zonder dat er sprake is van kruisreactiviteit met andere, niet-pathogene bacteriesoorten. Daarnaast dienen vaccinantigenen niet homoloog te zijn aan humane factoren. Het ideale vaccin om bacteriële OM te voorkomen beschermt tegen de 3 voornaamste pathogenen in OM: *S. pneumoniae, H. influenzae* (60) en *M. catarrhalis* (61). Daarbij zal een vaccin met een grotere dekkingsgraad, bijvoorbeeld op basis van eiwitten aanwezig bij alle serotypes, of toevoeging van een eiwit-gebaseerd vaccin aan het huidige pneumokokken conjugaatvaccin in de toekomst nodig zijn (58).

In tegenstelling tot invasieve ziekten zoals longontsteking, hersenvliesontsteking en sepsis, is OM een aandoening van de slijmvliezen. Om effectieve vaccins te ontwikkelen is het daarom van belang om te begrijpen hoe middenoor pathogenen interacteren met het mucosale immuunsysteem. Er zijn verscheidene obstakels in de ontwikkeling van mucosale vaccins die nog overwonnen moeten worden. Zo is er bijvoorbeeld nog geen goed correlaat om de mate van bescherming tegen mucosale infectie te meten. Er wordt momenteel onderzocht of bactericide testen, opsonofagocytose testen en vermindering van bacteriële aantallen in verschillende (dier)modellen een goede maat zijn. Een directe correlatie tussen immuunrespons en bacteriële klaring in het middenoor is echter nog niet gevonden.

Referenties

1. Daly KA, Hoffman HJ, Kvaerner KJ, et al. Epidemiology, natural history, and risk factors: panel report from the Ninth International Research Conference on Otitis Media. International journal of pediatric otorhinolaryngology 2010; 74(3): 231-40.
2. Brake MK, Jewer K, Flowerdew G, Cavanagh JP, Cron C, Hong P. Tympanocentesis results of a Canadian pediatric myringotomy population, 2008 to 2010. Journal of otolaryngology - head & neck surgery = Le Journal d'oto-rhino-laryngologie et de chirurgie cervico-faciale 2012; 41(4): 282-7.
3. Wiertsema SP, Kirkham LA, Corscadden KJ, et al. Predominance of nontypeable *Haemophilus influenzae* in children with otitis media following introduction of a 3+0 pneumococcal conjugate vaccine schedule. Vaccine 2011; 29(32): 5163-70.
4. Kaur R, Kim T, Casey JR, Pichichero ME. Antibody in middle ear fluid of children originates predominantly from sera and nasopharyngeal secretions. Clinical and vaccine immunology : CVI 2012; 19(10): 1593-6.
5. Schumacher SK, Marchant CD, Loughlin AM, Bouchet V, Stevenson A, Pelton SI. Prevalence and genetic diversity of nontypeable *Haemophilus influenzae* in the respiratory tract of infants and primary caregivers. The Pediatric infectious disease journal 2012; 31(2): 145-9.
6. Broides A, Dagan R, Greenberg D, Givon-Lavi N, Leibovitz E. Acute otitis media caused by *Moraxella catarrhalis*: epidemiologic and clinical characteristics. Clinical infectious diseases : an official publication of the Infectious Diseases Society of America 2009; 49(11): 1641-7.
7. Chantzi FM, Papadopoulos NG, Bairamis T, et al. Human rhinoviruses in otitis media with effusion. Pediatric allergy and immunology : official publication of the European Society of Pediatric Allergy and Immunology 2006; 17(7): 514-8.
8. Chattoraj SS, Ganesan S, Jones AM, et al. Rhinovirus infection liberates planktonic bacteria from biofilm and increases chemokine responses in cystic fibrosis airway epithelial cells. Thorax 2011; 66(4): 333-9.
9. Message SD, Laza-Stanca V, Mallia P, et al. Rhinovirus-induced lower respiratory illness is increased in asthma and related to virus load and Th1/2 cytokine and IL-10 production. Proceedings of the National Academy of Sciences of the United States of America 2008; 105(36): 13562-7.
10. Oliver BG, Lim S, Wark P, et al. Rhinovirus exposure impairs immune responses to bacterial products in human alveolar macrophages. Thorax 2008; 63(6): 519-25.
11. Proud D. Upper airway viral infections. Pulmonary pharmacology & therapeutics 2008; 21(3): 468-73.
12. Skovbjerg S, Roos K, Nowrouzian F, et al. High cytokine levels in perforated acute otitis media exudates containing live bacteria. Clinical microbiology and infection : the official publication of the European Society of Clinical Microbiology and Infectious Diseases 2010; 16(9): 1382-8.
13. Maeda K, Hirano T, Ichimiya I, Kurono Y, Suzuki M, Mogi G. Cytokine expression in

experimental chronic otitis media with effusion in mice. The Laryngoscope 2004; 114(11): 1967-72.
14. Scharer G, Zaldivar F, Gonzalez G, Vargas-Shiraishi O, Singh J, Arrieta A. Systemic inflammatory responses in children with acute otitis media due to *Streptococcus pneumoniae* and the impact of treatment with clarithromycin. Clinical and diagnostic laboratory immunology 2003; 10(4): 721-4.
15. Skotnicka B, Hassmann E. Proinflammatory and immunoregulatory cytokines in the middle ear effusions. International journal of pediatric otorhinolaryngology 2008; 72(1): 13-7.
16. Willett DN, Rezaee RP, Billy JM, Tighe MB, DeMaria TF. Relationship of endotoxin to tumor necrosis factor-alpha and interleukin-1 beta in children with otitis media with effusion. The Annals of otology, rhinology, and laryngology 1998; 107(1): 28-33.
17. Pichichero ME, Kaur R, Casey JR, Xu Q, Almudevar A, Ochs M. Antibody response to *Streptococcus pneumoniae* proteins PhtD, LytB, PcpA, PhtE and Ply after nasopharyngeal colonization and acute otitis media in children. Human vaccines & immunotherapeutics 2012; 8(6): 799-805.
18. Faden H, Brodsky L, Bernstein J, et al. Otitis media in children: local immune response to nontypeable *Haemophilus influenzae*. Infection and immunity 1989; 57(11): 3555-9.
19. Faden HS. Immunology of the middle ear: role of local and systemic antibodies in clearance of viruses and bacteria. Annals of the New York Academy of Sciences 1997; 830: 49-60.
20. Bakaletz LO, Holmes KA. Evidence for transudation of specific antibody into the middle ears of parenterally immunized chinchillas after an upper respiratory tract infection with adenovirus. Clinical and diagnostic laboratory immunology 1997; 4(2): 223-5.
21. Lebon A, Verkaik NJ, Labout JA, et al. Natural antibodies against several pneumococcal virulence proteins in children during the pre-pneumococcal-vaccine era: the generation R study. Infection and immunity 2011; 79(4): 1680-7.
22. Prevaes SM, van Wamel WJ, de Vogel CP, et al. Nasopharyngeal colonization elicits antibody responses to staphylococcal and pneumococcal proteins that are not associated with a reduced risk of subsequent carriage. Infection and immunity 2012; 80(6): 2186-93.
23. Bogaert D, Weinberger D, Thompson C, Lipsitch M, Malley R. Impaired innate and adaptive immunity to *Streptococcus pneumoniae* and its effect on colonization in an infant mouse model. Infection and immunity 2009; 77(4): 1613-22.
24. Lu YJ, Gross J, Bogaert D, et al. Interleukin-17A mediates acquired immunity to pneumococcal colonization. PLoS pathogens 2008; 4(9): e1000159.
25. Hallstrom T, Resman F, Ristovski M, Riesbeck K. Binding of complement regulators to invasive nontypeable *Haemophilus influenzae* isolates is not increased compared to nasopharyngeal isolates, but serum resistance is linked to disease severity. Journal of clinical microbiology 2010; 48(3): 921-7.
26. Nakamura S, Shchepetov M, Dalia AB, et al. Molecular basis of increased serum resistance among pulmonary isolates of non-typeable *Haemophilus influenzae*. PLoS pathogens 2011; 7(1): e1001247.
27. Gu XX, Sun J, Jin S, et al. Detoxified lipooligosaccharide from nontypeable *Haemophilus influenzae* conjugated to proteins confers protection against otitis media in chinchillas. Infection and immunity 1997; 65(11): 4488-93.
28. Hong W, Peng D, Rivera M, Gu XX. Protection against nontypeable Haemophilus influen-

zae challenges by mucosal vaccination with a detoxified lipooligosaccharide conjugate in two chinchilla models. Microbes and infection / Institut Pasteur 2010; 12(1): 11-8.
29. Sun J, Chen J, Cheng Z, Robbins JB, Battey JF, Gu XX. Biological activities of antibodies elicited by lipooligosaccharide based-conjugate vaccines of nontypeable Haemophilus influenzae in an otitis media model. Vaccine 2000; 18(13): 1264-72.
30. Gergova RT, Iankov ID, Haralambieva IH, Mitov IG. Bactericidal monoclonal antibody against Moraxella catarrhalis lipooligosaccharide cross-reacts with Haemophilus Spp. Current microbiology 2007; 54(2): 85-90.
31. Ryan AF, Ebmeyer J, Furukawa M, et al. Mouse models of induced otitis media. Brain research 2006; 1091(1): 3-8.
32. Sabirov A, Metzger DW. Intranasal vaccination of neonatal mice with polysaccharide conjugate vaccine for protection against pneumococcal otitis media. Vaccine 2006; 24(27-28): 5584-92.
33. MacArthur CJ, Hefeneider SH, Kempton JB, Parrish SK, McCoy SL, Trune DR. Evaluation of the mouse model for acute otitis media. Hearing research 2006; 219(1-2): 12-23.
34. Short KR, Diavatopoulos DA, Thornton R, et al. Influenza virus induces bacterial and non-bacterial otitis media. The Journal of infectious diseases 2011; 204(12): 1857-65.
35. Chen H, Ma Y, Yang J, et al. Genetic requirement for pneumococcal ear infection. PloS one 2008; 3(8): e2950.
36. Cripps AW, Otczyk DC, Kyd JM. Bacterial otitis media: a vaccine preventable disease? Vaccine 2005; 23(17-18): 2304-10.
37. Hava DL, Camilli A. Large-scale identification of serotype 4 Streptococcus pneumoniae virulence factors. Molecular microbiology 2002; 45(5): 1389-406.
38. Hendriksen WT, Bootsma HJ, Estevao S, et al. CodY of *Streptococcus pneumoniae*: link between nutritional gene regulation and colonization. Journal of bacteriology 2008; 190(2): 590-601.
39. Hermans PW, Adrian PV, Albert C, et al. The streptococcal lipoprotein rotamase A (SlrA) is a functional peptidyl-prolyl isomerase involved in pneumococcal colonization. The Journal of biological chemistry 2006; 281(2): 968-76.
40. Ogunniyi AD, LeMessurier KS, Graham RM, et al. Contributions of pneumolysin, pneumococcal surface protein A (PspA), and PspC to pathogenicity of Streptococcus pneumoniae D39 in a mouse model. Infection and immunity 2007; 75(4): 1843-51.
41. Tong HH, Long JP, Li D, DeMaria TF. Alteration of gene expression in human middle ear epithelial cells induced by influenza A virus and its implication for the pathogenesis of otitis media. Microbial pathogenesis 2004; 37(4): 193-204.
42. Tuomanen EI. Pathogenesis of pneumococcal inflammation: otitis media. Vaccine 2000; 19 Suppl 1: S38-40.
43. Adrian PV, Bogaert D, Oprins M, et al. Development of antibodies against pneumococcal proteins alpha-enolase, immunoglobulin A1 protease, streptococcal lipoprotein rotamase A, and putative proteinase maturation protein A in relation to pneumococcal carriage and Otitis Media. Vaccine 2004; 22(21-22): 2737-42.
44. Overweg K, Kerr A, Sluijter M, et al. The putative proteinase maturation protein A of *Streptococcus pneumoniae* is a conserved surface protein with potential to elicit protective immune responses. Infection and immunity 2000; 68(7): 4180-8.
45. Cron LE, Bootsma HJ, Noske N, Burghout P, Hammerschmidt S, Hermans PW. Surface-

associated lipoprotein PpmA of *Streptococcus pneumoniae* is involved in colonization in a strain-specific manner. Microbiology (Reading, England) 2009; 155(Pt 7): 2401-10.
46. Audouy SA, van Selm S, van Roosmalen ML, et al. Development of lactococcal GEM-based pneumococcal vaccines. Vaccine 2007; 25(13): 2497-506.
47. Bijlsma JJ, Burghout P, Kloosterman TG, et al. Development of genomic array footprinting for identification of conditionally essential genes in *Streptococcus pneumoniae*. Applied and environmental microbiology 2007; 73(5): 1514-24.
48. Armbruster CE, Hong W, Pang B, et al. LuxS promotes biofilm maturation and persistence of nontypeable *Haemophilus influenzae* in vivo via modulation of lipooligosaccharides on the bacterial surface. Infection and immunity 2009; 77(9): 4081-91.
49. Daines DA, Bothwell M, Furrer J, et al. *Haemophilus influenzae* luxS mutants form a biofilm and have increased virulence. Microbial pathogenesis 2005; 39(3): 87-96.
50. Munoz-Elias EJ, Marcano J, Camilli A. Isolation of *Streptococcus pneumoniae* biofilm mutants and their characterization during nasopharyngeal colonization. Infection and immunity 2008; 76(11): 5049-61.
51. Reid SD, Hong W, Dew KE, et al. *Streptococcus pneumoniae* forms surface-attached communities in the middle ear of experimentally infected chinchillas. The Journal of infectious diseases 2009; 199(6): 786-94.
52. Juneau RA, Pang B, Weimer KE, Armbruster CE, Swords WE. Nontypeable *Haemophilus influenzae* initiates formation of neutrophil extracellular traps. Infection and immunity 2011; 79(1): 431-8.
53. Chaney EJ, Nguyen CT, Boppart SA. Novel method for non-invasive induction of a middle-ear biofilm in the rat. Vaccine 2011; 29(8): 1628-33.
54. Magnus MC, Vestrheim DF, Nystad W, et al. Decline in early childhood respiratory tract infections in the norwegian mother and child cohort study after introduction of pneumococcal conjugate vaccination. The Pediatric infectious disease journal 2012; 31(9): 951-5.
55. Mawas F, Ho MM, Corbel MJ. Current progress with *Moraxella catarrhalis* antigens as vaccine candidates. Expert review of vaccines 2009; 8(1): 77-90.
56. Prymula R, Kriz P, Kaliskova E, Pascal T, Poolman J, Schuerman L. Effect of vaccination with pneumococcal capsular polysaccharides conjugated to *Haemophilus influenzae*-derived protein D on nasopharyngeal carriage of *Streptococcus pneumoniae* and *H. influenzae* in children under 2 years of age. Vaccine 2009; 28(1): 71-8.
57. Giebink GS. Vaccination against middle-ear bacterial and viral pathogens. Annals of the New York Academy of Sciences 1997; 830: 330-52.
58. Fitzwater SP, Chandran A, Santosham M, Johnson HL. The worldwide impact of the seven-valent pneumococcal conjugate vaccine. The Pediatric infectious disease journal 2012; 31(5): 501-8.
59. Rodgers GL, Klugman KP. The future of pneumococcal disease prevention. Vaccine 2011; 29 Suppl 3: C43-8.
60. Janeway CA, Travers P, M. W, Shlomchik MJ. Immunobiology: the immune system in health and disease. 6th edition ed. New York: Garland Science Publishing; 2005.
61. Murphy TF, Faden H, Bakaletz LO, et al. Nontypeable *Haemophilus influenzae* as a pathogen in children. The Pediatric infectious disease journal 2009; 28(1): 43-8.

Dankwoord
Curriculum vitae
List of publications
Abbreviations

Dankwoord

Peter, dank voor alle mogelijkheden die ik heb gekregen tijdens mijn promotietijd. Het werken binnen een Europees consortium was een fantastische ervaring! Ronald, dank voor je onvoorwaardelijk mentorschap. Ik hoop dat in de toekomst ook voor anderen te kunnen betekenen. Geniet van je welverdiende emeritaat. Adilia, dank voor de vrouwelijke tegenhang van Peter en Ronald. Iemand moet ze in het gareel houden en dat doe je met verve. Dank voor je advies.

Professor Kees Graamans en Joost Engel: dank voor de begeleiding vanuit de vakgroepen KNO van het Radboud Universitair Medisch Centrum en het Canisius-Wilhelmina ziekenhuis.

Willem Melchers, Patrick Sturm en Jaques Meis: dank voor jullie input en het beschikbaar stellen van werkplekken op de afdelingen Medische Microbiologie van bovengenoemde ziekenhuizen. Marion de Bruin en Carla Bartels: dank voor jullie coördinerende rol. Dank ook aan het personeel op de OK's voor de inclusie van patiënten voor de OMVac-studie.

Ook dank aan de medische en biomedische studenten (Peter, Mariëlle, Luc, Nienke, Marissa) betrokken bij de inclusie van patiënten en het opwerken van het patiëntenmateriaal. Sanne, je hebt me in het kader van jouw afstudeeronderzoek ondersteund met het opzetten van het otitis media model. Inmiddels ben je zelf druk bezig met de laatste fase van je promotieonderzoek, ik ben hartstikke trots op je.

Saskia, de verhalen over Vince en Bent waren als uit de Kameleon. Ondeugendheid is een groot goed, vooral als het de kinderen van je collega betreft. Naast je onderzoeksbegeleiding heb ik vooral veel geleerd van de manier waarop je in het leven staat. Hester, samen met Saskia heb je jarenlang gestreden voor de titel favoriete post-doc. Jullie staan nog steeds op een gedeelde eerste plaats (voor de goede orde: er waren geen andere deelnemers in deze competitie). Dank voor je begeleiding: gedetailleerd en recht voor zijn raap. Ik vind je een groots onderzoeker en een groots begeleider. Dimitri, in mijn laatste jaar kwam je als post-doc op ons laboratorium. Dank voor je kennis en begeleiding tijdens de laatste loodjes.

Kim B., Lori, Stefanie, Inge: gelukkig zaten jullie in hetzelfde (promotie)schuitje. Alle andere collega's van het laboratorium Kindergeneeskunde Infectieziekten: hard gewerkt en hard gelachen, beide soms op onmogelijke tijden.

Collega's van het OMVac consortium, in het bijzonder John Hays en Suzanne Ver-

haegh: dank voor de prettige samenwerking. Professor B.H. Normark, dear Birgitta, many thanks for your advise during the OMVac project and thank you for being one of the members of the committee.

Paranimfen: Arieke, 2013 is jouw jaar: een leuke vent, een eigen huis, een eigen tandartspraktijk. Dank voor je altijd luisterend oor, je wijze raad en je gevoel voor humor. Fijn dat je de taak van paranimf op je genomen hebt. Josefine, samen in het studentenhuis zijn wij medisch groot gebracht. Samen naar college en samen studeren voor tentamens. Inmiddels heb je één van de huisgenoten van destijds omgedoopt tot echtgenoot, heb je 2 prachtige dochters en werk je als huisarts in Den Haag. Ik waardeer je nuchtere kijk op het leven en het gegeven dat, hoe volwassen we dan ook inmiddels mogen zijn, we voornamelijk samen giebelen. Dank dat je paranimf wilt zijn.

Dank ook aan alle collega's van de afdeling Kindergeneeskunde in Tilburg: het is elke dag een feest om met jullie samen te werken.

Joris, Marloes, Len, Mark, Wessel, Nienke, Wout, Lot: zonder jullie zouden de feesten verjaardagen niet hetzelfde zijn. Ik hoop dat we nog veel mooie dingen samen mogen meemaken.

Lieve Arthur, jouw architectonische wereld is een gezond tegenwicht voor de beslommeringen in de medische praktijk. Met jouw ogen naast mij zie ik meer van de wereld. Max, wat gezellig dat je er bent! Wellicht weet je nu al veel over middenoorontsteking. Maak je geen zorgen over je genetische predispositie, die is er niet.

Niels, grote kleine broer, ik geef het 1 keer toe: jij bent inderdaad de leukste thuis (het staat wel zwart op wit). Maak er wat moois van samen met Noor. Pappa, mamma: dank voor jullie onvoorwaardelijke steun.

Curriculum Vitae

Kim Stol was born on the 18th of January 1980 in IJsselstein, Utrecht, The Netherlands. In 1998, she finished her secondary school education (VWO) at Elzendaalcollege in Boxmeer, and began further education at Leiden University, studying medicine. During her studies she went to Kanti's Children's hospital in Kathmandu, Nepal for an internship in Pediatrics and Pediatric surgery. In 2002, she went to the Department of Pediatrics at Cambridge University, Cambridge, United Kingdom, to perform a 7 months lasting research project on Androgen Insensitivity Syndrome entitled 'N/C interaction in the human Androgen Receptor' under supervision of Prof. Hughes and dr. Martin. After graduating in medicine, she worked as a resident at the Intensive Care Unit of Sophia's Children's hospital for one year. From 2006 till 2010 she performed her PhD project at the Radboud University Medical Centre in Nijmegen under supervision of Prof. dr. P.W.M. Hermans, Prof. dr. R. de Groot and dr. A. Warris. The majority of this research was performed as part of the European Union FP6 project 'Development of a prophylactic vaccine and diagnostic markers to prevent and diagnose otitis media (OMVac)', and the results obtained from the majority of the publications presented in this thesis. The results of her research were presented at several national and international scientific symposia and conferences, including the International Society of Pneumococci and Pneumococcal Diseases (ISPPD), the International Symposium on Recent Advances in Otitis Media and Europneumo. From July 2010 until May 2011 she worked as a resident in ENT Surgery. Kim is currently working as a resident in Pediatrics in Tilburg (head dr. C.C. Obihara) and Rotterdam (head dr. M. de Hoog). She is living together with Arthur Klijn in Tilburg and they have one son, called Max.

List of publications

1. Resistance to complement-mediated killing and IgM binding to non-typeable Haemophilus influenzae is not altered when ascending from the nasopharynx to the middle ears in children with otitis media.
   J.D. Langereis, T.M. van Dongen, **K. Stol**, R.P. Venekamp, A.G.M. Schilder, P.W.M. Hermans.
   Med Microbiol Immunol (2013) Jun 18; published online ahead of print.

2. Microbial profiling does not differentiate between childhood recurrent acute otitis media and chronic otitis media with effusion.
   K. Stol, S.J. Verhaegh, K. Graamans, J.A.M. Engel, P.D.J. Sturm, W.G.J. Melchers, J.F.G.M. Meis, A. Warris, J.P. Hays and P.W.M. Hermans.
   Int J Pediatr Otorhinolaryngol (2013), Apr;77(4): 488-93.

3. Inflammation in the middle ear of children with recurrent or chronic otitis media is associated with bacterial load.
   K. Stol, D. Diavatopoulos, K. Graamans, J.A.M. Engel, W. J.G. Melchers, H.F. Savelkoul, J.P. Hays, A. Warris and P.W.M. Hermans.
   Pediatr Infect Dis J (2012) Nov;31(11):1128-34.

4. Modified lipooligosaccharide structure protects nontypeable Haemophilus influenzae from IgM-mediated complement killing in experimental otitis media.
   J.D. Langereis, **K. Stol**, E.K. Schweda, B. Twelkmeyer, H.J. Bootsma, S.P.W. de Vries, P. Burghout, D.A. Diavatolpoulos and P.W.M. Hermans.
   MBio (2012), Jul 3;3(4):e00079-12.

5. Comparative analysis of the humoral immune response to Moraxella catarrhalis and Streptococcus pneumoniae surface antigens in children suffering from recurrent acute otitis media and chronic otitis media with effusion.
   S.J. Verhaegh, **K. Stol**, C.P. de Vogel, K. Riesbeck, E.R. Lafontaine, T.F. Murphy, A. van Belkum, P.W.M. Hermans and J.P. Hays.
   Clin Vaccine Immunol (2012) Jun;19(6):914-8.

6. Two DHH subfamily 1 proteins contribute to pneumococcal virulence and confer protection against pneumococcal disease.
L.E. Cron, **K. Stol**, P. Burghout, S. van Selm, E.R. Simonetti, H.J. Bootsma and P.W.M. Hermans.
Infect Immun (2011) Sep;79(9):3697-710.

7. Comparative analysis and supragenome modeling of twelve Moraxella catarrhalis clinical isolates.
J.J. Davie, J. Earl, S.P.W. de Vries, A. Ahmed, F.Z. Hu, H.J. Bootsma, **K. Stol**, P.W.M. Bootsma, R. M. Wadowsky, G.D. Ehrlich, J.P. Hays and A.A. Campagnari.
BMC Genomics (2011), Jan 26;12:70.

8. Evaluation of drug formularies for pediatric intensive care.
I. Ceelie, C. van der Starre, D. Tibboel, **K. Stol**, G. Koren and S.N. de Wildt.
Pediatr Crit Care Med (2011) Jan;12(1):e14-e19.

9. The pneumococcal serine-rich repeat protein is an intra-species bacterial adhesion that promotes bacterial aggregation in vivo and in biofilms.
C.J. Sanchez, P. Shivshankar, **K. Stol**, S. Trakhtenbroit, P. Sullam, K. Sauer, P.W.M. Hermans and C.J. Orihuela.
PLoS Pathog (2010), 6(8):e1001044.

10. Development of a non-invasive murine infection model for acute otitis media.
K. Stol, S. van Selm, S. van den Berg, H.J. Bootsma, W.A.M. Blokx, K. Graamans, E.L.G.M. Tonnaer and P.W.M. Hermans.
Microbiology (2009), Dec;155(Pt 12):4135-44.

Abbreviations

AA	Amino Acid
AOM	Acute Otitis Media
BA	Blood Agar
BAL	Bronchoalveolar Lavage
BCA assay	Bicinchonic Acid assay
BR	Basic Region
BSA	Bovine Serum Albumin
CBA	Cytometric Bead Array
CEP	Chromosomal Expression Platform
CFU	Colony Forming Unit
ChoP	Phosphorcholine
CI	Competitive Index
COME	Chronic Otitis Media with Effusion
COPD	Chronic Obstructive Pulmonary Disease
CV	Cristal Violet
DHH	the amino acid combination: asparagine-histidine-histidine
DNA	Deoxyribonucleic acid
Eno	Enolase
ENT	Ear-Nose-Throat
FACS	Fluorescence-Activated Cell Sorter
FCS	Fetal Calf Serum
GAF	Genomic Array Footprinting
GAPDH	Glyceraldehyde-3-phosphatedehydrogenase
gstBR	gst tagged recombinant Basic Region
HI	Heat Inactivated
HPS	Human Pooled Serum
i.n.	intranasally
IAV	Influenza A virus
IPD	Invasive Pneumococcal Disease
K10	Keratin 10
LOS	lipooligosaccharide
LPS	lipopolysaccharide

ME	Middle Ear
MEF	Middle Ear Fluid
MFI	Mean Fluorescence Intensity
MLST	Multilocus Sequence Typing
MOI	Multiplicity Of Infection
NHS	Normal Human Serum
NPL	Nasopharyngeal Lavage
NPS	Nasopharyngeal Swab
NR	Non-Repeat Region
NTHi	Nontypeable *Haemophilus influenzae*
OM	Otitis Media
OME	Otitis Media with Effusion
OMP	Outer Membrane Protein
ORL	Otorhinolaryngology
PAF	Platelet Activating Factor
PAMP	Pathogen Associated Molecular Pattern
PBS	Phosphate Buffered Saline
PCR	Polymerase Chain Reaction
PDE	Phosphodiesterase
PMN	Polymorphonuclear
PPI	Peptidyl-Prolyl Isomerases
PpmA	Pneumococcal proteinase maturation protein A
PRR	Pathogen Recognition Receptor
PsrP	Pneumococcal serine-rich repeat Protein
rAOM	recurrent Acute Otitis Media
rBR	recombinant Basic region
RNA	Ribonucleic Acid
RR	Response Regulators
Rt RT-PCR	realtime Reverse Transcriptase PCR
rt-PCR	realtime PCR
RT-PCR	Reverse Transcriptase PCR
SEM	Scanning Electron Microscopy
SEM	Standard Error of the Mean
SlrA	Streptococcal lipoprotein rotamase A
SPF	Specific-Pathogen-Free
SRR	Serine-rich Repeat Region

SRRP	Serine Rich Repeat Protein
STM	Signature Tagged Mutagenesis
TFP	Type IV pili
THY	Todd-Hewitt Yeast extract
TNF	Tumor Necrosis Factor
URI	Upper Respiratory tract Infection